



**Development of Rubber Allergy Protein Sensors by Using Molecular Imprinting
Technique**

Chonlatid Sontimuang

**A Thesis Submitted in Partial Fulfillment of the Requirements for the Degree of
Doctor of Philosophy in Pharmaceutical Sciences**

Prince of Songkla University

2011

Copyright of Prince of Songkla University

Thesis Title Development of rubber allergy protein sensors by using molecular imprinting technique
Author Mr. Chonlatid Sontimuang
Major Program Pharmaceutical Sciences

Advisory Committee :

.....Chairman

(Assoc. Prof. Dr. Roongnapa Srichana)

.....Committee

(Prof. Dr. Franz Ludwig Dickert)

Examining Committee :

.....Chairman

(Assoc. Prof. Dr. Proespichaya Kanatharana)

.....Committee

(Assoc. Prof. Dr. Roongnapa Srichana)

.....Committee

(Assoc. Prof. Dr. Teerapol Srichana)

.....Committee

(Assoc. Prof. Dr. Sanong Ekgasit)

.....Committee

(Asst. Prof. Dr. Juraithip Wungsintaweekul)

The Graduate School, Prince of Songkla University, has approved this thesis as partial fulfillment of the requirements for the Doctor of Philosophy in Pharmaceutical Sciences

.....

(Prof. Dr. Amornrat Phongdara)

Dean of Graduate School

ชื่อวิทยานิพนธ์	การพัฒนาเซ็นเซอร์สำหรับตรวจโปรตีนก่อแพ้จากยางพาราโดยการใช้เทคนิค พิมพ์ กระทบ โมเลกุล
ผู้เขียน	นายชลทิต สนธิเมือง
สาขาวิชา	เภสัชศาสตร์
ปีการศึกษา	2554

บทคัดย่อ

วิทยานิพนธ์นี้มุ่งเน้นที่การพัฒนาเซ็นเซอร์สำหรับตรวจวัดโปรตีนก่อแพ้จากยางพารา โดยอาศัยเทคนิคการพิมพ์กระทบ โมเลกุลบน โพลีเมอร์เป็นเลขอร์ที่สามารถให้ความไวและ เฉพาะเจาะจงต่อการตรวจวัดโปรตีนของเซ็นเซอร์ การพิมพ์กระทบ โมเลกุลที่พื้นผิวบนพอลิเมอร์ สามารถที่จะเตรียมได้โดยอาศัย เทคนิคการสแตมปีงหรือการละลายโปรตีนก่อแพ้ในน้ำกลั่นเป็นโพโร เจนตามด้วยการเกิดปฏิกิริยานอนโควาเลนต์ระหว่างหมู่ฟังก์ชันของเมทาไคลค เอซิด ไวนิลไพโรลิโดน เป็นฟังก์ชันนอล มอนอเมอร์ และไดไฮดรอกซีเอทิลีนบิสอะคริลาไมด์ เป็นสารครอสลิงค์เกอร์ โดยทำ ปฏิกิริยาพอลิเมอร์ไรเซชันภายใต้แสงยูวี ที่อุณหภูมิห้อง จากนั้นนำพอลิเมอร์ที่มีการพิมพ์กระทบ โมเลกุลโปรตีนก่อแพ้ที่ได้ไปทำให้ยึดบนซับสเตรตที่เป็นข้าวโอ๊ตเล็กโทรดที่เป็นโลหะทองคำ รอยจดจำ บนพอลิเมอร์ที่สังเคราะห์ได้นั้นสามารถให้การตอบสนองในการจดจำ ในแง่ของคุณสมบัติทาง เรขาคณิต เช่น ขนาด รูปร่าง และหมู่ฟังก์ชันของโปรตีนก่อแพ้ และสามารถนำไปใช้งานในการจับกับ โมเลกุลที่สนใจ ได้อีกหลังจากทำการล้าง โมเลกุลที่เชื่อมหลุดออกไปด้วยสารละลายที่เหมาะสม เซ็นเซอร์

สามารถที่จะให้ประสิทธิภาพของความไวในการวิเคราะห์ที่สูงและให้การคัดเลือกที่ดีและโดย
ทำการศึกษาคู่ประกอบของพอลิเมอร์เมตริกได้แก่ การศึกษาหาฟังก์ชันนอลมอนอเมอร์ ฟังก์ชันนอล
โครอสลิงเกอร์ อัตราส่วนของจำนวน โมลและพารามิเตอร์อื่นๆ ที่มีผลต่อการวัดสัญญาณ บนตัวแปร
สัญญาณของควอตซ์คริสตัล ไมโครบาลานซ์ อินเทอร์เน็ตจิจิต คาทาซิทีฟ และ เซอร์เฟสพลาสมอนเร
โซแนนซ์ และได้ตรวจความคงตัวทั้งทางด้านเชิงกลและกายภาพของพอลิเมอร์ที่มีรอยพิมพ์ประทับ
โมเลกุลสามารถประเมินได้ด้วยกล้องจุลทรรศน์แรงอะตอมก่อนที่จะนำไปประกอบใช้งานร่วมกับ
ตัวแปรสัญญาณต่างๆ

คุณสมบัติของรอยจดจำบนพอลิเมอร์ที่สังเคราะห์ได้ด้วยการพิมพ์ประทับโมเลกุลต่อ
โปรตีนก่อแพ้สามารถประเมินได้จากการศึกษาค่า อิมพริ้นดิงแฟกเตอร์ และค่าแฟกเตอร์ของการ
คัดเลือกของโปรตีนบนตัวแปรสัญญาณภายใต้สภาวะที่เหมาะสม การเข้าทำปฏิกิริยาระหว่างโปรตีน
ก่อแพ้และรอยจดจำที่สังเคราะห์ได้บนพื้นผิวของพอลิเมอร์สามารถก่อให้เกิดการเปลี่ยนแปลงทาง
กายภาพได้แก่การให้สัญญาณของความถี่ ความจุไฟฟ้าหรือ การเปลี่ยนแปลงมุมสะท้อนกลับ เป็นต้น
พอลิเมอร์เลเซอร์ที่สังเคราะห์ได้ทั้งหมดจะให้รอยจดจำของ Hev b1 อยู่ที่ระดับนาโนเมตร โดยอาศัย
การวัดด้วยกล้องจุลทรรศน์แรงอะตอม การเกิดปฏิกิริยาระหว่างโปรตีนก่อแพ้ในรอยจดจำบนพื้นผิว
ของพอลิเมอร์นั้น นอกจากจะให้การคัดเลือกที่ดีแล้วยังสามารถทำการวิเคราะห์โปรตีนก่อแพ้แบบ
ออนไลน์ได้ รอยจดจำบนพื้นผิวของพอลิเมอร์ให้ความเฉพาะเจาะจงต่อ Hev b1 เทมเพลตโปรตีนด้วย
ค่าอิมพริ้นดิงแฟกเตอร์อยู่ที่ 12 และให้การคัดแยกโปรตีนที่สัมพันธ์กันซึ่งสกัดได้มาจากน้ำยาง เช่น
Hev b1 Hev b2 และ Hev b3 ด้วยค่าแฟกเตอร์ที่มีความเฉพาะเจาะจงอยู่ในช่วง 4 ถึง 6

เซ็นเซอร์ที่พัฒนาด้วยการพิมพ์ประทับโมเลกุลบนพื้นผิวของพอลิเมอร์เลเซอร์ทำหน้าที่เป็นวัสดุในการจดจำบนตัวแปรสัญญาณ QCM และ IDC ได้พิสูจน์ถึงประสิทธิภาพในการให้ความไวของสัญญาณการตรวจวัดและความน่าเชื่อถือของสัญญาณการวิเคราะห์ที่ได้ในการหาปริมาณโปรตีนก่อแพ้ที่พบอยู่ในน้ำยางพาราและถุงมือยางพารา วิทยานิพนธ์นี้สามารถใช้เป็นแนวทางในการพัฒนาแอนติบอดีสังเคราะห์โดยอาศัยเทคโนโลยีการพิมพ์ประทับโมเลกุลร่วมกับตัวแปรสัญญาณซึ่งสามารถประยุกต์ใช้กับงานทางไบโอเซ็นเซอร์ได้

Thesis Title	Development of rubber allergy protein sensors by using molecular imprinting technique
Author	Mr. Chonlatid Sontimuang
Major Program	Pharmaceutical Sciences
Academic Year	2011

ABSTRACT

This thesis focuses on the development of rubber allergy protein sensors by using a molecular imprinted polymer as a sensitive layer. Surface imprinting techniques such as stamping or solution based polymerization were used to obtain the imprint made with Hev b1 as the template through noncovalent binding to chemical functionality of methacrylic acid (MAA) and 1-vinyl-2-pyrrolidone (NVP), as functional monomers, and *N,N'*-(1,2-dihydroxyethylene) bisacrylamide (DHEBA) as crosslinking agent as the recognition element after polymerization under UV light at room temperature. This surface imprinted polymer was then immobilized on a gold substrate to act as an electrode. The imprinted site on the polymer surface that mimicked the shape and surface functionality of the allergen protein and served as a recognition site for re-adsorption after removing the template by washing with an appropriate solvent. The composition of the polymer matrix including the functional monomers, functional cross-linkers and their molar ratios and also technological parameters were optimized to achieve good physical features of the sensitive layer with the best sensing response on three different transducers: a quartz crystal microbalance, an interdigitated capacitive and a surface plasmon resonance. The physical and mechanical stability of the MIP layers

can be properly investigated by atomic force microscopy (AFM) techniques to verify the integrity of sensing layer and the formed imprints. The binding characteristics of the MIP layer to Hev b1 were evaluated from the imprint factor and the cross-selectivity on the transducers under optimum conditions. Rebinding of the template to the recognition element-produced a change in the frequency, capacitance or SPR angle. For all of the cases, the molded polymer and surface-imprinted layer showed nano-sized Hev b1 imprints using an atomic force microscope. Re-inclusion of the latex allergen allowed for a selective on-line monitoring of these allergenic concentrations in distilled water. The imprinted cavities recognized specific binding sites on Hev b1 template proteins with a factor of 12 and could distinguish among closely related hevein latex allergenic proteins isolated from fresh natural rubber latex: Hev b1, Hev b2 and Hev b3 with a selectivity factor of from 4 to 6. The sensor prepared using Hev b1-imprinted thin layer as a sensitive element on QCM, and IDC transducer exhibited fast and reliable response to natural rubber latex protein even in real matrices stemming from glove extract. In the thesis project, a framework has been established to judge the feasibility of developing an artificial antibody based on molecular imprinting technology and interfacial protocols for supramolecular analysis. In light of this analysis, significant practical challenges have revealed the advantages of applying such technologies to produce biosensors.

ACKNOWLEDGEMENT

Firstly, I would like to gratefully acknowledge the enthusiastic supervision, encouragement and useful guidance of my advisor, Assoc. Prof. Dr. Roongnapa Srichana, during this work.

I would like to express my gratitude to Prof. Franz Ludwig Dickert, Dean of Chemistry Faculty and Head of Institute of Analytical Chemistry, University of Vienna, for giving me permission to commence this thesis in the first instance. I also want to thank Prof's team work for all their help, support, interest and valuable recommendations.

I would like to thank Mr. Perapong Peangyam and Assoc. Prof. Dr. Prapaporn Utarabhand, Department of Biochemistry, Faculty of Science, Prince of Songkla University who trained me to use the instrument in biochemical lab technique and Assoc. Pro.Dr. Wirote Youravong, Department of Food Science, Faculty of Agro-Industry, Prince of Songkla University allowed me to use the facilities and laboratory for my thesis work.

I would like to thank Dr. Brian Hodgson, Dr. Neelam Balekar and Dr. Gangadhar Katkam to suggest and guildline my writing skill to successful my thesis work.

I am deeply indebted the Department of Pharmaceutical Chemistry, Faculty of Pharmaceutical Science, Prince of Songkla University, where gave me an opportunity to complete this Ph.D. thesis and to permit me using departmental

accessories. I also would like to thank all those who gave me their kind support and guidance.

Finally, the financial support of National Research Council of Thailand, NANOTEC Center of Excellence, the Prince of Songkla University, Thailand and Faculty of Chemistry, University of Vienna is gratefully acknowledged.

Chonlatid Sontimuang

Contents

	Page
Contents	x
List of Tables	xx
List of Figures	xxii
Chapter	1
1 Introduction	1
1.1 Overviews and general introduction	1
1.2 Proteins in the latex fractions	6
1.2.1 Protein in rubber particle membrane	7
1.2.2 Protein in the C-serum	8
1.2.3 Protein in B serum	9
1.2.4 Protein in the bottom fraction	9
1.2.5 Protein from latex Glove	10
1.2.6 Rubber latex allergen proteins	12
1.3 Mechanisms of allergic reactions	18
1.3.1 Types of Allergy	19
1.3.1.1 <i>Irritant dermatitis</i>	19
1.3.1.2 <i>Delayed cutaneous hypersensitivity (type IV allergy)</i>	19

Contents (Continued)

	Page
1.3.1.3 <i>Immediate reaction (type I allergy)</i>	20
1.4 Quantification of total NRL protein and NRL antigenic proteins	21
1.5 Molecularly imprinted polymers (MIPs)	28
1.5.1 Molecular Recognition of MIPs	31
1.5.2 Polymer composition of MIP	32
1.5.2.1 Monomer	32
1.5.2.2 Crosslinkers	33
1.5.2.3 Porogenic solvents	33
1.5.2.4 Initiators	36
1.5.3 Polymerization conditions	37
1.5.4 Imprint polymerization processes	37
1.5.5 Materials in protein imprinting	40
1.6 Biosensor	43
1.7 Aims and objective of this thesis	45
2. Extraction and characterizations of the natural rubber latex proteins from natural rubber latex and rubber glove	47
2.1 Introduction	47
2.1.1 Sources of template proteins and Hev b related proteins	48
2.1.2 Method	52

Contents (Continued)

	Page
2.1.2.1 Gel electrophoresis	52
2.1.2.2 Mass spectrometry	56
2.2 Objective	62
2.3 Experimental	63
2.3.1 Chemical and Equipment	63
2.4 Methods	66
2.4.1 Natural rubber latex (NRL) and NRL glove samples	66
2.4.2 Preparation of rubber particles, C-serum and bottom fraction	66
2.4.3 Preparation of Hev b2 from bottom fraction membrane (BFM)	67
2.4.4 Preparation of protein from rubber particle (RP) (Hev b1 and Hev b3)	68
2.4.5 Extraction of the proteins from NRL gloves (Hev b1 and Hev b3)	68
2.4.6 Protein purification	70
2.4.7 Sodium dodecyl sulfate polyacrylamide gel electrophoresis (SDS- PAGE)	70
2.4.7.1 Stock solution	71
2.4.7.2 Working solution	71
2.4.8 Western blot analysis	74

Contents (Continued)

	Page
2.4.9 Peptide Mass Mapping of allergen protein (Hev b1, Hev b2 and Hev b3) by MALDI-TOF/MS	75
2.4.10 BCA method	75
2.5 Results and discussion	76
2.5.1 Allergen protein extraction from BFM (Hev b2) and rubber particle (Hev b1 and Hev b3)	77
2.5.2 Extraction of the proteins from NRL gloves (Hev b1 and Hev b3)	80
2.5.3 Determination of allergenicity of the purified proteins	81
2.5.4 Protein purification	85
2.5.5 Yield of extracted protein	90
2.5.6 BCA protein assay	91
2.5.7 Determination of molecular weight of allergen protein by SDS-PAGE	94
2.5.8 MALDI-TOF-MS Spectrometry	97
2.6 Conclusion	111
3 Studies for protein imprinting surface onto a substrate using a polymerizable monomer	112
3.1 Introduction	112
3.2 Objective	114
3.3 Experimental	114

Contents (Continued)

	Page
3.3.1 Chemicals and instruments	114
3.3.2 Preparation of Hev b1 imprinted polymer thin-film	115
3.3.3 Characterizations of MIP and NIP membranes	116
3.3.4 Binding experiment	117
3.4 Results and discussion	118
3.4.1. Preparation of Hev b1-MIP in cellulose and glass membrane	118
3.4.2 Investigation in protocol for protein template removal	125
3.5 Conclusions	127
4 The fabrication of latex protein allergen sensor using Hev b1 molecularly imprinted polymer as a sensor coating on quartz crystal microbalance	128
4.1 Introduction	128
4.1.1 Quartz crystal microbalance transducer	130
4.2 Objective	137
4.3 Experiment	138
4.3.1 Chemicals and materials	138
4.3.2 Equipment	140
4.3.3 QCM sensor	143
4.4 Method	144
4.4.1 Preparation of Hev b1(G)-surface imprinted polymer	144
4.4.2 Protein stamp preparation	145

Contents (Continued)

	Page
4.4.3 Sensor layers	145
4.4.4 AFM measurements	146
4.4.5 Flow Cell Design	148
4.4.6 QCM measurements	149
4.4.7 Binding isotherm	150
4.4.8 Method validation	151
4.4.8.1 Recovery	152
4.4.8.2 Linearity	152
4.4.8.3 The limit of detection (LOD)	153
4.4.8.4 Limit of quantitation (LOQ)	153
4.4.8.5 Precision	154
4.4.9 Quantitative analysis	155
4.4.9.1 Calibration curves	155
4.4.9.2 Standard addition method	156
4.4.10 Real-life analysis to rubber allergen proteins	156
4.5 Results and discussion	157
4.5.1 Protein stamp and imprints	157
4.5.2 Optimization of polymer compositions	162
4.5.3 The investigation of the technological parameters	165

Contents (Continued)

	Page
4.5.3.1 Influence of the background solutions on the sensor response	165
4.5.3.2 Influence of the medium pH on the sensor response	167
4.5.3.3 Influence of the polymerization temperature on the sensor response	169
4.5.4 Binding of template to Hev b1 (G) MIP	171
4.5.5 The effect of matrix on the Hev b1 analyses	174
4.5.6 Specific binding of Hev b1 protein surface-imprinted polymers	176
4.5.7 Method validation	180
4.5.7.1 Determination of percentage recovery of Hev b1 (G)	180
4.5.7.2 Determination of MDL and LOQ	181
4.5.7.3 Determination of precision for Hev b1 assay in MIP sensor	182
4.5.8 QCM assays using Hev b1 (G) surface-imprinted polymer	182
4.6 Conclusions	183
Chapter	
5 Hev b1 surface-molecularly imprinted polymer as a sensitive layer on interdigitated capacitive electrode for detection of rubber latex allergens	186
5.1 Introduction	186
5.1.1 Interdigital capacitors transducer	189

Contents (Continued)

	Page
5.2 Objective	193
5.3 Materials and methods	194
5.3.1 Chemicals and biologicals	194
5.3.2 Fabrication of MIP biosensors	196
5.3.3 Interdigitated capacitance electrode and measurements	197
5.3.4 Method validation	198
5.3.4.1 Recovery	198
5.3.4.2 Linearity	199
5.3.5 Sample and assays	199
5.4 Results and discussion	200
5.4.1 MIP immobilization	200
5.4.2 Sensor coating layer	201
5.4.3 Capacitance characteristics of the immobilization process	203
5.4.4 Optimum content of cross-linker	207
5.4.5 Chemical parameters	210
5.4.6 Capacitance measurements and optimization of the capacitive biosensor	212
5.4.7 Concentration dependence of the biosensors	216

Contents (Continued)

	Page
5.4.8 The selectivity and sensitivity of the Hev 1 (G) MIP layer on the IDC	223
5.4.9 Analytical characteristics	227
5.4.10 Analysis of rubber latex gloves	228
5.5 Conclusions	231
6 Molecularly imprinted a surface polymer as a sensor layer coated onto surface plasmon resonance electrodes	233
6.1 Introduction	233
6.1.1 Surface plasmon resonance (SPR)	236
6.2 Objective	242
6.3 Experimental	242
6.3.1 Chemicals and materials	242
6.3.2 Preparation of SPR sensor chip	243
6.3.3 Scatchard analysis	245
6.4 Results and discussion	245
6.4.1 Morphology of protein imprinting	245
6.4.2 Binding of Hev b1 (G) on surface Plasmon resonance	247
6.4.3 Scatchard analysis	249
6.4.4 The selectivity and sensitivity of the Hev 1 (G) MIP layer on the IDC	254

Contents (Continued)

	Page
6.5 Conclusions	256
7 General discussion and further work	257
7.1 Extraction and purification of rubber latex allergen	257
7.2 Hev b1-molecularly imprinted polymer coated quartz crystal microbalance sensor	258
Future work	262
VITAE	264
REFERENCES	266

List of Tables

	Page
Table 1 Composition of sap tapped from the rubber tree (De Beer <i>et al.</i> , 1999)	3
Table 2 Typical protein distribution in the centrifuged latex fractions	7
Table 3 Natural latex allergens registered at the IUIS (Yeang <i>et al.</i> , 2002)	11
Table 4 Purified allergen protein from NRL and NRL glove sample	93
Table 5 MS analysis data, molecular weight and <i>pI</i> of allergen proteins in NRL and rubber glove samples	100
Table 6 Tryptic peptides assigned to REF after the investigation of the protein originating from band GE1 and sequence coverage of the identified peptides	101
Table 7 Tryptic peptides assigned to rubber elongation factor protein originating from RP1 band after sequence coverage of the identified peptides	103
Table 8 Tryptic peptides assigned to beta-1, 3-glucanase originating from BM band after sequence coverage of the identified peptides	105
Table 9 Tryptic peptides assigned to beta-1, 3-glucanase (Hev b3) originating from RP2 band after sequence coverage of the identified peptides	108
Table 10 Polymer compositions of Hev b1-molecular imprinted polymer	116

List of Tables (Continued)

	Page
Table 11 Polymer compositions for preparing of Hev b1 rubber allergens surface-imprinted polymer	140
Table 12 Statistical values for the comparison between the slope for Hev b1 (G) standard curve and matrix match calibration curve of glove extract using two-way ANOVA of R software (R development Core Team, 2006)	176
Table 13 Percentage recovery of Hev b 1 (G) in glove sample at various spiked concentration	181
Table 14 Equilibrium dissociation constant and maximum number of binding sites value of two classes of binding sites in both imprinting polymers	223
Table 15 Equilibrium dissociation constant (K_d) and maximum number of bindings sites (Q_{max}) value of two classes of binding sites in both imprinting polymers	254

List of Figures

	Page
Figure 1 Chemical structure of cis-1, 4-polyisoprene in Hevea latex	2
Figure 2 Ultracentrifugation of <i>Hevea brasiliensis</i> latex (Gomez an dMoir, 1979)	4
Figure 3 Schematic drawing of the rubber molecule surface (Gomez an dMoir, 1979)	5
Figure 4 Mechanisms of allergic reactions modified from Larche <i>et al.</i> , (2006)	20
Figure 5 Principle of molecular imprinting (Molinelli, 2004)	29
Figure 6 Common functional monomers used in non-covalent molecular imprinting procedures	34
Figure 7 Chemical structure of common cross-linkers used in non-covalent molecular imprinting	35
Figure 8 Chemical structure of common initiator used in non-covalent molecular imprinting	36
Figure 9 The principles of protein identification by MALDI-MS. The protein of interest is digested by an enzyme (e.g. trypsin) and a MALDI-spectrum is recorded. The experimental obtained data are then analyzed against a peptide mass database. This database compiles data from a theoretical digest of already known proteins	58

List of Figures (Continued)

	Page
Figure 10 Matrix-assisted laser desorption ionization (MALDI) and time-of-flight mass analyzer (TOF) (Vicki <i>et al.</i> , 2005)	60
Figure 11 Ultracentrifugation of fresh latex	67
Figure 12 SDS-PAGE of an extract of the fresh natural rubber latex on a 12% acrylamide gel; (A): bottom fraction membrane (BFM) and (B): rubber particle. 1 (A): Protein from B-serum treated with distilled water at 4°C for overnight, 2 (A): Protein from BFM treated with 50mM Tris-HCl pH 7.4 and extracted with 0.2% Triton X-100 at 4°C; 1 (B): Protein from rubber particle extract with 1% SDS and 0.05 Triton X-100 in Tris-HCl, pH 7.4 at 4°C; S: Molecular weight markers	78
Figure 13 SDS-PAGE of an extract of allergen protein on a 12% acrylamide gel; 1 (A): protein from 0.9M NaCl in 200 M phosphate buffer at pH 7.4, 2 (A) : protein from 0.2% Triton X-100 in Tris-HCl, pH 7.4, 1 (B): Protein from 0.5% SDS in Phosphate buffer at pH 7.4, S: Molecular weight markers	81
Figure 14 SDS-PAGE and Western blot of Hevein proteins of the fresh natural latex and latex glove on a 12% gel acrylamide; (A): crude protein from rubber particle, (B): crude protein from BFM and (C): crude	

List of Figures (Continued)

	Page
protein from latex glove. 1(A): Crude protein from rubber particle 2(A): Crude protein from rubber particle incubated with IgE from patient sera, 3(A): Crude protein from rubber particle incubated with IgE from control sera, 1(B): Crude protein from BFM , 2(B): Crude protein from BFM incubated with IgE from patient sera 3(B): crude protein from BFM incubated with IgE from control sera 1(C): crude protein from latex glove, 2(C): crude protein from latex glove after incubating with IgE from patient sera, 3(C): crude protein from latex glove after incubating with IgE from control sera S: molecular weight markers.	83

Figure 15 SDS-PAGE of an extract of the curde and purified allergen proteins from fresh natural rubber latex and latex glove on a 12% acrylamide gel with visualization by Coomassie blue staining. M: Molecular weight marker 1(A): crude protein (14 and 22 kda) from latex glove, 2(A): purified protein (14 kda) from fraction number 30 of latex glove, 1(B): crude protein (14 and 22 kda) rubber particle 2(B): purified protein (22 kda) from fraction number 22 of rubber particle, 3(B): purified protein (14 kda) from fraction number 28 of rubber particle 1(C): curde protein (35 kda and 22 kda) from bottom fraction membrane, 2(C): purified

List of Figures (Continued)

	Page
protein (35 kda) from fraction number 20 of bottom fraction membrane	88
Figure 16 Process of gel filtration (Amersham, 2002)	90
Figure 17 The linear dynamic range of BCA assay using BSA as a protein reference	93
Figure 18 Molecular weight of protein obtained from B-serum by SDS-PAGE	95
Figure 19 Molecular weight of protein obtained from bottom membrane by SDS-PAGE	95
Figure 20 Molecular weight of protein obtained from rubber particle extract by SDS-PAGE	96
Figure 21 Molecular weight of protein obtained from glove extract by SDS-PAGE	96
Figure 22 SDS-PAGE of NRL extraction (A): BFM, (B) glove extract and (C) rubber particle for in-gel digestion	98
Figure 23 MALDI-TOF-MS spectrum of Hev b1 (G) within glove extraction (GE1) obtained by eluting from the gel pieces with methanol solvent and prepared with CHCA	101
Figure 24 MALDI-TOF-MS spectrum of Hev b1 (L) within rubber particle (RP1) obtained by eluting from the gel pieces by methanol solvent and prepared with CHCA	102

List of Figures (Continued)

	Page
Figure 25 MALDI-TOF-MS spectrum of the Hev b2 (L) within bottom membrane obtained from eluting from the gel pieces by methanol solvent and prepared with CHCA	104
Figure 26 MALDI-TOF-MS spectrum of Hev b3 (L) within rubber particle (RP2) obtained by eluting from the gel pieces and prepared with CHCA	107
Figure 27 Illustration of operating procedure in Mascot search algorithm with a probability-based molecular weight searching scoring algorithm for peptide mass fingerprint (Perkins, 1999).	110
Figure 28 The incorporation of surface-molecular imprinted polymer into the polymer matrix onto the substrate	119
Figure 29 Scanning electron microscopy images of bacterial cellulose membrane (A) before and (B) after grafting with a MIP layer	120
Figure 30 CLSM images of the Hev b1-FITC staining on: (A) a grafted MIP and (B) NIP layer on cellulose membrane, (C) MIP and (D) NIP on glass fiber membrane	123
Figure 31 Fluorescent spectram showing the diffences in emission and excitation between FITC (A) and FITC after addition of protein (B)	124
Figure 32 Absorbance spectrum of Hev b1 within a grated MIP layer of cellulose membrane after washing with 0.1% SDS in distilled water after the addition of BCA solution	126

List of Figures (Continued)

	Page
Figure 33 Illustration showing the piezoelectric effect generated of dipoles by deforming force (Bishop et al., 1981)	132
Figure 34 (A) AT-cut of a quartz crystal, (B) Piezoelectric crystal construction and (C) crystal vibrating in thickness shear mode (Suri, 2006 Marx, 2003)	133
Figure 35 The QCM sensor: Quartz crystal is sandwiched between two metal electrodes that are vapor deposited on either side of the crystal. The AC voltage is applied and quartz crystal will oscillate. Analyte molecules will be attached on the coated surface of QCM and the mass of the crystal increases, and therefore the resonance frequency of the quartz crystal changes	134
Figure 36 Schematic illustrating equivalence circuit for a QCM	135
Figure 37 Chemical structures of functional monomers and cross-linking monomers used in this study	139
Figure 38 MCP-Process Series Ismatec peristaltic pump	141
Figure 39 Illustration of an 8712ET RF network analyzer	142
Figure 40 Atomic force microscope apparatus	143
Figure 41 Schematic representation of the mass measurement circuit	144
Figure 42 Schematic for the preparation of the protein surface-imprinted polymer coating on a QCM electrode. A stamp with densely packed rubber	

List of Figures (Continued)

	Page
proteins is pressed into the pre-polymerized coating, templates are removed after polymerization	147
Figure 43 Flow Cell Design	148
Figure 44 Topographic AFM images of poly (MAA-NVP-DHEBA-polymer) layer: (a) Hev b1 (L) and (b) Hev b1 (G) self-assembled on a surface, (c) Hev b1 (L)-MIP, and (d) Hev b1 (G)-MIP coated on a QCM electrode showing regular patterns of latex allergen imprints. Layer heights are 200 nm (spin coated, layer height tested with AFM)	160
Figure 45 Effect of imprinted layer height on the frequency shift of the NIP and Hev b1 (G)-MIP (MAA-NVP-DHEBA-polymer) coated QCM exposed to Hev b1 (G) at a concentration level of 2 mg l^{-1} . Measurements were carried out in 0.1 mM phosphate buffer solution (pH 7.4) at room temperature, using an electrode polymerized at $25 \text{ }^{\circ}\text{C}$	161
Figure 46 Effect of the polymer components for an MIP- or NIP-modified QCM sensor on the frequency shift responses to $500 \text{ } \mu\text{g l}^{-1}$ Hev b1 (G) in phosphate buffer (pH 7.4) at room temperature	164
Figure 47 Effect of the background solution on the frequency responses of the NIP and Hev b1 (G)-MIP (MAA-NVP-DHEBA-polymer) layer coated 10 MHz-QCM using an electrode polymerized at $25 \text{ }^{\circ}\text{C}$. Measurements	

List of Figures (Continued)

	Page
were carried out in 0.1 mM phosphate buffer solution pH 7.4 and at room temperature. Responses were initiated by the addition of 500 $\mu\text{g l}^{-1}$ Hev b1 (G). Each value represents the average of three independent measurements	166
Figure 48 Effect of medium pH on the sensor response using 500 $\mu\text{g l}^{-1}$ of Hev b1 (G) for NIP sensor and MIP sensor using an electrode polymerized at 25 °C. Responses were initiated by the addition of 500 $\mu\text{g l}^{-1}$ Hev b1 (G)	168
Figure 49 Effect of polymerization temperature on the frequency shift response of the NIP sensor and MIP sensor. Responses were initiated by the addition of 500 $\mu\text{g l}^{-1}$ Hev b1	170
Figure 50 Linearized BET adsorption isotherm of Hev b1(G) on MIP at 25°C according to eq 6 (correlation coefficient of linear regression, $R^2 = 0.97$)	172
Figure 51 QCM sensor show the characteristics of NIP, and Hev b1 (G)-MIP coated 10 MHz QCM. Measurements were carried out in 0.1 mM phosphate buffer solution (pH 7.4) at room temperature	173
Figure 52 QCM sensor responses for non-imprinted reference and a Hev b1 (G)-MIP coated electrodes exposed to 10 $\mu\text{g l}^{-1}$ Hev b1 (G) solution. Measurements were carried out in 0.1 mM phosphate buffer solution	

List of Figures (Continued)

	Page
(pH 7.4) at room temperature	174
Figure 53 Calibration curve of Hev b1 either in the absence and presence of the matrix from latex glove sample measurement were performed with with poly-DHEBA-MAA-NVP, (2:6:2, w/w/w) coated on QCM sensor exposed with Hev b1 (G) between 10 to 1000 $\mu\text{g L}^{-1}$ in 0.1 mM phosphate buffer pH 7.4, a: a Hev b1 solution ; b: Hev b1 solution with added matriculate liquid of latex glove.	175
Figure 54 Selectivity profiles of the surface-imprinted polymers for Hev b1 (G) and Hev b1 (L) templates from stopped flow QCM experiments at an analyte concentration level of 500 $\mu\text{g l}^{-1}$ in phosphate buffer (pH 7.4)	178
Figure 55 Illustration of interdigitated electrodes	189
Figure 56 A cross-sectional drawing of interdigitated electrodes realized in the Cu foil on one side of a PCB	191
Figure 57 A cross-sectional drawing of interdigitated electrodes realized in the Cu foil on one side of a PCB where the red lines represent the electric field lines between the electrodes	191
Figure 58 Schematic illustration of the surface imprinting process of a pre-coated IDC microelectrode on the chip; The monomeric	

List of Figures (Continued)

	Page
solutions of the MAA and NVP functional monomers and DHEBA as a crosslinker and the Hev b1 (G) template in phosphate buffer (pH 7.4) is dripped onto the coated transducer surface to produce self-organizing receptor sites on the thin-film surface	195
Figure 59 Contact mode AFM images of: (A) MIP with partially removed template showing the rubber allergens retained in the polymerized material. (B) imprinted layer showing Hev b1 (G) pits on a MAA-NVP-DHEBA polymer after hardening of the layer and washing with distilled water for 24 h. (C) cross-section analyses of the scratch on the imprinted layer and the measured 200 nm layer	202
Figure 60 (a) SEM image of inter-digital capacitor and (b) equivalent circuits used to describe impedance spectra of coated electrodes: R_s electrolyte resistance; R_{ct} charge transfer resistance and C_{dl} is double layer capacitance. (c) Hev b1 (G)-MIP capacitive biosensor fabrication and process. (A) bare electrode; (B) with MIP layer; (C) with Hev b1 (G) binding. Circle = Hev b1 (G); Oval = matrix	205
Figure 61 Bode plot refer to representation of the impedance magnitude (or the real or imaginary components of the impedance) and phase angle as a function of frequency for IDC electrode	

List of Figures (Continued)

	Page
(open symbols) and IDC electrodes coated with an Hev b1 (G)-MIP (filled symbols), exposed to 0.1 mM phosphate buffer solution (pH 7.4) containing Hev b1 (G) at a concentration of 250 ng ml ⁻¹ at room temperature. Impedance = black line; phase degree = dotted line	207
Figure 62 Effect of the amount of cross-linking monomer (DHEBA) on the capacitive responses of the MIP and NIP layer on the IDC microelectrode biosensor exposed to Hev b1 (G) in phosphate buffer solution (pH 7.4) at a concentration of 400 ng ml ⁻¹ . The methacrylic acid and vinylpyrrolidone acted as functional monomers at a mole ratio of 6:2 were used	209
Figure 63 Effect of pH of the medium on the capacitance response upon 400 ng ml ⁻¹ of Hev b1 (G) MIP sensor and reference sensor at 1 kHz and at room temperature. (b) Effect of NaCl on the capacitive shift response of the MIP and NIP copolymer of DHEBA (pH 7.4). responses were initiated by the addition of 250 ng ml ⁻¹ Hev b1 (G)	211
Figure 64 Effect of NaCl on the capacitive shift response of the MIP and NIP copolymer of MAA and NVP at 6:2 mole ratio and 15 mol% DHEBA (pH 7.4). Responses were initiated by the addition of 250 ng ml ⁻¹ Hev b1 (G)	213

List of Figures (Continued)

	Page
Figure 65 A typical sensor response of both a non-imprinted control polymer and Hev b1 (G)-MIP illustrates the effectiveness of rubber allergen adhesion via surface imprinting using solution-based polymerization with Hev b1 (G) proteins (pH 7.4, room temperature and flow rate of 1 ml min ⁻¹)	214
Figure 66 Reproducibility of the response from the Hev b1 (G)-MIP modified electrode to injections of fixed volume of a standard solution of Hev b1 (G) (250 ng ml ⁻¹) with regeneration and reconditioning steps between each individual assay	216
Figure 67 Concentration dependence of the capacitance response to Hev b1 (G) for the imprinted poly(MAA-NVP-DHEBA) coated IDC and the control. Each point represents the average of three independent measurements. A separate regression line has been fitted for the data in each stratum. Those regression lines are the dashed lines in the plot	218
Figure 68 Scatchard plot of the binding of Hev b1 (G) to MIP. Q: bound Hev b1 (G) [Hev b1(G)]:concentration of free Hev b1 (G)	221
Figure 69 Scatchard plot of the binding of Hev b1 (G) to NIP. Q: bound Hev b1 (G) [Hev b1 (G)]:concentration of free Hev b1 (G)	222
Figure 70 The Hev b1 (G) imprinted MAA-NVP-DHEBA copolymer	

List of Figures (Continued)

	Page
on the IDC transducer. The sensor response shows different degrees of enrichment for Hevein latex allergenic proteins tested at an analyte concentration level of 250 ng ml ⁻¹ , room temperature and pH 7	225
Figure 71 The selectivity pattern of Hev b1 (G)-imprinted polymer as obtained by IDC measurements. The proteins Hev b and non-Hev b are detected at a concentration of 250 ng ml ⁻¹ in phosphate buffer (pH 7.4) at room temperature. Each value represents the average of three independent measurements	227
Figure 72 Response of Hev b1 (G)-imprinted polymer layer coated IDC sensors for the rubber latex allergen proteins to Hev b1 (G) from powder-free (G1) and powdered rubber latex gloves (S1, S2, S3) and powdered gloves (S1) spiked with Hev b1 (G) standards, and pure Hev b1 (G) standards. Measurements were carried out in 0.1 mM phosphate buffer solution (pH 7.4) at room temperature and flow rate of 1 ml min ⁻¹ . Each value represents the average of three independent measurements	230
Figure 73 Response of non-imprinted reference polymer layer coated IDC sensors for the rubber latex allergen proteins to Hev b1 (G) from	

List of Figures (Continued)

	Page
powder-free (G1) and powdered rubber latex gloves (S1, S2, S3) and powdered gloves (S1) spiked with Hev b1 (G) standards, and pure Hev b1 (G) standards. Measurements were carried out in 0.1 mM phosphate buffer solution (pH 7.4) at room temperature and flow rate of 1 ml min ⁻¹ . Each value represents the average of three independent measurements	231
Figure 74 Three-layer Kretschmann configuration of SPR	234
Figure 75 Change in permittivity shifts SPR excitation: this phenomenon is analogous to resonant frequency in a mechanical system in that there must be a precise match between the light's frequency and momentum and the characteristics of the gold	237
Figure 76 Depiction of measurable shift in SPR curve	238
Figure 77 Spreeta's multiple SPR interrogation design	239
Figure 78 Internal design of spreeta sensor	241
Figure 79 Spreeta flow cell	243
Figure 80 Self-assembly of protein solution based imprinting coated on gold surface as a sensitive recognition layer of SPR sensor chip	244
Figure 81 Contact mode AFM images: (A) MIP with partially removed template showing the rubber allergens retained in the polymerized material; (B) imprinted layer	246

List of Figures (Continued)

	Page
Figure 82 Schematic diagram depicting a typical surface plasmon resonance (SPR)	248
Figure 83 Concentration dependence of the SPR angle shift to Hev b1 (G) for the specific Hev b1-imprinted polymer coated gold surface SPR chip in 0.1mM phosphate buffer (pH 7.4) at 25°C with a flow rate 0.25 ml min ⁻¹	250
Figure 84 Scatchard plot of the binding of Hev b1 (G) to MIP. Q: bound Hev b1 (G) [Hev b1 (G)]:concentration of free Hev b1 (G)	252
Figure 85 Scatchard plot of the binding of Hev b1 (G) to NIP. Q: bound Hev b1 (G) [Hev b1 (G)]:concentration of free Hev b1 (G)	253
Figure 86 Selectivity test of Hev b1, related Hev b1 and non-related Hev b1 on the Hev b1 (G)-imprinted polymer coated gold surface SPR chip in 0.1mM phosphate buffer (pH 7.4) at 25°C with a flow rate 0.5 ml min ⁻¹	255

LISTS OF ABBREVIATIONS AND SYMBOLS

SYMBOLS OF COMMON TERM

ACM	=	Acrylamide
AIBN	=	Azobisisobutyronitrile
AFM	=	Atomic force microscope
ASTM	=	American Society of Testing Materials
BCA	=	Bicinchoninic acid
BFM	=	Bottom fraction membrane
BSA	=	Bovine serum albumine
CHCA	=	Cyano-4-hydroxycinnamic acid
CLSM	=	Confocal laser scanning microscopy
DAB	=	3,3'-Diaminobenzidine tetrahydrochloride
DHEBA	=	<i>N,N'</i> -(1,2-dihydroxyethylene)bisacrylamide
EDMA	=	Ethylene glycol dimethacrylate
EDTA	=	Ethylene diaminetetracetate
ELISA	=	Enzyme-linked immunosorbent assay
FITC	=	Fluorescein isothiocyanate
FDA	=	Food and Drug Administration
HPLC	=	High performance liquid chromatography
IDC	=	Interdigitate capacitance

ITA	=	Itaconic acid
LEAP	=	Latex ELISA for antigenic protein
LC-MS	=	Liquid chromatography-mass spectrophotometry
MAA	=	Methacrylic acid
MALDI-TOF	=	Matrix-assisted laser desorption ionization and time-of-flight
MBA	=	<i>N,N'</i> -methylene bisacrylamide
MIP	=	Molecularly imprinted polymer
3-MPS	=	3-trimethoxysilylmethacrylate
MSDB	=	Matrix Science Database
MW	=	Molecular weight
NCBI	=	National Center for Biotechnology Information
NIP	=	Non-imprinted polymer
NRL	=	Natural rubber latex
QCM	=	Quartz crystal microbalance
SB	=	Spina bifida
SDS	=	Sodium dodecyl sulfate
SDS-PAGE	=	Sodium dodecyl sulfate-polyacrylamide gel electrophoresis
SEM	=	Scanning electron microscope
SPR	=	Surface plasmon resonance
SY	=	Styrene
TSM	=	Thickness shear mode

CHAPTER 1

INTRODUCTION

1.1 Overviews and general introduction

Natural latex is a well known natural product, already used by Aztec Indians to prepare shoes, bottles, balls and other products. Fresneau described the rubber tree *Hevea brasiliensis* for the first time. Two centuries after its discovery by the Europeans in the 15th century. By the end of the 18th century the development of rubber mastication and the water proofing process made rubber an industrial product. The industrial success of rubber was finalized by Dunlop in 1888.

Natural rubber (*cis*-1,4-polyisoprene) is a vital raw material used in enormous quantities by commercial, medical, transportation and defense industries (Cornish and Siler, 1996; Backhaus, 1998). Even though synthetic rubber has been developed with the help of a modern technology to match with the natural rubber, it cannot replace natural rubber. Therefore natural rubber is preferred over synthetic rubber because of its elasticity, tensile strength, resilience, tackiness and low heat built-up. Compare to the production of synthetic rubber from petroleum, the rubber tree (*Hevea brasiliensis*) has been called “the green rubber factory” (D’Auzac, 1988).

The world supply of natural rubber is produced from *Hevea brasiliensis*, the cultivation of which is confined to the Southeast Asia. In the recent years, the demand for natural rubber has been increasing tremendously and is believed to exceed the expected production from the existing Hevea plantations, resulting in a worldwide shortage of natural rubber (Cornish and Siler, 1996; Backhaus, 1998). Latex is produced in so called laticifers, these are individual cells located directly under the bark of the tree and it is harvested by periodic incision of the bark or tapping (De Fay and Jacob, 1989). The NRL has a high content of polyisoprene; this may either be in the all-cis form (Figure 1) or all-trans (gutta). Rubber latex is a colloidal dispersion which consists of several compounds as shown in Table 1.

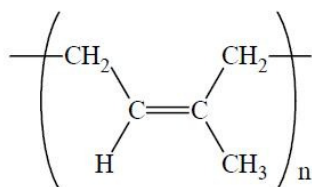


Figure. 1 Chemical structure of cis-1, 4-polyisoprene in Hevea latex

Table 1: Composition of sap tapped from the rubber tree (De Beer *et al.*, 1999)

Content	%
Hydrocarbon	36.0
Protein	1.4
Carbohydrate	1.6
Neutral lipid	1.0
Glycolipid+Phospolipid	0.6
Inorganic substances	0.5
Others	13.9
Water	45.0
Total	100.0

It has long been known that *Hevea* latex contains a large number of non-rubber constituents present in relatively small amounts in natural rubber, as well as rubber particles. Many of these are dissolved in the aqueous serum of latex, while others are adsorbed on the surface of the rubber particles or suspended in the latex. Non-rubber compounds are not only of biological significance with regard to the structure and origin of rubber, but also affect the physical and chemical properties of the latex. The major components of the non-rubber compounds are identified as inorganic salts, amino acids, proteins, inositols and carbohydrates. Detailed microscopic observation of the laticifers in

Hevea brasiliensis shows that latex contained in the cytoplasm, with three main particulate components which are rubber particles, lutoid particles and Frey-Wyssling complex are present in major amounts, in addition to typical components such as nuclei, mitochondria and ribosomes (Dickenson, 1969). As shown in Figure 2, Hevea latex when ultracentrifuged is separated into three fractions: (i) rubber particles in the top layer; (ii) Frey-Wyssling particles and the clear serum in the yellow layer; and (iii) the predominant the lutoid in the bottom layer.

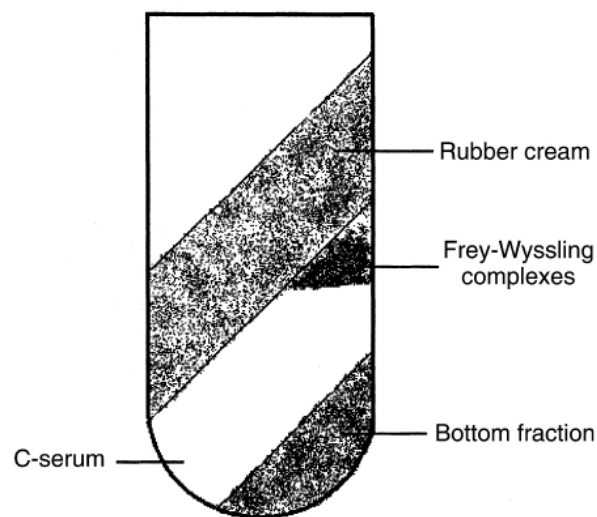


Figure 2. Sedimentation profile of *Hevea brasiliensis* latex after ultracentrifugation (Gomez and Moir, 1979)

The rubber particles, which constitute 25 - 45% of the volume of the fresh Hevea latex range in diameter from 0.5 to 3 μm (Gomez and Moir, 1979). The particles are usually spherical, but the larger ones in latex from mature trees are often pear-shaped

(Schoon and van der Bie, 1955; Dickenson, 1963). The hydrophobic rubber molecules are protected from the hydrophilic medium by a complex film of proteins and lipids (Ho *et al.*, 1975).

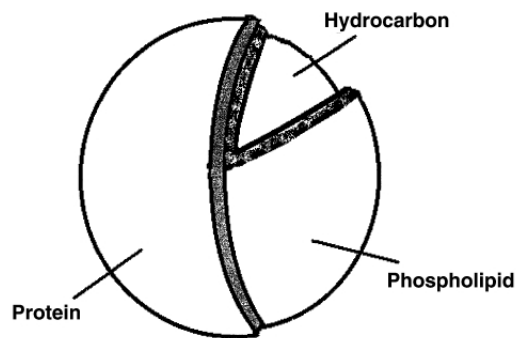


Figure 3. Schematic drawing of the rubber molecule surface (Gomez and Moir, 1979)

As illustrated in Figure 3, the rubber particles comprise a sphere consisting of rubber, and are surrounded by spherical shells inside which contained phospholipids and proteins (Gomez and Moir, 1979). Triglycerides, sterols, sterol esters, tocotrienols and other lipids also are combined with rubber particles. The fresh Hevea rubber particles have isoelectric points ranging from pH 4.0 to 4.6, depending on the clone, indicating that the relative proportions of the adsorbed proteins are clonal characteristic (Bowler, 1953).

1.2 Proteins in the latex fractions

Latex proteins are found in the latex sera and are also associated with latex organelles that can be separated by ultracentrifugation at 53,000g (Moir, 1959). About 70% of latex proteins are soluble, with the remaining being associated with membranes. There are basically three main fractions that are easily discerned such as rubber phase, the C-serum, and the bottom fraction (Cook and Sekhar, 1953). The rubber phase comprises the rubber particles that are packed centripetally by centrifugation. With the C-serum in the interstices between rubber particles removed, two main proteins are extractable from the surface of the rubber particles. Whereas most of the C-serum and B-serum proteins are water-soluble, those of the rubber particles are generally insoluble. About 11 mg of proteins is bound to each gram of rubber. A typical distribution of proteins in the rubber particles, the C-serum, the B-serum, and the lutoid membranes is shown in Table 2.

Table 2. Typical protein distribution in the centrifuged latex fractions

Latex fraction	Protein concentration (mg/ml latex)	%
Rubber particle membranes	3.5	25
C-serum	6.0	43
B-serum	3.6	26
Bottom fraction membranes	0.9	6
Total	14.0	100

1.2.1 Protein in rubber particle membrane

The rubber particles are believed to be covered by some proteins and phospholipids, concerning with the colloidal stability of natural rubber latex. Phospholipids are strongly adsorbed to the surfaces of the rubber particles, and believed to be intermediate by which the proteins are anchored on the rubber particles. This phospholipid protein layer imparted a net negative charge to the rubber particle, thereby contributing to the colloidal stability of these particles (Bowler, 1953). The major protein on the rubber surface has been shown to be negatively charged of 14.6 kDa protein (Hev b1). This protein is water insoluble protein and mainly on large rubber particles (>350 nm in diameter) which is involved in rubber biosynthesis (Czuppon *et al.*, 1993).

1.2.2 Protein in the C-serum.

The C-serum refers to the aqueous medium in which all the latex organelles are suspended. Being the cytoplasm of the laticifer, latex C-serum contains a large variety of proteins associated with cellular metabolism, as might be expected. For example, all the enzymes of the respiratory pathway are present. Various enzymes specific to latex, such as the enzymes associated with the rubber biosynthesis pathway, are also found in the latex C-serum. A typical sample of C-serum contains about 12 mg proteins per milliliter. The first protein to be isolated from Hevea latex was from C-serum. It was named α -globulin by (Archer and Cockbain, 1955). This protein is the major protein component of C-serum. It is readily adsorbed at a water-air or oil-water interface with a resulting fall in the interfacial tension. This led to the suggestion that α -globulin was one of the proteins on the surface of rubber particles and that it contributed to the colloidal stability of fresh latex. Moreover, Tata and Moir (1964) reported the presence of twenty-two protein bands in C-serum by starch gel electrophoresis. Seventeen of these were anionic at pH 8.2 whilst five were cationic and existed much concentration. A comparative study on the protein in the C-serum from four clones viz PRIM 501 revealed very little difference between their general electrophoretic patterns. There was also no significant difference in the proteins with seasonal variation within a single clone (Tata and Moir, 1964).

1.2.3 Protein in B serum

The B-serum is commonly thought of as the luteoidic serum, it also contains minute constituents derived from the other minor organelles deposited in the bottom fraction. The latex B-serum is obtained by repeated freezing and thawing of the bottom fraction of centrifuged latex. B-Serum contains about 24 mg proteins per milliliter (Hsia, 1958). Compared with the C-serum, there are a smaller number of proteins (fewer than 20 major peptides), with a single protein, hevein, making up 50–70% of the total B-serum soluble proteins (Archer *et al.*, 1969). Whereas the rubber particle proteins and practically all the C-serum proteins are generally acidic proteins, B-serum has a mixture of acidic and basic proteins (Moir and Tata, 1960).

1.2.4 Protein in the bottom fraction

Proteins in the bottom fraction are essentially studied as the soluble proteins in B-serum. These have been examined with various techniques, including starch gel electrophoresis and polyacrylamide gel electrophoresis (Tata, 1975; Yeang *et al.*, 1977). According to the techniques used, the proteins of B-serum were found to be marked different from those C-serum (Archer, *et al.*, 1969). The major protein in B-serum is hevein, which accounts for about 70% of the water soluble proteins in the bottom fraction. Hevein is a low molecular weight anionic protein (5 kDa) with a higher (5%) sulphur content (Archer and Cockbain, 1960 and Tata, 1976). All the sulphur in

hevein exists as eight disulphide (S-S) bridge of cysteine. It contained 43 amino acid residues in a single polypeptide chain with glutamic acid at the N-terminus. Because of its low molecular weight and number of S-S bridge, hevein is heat stable. Moreover, the presence of basic proteins in B-serum was first demonstrated when B-serum or an aqueous extract of freeze-dried bottom fraction was carried out by 12% gel of sodium dodecyl sulfate polyacrylamide gel electrophoresis denaturation (Tata and Edwin, 1970). In addition, the proteins were also shown to have lysozyme and chitinase activities (Tata *et al.*, 1983).

1.2.5 Protein from latex Glove

To date, thirteen NRL proteins, Hev b 1 to Hev b 13 are recognized by the International Union of Immunological Societies (IUIS) as the causal agents of NRL allergy (Table 3).

Table 3. Natural latex allergens registered at the IUIS (Yeang *et al.*, 2002)

Latex Allergen	Molecular Mass	Protein name	Significance as latex allergen
Hev b1	14.6	Rubber elongation factor (REF)	High
Hev b2	34-36	β -1,3-glucanase	Medium
Hev b3	24-27	Small rubber particle protein	High
Hev b4	50-57	Beta-glucosidase (microhelix compound)	ND
Hev b5	16-24	Acidic structure protein	High
Hev b6.01	20	Prohevein (hevein precursor)	High
Hev b6.02	4.7	Hevein	High
Hev b6.03	14	C-domaine of prohevein	High
Hev b7.01	42	Patatin-like protein (esterase) from latex B-serum	Low
Hev b7.02	44	Patatin-like protein (esterase) from latex C-serum	Medium
Hev b8	14	Profilin (actin-binding protein)	Low
Hev b9	51	Enolase	Low
Hev b10	26	Manganese superoxide dismutase (MnSOD)	Low
Hev b11	32	Class I chitinase	Low
Hev b12	9	Lipid transfer protein	Low
Hev b13	42	Esterase	High

ND= non detectable

1.2.6 Rubber latex allergen proteins

Hev b1 (rubber elongation factor) is a very hydrophobic protein with length of 137 amino acid residues and a molecular mass of 14.6 kDa that tetramerizes with a molecular mass of about 58 kDa in native form. Amino acid residue like cysteine, methionine, histidine, and tryptophan are completely absent. The N-terminus of Hev b1 includes a cluster of acidic amino acid residues and is acetylated. This protein is tightly bound to rubber particles but can be solubilized by detergents. Hev b1 was the first NRL allergen characterized at the molecular level and was suggested to be the major allergen in NRL and the only allergen present in one latex surgical glove (Czuppon *et al.*, 1993). This protein is characterized, cloned, and sequenced, and both B cell and T cell epitopes have been identified which they found that the main epitope areas are localized in the carboxy-terminal part of Hev b1 and in a region between amino acid residues 31-64. The clinical relevance of Hev b1 has been demonstrated by the high prevalence of IgE antibodies among *spina bifida* (SB) patients with latex allergy. Studies showed that Hev b1 represented a target for IgE antibodies of up to 80% of SP patients sensitized to latex (Yeang, 1977 and Ylitalo *et al.*, 1998). The prevalence of the presence of Hev b1-specific IgE antibodies in latex sensitized healthcare workers (HCWs) was reported to be between 18 and 49% by using different serum samples and test methods (Akasawa, 1995 and Alenius *et al.*, 1996). Hev b1, eluted from latex glove may also occur in other molecular masses such as 8, 14, and 42 kDa (Chen *et al.*, 1997).

Hev b2 (β -1,3-glucanase) is a basic protein with a *pI* of about 9.5 which precipitates out when the protein solution is diluted or dialyzed. The allergen therefore resists being washed away with water during the manufacture of latex gloves, but subsequently dissolves in the sweat of the glove user (Sunderasan *et al.*, 1995). The molecular mass of this protein appears to be 34–36 kDa from B-serum isolated from fresh latex by SDS polyacrylamide gel electrophoresis. Hev b2 showed binding to IgE from sera of patients with latex allergy. Both patients with SB and HCWs with latex allergy showed strong IgE-binding reactivity to the native Hev b2 (Sunderasan *et al.*, 1996 and Kurup *et al.*, 2000). Depending on the methods used, the reactivity varied from 20% to 61% in patients with latex allergy. However, only 2 of 29 patients showed skin prick test (SPT) reactivity to Hev b2 (Yip *et al.*, 2000).

Hev b3 is a small rubber particle protein of molecular mass between 22-23 kDa when was identified using mass spectrometry analyses (Yeang *et al.*, 1998). Hev b3 shares 47% sequence identity with Hev b1 on the amino acid level (Wagner, 1999). The proteins also possess structural similarity, consequently leading to IgE cross-reactivity. When only the matching regions of the paired proteins are considered, amino acid identity is increase to 72% between Hev b1 and Hev b3. In immunoblotting, 83% of NRL allergic patient with SB revealed IgE binding to Hev b3. These findings suggest that Hev b3 is a highly important allergen for SB patients. Hev b1 and 3 have increased reactivity in SB patients in comparison to HCW, suggesting the potential for genetic factors or route of exposure to influence the IgE response to latex.

Hev b4 is a glycoprotein, which is known as the microhelix comprised a triplet of allergenic peptides of molecular mass 50-57 kDa when separated electrophoretically under reducing conditions. In its unreduced form, a band of about 100 kDa was discernible. Hev b4 might have related biochemical functions in the latex and may be components of a protein complex. A lecithinase homolog is the major protein component of Hev b4, a latex allergen that is reactive in skin prick tests. The IgE epitopes of the Hev b4 major protein reside in its carbohydrate moiety that is responsible for the discrepancy between observed and calculated molecular weights (Sunderasan *et al.*, 2005).

Hev b5 is a 163 amino acid protein that is one of the most acidic proteins in the laticifer cells of the rubber tree, and is exceptionally rich in glutamic acid. Hev b5 has been isolated from ammoniated latex and from heat-treated latex and glove extracts. Hev b5 is a major latex allergen as indicated by its strong IgE binding with IgE from sera of both HCWs and patients with SB. 92% of HCWs showed reactivity to Hev b 5, and 56% of patients with SB showed specific IgE binding. Sixty-two percent of HCWs who were skin tested with Hev b5 had a positive response (Beezhold *et al.*, 1994).

Hev b6.01 (prohevein), Hev b6.02 (hevein) and Hev b6.03 (prohevein C-domain) were found to be predominant protein in NRL and heat stable which they have also been suggested to be involved in the coagulation of rubber. Alenius and coworkers (1995) reported that 69% of NRL allergic patients had IgE antibodies of purified prohevein, whereas 21% of these patients had IgE against the purified prohevein C-domain. Moreover, 56% of 45 NRL allergic patient sera showed IgE antibodies to

purified N-terminal hevein domain (Alenius *et al.*, 1995). In the study of Chen and coworker reported that the skin prick test showed a positive reaction to purified hevein in 81% of patients with NRL allergy. All the available data indicate that prohevein and its N-terminal hevein domain are major NRL allergens (Chen *et al.*, 1996).

Hev b7 was identified as a 43-kDa protein with structural homology to a potato protein called patatin. Patatins are storage proteins but also have phospholipase activities and defense functions in plants. The protein has been cloned and characterized (Kostyal *et al.*, 1998; Sowka *et al.*, 1998) and multiple isoforms have been identified with similar IgE reactivities. Hev b 7 showed IgE-binding reactivity in 23% of HCWs with latex allergy. Both patients with spina bifida and HCWs with latex allergy reacted to this allergen and SPT reactivity was demonstrated in 41% of HCWs (Kurup *et al.*, 2000).

Hev b8 (profilin) is a member of a group of plant allergens cause cross-reactivity between pollen and food of plant origin. Hevea profilin was first shown to be allergenic by IgE inhibition assays. Native Hevea profilins that separated as peptides of 10.2, 14.2, and 15.7 kDa were described by Nieto and coworker (1998). Profilin expressed in Hevea latex has a predicted molecular weight of 14.0 kDa and a *pI* of 4.9 and has been shown in a study to be allergenic to latex-allergic patients who were also sensitized to pollen or plant food (Ganglberger *et al.*, 2001). The purified latex profilin, when used in skin prick testing, showed positive reactions in all 24 patients with SB and latex allergy but in only 6 of 17 HCWs with latex allergy (Fuchs *et al.*, 1997 and Nieto *et al.*, 1998).

Hev b9 is a minor latex allergen in NRL C-serum. Recently, the cloning of a 1651 bp cDNA encoding a protein of 445 amino acids (47.6 kD; pI 5.6) from *Hevea* latex was described. Sixteen out of 110 NRL allergic patients (14.5%) showed IgE binding to rHev b9, suggesting that Hev b9 is a minor NRL allergen. Latex enolase has 72% overall amino acid sequence identity with human enolase. IgE from patients sensitized to enolases of the molds *Cladosporium herbarum* and *Alternaria alternata* cross-react with Hev b9. Comparisons of protein sequences show that *Hevea* enolase displays about 60% sequence identity with the mold enolases. Its active enzyme catalytic site is well conserved (Wagner *et al.*, 2000).

Hev b10 is manganese superoxide dismutase: MnSOD consisting of 206 amino acid residues and was cloned and expressed in *Escherichia coli* (Wagner *et al.*, 2001). In 1997, Yosof and Abdullah purified native Hev b10 from the latex B-serum and estimated its molecular mass about 45 kDa when was separated on SDS-polyacrylamide gel. In immunoblotting both NRL as well as *Aspergillus fumigatus* allergic patients revealed IgE binding to rHev b10. Cross reactivity to Asp f 6, the MnSOD from *A. fumigatus*, and human MnSOD was determined by inhibition of IgE binding to these MnSODs by rHev b10. Hev b10 is a new cross-reactive allergen of *H. brasiliensis* which belongs to the “latex mould” group of latex allergens.

Hev b11 (class I chitinase) is a type I chitinase of NRL. It has a molecular size of 33 kDa and an isoelectric point of 5.1 (Martin, 1991). Chitinases and lysozymes constitute about 25% of the proteins in the lutoid fraction of rubber latex (B-serum). The class I chitinases share homology with N-terminal hevein domain and probably also share

epitopes with similar allergens from avocado and banana. Although Hev b 11 is considered a minor allergen in latex allergy, detailed cross-reactivity with other allergens and its immune responses and allergy effect are not known (Akasawa *et al.*, 1996).

Hev b12 (lipid transfer protein, LTP) was cloned from *Hevea brasiliensis* RNA and produced as a recombinant protein by Beezhold and coworker (2003). The DNA sequence predicts a mature Hev b 12 protein of 9.3 kDa with an isoelectric point of 10.8. A 24 amino acid signal peptide precedes the amino acid sequence of the mature protein, but not yet know in vacuole targeting sequence at the C-terminus (that might suggest a lutoid protein) has been identified. Immunoblots of the recombinant protein demonstrated Hev b 12-specific IgE in the sera of nine out of 37 latex allergic individuals (24%). The reactivity of IgE from latex-allergic patients to Hev b 12 occurred under reducing conditions of the protein, but fruit LTP-allergic sera reacted only with the non-reduced form of Hev b 12. Configuration in the molecule might therefore play a role in IgE recognition (Beezhold *et al.*, 2003).

Hev b13 (lipolytic esterase) is a highly allergenic 42–46 kDa protein in *Hevea brasiliensis* latex appeared to have been resolved with the discovery of a 43 kDa allergenic latex protein that was a homologue to patatin. However, the low to moderate prevalence of sensitization to the protein, Hev b13, is a glycoprotein isolated from Hevea latex (Arif *et al.*, 2002). The allergenicity of Hev b13 has been assessed by various approaches. IgE reactivity was 61% by IgE-dot blot and 78% by IgE-enzyme-linked immunosorbent assay (Yeang *et al.*, 2000 and Bernstein *et al.*, 2003).

1.3 Mechanisms of allergic reactions

The first phase of an allergic reaction is called the sensitization phase, in which contact with allergens leads to the activation of antigen presenting cells and subsequent generation of allergen specific effector and memory T-cells (Kay 2001, Janeway, *et al.*, 2005; Larche *et al.*, 2006). A subpopulation of specific T-cells facilitates B-cell activation and this in turn leads to the production of allergen-specific IgE and IgG antibodies (see Figure 4A). IgE antibodies binding to IgE receptors on mast cells in the tissue and on basophils in the circulation. In the elicitation phase, cross-linking of cell-bound IgE by allergens induces the release of bioactive mediators which elicits the appearance of the immediate allergic symptoms (Figure 4B). Secretion of inflammatory mediators from IgE-activate mast cells also results in recruitment of allergen specific T-cells into the inflammation site. Allergen activated T-cells proliferate and secrete a variety of inflammatory mediators which attract other leukocytes, e.g. eosinophils, to the inflammatory. The coordinated action different leukocytes results in the clinical features that are characteristic of late phase reaction as shown in Figure 4C. Although innate immunity also plays an important role in the sensitization and elicitation phases, as well as in the regulation of allergic responses.

1.3.1 Types of Allergy

Allergy to the NRL allergen protein is an immunologic reaction that can be classified into three types of allergic responses.

1.3.1.1 *Irritant dermatitis*

A skin irritation that does not involve the body's immune response. Although it is not an allergic reaction, irritant hand dermatitis can cause breaks in the skin allowing easier entry of the sensitizing latex protein or glove chemicals, leading to latex allergy.

1.3.1.2 *Delayed cutaneous hypersensitivity (type IV allergy)*

A contact dermatitis due to the chemicals used in latex glove mediated via T-cells. The skin reaction is seen 6-48 hours after contact. The reaction is limited to the local area of skin that has contacted the glove. This is not life threatening but those with type IV allergy will be at increased risk to develop type I allergy.

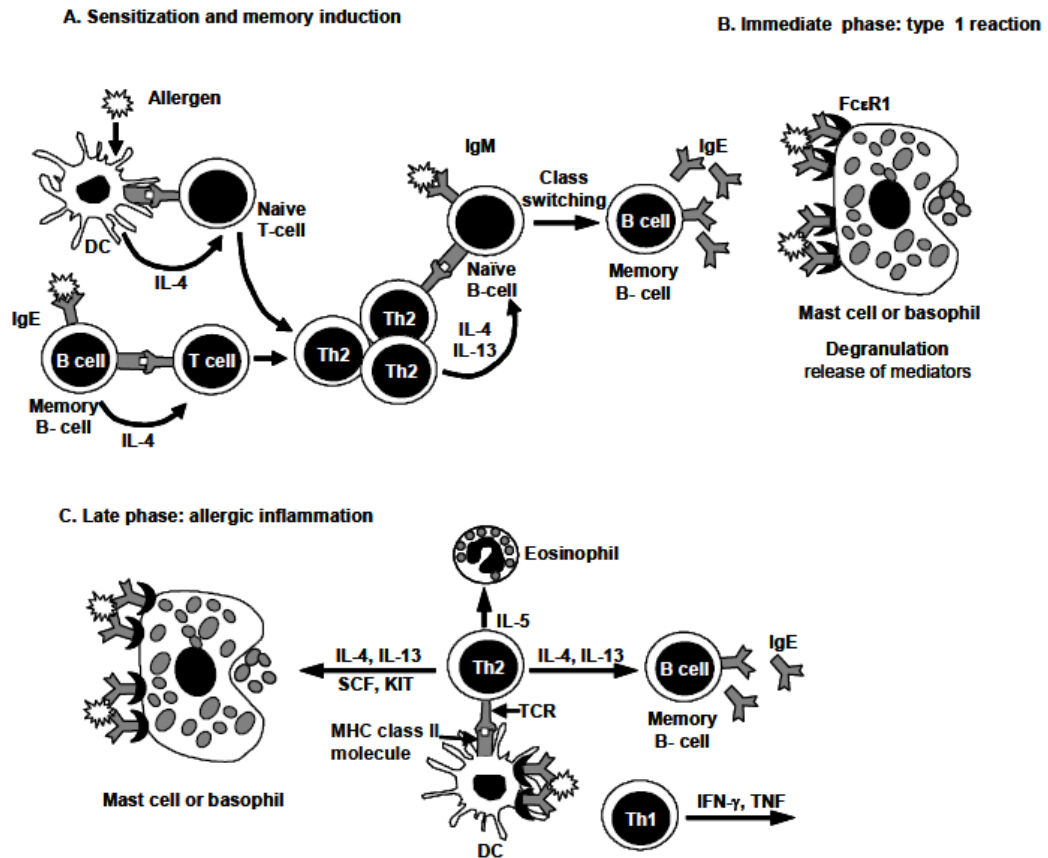


Figure 4. Mechanisms of allergic reactions modified from Larche *et al.*, (2006)

1.3.1.3 Immediate reaction (type I allergy)

These are systemic allergic reactions caused by circulating IgE antibodies to the proteins in natural latex. The reactions vary from contact urticaria to systemic anaphylaxis and laryngeal edema. Systemic allergic symptoms can include itching eyes, swelling of lips or tongue, breathlessness, dizziness, abdominal pain,

nausea, hypotension, shock and potentially death. Symptoms occur soon after exposure to the latex (within about 30 minutes). This results from binding of the latex allergen to sensitised receptors on mast cells. The routes of exposure are cutaneous, mucosal, parenteral, and aerosol (from inhaling latex glove powder). No immunotherapy or desensitization currently exists for latex allergy. Each systemic reaction occurs with less provocation and presentation of a greater magnitude. Unlike natural latex, synthetic rubber does not produce type I allergy (anaphylaxis). Hence these gloves are preferred in people with known type I hypersensitivity or type IV allergy (contact dermatitis). However, this is the feasibility of occurrence a serious type IV allergic reaction to a synthetic rubber. Synthetic rubber used in latex paint and rubber-stopped vials, are not a risk to latex-sensitive individuals.

1.4 Quantification of total NRL protein and NRL antigenic proteins

NRL allergy results from extended and repeated exposure to NRL proteins. The dose, the duration, and the route of exposure are the determining factors for allergic system of rubber latex proteins (Bernardini *et al.*, 1998; Levy *et al.*, 1999). From the Food and Drug Administration's perspective, the safety and effectiveness of regulated medical devices are the main concerns. The available data clearly support the fact that NRL medical gloves are effective products, providing an excellent infection barrier. The problem of allergic reaction to NRL proteins has raised concerns regarding the safety of NRL gloves. Reducing the overall protein levels of NRL in medical devices

was an initial approach, but to ensure safety, it is essential to identify and protect sensitized individuals and to prevent or minimize further sensitization by controlling exposure to allergenic proteins. This cannot be accomplished without adequate diagnostic tests and reliable methods for allergen quantitation. Although ongoing research is directed toward quantitation of biologically relevant proteins in NRL, no standard allergen test has been developed.

Many quantitative methods for measurement of total NRL protein which was premise that the total level of protein is proportional to the level of potential allergens have been developed (Tomazic-Jezic *et al.*, 2002). The Biuret method depends on the reaction of compounds containing several peptide bonds with Cu^{2+} under alkaline conditions to form a violet-coloured species. This method is relatively insensitive to amino acid composition since it relies on reaction with peptide bonds; it is however a very insensitive technique and reagents such as NH_4^+ , Tris and Good's buffers interfere with the reaction (Pingoud, *et al.*, 2002; Itzhaki, 1964). The sensitivity of the Biuret method, which is in the mg range, can be increased by a factor of about 100 by the addition of Folin-Ciocalteu reagent which is the basis of the celebrated Lowry assay (Lowry *et al.*, 1951). This method has been introduced by modification of the biuret reaction to give a more sensitive determination of protein. Two color reactions are used: the biuret reaction with alkaline copper (II) and the reaction of a complex salt of phosphomolybdotungstate, called the Folin-Ciocalteu phenol reagent, which gives an intense blue-green color with the biuret complexes of tyrosine and tryptophan. The clear advantage of the Lowry method over Biuret is its much higher sensitivity. However, the

disadvantages of this method are that it takes longer, the coloration is unstable, it depends on the tyrosine and tryptophan content, and mercapto-compounds interfere with the assay (Robyt, 1987). Alternative method has been introduced and very popular that is the bicinchoninic acid assay (BCA) (Smith *et al.*, 1985). This relies on the production of Cu^{2+} which in this case is converted into a violet-coloured substance by reaction with bicinchonate. The method has comparable sensitivity to the Lowry method, but is easier and less subject to interference. The BCA assay has the advantage of being insensitive to detergents such as Triton-X100 and SDS (1%).

Next the method is Bradford assay, which this method depends on the binding of the dye Coomassie brilliant blue G-250 to proteins under acid conditions which that causes a shift in the absorption maximum from 465 nm to 595 nm (Bradford, 1976). This assay can be used to measure protein concentration in the μg range. The colour reaction is dependent on the content of basic amino acids, particularly arginine, and of aromatic amino acid residues. The advantages of this method are relatively insensitive to interferences from reagents that are commonly found in protein solution. In additionally, UV spectroscopy can be used for measured of the protein that proteins contain chromophoric residues that absorb in the near and far UV (Manchester, 1996). The advantage of this method is that it does not destroy the protein, however the procedure is not very sensitive in the near-UV (280 nm), and is very subject to interference in the far-UV (205 nm); furthermore, exact determination of concentrations from near-UV data do require knowledge of the amino acid composition. All mentioned method, the Modified Lowry method, a chemical assay that measures all proteins,

became the American Society for Testing Materials (ASTM) standard (D5712) in 1995. It was the first standardized and validated method with great utility for screening NRL products.

The Food and Drug Administration could issue a recommendation that manufacturers may state a total protein level on their products as a guide for users in product selection (FDA, 1996). As manufacturers successfully decreased the protein levels in NRL products, the assay was not sufficiently sensitive to accurately quantitate the remaining proteins. However, NRL proteins even below the detection level could induce a positive skin reaction. Furthermore, the Lowry assay is prone to the interference of chemical additives in NRL products and also includes in the measurement other proteins, which may have been added during the manufacturing process. These factors are probably responsible for the generally poor correlation of the Lowry method with the biologically active protein content of the product.

The latex ELISA for antigenic proteins (LEAP) test, designed by Guthrie Research Institute. It has a greater sensitivity than the Modified Lowry standard test and is available as a kit. However, the test formats require binding of unknown protein samples to the assay plate, to which rabbit anti-NRL serum is then applied. The protein binding to the plate depends on the overall concentration and the molecular weight of individual proteins. Two other tests used in research laboratories, the RAST inhibition and the ELISA inhibition test, have avoided this problem by applying a different format. The measurement of antigenic protein levels in both tests is based on the capacity of rabbit anti-NRL serum to react with the NRL protein sample. A test protein is exposed to

anti-NRL serum in a separate inhibition step. After the antigen-antibody reaction is completed, the unbound antibodies are exposed to the reference antigen, and the percent of serum inhibition represents the amount of protein in the test sample. The reference antigen is a defined source of NRL protein, which is either passively attached to the assay plates or covalently bound to a solid phase. The inhibition format is both sensitive and reproducible. In addition, this format can be easily used for the quantitation of antigenic proteins with rabbit anti-NRL serum and the quantitation of specific NRL allergenic proteins with human anti-NRL serum. However, neither of these methods can be developed into a standard allergen assay because the potency and specificity of human anti NRL IgE antibodies cannot be standardized as a reference antiserum.

For characterization and identification the molecular mass of protein, sodium dodecyl sulfate (SDS) polyacrylamide gel electrophoresis (PAGE) and LC-MS have been applied. SDS-PAGE is the most widely used method for qualitatively analyzing protein mixtures. It is particularly useful for monitoring protein purification, and because the method is based on the separation of proteins according to size, the method can also be used to determine the relative molecular mass of proteins. Because the principle of this technique is the separation of proteins based on size differences, by running calibration proteins of known molecular weight on the same gel run as your known protein, the molecular weight of the unknown protein can be determined. For most proteins a plot of \log_{10} molecular mass vs relative mobility provides a straight line graph, although one must be aware that for any given gel concentration this relationship is only linear over a limited range of molecular mass. An approximate guide, using the

system described here, the linear relationship is true over the following ranges: 15% acrylamide, 10,000-50,000; 10% acrylamide 15,000-70,000; 5% acrylamide 60,000-200,000. It should be stressed that this relationship only holds true for proteins that bind SDS in a constant weight ratio. Two-dimensional polyacrylamide gel electrophoresis (2-DE) provides not only the ability to resolve and quantify thousands of proteins, but it also gives those in research and industry the ability to monitor in-process protein purification, quickly and easily. Two-dimensional polyacrylamide gel electrophoresis (2-DE) is also used to identify variability in protein expression in a variety of cell lines. It is known that many parameters and laboratory conditions can influence the resolution of proteins on 2-DE, such as the pH range of carrier ampholytes used, the quality of reagent and equipment used, temperature, voltage, and the skill of the operators.

Liquid chromatography-mass spectrophotometry (LC-MS) also has been used for identification and characterization of proteins. A mass spectrometer is a device that determines the molecular weight of a compound by separating out molecular ions of the compound according to their mass-to-charge ratio (m/z). Mass spectrometry is the method of choice if one requires a highly accurate molecular mass. This technique allows protein molecular weights to be routinely measured with an accuracy of <0.01% which corresponds to < 5 Da for a 50,000 kDa protein (c.f. an accuracy of 500–1,000 Da for SDS-PAGE). A mass spectrometer consists of three fundamental parts: the ionization source, the analyzer, and the detector. The protein sample is introduced into the ionization source which induces ionization of the protein molecules. The ionized molecules are then extracted into the analyzer region of the instrument, which separates

the ions on the basis of their m/z . The separated ions are then sent to the detector where the signal is detected and recorded. Mass spectrometers are usually classified according to their ionization source, but they may also vary in the types of analyzers and detectors employed. Two different types of ionization are normally employed for protein studies: electrospray ionization (ESI) and matrix-assisted laser desorption ionization (MALDI). Electrospray ionization mass spectrometry (ESI-MS) has had a profound influence on biological research over the last decade. With this technique it is possible to generate and characterize gas-phase analyte ions from aqueous solutions of proteins, peptides, and other classes of biomolecules, ESI is performed at atmospheric pressure, which simplifies sample preparation and handling and allows on-line coupling of chromatography, such as capillary high-performance liquid chromatography (HPLC), to mass spectrometers (LC-MS). The use of ESI in combination with tandem mass spectrometry (MS/MS) provides the capability for amino acid sequencing of peptides. The optimization and miniaturization of peptide sample preparation method for ESI as well as the development of highly sensitive tandem mass spectrometers, such as triple quadrupoles, ion traps, and quadrupole-time-of-flight (Q-TOF) hybrid instrument, makes it possible and almost routine to obtain amino acid sequences from subpicomole levels of protein in many laboratories. Peptide sequencing is typically performed by nonoelectrospray MS/MS analysis of crude, concentrated peptide mixtures or by hyphenated techniques, such as capillary HPLC coupled to micro/nanoelectrospray-MS/MS. The sets of peptide tandem mass spectra generated in such experiments are used to query biological sequence databases with the aim to identify all protein components present in the sample.

1.5 Molecularly imprinted polymers (MIPs)

Molecularly imprinted polymers (MIPs) are a synthetic crosslinking polymer contains of recognition site of imprinted cavities. MIPs were prepared by cross-linking copolymerization of appropriate functional monomer with crosslinker in the presence of template molecule in appropriate porogen solvent. After template removal the recognition site within the polymer matrix is formed which thus are complementary to the analyte molecule in the shape and positioning of functional groups. Essentially, two kinds of molecular imprinting strategies have been established based on covalent bonds or non-covalent interactions between the template and functional monomers (Figure 5). In both cases, the functional monomers, chosen so as to allow interactions with the functional groups of the imprinted molecule which monomer mixtures are polymerized in the presence of the imprinted molecule. The special binding sites are formed by covalent or, more commonly, non-covalent interaction between the functional group of imprint template and the monomer, followed by a crosslinked co-polymerization (Takeda, 2005). Non-covalent approach has been used more extensively due to follow three reasons:

- (1) Non-covalent protocol is easily conducted, avoiding the tedious synthesis of prepolymerization complex.
- (2) Removal of the template is generally much easier, usually accomplished by continuous extraction.

(3) A greater variety of functionality can be introduced into the MIP binding site using non-covalent methods.

Non-covalent approach is the most frequently used method to prepare MIP due to its simplicity. During the non-covalent approach, the special binding sites are formed by the self-assembly between the template and monomer, followed by a crosslinked copolymerization (Svenson, 2004 and Ekberg, 1989). The imprint molecules interact, during both the imprinting procedure and the rebinding, with the polymer via non-covalent interactions, e.g. ionic, hydrophobic and hydrogen bonding. The non-covalent imprinting approach seems to hold more potential for the future of molecular imprinting due to the vast number of compounds, including biological compounds which are capable of non-covalent interactions with functional monomers (Michael, 1995 and Sellergren, 1993).

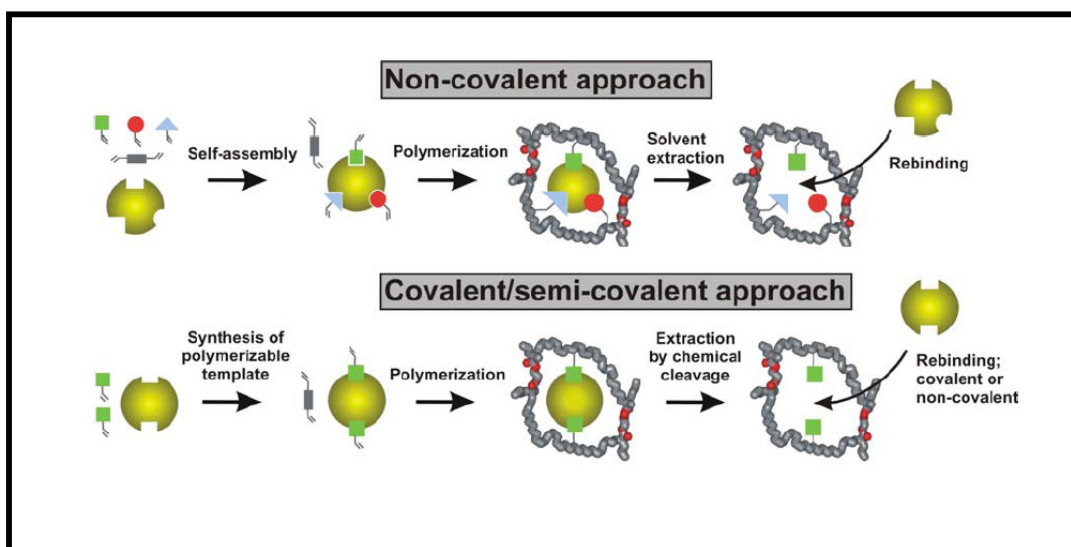


Figure 5. Principle of molecular imprinting (Molinelli, 2004)

Most of fact, the formation of interactions between monomers and the template are stabilized under hydrophobic environments, while polar environments disrupt them easily. Another limit is represented by the need of several distinct points of interactions: some molecules characterized by a single interacting group, such as an isolated carboxyl, generally give imprinted polymers with very limited molecular recognition properties, which have little interest in practical applications. Understanding the basic optimization of non-covalent methods is important for two reasons: the methodology is far easier than covalent methods, and it produces higher affinity binding sites, versus covalent methods.

The trends in binding and selectivity in non-covalently imprinted polymers are explained by incorporates multiple functional monomers for the highest affinity binding sites. The increased number of binding interactions in the polymer binding site may account for greater fidelity of the site, and thus impart greater affinity and selectivity to the site. This would suggest that the number of functional groups in the polymer binding site is not determined directly by the solution phase pre-polymer complex; rather, it is determined during polymerization. Because of the difficulty to characterizing the binding site structures during and after polymerization, the actual events determining the final binding site structure are still a main challenge.

MIPs possess several advantages over their biological counterparts including low cost, ease of preparation, storage stability, repeated operations without loss of activity, high mechanical stability, durability to heat and pressure, and applicability in harsh chemical media. MIP has become increasingly attractive in many fields of

chemistry and biology, particularly as an affinity material for sensors, binding assays, artificial antibodies, adsorbents for solid phase extraction, and chromatographic stationary phases.

1.5.1 Molecular recognition of MIPs

Molecular recognition ability of MIPs is dependent on several factors, such as shape complementarity, functional complementarity, contributions from the surrounding environment. As for the functional complementarity, even though all non-covalent interactions are applicable to the molecular recognition between a target molecule and a molecular recognition site formed by a molecular imprinting, the nature of the template, monomers and the polymerization reaction itself determine the quality and performance of the polymer product. Moreover, the quantity and quality of the molecularly imprinted polymer recognition sites are attributed to direct function of the mechanisms and extent the monomer-template interactions present in the pre-polymerization mixture. The recognition of the polymer constitutes an induced molecular memory, which makes the recognition sites capable of selectively recognizing the imprint species. The imprinted molecules interact, during both the imprinting procedure and the rebinding, with the polymer via non-covalent interactions, e.g. ionic, hydrophobic and hydrogen bonding. Hydrogen bond is most often applied as a molecular recognition interaction of molecularly imprinted polymers. These non-covalent interactions are easily reversed, usually by a wash in aqueous solution of an acid, a base,

or methanol, thus facilitating the removal of the template molecule from the network after polymerization. In addition to the better versatility of this more general approach, it allows fast and reversible binding of the template.

1.5.2 Polymer composition of MIP

1.5.2.1 Monomer

For non-covalent imprinting, the optimal template /monomer ratio is achieved empirically by evaluating several polymers made with different formulations with increasing template (Kim, 2003). From the general mechanism of formation of MIP binding sites, functional monomers are responsible for the binding interactions in the imprinted binding sites, and for non-covalent molecular imprinting protocols, are normally used in excess relative to the number of moles of template to favor the formation of template-functional monomer assemblies. It is very important to match the functionality of the template with the functionality of the functional monomer in a complementary fashion (e.g. H-bond donor with H-bond acceptor) in order to maximise complex formation and thus the imprinting effect. Higher retention and resolution was found by the two co-monomer imprinting polymer than the single monomer imprinting polymer, which indicated an increase in the affinity of the MIP with the sample as a result of the cooperation effect of the binding sites. However, it is important to bear reactivity ratios of the monomers to ensure those copolymerisations are feasible.

1.5.2.2 Crosslinkers

The selectivity is greatly influenced by the kind and amount of cross-linking agent used in the synthesis of the imprinted polymer. The careful choice of functional monomer is another importance choice to provide complementary interactions with the template and substrates. In an imprinted polymer, the cross-linker fulfils three major functions: first of all, the cross-linker is important in controlling the morphology of the polymer matrix, whether it is gel-type, macroporous or a microgel powder. Secondly, it serves to stabilize the imprinted binding site. Finally, it imparts mechanical stability to the polymer matrix. From a polymerization point of view, high cross-link ratios are generally preferred in order to access permanently porous (macroporous) materials and in order to be able to generate materials with adequate mechanical stability. So the amount of cross-linker should be high enough to maintain the stability of the recognition sites. There are a variety of functional monomer and cross-linker used in non-covalent molecular imprinted polymer and some examples shown in Figure 6 and 7, respectively.

1.5.2.3 Porogenic solvents

Porogenic solvents play an important role in formation of the porous structure of MIP, which known as macroporous polymers. It is known that the nature and level of porogenic solvents determines the strength of non-covalent interactions and influences polymer morphology which, obviously, directly affects the

performance of MIP. Firstly, template molecule, initiator, monomer and cross-linker have to be soluble in the porogenic solvents. Secondly, the porogenic solvents should produce large pores, in order to assure good flow-through properties of the resulting polymer. Thirdly, the porogenic solvents should be relatively low polarity, in order to reduce the interferences during complex formation between the imprint molecule and the monomer, as the latter is very important to obtain high selectivity MIP.

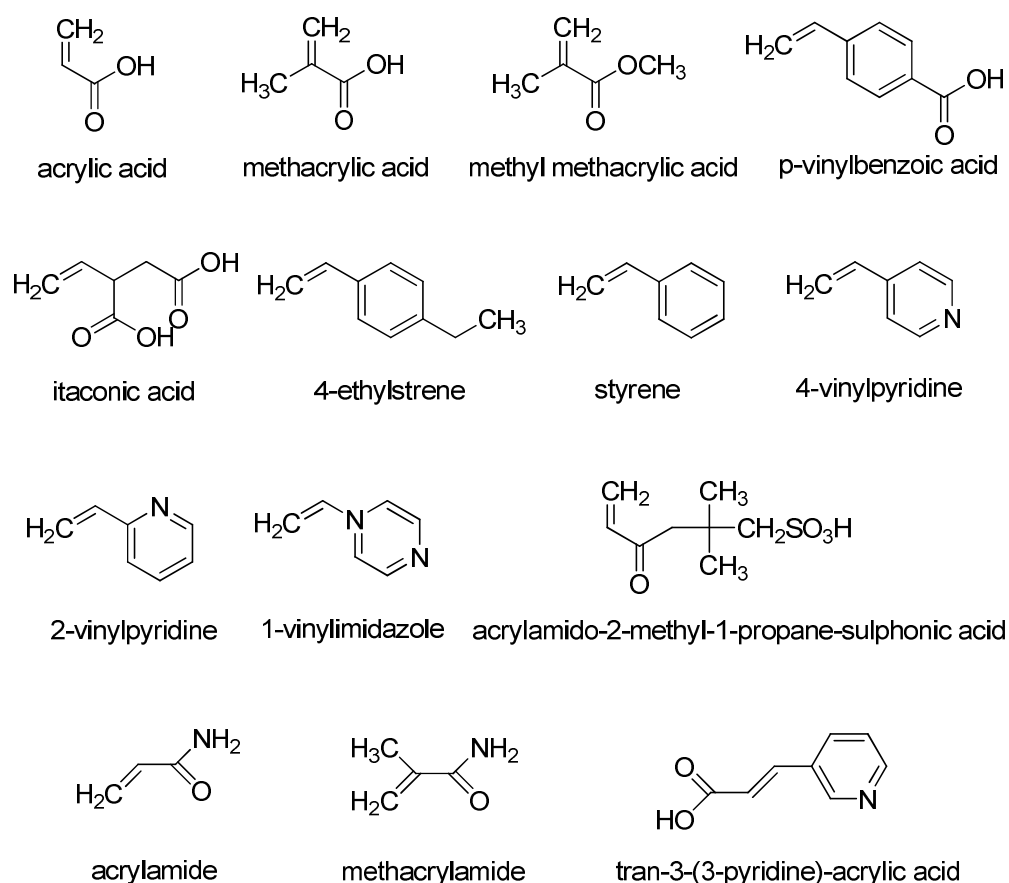


Figure 6. Common functional monomers used in non-covalent molecular imprinting procedures

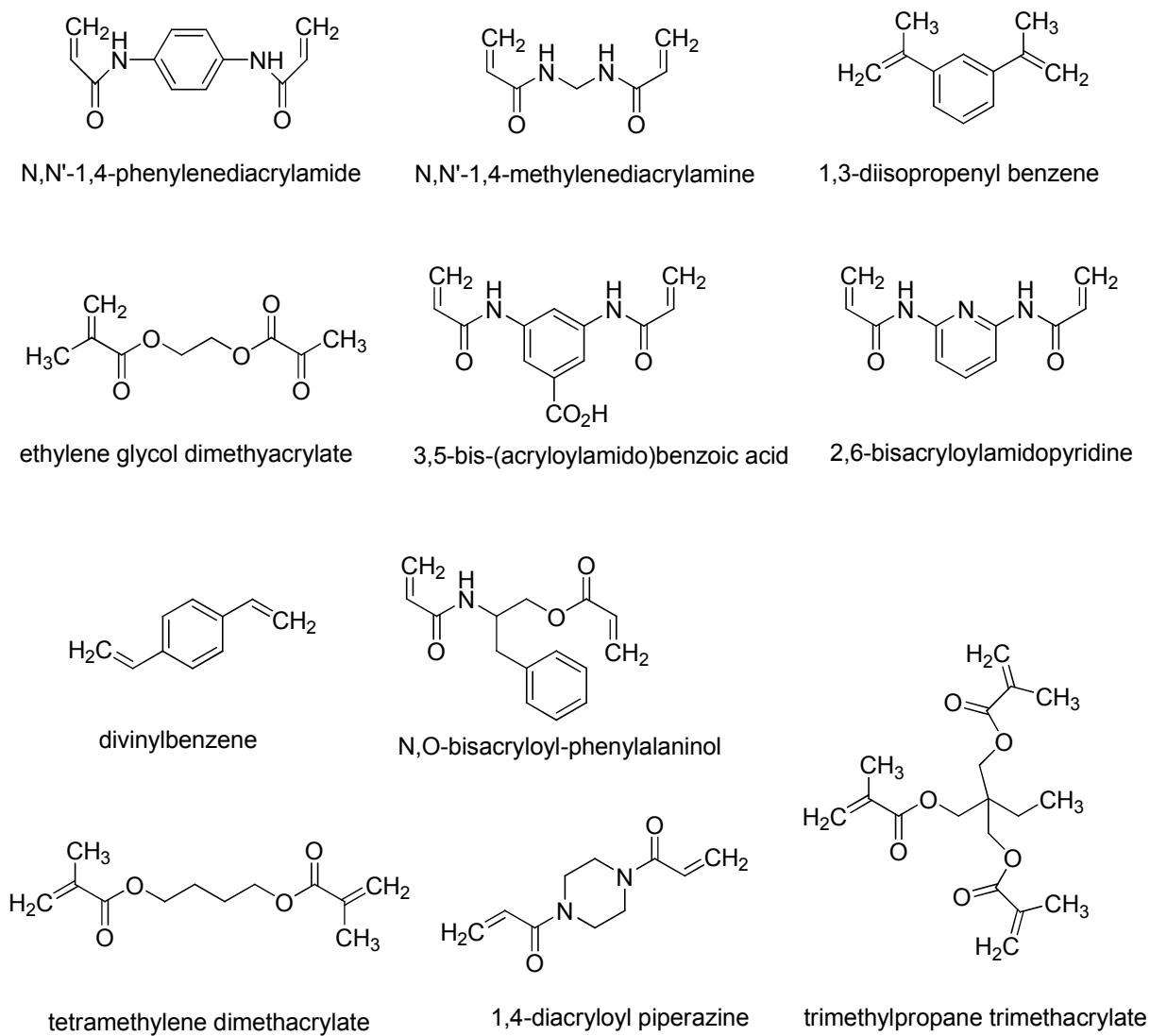


Figure 7. Chemical structure of common cross-linkers used in non-covalent molecular imprinting

1.5.2.4 Initiators

Many of initiators with different chemical properties (see chemical structure in Figure 8) can be used as the radical source in free radical polymerization. Normally they are used at low levels compared to the monomer, e.g. 1 wt. %, or 1 mol. % with respect to the total number of moles of polymerisable double bonds. The rate and mode of decomposition of an initiator to radicals can be triggered and controlled in a number of ways, including heat, light and by chemical/electrochemical means, depending upon its chemical nature. For example, the azoinitiator azobisisobutyronitrile (AIBN) can be conveniently decomposed by photolysis (UV) or thermolysis to give stabilised, carbon-centred radicals capable of initiating the growth of a number of vinyl monomers.

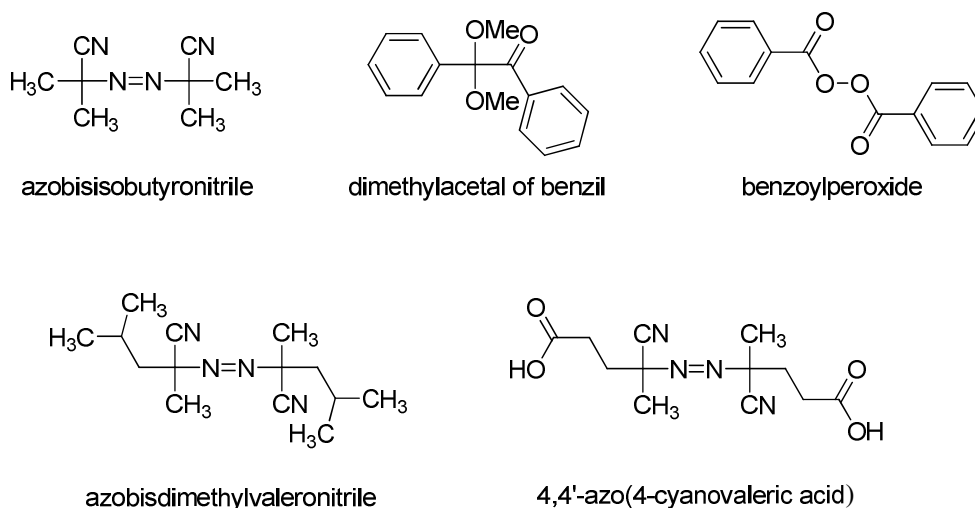


Figure 8. Chemical structure of common initiators used in non-covalent molecular imprinting

1.5.3 Polymerization conditions

Several studies have shown that polymerization of MIP at lower temperatures forms polymers with greater selectivity versus polymers made at elevated temperatures. However, the initiation of the polymerization reaction was very fast and therefore hard to control at high temperature and resulted in low reproducibility of molecular imprinted polymer. Furthermore, the relatively high temperatures have a negative impact on the complex stability, which reduced the reproducibility of the monolithic stationary phases and produced high column pressure drops. Thus, the relatively low temperatures of with a prolonged reaction time were selected in order to yield a more reproducible polymerization. Where complexation is driven by hydrogen bonding then lower polymerization temperatures are preferred, and under such circumstances photochemically active initiators may well be preferred as these can operate efficiently at low temperature.

1.5.4 Imprint polymerization processes

From the 1990s, MIP technology has been extensively exploited to create recognition sites for a range of different templates. Some examples are: polypeptides (Kempe and Mosbach, 1995; Anderson *et al.*, 1995; Minoura and Rachkov, 2000), cells and viruses (Dickert and Hayden, 2002), low molecular mass compounds (Katz and Davis, 2000; Pampi and Kofinas, 2004; Yilmaz *et al.*, 2000) and proteins (Burow and

Minoura, 1996; Bossi *et al.*, 2001; Guo *et al.*, 2004). However, imprinting of proteins represents one of the most challenging tasks. The reason for this could be found in several factors related to the properties of the protein templates as follows. Proteins are water-soluble compounds that are not always compatible with mainstream MIP technology, which relies on using organic solvents for the polymer preparation. Proteins have a flexible structure and conformation, which can be easily affected by change in temperature or in the environment. Practically, it is difficult to develop successful imprints for such biomolecules. Proteins have large number of functional groups available for the interaction with functional monomers. There is always a trade-off involved in the selection of imprinting protocols which rely in some cases on using strong/dissociable (e.g. methacrylic acid) or in others on weak/neutral binding monomer (e.g. acrylamide) for the template recognition. Moreover, proteins are sensitive to temperature, pH and ionic strength, extremes of which can result in denaturation, conformational changes or aggregation.

Protein imprinting can be done successfully by bulk imprinting or surface imprinting depending on the whole or epitope/heptane of protein template. The imprinting procedures for protein on the polymer material are the following:

Bulk imprinting is the most straightforward approach because whole protein can be removed through either extraction or washing and is then able to rebind in the three-dimensional cavity within the MIP. Owing to the large size of proteins, controlling the size and number of pores that are generated during the synthesis and

spread onto the MIP surface, together with the density of MIP network, is essential for effective MIP design and synthesis.

Surface imprint is an engineered method for imprinting protein molecule which is known to produce surface with a heterogeneous covering of binding sites, which are close to the surface, thereby, making the binding site more accessible and therefore, template/polymer interactions are not limited by diffusion problem which this decrease the equilibrium time and enhance the binding kinetics (Hillberg *et al.*, 2008). Surface imprinting has been tackled by a number of research groups using a variety of different approaches. The main steps of surface imprinting of thin films for chemical sensing can be classified into three main approaches.

1. The self-organization of the polymer-template interaction of the template into the polymerizing matrix: the monomer solution is pre-polymerized where highly viscous spin-coated thin-films are formed. There are various approach in order to accomplish an interfacial contact between the thin-film surface and the templates. Templates can be deposited on a stamp and subsequently pressed against the pre-coated transducer. Due to the minor mechanical force applied, the micron-sized templates are effectively embedded in the polymerizing matrix. The stamp is peeled off after polymerization and the templates removed. In case of smaller bioanalytes the interfacial contact can be achieved by immobilizing the templates on beads or crystallized proteins, which can be placed again on a stamp.

2. The self-assembly and polymerization in the solution phase: templates can also be deposited from an aqueous monomer solution onto a transducer, which can be pre-coated.

The transducers are placed in reaction chambers and the aqueous template solution that is drop or spin-coated onto the film. The chamber is filled with an inert gas and is saturated with humidity and volatile monomers, if appropriate. The monomers self-assemble template-directed as thin film during the polymerization. Depending on the nature of the template the imprinting process can be adapted by varying the template concentrations, the buffer system or the pH.

3. The interaction by spray deposition of templates and monomers which is an alternative approach to surface imprinted thin-films uses an aerosol spray. Template/monomer mixtures are sprayed on the transducer surface, which works even well for cellular template.

1.5.5 Materials in protein imprinting

Polyacrylamides are among the most extensively used polymeric materials for bulk imprinting of protein. Recent examples include haemoglobin (Hb) (Gu *et al.*, 2004), lysozyme (Ou, *et al.*, 2004) and bovine serum albumin (BSA) (Huagn *et al.*, 2005) imprinted polyacrylamides. However, the decreased density of polymers inevitable means that their recognition and binding efficiency are reduced after as few rounds of regeneration. Also, the pore size and functional groups on the polymer surface can change over time under harsh condition. Finally, larger proteins are more difficult to imprint, because it is more problematic to retain selectivity and adsorption with increasing template size.

Sol-gels are another group of advanced polymeric materials applied to bulk imprinting of proteins. They are colloidal suspensions of silica particles that are gelled to form a solid. The advantages of water involvement and the mild condition (i.e. pH and ionic strength) in the sol-gel process have been exploited for BSA, Hb, myoglobin (Mb) and urease imprinting (Venton *et al.*, 1995). Recently, Tao and coworker (2006) described an ovalbumin-imprinted polymer using xero-gel, a sol-gel-derived product that exhibits remarkable stability over time. In addition, its physicochemical properties can be tailored by using different precursors or protocols. A novel strategy for the selective detection and quantification of proteins was established by installing a luminescently tagged molecule within the imprinted site and by monitoring the changes in luminescence upon binding of the analyte. The resulting polymer was able to discriminate between the same proteins from different animal species (e.g. human and porcine interleukin-1a) (Tao *et al.*, 2006).

Polyurethanes are widely used in adhesives, surface coatings manufactured and soft-lithography for sensor fabrication because they are high elasticity, good tear strength, and excellent mechanical properties. Dickert and coworker (2001) have been introduced yeast polyurethane imprinting coated on mass-sensitive device for the selective detection of various groups of analyte in aqueous phase. The mixture of bisphenol A, phloroglucinol and *p,p'*-diisocyanatodiphenylmethane was dissolved and pre-polymerized in THF at 70 °C. The diluted pre-polymers are coated on QCM electrode and the subsequent surface imprinting procedure which glass slides were coated with active dry cells and flattened by pressing the cell stamp onto a Teflon

surface. After the template removal, resulted with yeast imprinted polyurethane using hydroxyl or amino functionalities for the polymerization process enable to differentiate between yeast strains of the same genera (*S. cerevisiae*, *S. bayanus* and *S. diastaticus*) and equal cell concentrations. Beside yeast detection, nano-structured pattern of tobacco mosaic viruses (TMV) on polyurethane that coated on QCM sensor is able to re-adsorption after washing out of the template which provided detection ranging from 100 ng mL⁻¹ to 1 mg mL⁻¹ within minutes (Dickert, 2004). Moreover, polyurethane stamp imprinting layer coated on mass sensitive can be generated the patterned polyurethane layer that depict the geometrical features of the template virus, as confirmed by AFM. The cavities are not only selective to shape but also to surface chemistry: different HRV serotypes (HRV1A, HRV2, HRV14, and HRV16, respectively) can be distinguished (Jenik *et al.*, 2009).

Acrylate acid can be prepared in water and are initiated radically. Thus the environment for MIP generation is very suitable for imprinting cells and viruses, because aqueous buffer systems can be chosen. Moreover, the mixture of acrylic/methacrylic acid, and 1-vinyl-2-pyrrolidone (NVP) were used as monomer with ethylene glycol dimethacrylate (EDMA) as crosslinker was applied as a sensitive layer on QCM sensor to detect trypsin. The SDS solution (1%) was used to remove the protein template. Selective trypsin was distinguishable from the native enzyme. Thus, the combination of a mass sensitive transducer with a surface imprinting technique is a versatile approach for chemical sensing of proteins (Hayden *et al.*, 2006).

1.6 Biosensor

To overcome the disadvantages of conventional methods, high sensitive and selective method has been introduced. A sensor can be explained as a device incorporating a sensing element connected to a transducer. Sensing element is a high specific and selective to analyst or substrate in the sample whereas transducer converts an observed change (physical or chemical) into a measurable signal, usually an electronic signal whose magnitude is proportional to the concentration of a specific chemical or set of chemicals (Brian *et al.*, 1996). Biosensor have been used extensively in diagnostics, environmental monitoring and food processes. They utilize various biological molecules, such as microbes, antibodies or enzymes, which are capable of recognizing a specific target molecule. However, many difficulties, such as instability against high temperature, pH and organic solvents, exist for their practical use. Furthermore, in many cases it is hard to find and purify a natural candidate which possesses the desired properties. Moreover, biomedical applications, natural receptors, such as antibody/antigen, enzymes, nucleic acid, cells, are the most common choice for sensing element in biosensor, due to their evolved high affinity and specificity. In contrast, biomimetic sensing elements that incorporate synthetic sensing elements, such as molecularly imprinted polymers, can be advantageous over their biological counterparts, because they can be designed to mimic biological recognition pathways and the same time exhibit other a biotic properties that are more favorable, such as greater stability in harsh environments. The transduction of the interaction between the sensing element and its target molecule can be done by a

variety of transducing elements, including gravimetric, optical and electrochemical sensor.

A sensor is defined as a measuring device that exhibits a characteristic of an electrical nature (charge, voltage or current when it is subjected to a phenomenon that is not electric. The electrical signal it produces must carry all the necessary information about the process under investigation. Sensor devices are combined with molecular recognition elements which are specific reaction to the target analyte in chemical compound and the transducer system that could be specific converted, transferred and amplified the physicochemical signal as an electrical signal for analytical information. The specific binding interaction of target protein to molecular recognition of MIP modified on surface electrode can be measured and verified by electrochemical, piezoelectric and optical devices due to ease of measuring and the availability of instrumentation. Therefore, the selection of a transducer for quantification of allergen protein is based on many factors of the protein, such as the effect of binding interaction, capacitance of protein on surface of polymer, size or weight which could be related to sensitivity of related transducers. The transducers when fabricated with the MIP is able to provide the high sensitive and selective method to detect the low level of allergen proteins in this thesis study includes inter-digital capacitance (IDC), quartz crystal microbalance (QCM) and surface plasmon resonance (SPR).

1.7 Aims and objective of this thesis

This research was concerned with the investigation of the specific MIP system onto the favorable selected transducer system for application as recognition element for biosensor. The main objective was to investigate their use as sensor coating in allergen protein assay. This involved the specific binding interaction of polymerizing MIP compositions on the transducer surface with the target protein and convert physicochemical properties of protein-MIP introduction and amplify as an electrical signal.

The specific aims were:

1. to study possibility of preparing surface imprinting of natural rubber allergen proteins from copolymerization of selected functional monomers [*i.e.* acrylamide (ACM), 1-vinyl-2-pyrrolidone (NVP), methacrylic acid and cross-linking monomer [*i.e.* *N,N'*-(1,2-dihydroxyethylene) bisacrylamide (DHEBA), *N,N'*-methylene-bisacrylamide (MBAA)] to use as a recognition element onto both the quartz crystal microbalance (QCM) and interdigital capacitor (IDC), and also surface plasmon resonance (SPR) transduction systems.
2. for quartz crystal microbalance, interdigital capacitor and surface plasmon resonance transduction system, to characterize the allergen protein surface imprinted polymer.

3. on the basis of the results achieved in 1 and 2 to develop the MIP-QCM, MIP-IDC, and MIP-SPR sensor method to analyze and on the basis of the results achieved in 1 and 2 identify the allergen proteins from rubber latex and latex glove.

4. to determine the amount of rubber allergen proteins by the newly developed MIP-based sensor method using surface-imprinted polymer as a recognition element to the real-life samples.

CHAPTER 2

EXTRACTION AND CHARACTERIZATIONS OF THE NATURAL RUBBER LATEX PROTEINS FROM NATURAL RUBBER LATEX AND RUBBER GLOVE

2.1 Introduction

In order to develop chemical sensor device included a sensitive layer preparing by molecularly imprinted polymer technique the target proteins can be purified from two mainly sources either fresh natural rubber or NRL glove. The target protein from fresh natural rubber latex have been reported in all three major fractions obtained during ultracentrifugation (Moir, 1959) such as a rubber phase, C or B-serum and bottom fraction membrane. Two major water-insoluble proteins are located on the surface of rubber particles in *Hevea brasiliensis* latex. A 14.6 kDa protein (Hev b1), found mainly on large rubber particle (>350 nm in diameter), and a 24 kDa protein (Hev b3), found mainly on small rubber particles (average diameter, 70 nm), are recognized by IgE from patients with SB and latex allergy (Yeang *et al.*, 1996). In spite of fresh natural rubber latex as a source for template protein, in manufacture glove, fresh NRL containing of 0.7% ammonia was centrifuged to be 60% NRL concentrate which this process reduced water soluble protein from 2.0% to 1.0% and this solution was used as raw material

before producing latex gloves. After compounding and dipping process, protein reduction in NRL gloves was removed out by leaching the wet coagulated rubber gel following leaching the surface of the dry rubber film. Moreover, the most efficient way of reducing water-soluble protein is the use of chlorination process. However, high sensitive method were still detect allergen proteins residue on glove surface, especially Hev b1 and Hev b3 allergen proteins. Therefore, these allergen proteins were used as the template protein

2.1.1 Separation and purification of proteins

In order to isolate intracellular proteins, cells must be disrupted. Several disruption techniques, both mechanical and chemical are available. An efficient protocol for cell disruption must be developed to release the protein in a soluble form from its intracellular compartment. The disruption protocol should be as gentle as possible to the protein, as the extraction step is the starting point for all subsequent procedures. The success of cell disruption depends on choice of buffer, the presence of protease inhibitors, and the osmolarity of the resuspension buffer (Scopes, 1994). The condition and the constituent of the extraction buffer depend on the nature of the cell type, the target protein, and further target application. The purification of latex allergen proteins is as essential first step for the study of its molecular and biological properties in order to understand its biological function. There are several properties such as molecular weight, charge, hydrophobicity that can be exploited to purify a protein from a mixture. Based

on those properties, several chromatographic and non-chromatographic methods such as electrophoretic, precipitation, membrane-filtration can be applied (Ahmed, 2005). In protein purification it is important to adopt procedures that do not cause denaturation of proteins. The choice of purification methods is also influenced by factors such as how the purified protein is to be used, the quantity of the purified protein needed, and the cost of the materials and reagents used in the purification. A purification step that may denature purified protein is not suitable for studies of its biological properties, but may be suitable for the determination of its primary structure, subunit size. The purification protocol for obtaining a microgram level of purified protein (for partial peptide sequence in order to construct a gene probe) may be different from those that yield larger quantities of purified protein. The cost of ligands used for immobilization of matrix and for elution of a bound protein in affinity chromatography may be limiting factors for large-scale purification. A protein may be purified by a single step (for example, affinity chromatography) or by a combination of several steps, for example, salt fractionation, ion exchange, gel filtration (Ahmed, 2005).

The methods available for protein purification range from simple precipitation procedures to sophisticated chromatographic and affinity techniques that are constantly undergoing development and improvement (Kaur-Atwal *et al.*, 2007). Methods can be classified in several alternative ways perhaps one of the best is based on the properties of the proteins that are being exploited. Thus the methods can be divided into four distinct but interrelated groups depending on protein characteristics: surface features, size and shape, net charge, and bioproperties.

Surface features include charge distribution and accessibility, surface distribution of hydrophobic amino acid side chains, and, to a lesser extent, net charge at a given pH. Methods exploiting surface features mainly depend on solubility properties. Differences in solubility result in precipitation by various manipulations of the solvent in which the proteins are solubilized. Factor affecting the extraction of proteins such as ionic strength, dielectric constant, pH, temperature, and detergent content, any of which may selectively precipitate some of the proteins present. Conversely, proteins may be selectively solubilized from an insoluble state by manipulation of the solvent composition. The surface distribution of hydrophobic residues is an important determinant of solubility properties; it is also exploited in hydrophobic chromatography, both in the reversed phase mode and in aqueous phase hydrophobic-interaction chromatography (Kaur-Atwal *et al.*, 2007). Also the highly specific technique of immunoaffinity chromatography, in which an antibody directed against an epitope on the protein surface is used to pull out the desired protein from a mixture.

Although the size and shape of proteins can have some influence on solubility properties, the main process of exploiting these properties is gel-filtration chromatography. In addition, preparative gel electrophoresis makes use of differences in molecular size to separate polypeptides (~5000 Da) upto macromolecular complexes of many million daltons. Many proteins in the bioactive state are oligomers of more than one polypeptide and these can be dissociated, though normally with loss of overall structure. Thus many proteins have two “sizes”: that of the native state, and that (or those) of the polypeptides in the denatured and dissociated state. Gel-filtration

procedures normally deal only with native proteins, whereas electrophoretic procedures commonly involve separation of dissociated and denatured polypeptides.

The two techniques that exploit the overall charge of proteins are ion-exchange chromatography (by far the most important) and electrophoresis. Ion exchangers bind charged molecules, and there are essentially only two types of ion exchangers, anion and cation. The net charge of a protein depends on the pH positive at very low pH ($\text{pH} < pI$), negative at high pH ($\text{pH} > pI$), and zero at some specific point in between, termed the isoelectric point (pI). It should be stressed that at the pI a protein has a great many charges; it just happens that at this pH the total negatives exactly equal the total positives. The most charged state (disregarding the charge sign) is in the pH range 6.0 to 9.0. This is the most stable pH range for most proteins, as it encompasses common physiological pH values. Ion exchangers consist of immobilized charged groups and attract oppositely charged proteins. They provide the mode of separation that has the highest resolution for native proteins. High-performance reversed phase chromatography has equivalent or even better resolution, but it generally involves at least partial denaturation (Scopes, 1995) during adsorption and so this is not recommended for sensitive proteins such as enzymes. Protein purification using ion-exchange chromatography has mainly employed positively charged anion exchangers since the majority of proteins at neutral pH are negatively charged. A powerful method for separating the desired protein from others is to use a biospecific method in which the particular biological property of the protein is exploited. The affinity approach is limited to proteins that have a specific binding property, except that proteins are theoretically

able to be purified by immunoaffinity chromatography, which is the most specific of all affinity techniques (Ward and Swiatek, 2009).

Most proteins of interest do have a specific ligand: enzymes have substrates and cofactors, and hormone-binding proteins and receptor molecules are designed to bind specifically and tightly to particular hormones and other factors. Immobilization of the ligand to which the protein binds (or of antibody to the protein) enables selective adsorption of the desired protein in the technique known as affinity chromatography. There are also nonchromatographic modes of exploiting biospecific interactions.

2.1.2 Methods

In the following section a short overview of the methods applied during this doctoral thesis is presented. The attention is turned on historically relevant approaches as well as on state of the art technique.

2.1.2.1 Gel electrophoresis

Gel electrophoresis provides information about the molecular weights and charges of proteins, the subunit structures of proteins, and the purity of a particular protein preparation (Laemmli, 1970). It is relatively simple to use and it is highly reproducible. The most common use of gel electrophoresis is the qualitative analysis of

complex mixtures of proteins. The technique provides the highest resolution of all methods available for protein separation. Polypeptides and proteins differing by less than 0.1 pH unit in their isoelectric points are routinely resolved in gels. Gel electrophoresis is a broad subject encompassing many different techniques. Sodium dodecyl sulfate-polyacrylamide gel electrophoresis (SDS-PAGE) is the most commonly used for separation and characterization of proteins. The method provides an easy way to estimate the number of polypeptides in a sample and thus assess the complexity of the sample or the purity of a preparation. SDS-PAGE is particularly useful for monitoring the fractions obtained during chromatographic or other purification procedures. It also allows samples from different sources to be compared for protein content. One of the more important features of SDS-PAGE is that it is a simple, reliable method which can be used to estimate the molecular weights of proteins. SDS-PAGE requires that proteins have to be denatured to their constituent polypeptide chains, so that it is limited in the detail information. In those situations where it is desirable to maintain biological activity or antigenicity, non-denaturing electrophoresis systems must be employed. The subject of electrophoresis deals with the controlled motion of charged particles in electric fields. Since proteins are charged molecules, they migrate under the influence of electric fields. From the point of view of electrophoresis, the two most important physical properties of proteins are their electrophoretic mobilities and their isoelectric points. The electrophoretic mobility of a protein depends on its charge, size, and shape, whereas its isoelectric point depends only on its net overall charge. Various electrophoresis systems

have been developed to exploit the differences between proteins in these two fundamental properties (Kaur-Atwal, *et al.*, 2007).

The rate of migration of a protein per unit of field strength is called “electrophoretic mobility”. The units of electrophoretic mobility are those of velocity (cm/sec) divided by the units of electric field (V/cm), or $\text{cm}^2/\text{V}\cdot\text{sec}$. Separations between proteins result from differences in their electrophoretic mobilities. Both quantities are established by the composition of the protein and by the make-up of the surrounding medium. Electrophoretic mobilities are influenced by many factors such as pH and the amounts and types of counter ions and denatures that are present in the medium. For every protein there is a specific pH at which its net charge is zero. This pH is called that “isoelectric point”, or *pI*, of the protein. A protein is positively charged in solution at pH values below its *pI* and negatively charged when the pH is above its *pI*. Gels can act as molecular sieves for molecules the size of proteins. They consist of three-dimensional networks of solid material and pores. During electrophoresis in gels, the polymer material acts as a barrier to the motion of proteins forcing them to move between the buffer-filled pores of the gels. In order to confirm the allergenicities of purified protein, immuno analytical method was carried out to identify IgE reactivity to human serum. Western blotting refers to the electrophoretic transfer of the resolved proteins from a polyacrylamide gel to a membrane such as nitrocellulose and polyvinylidene difluoride (PVDF) (Kaur-Atwal *et al.*, 2007).

In most applications, immobilized proteins can be identified and visualized by using very specific and sensitive detection techniques. For example, as low

as 1 to 10 pg of protein can be detected by this way employing immunological techniques. Because of its applicability and flexibility in protein detection methods, Western blotting has become a very popular and convenient method for analysis of denatured proteins. Proteins are transferred from the SDS-PAGE gels, in which all proteins are negatively charged due to the SDS treatment. In an electric field, these negatively charge proteins migrated towards the positive and immobilized on the membrane. The efficiency of Western transfer depends on several factors such as composition of buffer, time, voltage, and size of the protein; percent acrylamide; and the thickness of the gel. An optimization is required for each protein and the efficiency of transfer can be assessed by staining the blots with any blot stain. In general, proteins with low molecular weight transfer more easily than those of high molecular weight and transfer more effectively from low-percent acrylamide gels than from high-percent gels.

For characterization and identification the molecular mass and structure analysis of purified protein, mass spectrometry and tandem mass spectrometry (MS/MS) experiments are major tools used in protein identification. Mass spectrometers measure the mass/charge ratio of analytes; for protein studies, this includes intact proteins and protein complexes (Sobott *et al.*, 2002) fragment ions produced by gas-phase activation of protein ions (top-down sequencing) (Loo *et al.*, 1990, Senko *et al.*, 1994; Little *et al.*, 1994), peptides produced by enzymatic or chemical digestion of proteins (mass mapping) (Kleno *et al.*, 2004; Pan *et al.*, 2003) and fragment ions produced by gas-phase activation of mass-selected peptide ions (bottom-up sequencing) (Yates *et al.*, 1998).

2.1.2.2 Mass spectrometry

The application of mass spectrometry and MS/MS to proteomics takes advantage of the vast and growing array of genome and protein data stored in databases. The information produced by the mass spectrometer, lists of peak intensities and mass-to-charge (m/z) values, can be manipulated and compared with lists generated from “theoretical” digestion of a protein or “theoretical” fragmentation of a peptide (Figure 9). Applications to analyze ever smaller quantities of sample are driving the development of more sensitive mass spectrometers, as well as low flow, high resolution separation technologies, to provide structural information on individual components in complex mixtures of thousands of proteins derived from biological samples (Wysocki *et al.*, 2005). Protein identification by mass spectrometry requires an interplay between mass spectrometry instrumentation (how molecules are ionized, activated, and detected) and gas-phase peptide chemistry (which bonds are broken, at what rate, and how cleavage depends on factors such as peptide/protein charge state, size, composition, and sequence) (Lewis *et al.*, 2000). In traditional protein chemistry, proteins were identified by de novo sequencing using automated Edman degradation. Nowadays, this technique tends to be replaced by mass spectrometry, which is becoming one of the most powerful techniques in protein chemistry. The reason for this is a 100 fold increase in sensitivity and 10 fold increase in speed. In most cases sequence-specific proteolysis of the protein, in addition to accurate measuring of the mass-to-charge ratio of the resulting peptides gives enough information to identify the proteins in the sample. This can easily be done

using the matrix-assisted laser desorption ionization mass spectrometry (MALDI-MS) procedure (see Figure 10). This technique offers a unique application for the particular protein or protein mixtures. The experimental obtained mass-to-charge values that can be matched against theoretical obtained for mass data from already identified protein sequences and a score depending on the correlation can be given. Correct identification of course requires that the database contain the specific protein sequences (or the corresponding DNA sequences). Therefore, the approach is best suited for generically well characterized organisms where the entire genome is known, but can also be used for organisms which only part of the genome is known or for which very homologous sequences are available. This way of identifying proteins is called peptide mass searching or fingerprint (PMS or PMF). A low amount of 0.2-2 pmol of protein starting material in a gel is sufficient for identification by peptide mass fingerprinting. In practice these identifications are made by complex search-algorithms build into simple-to-use programs.

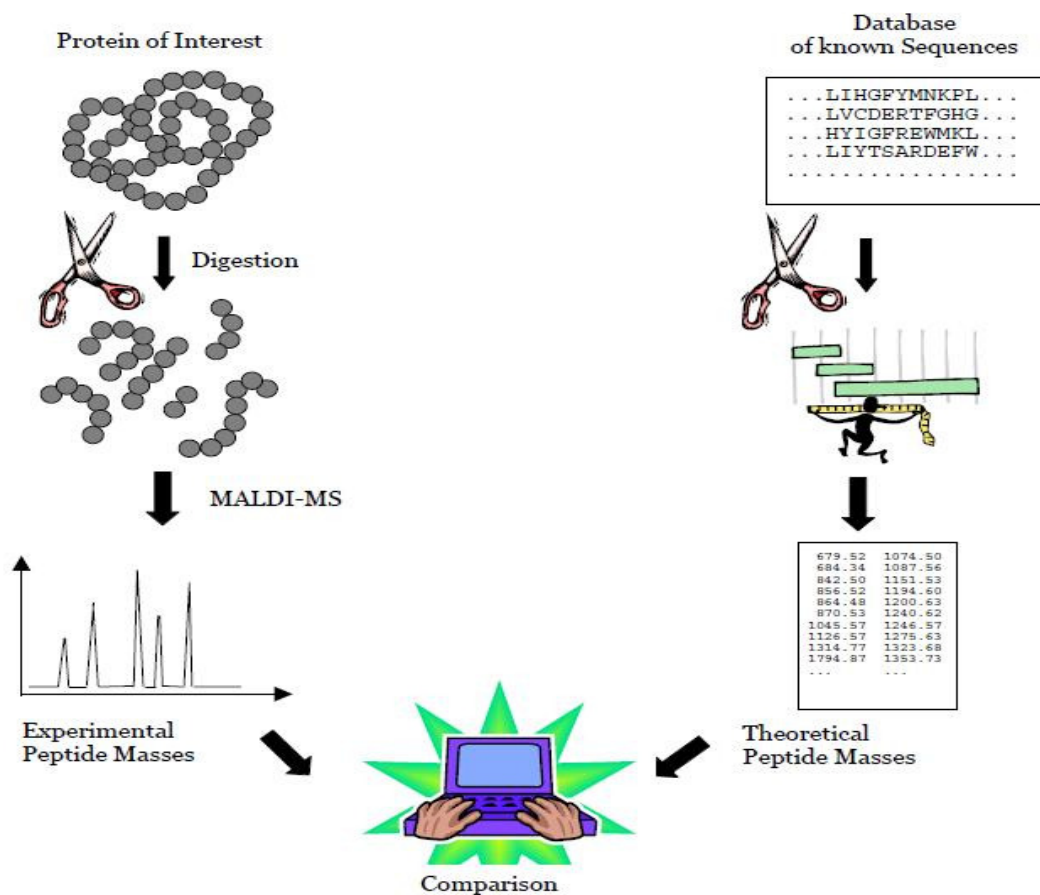


Figure 9. The principles of protein identification by MALDI-MS. The protein of interest is digested by an enzyme (e.g. trypsin) and a MALDI-spectrum is recorded. The experimental obtained data are then analyzed against a peptide mass database. This database compiles data from a theoretical digest of already known proteins

The analysis with matrix-assisted laser desorption/ionization mass spectrometry, only solid sample, can be analyzed (see Figure 12). The sample has to co-

crystallize with a so-called matrix on the sample slide and the desorption is carried out by means of a laser shot. Matrix molecules are applied in a great excess, their function is to isolate the sample molecules from each other and absorb the laser light to help with the vaporization and ionization of the substances to analyze. There are special types of matrices for each application. In our experiments sinapic acid (SA) and α -cyano-4-hydroxycinnamic acid (CHCA) matrices were used. SA is an ideal matrix for proteins, which CHCA is applied for peptide or small proteins (<20 kDa).

The sample compounds will be ionized and accelerated into a flight tube. The time needed to reach the detector situated at the end of the drift tube is characteristic and proportional to the mass of the ionic species. The mass of the ions can be calculated via the exact measurement of the time of flight. Ions having the same molecular mass, but slightly different starting speed can decrease the accuracy of the measurement. To overcome this difficulty most instruments are furnished with a time delayed extraction possibility to correct for the initial spread of velocity or with a so-called reflectron or ion mirror, to focus the ions, having the same molecular mass, into small "packages". With these options the mass accuracy can be substantially increased (reflectron mode). However, the decrease in sensitivity at reflectron mode must be taken into consideration.

The extraction of the proteins without enzymatic digestion was carried out according to the method of Ehring and coworker. The gel was stained with Coomassie stain. The peptide mapping experiments were carried out with proteins purified by means of HPLC. In this work, the mass spectra were obtained by a MALDI-TOF mass spectrometer (Ultraflex III TOF/TOF 200, Bruker Daltonik GmbH, Bremen Germany).

All measurements were performed in the positive-ion reflector made at an accelerating voltage of 20 kV, 70% grid voltage, 0.05% guide wire voltage and a delay of 100 ns. MALDI-TOF spectra were recorded at 256 scans per spectrum. The low-mass gate was set at 500 m/z.

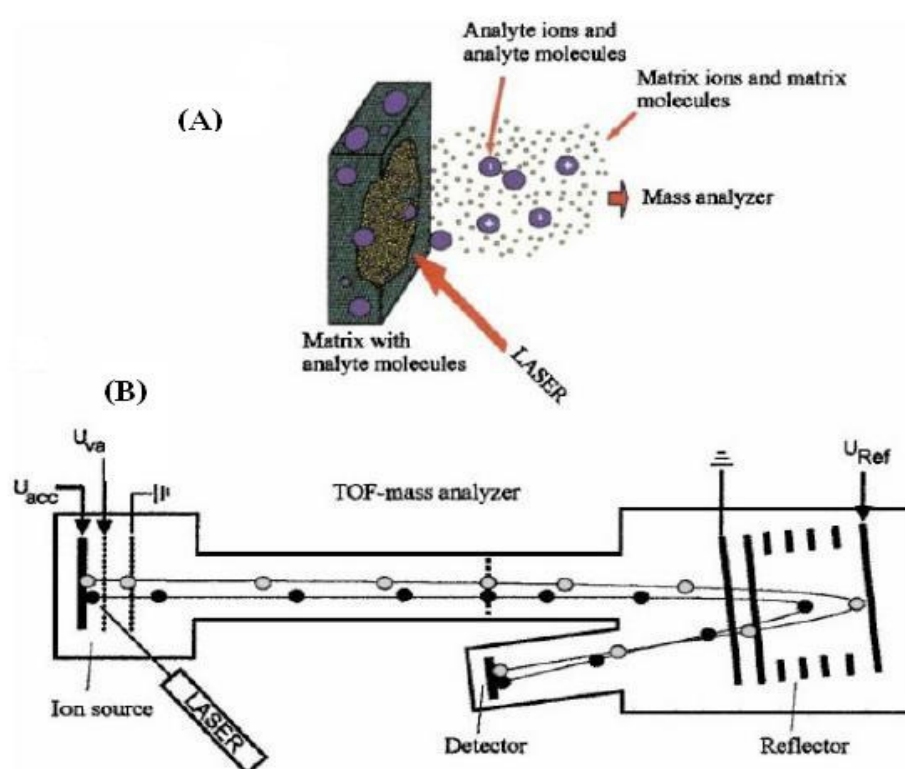


Figure 10. Matrix-assisted laser desorption ionization (MALDI) and time-of-flight mass analyzer (TOF) (Vicki *et al.*, 2005)

Hev b1 (14.6 kDa) and Hev b3 (24 kDa) are hydrophobic protein (Rish *et al.*, 2000) and major latex allergens found tightly associated to rubber particles of natural rubber latex (NRL) (Czuppon *et al.*, 1993; Alenius *et al.*, 1993; Yeang *et al.*, 1996) and

NRL glove product. Two major rubber particle proteins of 14.6 and 24 kDa had been classified as proteolipids and identified in washed rubber particle obtained from ultracentrifuged fresh latex (Hasma, 1987; Wititsuwannakul *et al.*, 2004). The genes encoding two major proteins were found to be most abundant in the analysis of the *Hevea laticifer* transcriptome (Ko and Chow, 2003). A deduced amino acid sequence obtained from a full-length cDNA encoding the 24 kDa protein was shown to have a high homology to that of the 14.6 kDa (Hev b1). Moreover, Hev b2 (34–36 kDa) is a basic protein and solubilized in high ionic (salt) content. Hev b2 appeared to show the ability of binding to IgE from sera of patients with latex allergy which appears in bottom fraction membrane or B-serum when isolated from fresh latex. Therefore, the fresh NRL and NRL glove were used as a starting material for purification of allergen protein.

Generally, hydrophobic protein required disruption of the phospholipids bilayer or cleavage of the polypeptide from its membrane anchor which usually achieved with detergent (Harris and Angal, 1990). Then the next step is the isolation and purified protein which could be achieved by physical properties of protein such as surface charge, hydrophobic nature, solubility, biospecificity and molecular mass. In this thesis work, the isolation and purification procedures of allergen proteins from NRL have been carried out using the method as described previously by Yeang and coworker (1996) and Wititsuwannakul *et al.*, 2008 which in brief, the first step for fresh latex is to centrifuge the latex to separate out the latex fractions and the proteins on the surface of the rubber particles and bottom fraction membrane were then solubilized and extracted by adding an equal volume of detergent. The mixture was stirred and then centrifuged to obtain the

supernatant that contained solubilized proteins. For purification of allergen protein achieving from NRL glove was carried using method as described by Czuppon *et al.*, (1993) which in brief, the glove was cut to a small pieces and extracted by 1% sodium dodecylsulfate (SDS) in phosphate buffer solution (Czuppon *et al.*, 1993). For purified allergen protein gel filtration and SDS-PAGE were used to isolate and monitor the amount of allergen protein during purification step. Moreover, SDS-PAGE, western blotting, and mass spectrometry are being used to characterize proteins in terms of molecular mass allergenicity and their mass spectra.

2.2 Objective

The aim of this work was to isolate and purify the natural rubber latex proteins from rubber latex and latex glove in order to use as a template molecule in studying the preparation of protein surface-imprinted layer onto the transducers. It was planned to employ these extracted proteins to evaluate specificity of sensor system. Other related allergen proteins of extractable Hev b2 (L) and Hev b3 (L) were purified and characterized to study the selectivity of sensor system. Note that allergenic proteins isolated from rubber tree sap are identified with an “L” in parenthesis, and proteins extracted from rubber latex gloves as identified with a “G” in parenthesis.

2.3 Experimental

2.3.1 Chemicals and Equipment

2.3.1.1 Buffers and additives

- Glycine (AR grade, Sigma-Aldrich, USA)
- Hydrochloric acid (AR grade, Lab-scan, Thailand)
- Methanol (AR grade, Lab-scan, Thailand)
- Sodium dodecyl sulfate (AR grade, Sigma-Aldrich, USA)
- Tris(hydroxymethylaminomethane) (AR grade, Sigma-Aldrich, USA)
- Triton X-100 (AR grade, Fluka, Belgium)
- Tween 20 (Molecular biology grade, AppliChem, Germany)

2.3.1.2 Electrophoresis reagents

- Acrylamide (AR grade, Sigma-Aldrich, USA)
- Bromphenol blue (AR grade, Sigma-Aldrich, USA)
- Coomassie brilliant blue (AR grade, Sigma-Aldrich, USA)
- Ethylene diaminetetraacetate (EDTA) (AR grade, Sigma Aldrich, USA)
- Glycerol (AR grade, Sigma-Aldrich, USA)
- Glycine (AR grade, Sigma-Aldrich, USA)
- 2-mercaptoethanol (AR grade, Sigma-Aldrich, USA)

- *N, N, N'*, *N'*-tetramethylenediamine (AR grade, Sigma-Aldrich,USA)

2.3.1.3 Protein determination reagents

- Bovine serum albumin (Molecular biology grade, Sigma-Aldrich,USA)
- Lysozyme (Molecular biology grade, Sigma-Aldrich,USA)
- Ovalbumine (Grade II, Crude, Dried Egg, White, Sigma-Aldrich,USA)
- Copper sulfate (AR grade, Sigma-Aldrich,USA)
- Sodium hydroxide (AR grade, Sigma-Aldrich,USA)
- Sodium carbonate (AR grade, Sigma-Aldrich,USA)
- Sodium bicarbonate (AR grade, Sigma-Aldrich,USA)
- Sodium tartrate (AR grade, Sigma-Aldrich,USA)
- Binichoninic acid disodium salt hydrate (AR grade, Sigma-Aldrich,USA)

2.3.1.4 Immunochemicals

- Alkaline phosphatase conjugate substrate (Molecular biology grade, Sigma-Aldrich,USA)
- Anti-human IgE antibody (Bio-Rad) (Molecular biology grade, Sigma-Aldrich,USA)

- Bovine serum albumin (BSA) (Molecular biology grade, Sigma-Aldrich,USA)
- 3,3'- Diaminobenzidine tetrahydrochloride (Molecular biology grade, Sigma-Aldrich,USA)
- Hydrogen peroxide
- Peroxidase conjugated goat anti-human IgE antibody (Molecular biology grade, Sigma-Aldrich,USA)
- Ponceau-S (Molecular biology grade, Sigma-Aldrich,USA)

2.3.1.5 Electrophoresis cell (ATTO, Dual Mini Slab, Japan)

2.3.1.6 Power supply (Bio-Rad, Model; Power Pac 300, USA)

2.3.1.7 Protein blotting cell (Bio-Rad, Mini Trans-Blot, Japan)

2.3.1.8 UV spectrophotometer (Beckman, Model: DU 650 I, USA)

2.3.1.9 Ultracentrifuge (Beckman, Model: L8-70M, USA)

2.3.1.10 Whatman 3M paper (GE Healthcare, UK)

2.3.1.11 Polyvinylidene Fluoride membrane (0.45 μm , Pall Corporation, USA)

2.3.1.12 Magnetic stirrer (model; LMS100, LabTech, Korea)

2.3.1.13 Speed Vac concentrator (SVC 100, Thermo Scientific Savant, USA)

2.3.1.14 Fraction collector (model 2110, Bio-Rad, USA)

2.4 Methods

2.4.1 Natural Rubber Latex (NRL) and NRL glove samples

The fresh Hevea latex used throughout this study was obtained from the clone RPIM 600 which grown at farmer plant in Hat Yai, Songkhla, Thailand. The trees were tapped by “jebong” knife on panel BO-1 under $\frac{1}{2}$ S d/2 tapping system. Tapping starts about 06.00 hours and the exuded latex was collected in beakers which were chilled on ice. Latex collection period of sixty minutes was done on each tapping. NRL glove was collecting from local market in Hat Yai, Songkhla, Thailand. One brand (Powder gloves) was collected form High Care Co., Ltd.

2.4.2 Preparation of rubber particles, C-serum and bottom fraction

The chilled latex was filtered through 4 layers of cheese cloth to remove the particulated materials and bark tissue debris. The filtrate was collected and centrifuged at 60,000 g for 45 min at 4 °C in an ultracentrifuge (Beckman, Model: L8-70M). After centrifugation, the latex was separated into three distinct layers with the rubber cream and Frey Wyssling complexes on the top, the bottom fraction at the bottom and C-serum in between (Figure 11). By this separation, the bottom fraction consists mainly of lutoid particles and some heavy fraction of Frey-wyssling complexes as described by Gomez and Samsidar Hamzah (1989).

2.4.3 Preparation of Hev b2 from bottom fraction membrane (BFM)

The intact bottom fraction separated from ultracentrifuged latex was washed 2 times to remove the contaminated C-serum and rubber particles by suspending the bottom fraction in five volumes of isotonic buffer and recovered by centrifugation at 60,000 g for 45 min. The washed bottom fraction was then suspended in ten volumes of distilled water (DW) with overnight stirring at 4 °C. The remaining insoluble BFM was collected by centrifugation at 10,000 g for 30 min and further washed 3 times with isotonic buffer to eliminate residual B-serum. The intrinsic proteins of washed BFM obtained from preparation were extracted by suspending the BFM in 50 mM Tris-HCl, pH 7.4 containing 0.2% Triton X-100 with overnight stirring at 4 °C. The crude protein was recovered by centrifugation at 10,000 g for 30 min (Wititsuwannakul *et al.*, 2008).

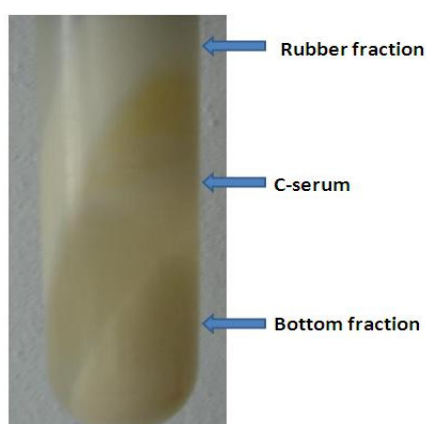


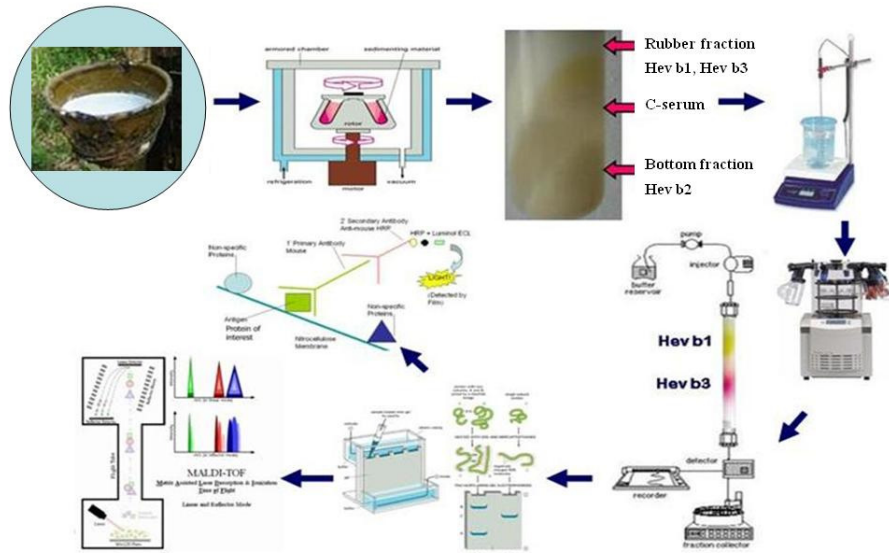
Figure 11. Ultracentrifugation of fresh latex

2.4.4 Preparation of protein from rubber particle (RP) (Hev b1 and Hev b3)

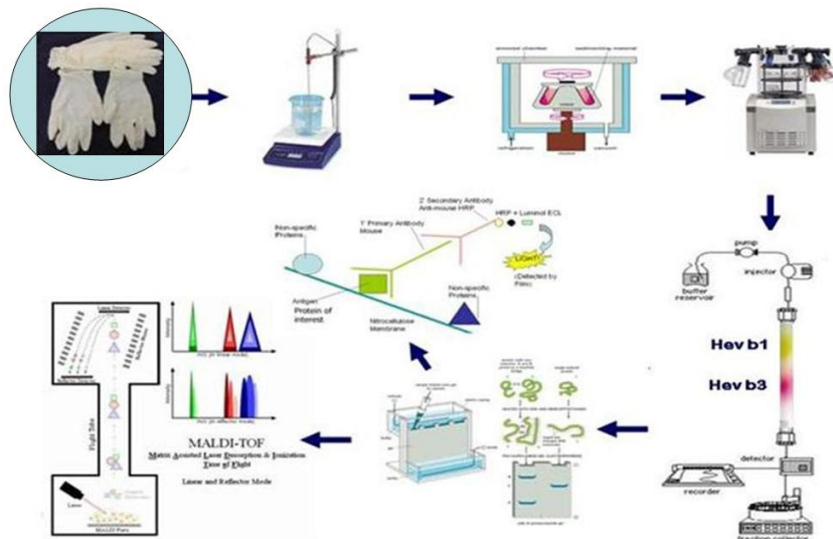
The rubber cream from centrifuged latex was collected in its entirety. For some experiments the portions of the cream representing Zone 1 and Zone 2 were sampling separately. The rubber particles in the rubber cream samples were washed by resuspension in 30% sucrose and recovered by centrifugation. The proteins on the surface of the rubber particles were then solubilized and extracted by adding an equal volume of detergent comprising 0.1% Triton-X 100 and 1% sodium dodecylsulfate (SDS) to the rubber cream. The mixture was vortexed and then centrifuged to obtain the supernatant that contained solubilized proteins (Yeang *et al.*, 1996).

2.4.5 Extraction of the proteins from NRL gloves (Hev b1 and Hev b3)

Scheme 1 and 2 show the extraction protocol and setup of purification for Hev b1 and Hev b3 from NRL and latex glove samples, respectively. The NRL gloves chosen for the investigations were cut into a small piece and were extracted in extraction buffer containing varies surfactant. There are several methods described by different groups for the extraction of proteins from natural latex articles. Sodium dodecyl sulfate (SDS), Triton X-100 and Phosphate buffer saline were tested at 120 min in room temperature. Thereafter the rubber pieces were removed by centrifugation, the supernatant was dialyzed through a cellulose bag (molecular weight cutoff of 3700 Da) against distilled water for 48 hours at 4 °C, and then lyophilized (Chen *et al.*, 1997).



Scheme 1. Diagram of extraction protocols and purification of allergen proteins from NRL samples



Scheme 2. Diagram of protocol for extraction and purification of NRL allergen proteins latex gloves

2.4.6 Protein purification

The concentrated crude (2 ml) solution of NRL and NRL glove was loaded onto a SephacrylTMS-100 (High Resolution) column (1.5 x 64 cm), which was equilibrated and eluted with 50 mM phosphate buffer (pH 7.4) containing 0.1% SDS and 0.15 M NaCl. Fractions of 2.0 ml were collected and examined by SDS-PAGE. The active fractions were pooled, concentrated and examined their peptide mapping by MALDI-TOF (Marchetti-Deschmann *et al.*, 2009).

2.4.7 Sodium dodecyl sulfate polyacrylamide gel electrophoresis (SDS-PAGE)

The extractable proteins were examined by SDS-PAGE according to the method of Leammli (1970). The separating and stacking gel used in this study include 12% and 4% of acrylamide, respectively. A protein sample was treated with solubilizing buffer and boiling in water at 100°C for 5 min. The SDS-PAGE was performed at room temperature and electrode buffer at pH 8.3. A constant electrical current of 14-20 mA per one slab gel was applied until the tracking dye marker approached the bottom of gel. After completed, the protein bands were fixed and stained with Coomassie brilliant blue R. Destaining of excess dye was achieved by changing several times of solution until the clear background was obtained.

2.4.7.1 Stock Solutions

1. 2 M Tris-HCl (pH 8.8), 1 liter: weight out 242 gram Tris base and add 900 ml distilled water. Adjust pH to 8.8 by adding concentrated HCl slowly and finally add distilled water to a total volume of 1 liter.
2. 1 M Tris-HCl (pH 6.8), 100 ml: to 12.1 gram of Tris base add 80 ml distilled water and adjust pH to 6.8 with concentrated HCl. Add distilled water to a total volume of 100 ml.
3. 10% SDS (w/v), 100 ml: weight out 10 gram SDS and add distilled water to a total volume of 100 ml. Store solution at room temperature.
4. 50% glycerol (v/v), 100 ml: add 50 ml distilled water to 50 ml 100% glycerol.
5. 1% bromophenol blue (w/v), 10 ml: weigh out 100 mg bromophenol blue and add 10 ml distilled water. Stir until dissolved and filter to remove particulates.

2.4.7.2 Working Solutions

1. 30% acrylamide stock solution: dissolve 29.2 gram acrylamide and 0.8 gram bisacrylamide with distilled water to make 100

ml. The solution is stable at 4 °C for months. (Note: unpolymerized acrylamide is a skin irritant and a neurotoxin and thus should be handled with gloves. Use of a mask is also recommended to avoid inhalation. Unused acrylamide solution should be polymerized and disposed of with solid waste).

2. 4 × separating gel buffer, 100 ml
 - a. 75 ml 2 M Tris-HCl (pH 8.8); final concentration 1.5 M
 - b. 4 ml 10% SDS; final concentration 0.4%
 - c. 21 ml water(The solution is stable for months at 4 °C)
3. 4 × stacking gel buffer, 100 ml
 - a. 50 ml 1 M Tris-HCl (pH 6.8): final concentration 0.5 M
 - b. 4 ml 10% SDS; final concentration 0.4%
 - c. 46 ml water(The solution is stable for months at 4 °C)
4. 10% ammonium persulfate, 5 ml: dissolve 0.5 gram ammonium persulfate in 5 ml distilled water. Aliquot 100 µl in 0.5 ml microfuge tubes and store at -20 °C (stable for months)
5. Electrophoresis buffer, 1 liter:
 - a. 3 gram Tris base; final concentration 25 mM
 - b. 14.4 gram glycine; final concentration 192 mM
 - c. 1 gram SDS; final concentration 0.1%

- d. Water to make 1 liter

(pH should be approximately 8.3; 10x stock solution can also be made and stored at 4 °C; stable for months.)

6. 5×sample buffer, 10 ml:

- a. 0.6 ml 1 M Tris-HCl (pH 6.8); final concentration 60 mM
- b. 5 ml 50% glycerol; final concentration 25%
- c. 2 ml 10% SDS; final concentration 2%
- d. 0.5 ml 2-mercaptoethanol; final concentration 14.4 mM
- e. 1 ml 1% bromophenol blue; final concentration 0.1%
- f. 0.9 ml water

(Aliquot in small volume in microfuges and store at - at -20 °C (stable for months)

7. Coomassie gel stain stock solution, 1 liter:

Coomassie Brilliant Blue R-250	1 g
Methanol	450 ml
Water	450 ml
Glacial acetic acid	100 ml

8. Coomassie gel destain stock solution, 1 liter:

Methanol	100 ml
Water	800 ml
Glacial acetic acid	100 ml

2.4.8 Western blot analysis

Electrophoretic blotting was performed according to the method described by Towbin (1979). Nitrocellulose was immersed in a blotting buffer. Upon completion of electrophoresis, the gel was placed on a Scotch-Brite pad. The transfer membrane was put on the top of the gel. The membrane was covered with two sheets of Whatman 3 M paper and a second Scotch-Brite pad. Proteins transfer was carried out at 100 V for 1 h at 4°C. After blotting, the sheets of blotted membrane were blocked with bovine serum albumin and human sera diluted 1:10 in blocking buffer were added and incubated for 18 h at 4°C with continuous shaking. The sheets of cellulose membrane were incubated by peroxidase conjugated goat anti-human and DAB substrate was added to form color. In the presence of peroxide (H_2O_2), HRP catalyzes the oxidation of phenols, naphthols, diamines, aminophenols, indophenols, etc. forming chromogenic products visible by light microscopy. Most commonly employed is diaminobenzidine (DAB). DAB is the most widely accepted donor substrate for peroxidase immunoblot, since it provides a reaction product insoluble in alcohols and xylene. The oxidation of DAB results in formation of a free radical intermediate which polymerizes to form a brown product.

2.4.9 Peptide Mass Mapping of allergen protein (Hev b1, Hev b2 and Hev b3) by MALDI-TOF/MS

A. Trypsin in gel digestion

Excised protein spot/band was cut into small pieces (< 1 mm) and dehydrated in acetonitrile for 10 min. The acetonitrile was removed by a rotary evaporator and then reswell the gel at 4° C for 45 min in buffer containing trypsin and 50 mM ammonium bicarbonate. Gel piece was digested overnight at 37° C for 3 h.

B. MALDI-TOF mass spectrometry

The mass spectra were obtained by a MALDI-TOF mass spectrometer (Ultraflex III TOF/TOF 200, Bruker Daltonik GmbH, Bremen Germany). All measurements were performed in the positive-ion reflector made at an accelerating voltage of 20 kV, 70% grid voltage, 0.05% guide wire voltage and a delay of 100 ns. MALDI-TOF spectra were recorded at 256 scans per spectrum. The low-mass gate was set at 500 m/z.

2.4.10 BCA method

1. Reagent A: Na₂CO₃.H₂O (0.8 g), NaOH (1.6 g), sodium tartrate

(dehydrate) (1.6 g), made up to 100 mL with water, and adjusted to pH 11.25 with 10 M NaOH.

2. Reagent B: BCA (4.0 g) in 100 mL of water.
3. Reagent C: $\text{CuSO}_4 \cdot 5\text{H}_2\text{O}$ (0.4 g) in 10 mL of water.
4. Standard working reagent (SWR): mix 1 volume of reagent C with 25 volume of reagent B, then add 26 volume of reagent A.

The bovine serum albumin (BSA) and analyte were incubated added with 1 mL of SWR at 60 °C for 30 min. Then, this mixture was cooled to room temperature, before measuring UV adsorption at 562 nm. The amount of protein was determined by BSA standard calibration curve (Ahmed, 1959).

2.5 Results and discussion

The allergen proteins were isolated and purified from latex gloves to use as a template for molecularly imprinted polymer. However, latex proteins may be modified (denatured, fragmented, aggregated) during glove production or during latex ammoniation prior to the manufacturing process when comparable to native form of protein from fresh natural rubber latex. Therefore, fresh natural rubber latex and latex glove were used as a raw material to extract target allergen proteins (Hev b1, Hev b2 and Hev b3). Fresh Hevea latex can be isolated as a three major fractions by ultracentrifugation namely: (1) a white creamy layer at the top which contains virtually of the rubber particles; (2) a translucent fluid (C-serum); and (3) a bottom fraction

containing organelles, including the lutoids and Frey-Wyssling (Moir, 1959). As well known the most of allergen proteins in centrifuged NRL is into three fractions i.e. 25% rubber particles containing, 43% C-serum containing, 26% B-serum containing and 6% bottom fraction membrane. However, first part of the experiments will focus in the rubber particles and BFM samples as a first priority because both sources of allergy protein reported that have more reactive in binding to anti-glove IgG than those of C-serum (Jewtragoon, 1995 and Yeang, 1996). By using HRP as the enzyme conjugate for immunological detection on the rubber particle and BFM blotted membrane in *spina bifida* and latex-sensitive revealed IgE-reactive rubber particle and BFM proteins at several regions; 14.6 and 24 kDa and 14, 17, 22, 30, 43, 55, 58 and 94 kDa, respectively. Thus, rubber particle and bottom fraction membrane obtained from fresh natural rubber latex were used as a first source for purified allergen protein.

2.5.1 Allergen protein extraction from BFM (Hev b2) and rubber particle (Hev b1 and Hev b3)

The first step is to remove contaminating cytosolic proteins (B-serum and C-serum). Soluble cytoplasmic proteins are extracted by cell disruption in a neutral, isotonic, and detergent-free buffer and are removed components of the cell extract. In the second step of isolating membrane proteins, a highly purified membrane fraction is obtained. In this experiment, the extraction of BFM protein must remove B-serum and C-serum residue with distilled water treatment. These proteins were classified

as hydrophobic type contained luteoid organelles and other colloidal substances within bottom fraction after removal B-serum and C-serum. BFM protein was extracted with the buffer containing 0.2 % Triton X-100 due to its medium environmentally condition that maintain their native states of conformation and activity. Figure 12 showed SDS-PAGE of three major protein-bands of B-serum at 14, 20 and 30 kDa (lane 1) and several protein bands of BFM at 14, 23, 31, 38, 40, 60 and 65 kDa (lane 2) in comparison to standard molecular weight.

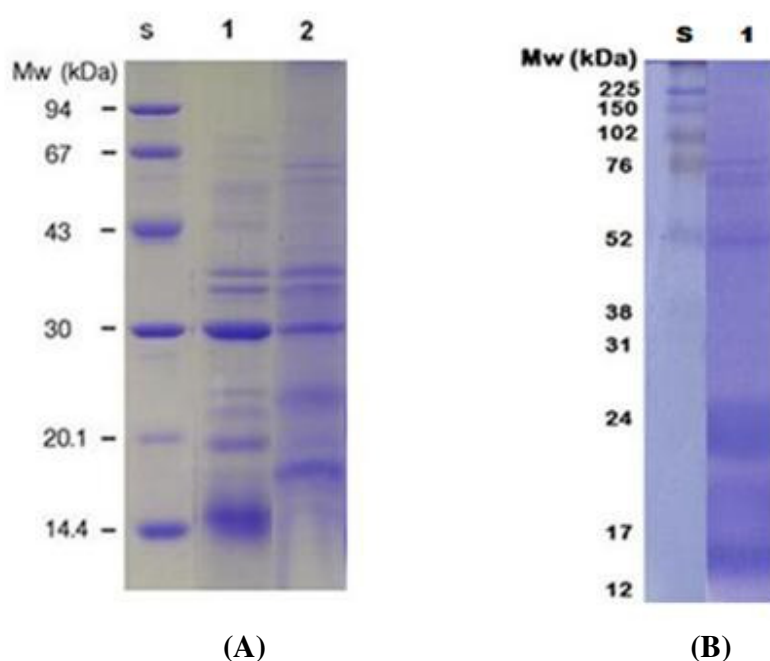


Figure 12. SDS-PAGE of an extract of the fresh natural rubber latex on a 12% polyacrylamide gel; (A): bottom fraction membrane (BFM) and (B): rubber particle. **1** (A): Protein from B-serum treated with distilled water at 4°C for overnight, **2** (A): Protein

from BFM treated with 50mM Tris-HCl, pH 7.4 and extracted with 0.2% Triton X-100 at 4°C; **1 (B)**: Protein from rubber particle extract with 1% SDS and 0.05 Triton X-100 in Tris-HCl, pH 7.4 at 4°C; **S**: Molecular weight markers

These results could be explained that B-serum proteins (Figure 12A, lane 1) may be identified as hydrophilic group or globular protein due to their water solubility properties during BFM treatment process. Their structure may be polar and ionic group of amino acid positioning of their surface area. In contrast, BFM proteins composed of integral or peripheral membrane proteins interact with phospholipid bilayer and possess a hydrophobic property due to their solubility in mild surfactant (Triton X-100). The process of solubilization of membrane proteins depends on the amount of the detergent relative to membrane protein. Detergent extraction of a membrane protein occurs as follows: (a) binding of detergent to the membrane and initiation of lysis; (b) solubilization of the membrane in the form of detergent-lipid-protein complex; and (c) further solubilization of the detergent-lipid-protein complexes to give detergent-protein complexes and detergent-lipid complexes. The BFM proteins (Figure 12A, lane 2) were found to be distinct protein bands of similar masses, around 14 kDa and 30-35 kDa, to those observed in the B-serum. These distinct detergent and lipid-soluble proteins found in the BFM should, therefore, be another attractive source of hydrophobic proteins in the latex allergens.

2.5.2 Extraction of the proteins from NRL gloves (Hev b1 and Hev b3)

According to the hydrophobic character of major latex allergens (Hev b1 and Hev b 3), research of effect of varies solvenet to extract proteins in glove such as sodium dodecyl sulfate (SDS), Triton-X-100 and phosphate buffer saline was carried out. The result of SDS-PAGE (Figure 13) showed no protein that was obtained from using phosphate buffer (lane 1) and Triton X-100 (lane 2) because a membrane protein composed of integral or peripheral membrane proteins interact with phospholipid bilayer and possess a hydrophobic property due to their solubility in isotonic buffer or mild surfactant of Triton X-100 can not break strong binding interaction between hydrophobic protein type and rubber particle. The results can be explained that phosphate buffer is not suitable for extraction protein of hydrophobic type remained on glove surface. Although, Triton X-100 buffer was suitable to extract protein from BFM in NRL as mentioned above, it revealed no proteins extract in glove product. This detergent is non-ionic with uncharged hydrophilic head groups and less denaturing properties than ionic detergents. Thus, it is not suitable to extract membrane protein which may be used disulfide linkage (S-S) between lipid bilayer of membrane particle and itself. With using SDS buffer emerged four bands protein at 14, 24 kDa. It seems that SDS detergent has more efficiency protein extraction than Triton X-100 because it allowed for the micelle formation of hydrophobic tail and hydrophilic head (Figure 13B). Solubilized membrane proteins from mixed micelles were added with detergents, which shield the hydrophobic (or transmembrane) domain of the protein from contact with the aqueous buffer.

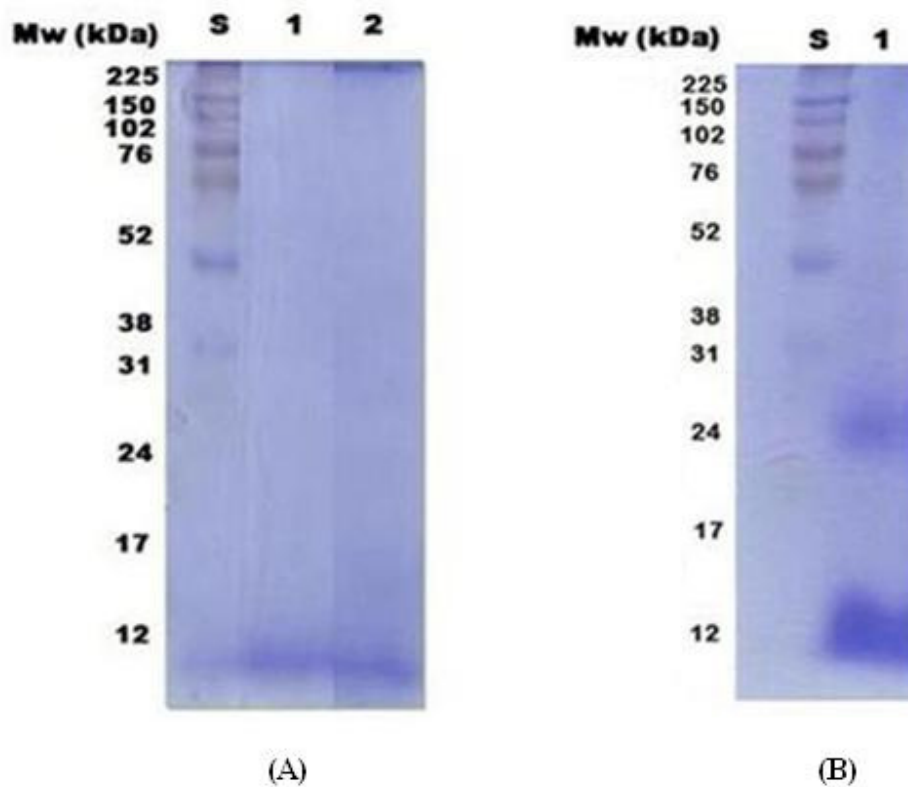


Figure 13 SDS-PAGE of an extract of allergen protein on a 12% acrylamide gel; 1 (A): protein from 0.9M NaCl in 200 M phosphate buffer at pH 7.4, 2 (A) : protein from 0.2% Triton X-100 in Tris-HCl, pH 7.4, 1 (B): protein from 0.5% SDS in phosphate buffer at pH 7.4, S: molecular weight markers

2.5.3 Determination of allergenicity of the purified proteins

In order to identify allergenicity of protein, each protein band obtained from rubber particle, BFM and glove extract were tested with serum of one patient from

Songklanagarind Hospital who has been evident-based allergic to NRL. An immunoblot is used for the detection and visualization of proteins in a mixture (Yeang *et al.*, 1996). In this case, proteins were transferred onto a membrane after one dimensional gel electrophoresis by means of electroblot. Molecules adsorbed on the membrane surface were free from the detergents and salts of the gel electrophoresis and available for the reaction with macromolecular ligands, such as antibodies. Before the detection free binding sites of the membrane have to be blocked to avoid the unspecific binding of antibodies. The membrane was then incubated with the antibodies against the protein of interest and an additional marker protein was used to identify the labeled protein. This second antibody carries a conjugate horseradish peroxidase which makes the protein-antibody complex and DAB substrate was added to form color. The proteins from SDS-PAGE were examined for their allergenicity by Western blot Figure 14 shows SDS-PAGE and Western blot analysis for rubber latex proteins. The IgE in the serum of a sensitized patient from Songklanagarind Hospital bound to two proteins (14 and 22 kDa) that were obtained from the fractin of rubber particle and glove extract. This fact indicated that multiple allergenic proteins existed in the latex serum and that two rubber latex allergens were found to be the 14 and 22 kDa. Two allergenic protein bands were observed in the lanes by SDS-PAGE, but the densities of these bands were different from those obtained from glove extract sample. None of the protein bands appeared when the control serum or the plasma was used instead of the patient's serum. The IgE binding epitopes of the major latex allergens, Hev b1 and Hev b3 may have an important role in the immune mechanism of latex hypersensitivity (Chen *et al.*, 1996).

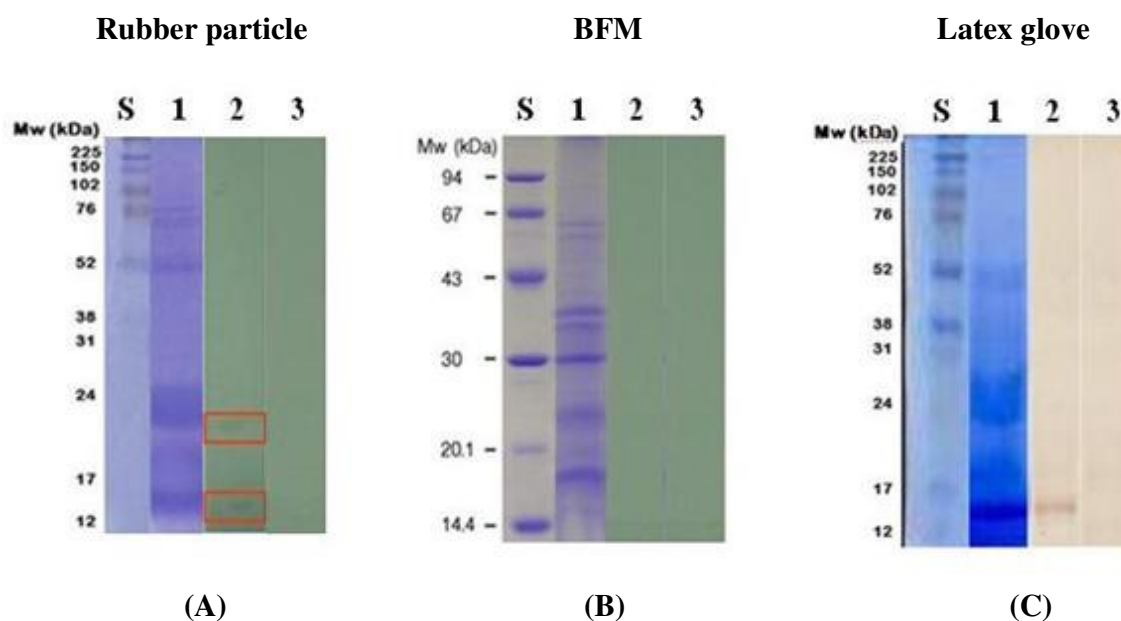


Figure 14. SDS-PAGE and Western blot of Hevein proteins of the fresh natural latex and latex glove on a 12% gel acrylamide; (A): Crude protein from rubber particle, (B): Crude protein from BFM and (C): Crude protein from latex glove. 1(A): Crude protein from rubber particle, 2(A): Crude protein from rubber particle incubated with IgE from patient sera, 3(A): Crude protein from rubber particle incubated with IgE from control sera, 1(B): Crude protein from BFM, 2(B): Crude protein from BFM incubated with IgE from patient sera, 3(B): Crude protein from BFM incubated with IgE from control sera 1(C): Crude protein from latex glove, 2(C): Crude protein from latex glove after incubating with IgE from patient sera, 3(C): Crude protein from latex glove after incubating with IgE from control sera, S: Molecular weight markers

The prevalence and severity of latex hyper-sensitivity reactions in both children and adults and involvement of B cell epitopes in the clinical manifestation of the disease which the IgE binding epitopes are located near the C-terminal regions of Hev b3 (60-69, YYIPLEAVKE), while for Hev b1 the specific epitope binding to SB patients were seen at the amino acid residues (16-25, KYLGFVQDAA) and (46-55, LQPGVDIIEG). Both allergens demonstrated significant sequence homology and showed similar IgE binding with sera from SB patients (Alenius *et al.*, 1993; Chen *et al.*, 1996 and Yeang *et al.*, 1996). Moreover, Chen and coworker (1996) mapped the B-cell epitope of Hev b1 using sera from SB patients, monoclonal antibodies and rabbit antisera against Hev b1 and identified common allergenic and antigenic epitopes in the amino acid residue of 31-64 and 121-137. In contrast to their findings, they identified a specific Hev a1 epitope having amino acid residues from 16-25 reacting with IgE of SB patients. Similarly, IgE epitopes for Hev b3 could be detected near the C-terminal region of the protein in the amino acid residue of 138-188. However, the IgE binding specificity of Hev b3 for SB patients were found to be located near the N-terminal region of the protein. Hence the specific IgE binding of these two proteins with sera from SB patients could be attributed to the presence of unique epitopes in these molecules. Finally, this result showed similarly the data obtained Jewtragoon's work that patient's sera from Siriraj and Songklanagarind Hospital revealed IgE-reactive BFM proteins in the region of 14 and 22 kDa.

2.5.4 Protein purification

In this section, the extracted proteins from NRL glove were purified. For this purpose concentrated crude (2 ml) of NRL glove was loaded onto a SephacrylTMS-100 (High Resolution) column (1.5 x 64 cm), which was equilibrated and eluted with 50 mM phosphate buffer (pH 7.4) containing 0.1% SDS and 0.15 M NaCl. Fractions of 2.0 ml were collected and examined by SDS-PAGE. The active fractions were pooled, concentrated and the sequence of target protein was confirmed using peptide mapping by MALDI-TOF. There are several influence parameters of gel filtration chromatography on the extraction of allergen protein from manufactured glove product that should be considered such as column dimension, gel filtration material, sample volumes, component of buffer solution and flow rate. For protein purification by gel filtration chromatography, column dimensions are important, shape as well as total volume a long and thin column is suitable for separation of target protein because it gave potentially good resolution. In addition to column dimension, gel filtration materials suitable for protein separation also should be considered since it gives directly resolution of target protein.

In this work, SephacrylTMS-100 (High Resolution), extra cross-linking of the dextran with acrylamide, is suitable for separation of target protein due to its large working range of 1,000 Da to 100,000 Da. Moreover, it has more rigid bead, chemical stability which can be operated under higher pressure and so faster flow rates comparable with Sephadex (cross-linked dextran). Sample application is a most important

consideration, a small volume, because the volume containing each component protein will keep increasing due to the diffusion and non-ideal flow effects. Since the effective fractionation volume is approximately half the volume of the column. This should not exceed 3% of the total column volume; smaller volumes than this will give slightly better results, down to about 1% of the column volume. Furthermore, buffer composition does not directly influence the resolution obtained in gel filtration since the separation depends only on the sizes of the different molecules. The most important consideration is the effect of buffer composition on the shape or biological activity of the molecules of interest. For example, the pH and ionic strength of the buffer and the presence of denaturing agents or detergents can cause conformational changes, dissociation of either the proteins into subunits, enzymes and cofactors, or hormones and carrier proteins. Select a buffer and pH that are compatible with protein stability and activity and in which the product of interest should be collected. Use a buffer concentration that eluent has to be desirable avoiding the side effects and the high concentration of NaCl in non-specific ionic interaction of the matrix (shown by delays in peak elution). Note that some proteins may precipitate in low ionic strength solutions. Flow rates are restricted to the maximum attainable under a buffer head which flow rates of upto 30 cm h^{-1} are recommended for Sephacryl, which flow rates of upto 30 cm.h^{-1} are recommended for Sphacryl. Rigid materials can also the elution of the target molecule which some cognizance of the manufacturer's recommendations is needed.

In this work, the composition of mobile phase was 50 mM phosphate buffer (pH 7.4) containing 0.1% SDS and 0.15 M NaCl. Phosphate buffer (pH 7.4) has a

function to control pH capacity of mobile phase system because it may affect to biological activity or conformation of target proteins. The experimental of gel filtration chromatography was performed by the use of 0.15 M NaCl due to it can be ionized as Na^+ and Cl^- and formed as opposite ion of protein which protect non-specific interaction of protein and gel matrix. Moreover, detergents are useful as solubilizing agents for proteins with low aqueous solubility such as membrane components and will not affect the separation. Note that high concentrations of detergent will increase the viscosity of the buffer so that lower flow rates may be necessary to avoid over-pressuring the column packing. If proteins that have been solubilized in a denaturant or detergent are seen to precipitate, elute later than expected or be poorly resolved during gel filtration, add a suitable concentration of the denaturing agent or detergent to the running buffer. Surfactant is important for hydrophobic protein due to its solubilization of target protein. 0.1% of SDS in buffer system can support completely separated by gel matrix with good resolution which could be seen in SDS-PAGE (Figure 15) that target protein can be completely separated from gel filtration chromatography. Detergents are useful as solubilizing agents for proteins with low aqueous solubility such as membrane components and will not affect the separation. If denaturing agents or detergents are necessary to maintain the solubility of the proteins, they are usually mixed in both the running buffer and the sample.

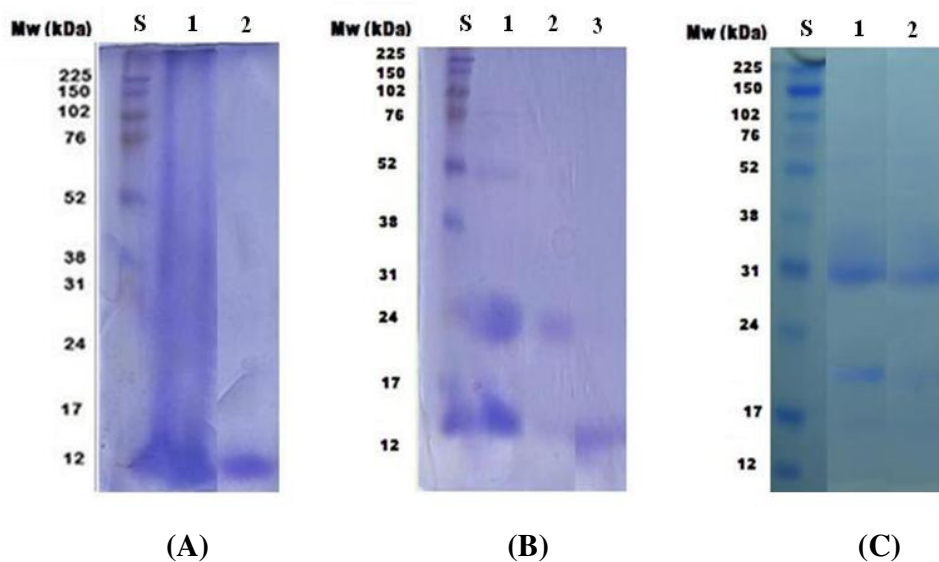


Figure 15 SDS-PAGE of an extract of the curde and purified allergen proteins from fresh natural rubber latex and latex glove on a 12% acrylamide gel with visualization by Coomassie blue staining. M: Molecular weight marker, 1(A): crude protein (14 and 22 kDa) from latex glove, 2(A): purified protein (14 kDa) from fraction number 30 of latex glove, 1(B): crude protein (14 and 22 kDa) rubber particle, 2(B): purified protein (22 kDa) from fraction number 22 of rubber particle, 3(B): purified protein (14 kDa) from fraction number 28 of rubber particle, 1(C): crude protein (35 kDa and 22 kDa) from bottom fraction membrane, 2(C): purified protein (35 kDa) from fraction number 20 of bottom fraction membrane

The target protein of glove extract could be observed from fraction number 30 on the SDS-PAGE is the molecular weight appeared at 14.0 kDa (Figure 15). Moreover, the protein of rubber particle from fraction number 22 and 28 could be observed on SDS-PAGE at 22 kDa and 14 kDa, respectively. The BFM protein from

fraction number 20 could be observed on SDS-PAGE at 35 kDa. The mechanism underlying separation system by this filtration medium is related to difference in size of proteins by which the protein molecules along with detergent were separated on SDS-PAGE. As shown in Figure 16, buffered solvent and sample moved through the column, the protein molecules diffused in and out of the pores of the matrix, which smaller molecules moved further into the matrix and so stay longer on the column. As buffer passes continuously through the column, molecules that are larger than the pores of the matrix was unable to diffuse into the pores and pass through the column. Smaller molecules diffuse into the pores and are delayed in their passage down the column. Large molecules leave the column first followed by smaller molecules in order of their size. The entire separation process takes place as one total column volume (equivalent to the volume of the packed bed) of buffer passes through the gel filtration medium.

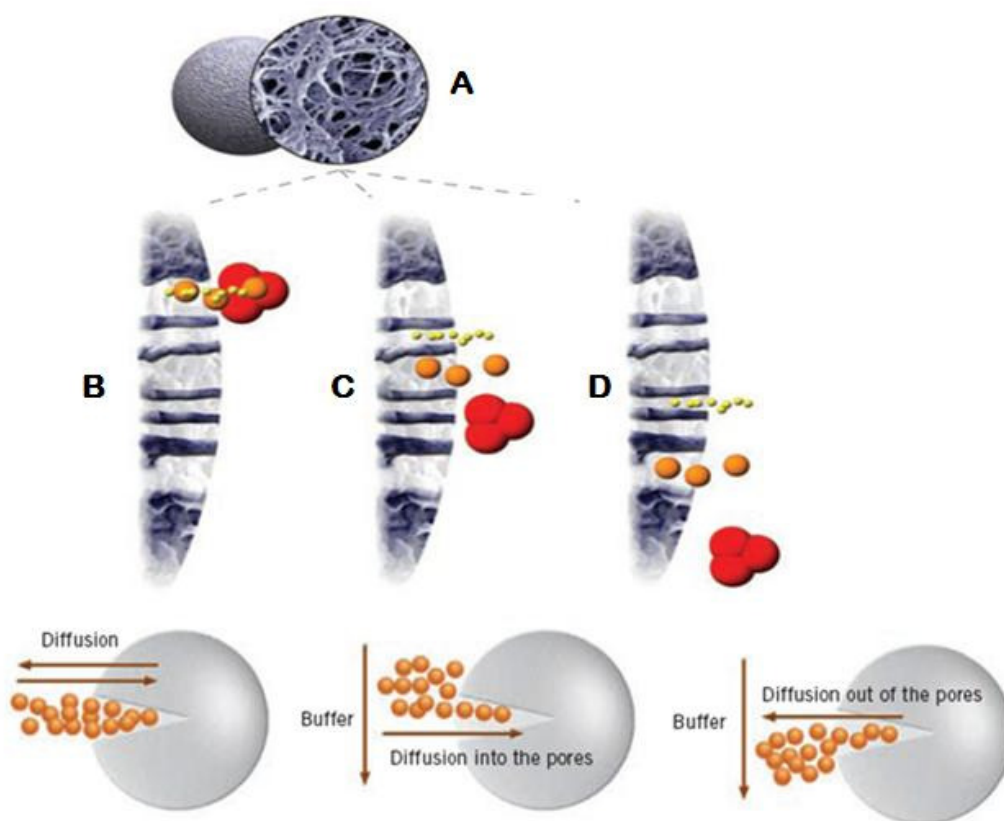


Figure 16. Process of gel filtration (Amersham, 2002)

2.5.5 Yield of extracted protein

It is currently not possible to routinely determine the total amount of protein in a NRL or rubber latex glove sample prior to solubilization. The yield of extracted proteins will therefore, by necessity, be an indirect measure. The best measurements are percentage of solubilization of total wet or dry weight of the NRL or

rubber latex glove sample or the total amount of solubilized protein per weight unit of sample, which both can readily be determined as equation (1).

$$\% \text{ Yield of protein} = \frac{\text{Total protein contain after gel filtra} \times 100}{\text{Crude protein}} \quad (1)$$

2.5.6 BCA protein assay

During a protein purification process, the measurements of the total protein and of the amount of the desired protein must be made. An assay, either quantitative or at least semiquantitative, indicating which fraction contains the most of the desired protein is essential. Measurement of total protein is useful, as it indicates the degree of purification at each step. Some of the interferences associated with the Lowry assay can be overcome by using bicinchonic acid (BCA) because this assay is stable and highly specific for cuprous ion. The reaction was carried out when peptide bond of protein first reduce cupric ion (Cu^{2+}) to produce tetradentate-cuprous ion (Cu^+) complex in alkaline medium. The cuprous ion complex then reacts with BCA (2 molecules per Cu^+ ion) to form an intense purple color that can be measured at 562 nm. The presence of four amino acids (cysteine, cystine, tryptophan, and tyrosine) in the protein is responsible for the color development.

The linear dynamic range was investigated by serial dilutions of BSA stock standard solution. The calibration curve was obtained by plotting the absorbance

versus the known concentration of analytes. Linearity is achieved when the coefficient of determination (R^2) is equal or greater than 0.990 (FDA, 2000), close to 1. The slope of the regression line provided the sensitivity. Figure 17 shows the calibration curves of BSA as a reference protein with a linear dynamic range around 10 to 100 mg/ml with UV-visible spectrophotometry. Quantitative analyzes of crude protein or purified protein was allowed on the response of the absorbance that was proportional to the amount of BSA. The purified allergen proteins in each step are able to verify by monitoring the yield that calculate from the purified protein divided by the crude protein.

Employing the purification protocol described above, the purified allergen proteins were obtained the yields of which are summarized in Table 4. The amounts between 52 to 76 mg of purified protein per lot of fresh natural rubber latex and latex glove (1 kg) were obtained in this study.

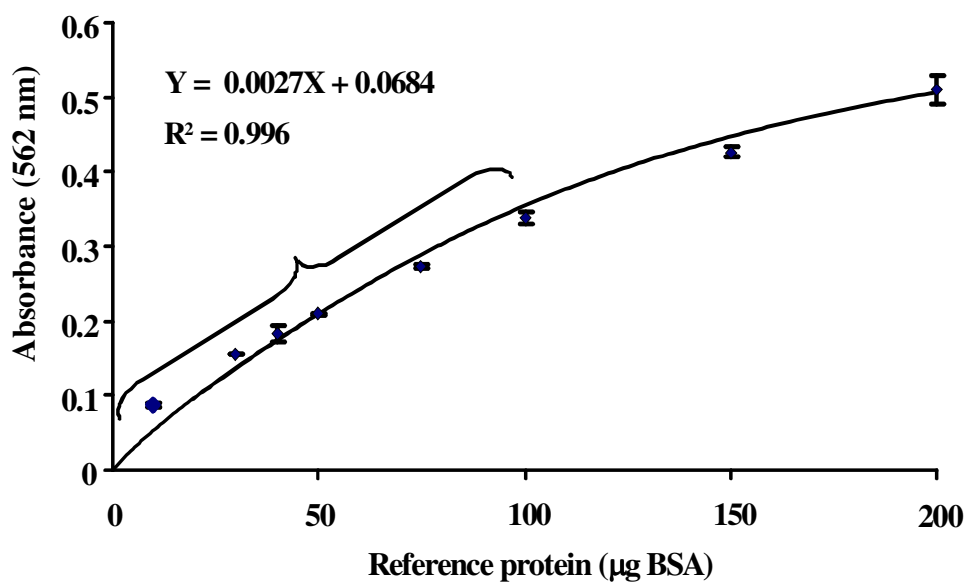


Figure 17. The linear dynamic range of BCA assay using BSA as a protein reference

Table 4. Purified allergen protein from NRL and NRL glove samples

Treatment	Total protein (µg)			
	Hev b1 (G)	Hev b1 (L)	Hev b2 (L)	Hev b3 (L)
Crude extracted	5250±630	8950±188	8950±188	8950±188
Gel filtration	3710±105	4820±160	730±20	1780±33
% Yield	70	53	8	19

2.5.7 Determination of molecular weight of allergen protein by SDS-PAGE

Subunit molecular weight of protein samples were evaluated by SDS-PAGE, since the migration of protein is proportional to the mass. A standard curve is generated from proteins of known molecular weight (known as standard proteins), and the molecular weight of unknown protein is determined from the curve. The standard curve is obtained by plotting the relative mobility (R_f) value (in x-axis) and \log_{10} of the molecular weight (in y-axis). R_f value is determined as follows equation (2).

$$R_f = \frac{\text{Distance of protein migration}}{\text{Distance of tracking dye migration}} \quad (2)$$

The molecular weight of proteins obtained from each source were determined by a SDS-PAGE method (Pingoud *et al.*, 2002) in subunit form as shown in Fig. 18-21. The B-serum fraction had five proteins of 11.5, 14.8, 24.4, 40.5 and 52.1 kDa band on SDS-PAGE (Figure 18). The BFM fraction showed seven protein bands at 17.2, 23.5, 31.7, 38.2, 40.7, 60.1, 65.1 kDa (Figure 19). whilst glove extract gave two protein bands at 13.2 and 29.5 kDa (Figure 20) and rubber particle showed two protein bands at 13.9 and 23.0 kDa (Figure 21). Subsequently all the purified proteins were identified by MALDI TOF-MS as a finally step.

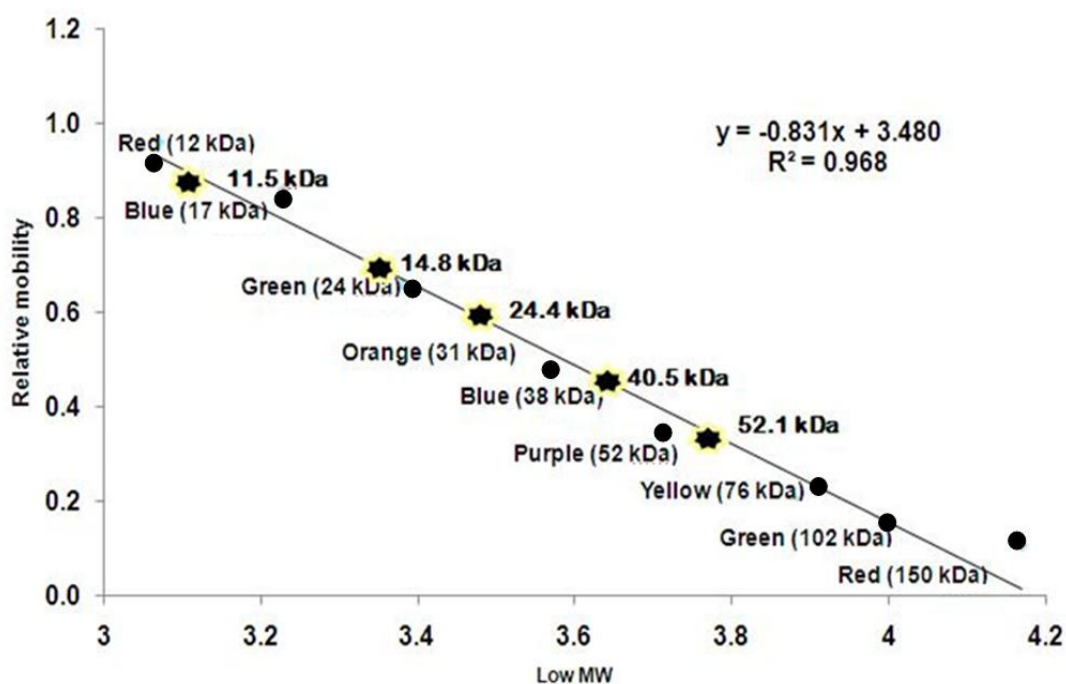


Figure 18. Molecular weight of protein obtained from B-serum by SDS-PAGE

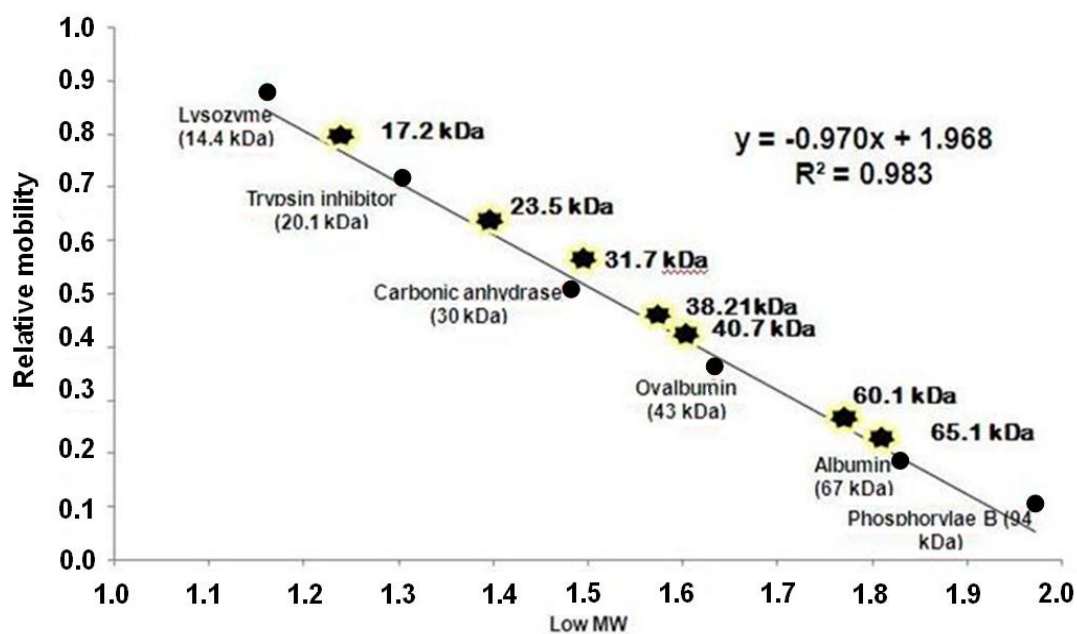


Figure 19. Molecular weight of protein obtained from bottom membrane by SDS-PAGE

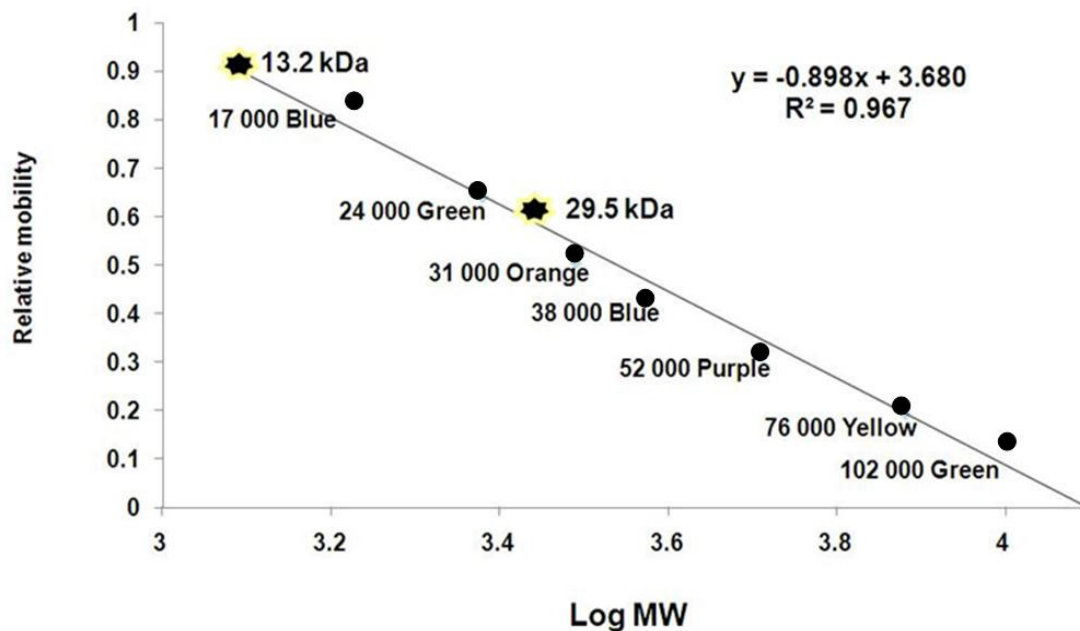


Figure 20. Molecular weight of protein obtained from rubber particle extract by SDS-PAGE

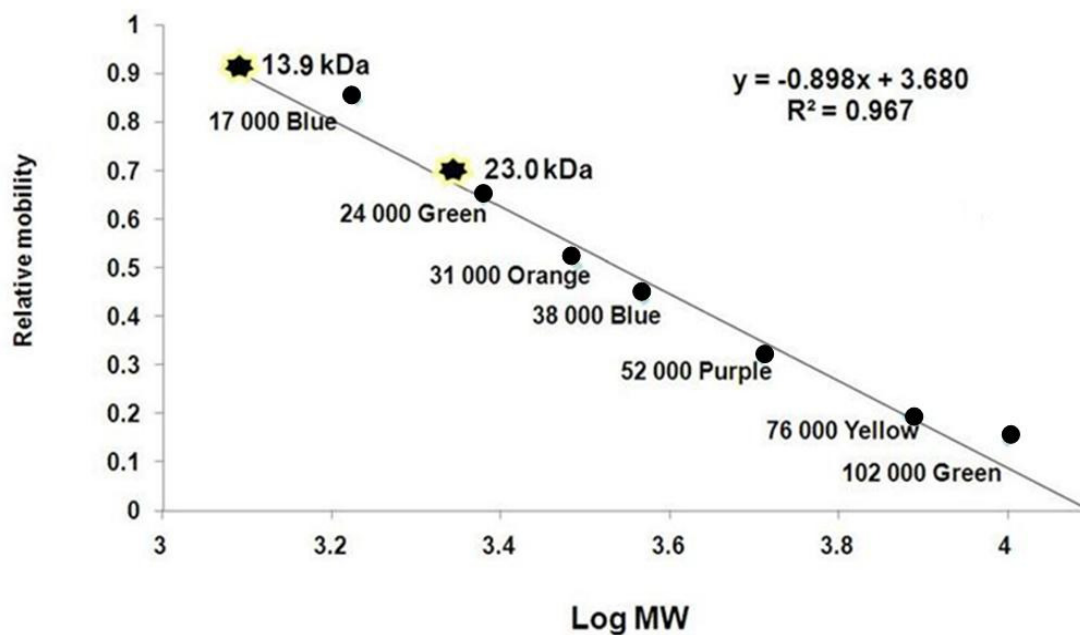


Figure 21. Molecular weight of protein obtained from glove extract by SDS-PAGE

2.5.8 MALDI-TOF-MS Spectrometry

The BFM fractions contain six protein bands on SDS-PAGE, two bands of glove extract and two bands of rubber particle were appeared. These protein bands were verified further by means of MALDI-TOF and their mass spectrum would be evaluated and peptide sequences were compared to those from standard data bank of NCBI NR database (Perkins *et al.*, 1999). The protein bands visualized by Coomassie staining and separated proteins for each lane were shown in Figure 22 for BFM (BM1, BM2, BM3, BM4, BM5 and BM6), glove extract (G1, G2 and G3) and rubber particle (PR1 and RP2). The protein bands were then cut and completely destained and the intact protein were extracted from the gel pieces. The solutions containing the proteins of interest were concentrated and then examined by MALDI-TOF spectrometry in a vacuum concentrator. CHCA was used as MALDI matrix and the “sandwich” method was applied to MALDI-TOF spectra.

Typically, mass fingerprint of a pure protein or a very simple mixture can be obtained by a procedure of proteases and/or chemicals. Trypsin is a very stable and efficient protease that specifically cleaves at the C-terminal side of lysine and arginine residues. Trypsin cleavage of proteins produce a basic residue at the carboxy-terminus and with the right size to be useful for detection and and it is possible in sequencing by a mass spectrometry. The mixture of peptides was analysed by mass spectrometry, this yields a set of molecular mass values, which is able to be searched to match a database of protein sequences by using a search engine. For each entry in the

protein database, the search engine simulates the known cleavage specificity of the enzyme, calculates the masses of the predicted peptides, and compares the set of calculated mass values with the set of experimental mass values. Some type of scoring is used to identify the entry in the database that gives the best match, and a report is generated.

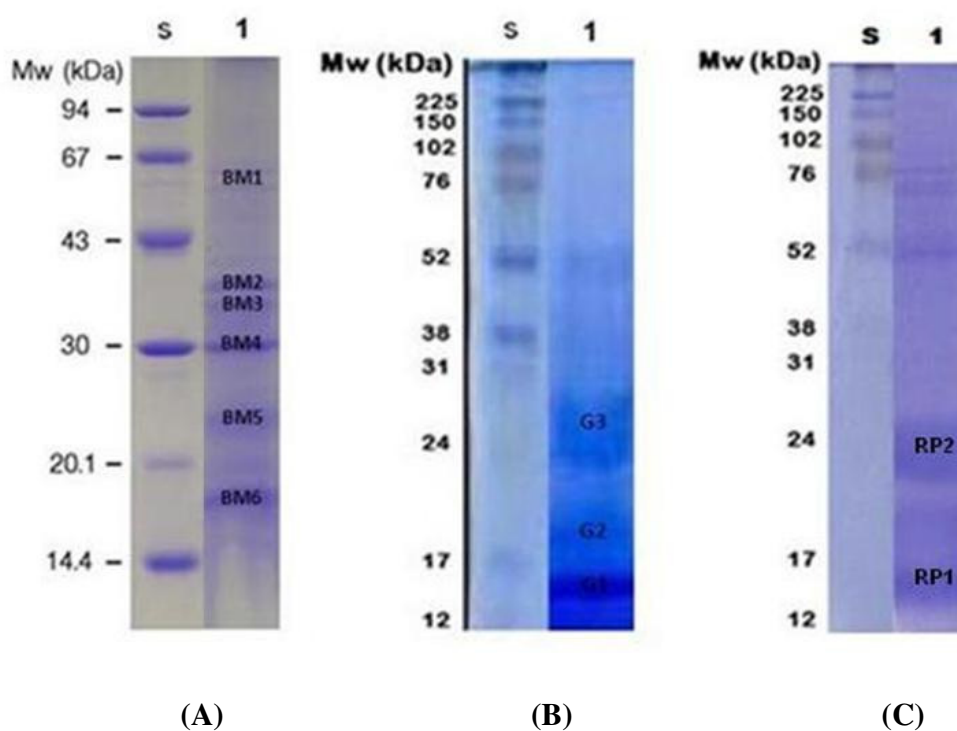


Figure 22. SDS-PAGE of NRL extraction (A): BFM, (B) glove extract and (C) rubber particle for in-gel digestion

Peptide mass fingerprint data from MALDI-Q-TOF were compared match the protein candidates in NCBIInr, MSDB and Swiss-Prot protein databases.

Further, the product ion spectra data of MALDI-TOF MS mass spectrometry were then compared against the NCBI Inr and Swiss-Prot databases and an exact match was found through the Mascot search program (Wan et al., 2001; Ahram et al., 2002). Database searching (NCBI Inr) and protein identification were performed with the Mascot computer program (Matrix Sciences, London, UK) according to a recently described procedure (D'Amato et al., 2010) and recorded as in Table 5. Peptide identifications were accepted if they could be established at greater than 95.0% probability as specified by the Peptide Prophet algorithm (Craig, 2004) as listed in Table 6-9. Figures 23-26 show some mass spectra of the rubber latex allergen proteins of this study.

After the enzymatic digestion the extracted proteins were identified to be beta-1, 3-glucanase (Hev b2, L) from BM3 and BM4, rubber elongation factor (Hev b1, G) from GE1 and rubber elongation factor (Hev b1, L) and small rubber particle protein (Hev b3, L) from RP1 and RP2, respectively. Table 5 shows the score and sequence coverage (%) MALDI-TOF MS spectrum of beta-1, 3-glucanase, rubber elongation factor (GE1), small rubber particle and bottom membrane. The percentage sequence coverage showed the degree of matching between the amino acid sequence of purified protein and protein form data bank. Moreover, the data of molecular weight and *pI* values of purified allergen proteins from BFM fractions, glove extract and rubber particle in NRL are shown in Table 5.

Table 5. MS analysis data, molecular weight and pI of allergen proteins in NRL and rubber glove samples

Protein purification	Protein Name	MW (Da)	pI	Score	Sequence coverage	Allergen protein
BM3	Beta-1, 3-glucanase	41543	9.4	88	35	Hev b2 (L)
BM4	Beta-1, 3-glucanase	41543	9.4	87	34	Hev b2 (L)
GE1	Rubber elongation factor (REF)	14713	5.0	74	68	Hev b1 (G)
RP1	Rubber elongation factor (REF)	14713	5.0	132	68	Hev b1 (L)
RP2	Small rubber particle	22331	4.8	117	89	Hev b3 (L)

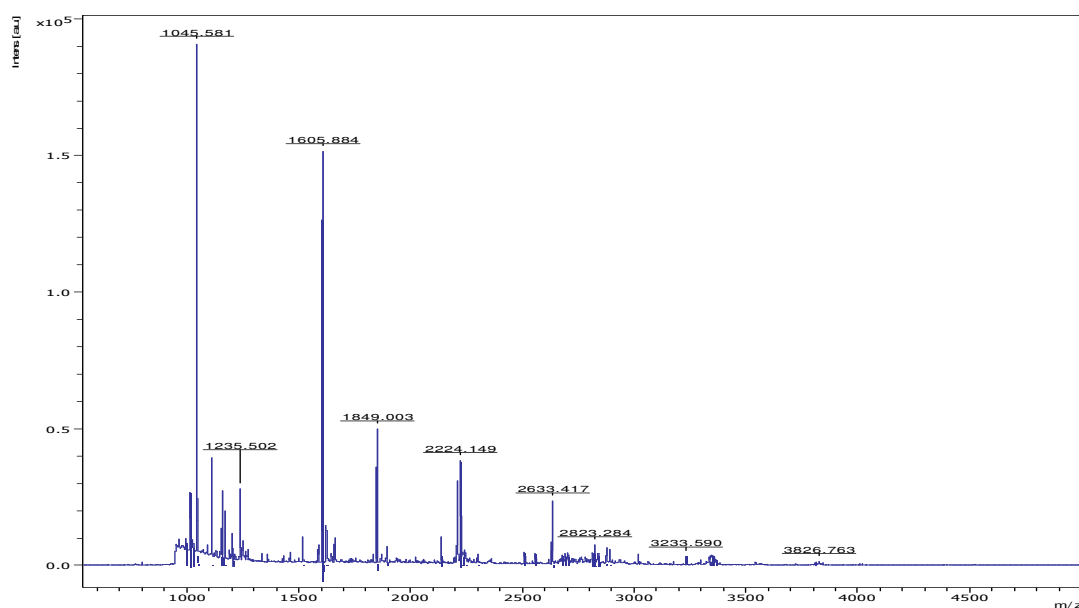


Figure 23. MALDI-TOF-MS spectrum of Hev b1 (G) within glove extraction (GE1) obtained by eluting from the gel pieces with methanol solvent and prepared with CHCA

Table 6. Tryptic peptides assigned to REF after the investigation of the protein originating from band GE1 and sequence coverage of the identified peptides

Amino acid residues ¹	Molecular mass ¹	# ²	Sequence ¹
43-58	1605.8	0	K.SGPLQPGVDIIEGPVK.N
59-67	1045.5	0	K.NVAVPLYNR.F
68-77	1109.6	0	R.FSYIPNGALK.F
78-92	1621.8	0	K.FVDSTVVASVTIIDR.S
100-110	1158.6	0	K.DASIQVVS AIR.A

¹according to the NCBI NR database

²number of missed cleavages

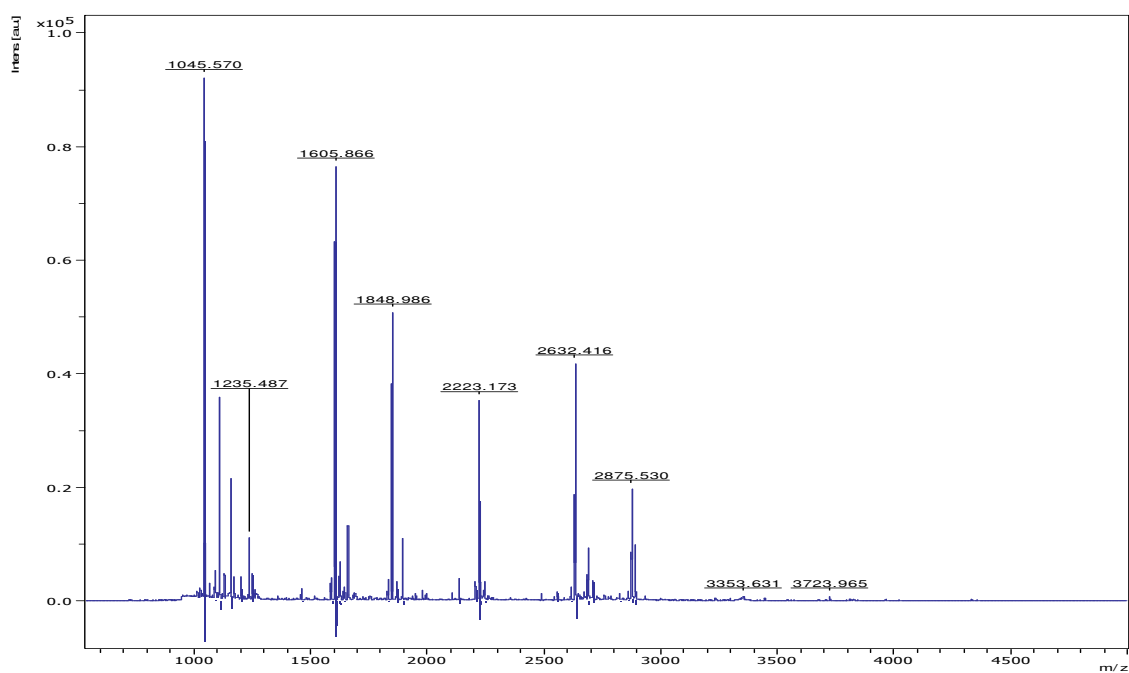
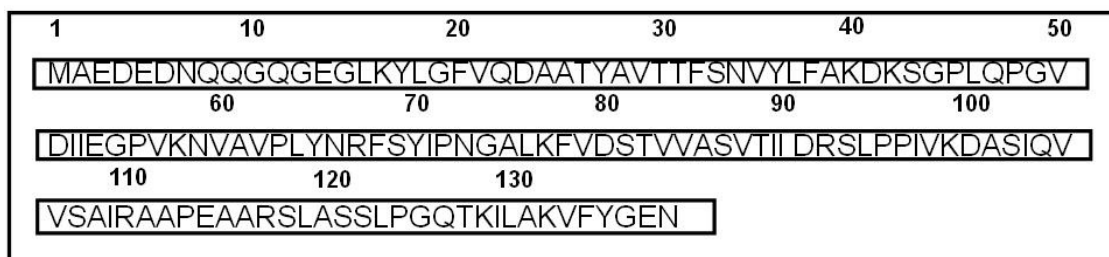


Figure 24. MALDI-TOF-MS spectrum of Hev b1 (L) within rubber particle (RP1) obtained by eluting from the gel pieces by methanol solvent and prepared with CHCA

Table7. Tryptic peptides assigned to rubber elongation factor protein originating from RP1 band after sequence coverage of the identified peptides

Amino acid Residues ¹	Molecular mass ¹	# ²	Sequence ¹
17 - 40	2689.3375	0	K.YLGFVQDAATYAVTTFSNVYLFAK.D
41 - 58	1848.9858	1	K.DKSGPLQPGVDIIEGPVK.N
43 - 58	1605.8658	0	K.SGPLQPGVDIIEGPVK.N
43 - 67	2632.4156	1	K.SGPLQPGVDIIEGPVKNVAVPLYNR.F
59 - 67	1045.5699	0	K.NVAVPLYNR.F
59 - 77	2136.1315	1	K.NVAVPLYNRFSYIPNGALK.F
68 - 77	1109.5877	0	R.FSYIPNGALK.F
78 - 92	1621.8527	0	K.FVDSTVVASVTIIDR.S
93 - 110	1893.0942	1	R.SLPPIVKDASIQVVS AIR.A
100 - 110	1158.6362	0	K.DASIQVVS AIR.A

¹according to the NCBI NR database

²number of missed cleavages

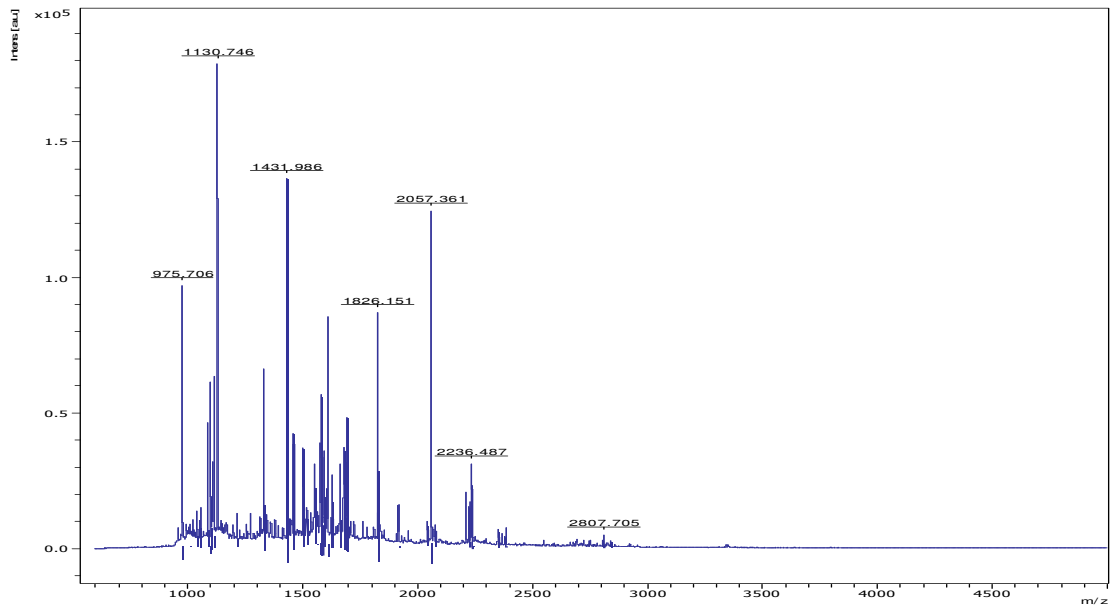
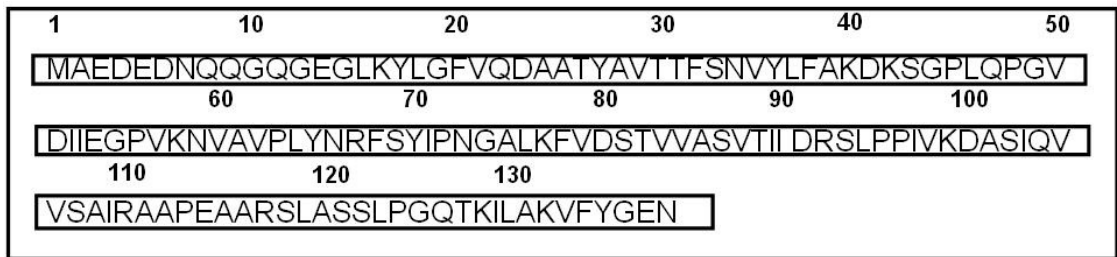


Figure 25. MALDI-TOF-MS spectrum of the Hev b2 (L) within bottom membrane obtained from eluting from the gel pieces by methanol solvent and prepared with CHCA

Table 8. Tryptic peptides assigned to beta-1, 3-glucanase originating from BM band after sequence coverage of the identified peptides

Amino acid Residues ¹	Molecular mass ¹	# ²	Sequence ¹
69 - 81	1502.0	0	R.IYDPNQAVLEALR.G
124 - 136	1431.9	0	R.YIAVGNEISPVNR.G
137 - 150	1577.1	0	R.GTAWLAQFVLPAMR.N Oxidation (M)
167 - 188	2236.5	0	K.VSTAILTLVGNSYPPSAGAFR.D
193 - 200	975.7	0	R.SYLNPIIR.F
207 - 224	2057.4	0	R.SPLLANIYPYFTYAGNPR.D
225 - 245	2350.6	0	R.DISLPYALFTSPSVVWWDGQR.G
249 - 264	1812.2	0	K.NLFDATLDALYSALER.A
335 - 343	1106.8	0	K.HFGLFFPNK.W

¹according to the NCBI NR database

²number of missed cleavages

1	10	20	30	40	50
MAISSSTSGTSSSLPSRTTVMLLLFFFTASVGITDAQVGVICYGMQGNLPPV					
60	70	80	90	100	
SEVIALYKKSNIITRMRIYDPNQAVLEALRGSNIELILGVPNSDLQSLTNPSNAK					
110	120	130	140	150	
SWVQKNVRGFWSSVRFRIYAVGNEISPVNRGTAWLAQFVLPAMRNIHDAIR					
160	170	180	190	200	210
SAGLQDQIKVSTAILTLVGN SYPPSAGAFRDDVRSYLNPIIRFLSSIRSPLLA					
220	230	240	250	260	
NIYPYFTYA GNPRDISLPY ALFTSPSVV WDGQRGYKNLFDATLDALYSAL					
270	280	290	300	310	
ERASGGSLEVWVSESGWPSAGAF AATFDNGRTYLSNLIQHVKRGTPKRPKR					
320	330	340	350	360	
AIETYLEAMFDENKKQPEVEKHFGLEFFPNKWQKYNLNFSAEKNWDISTEHNA					
370					
TILFLKSDM					

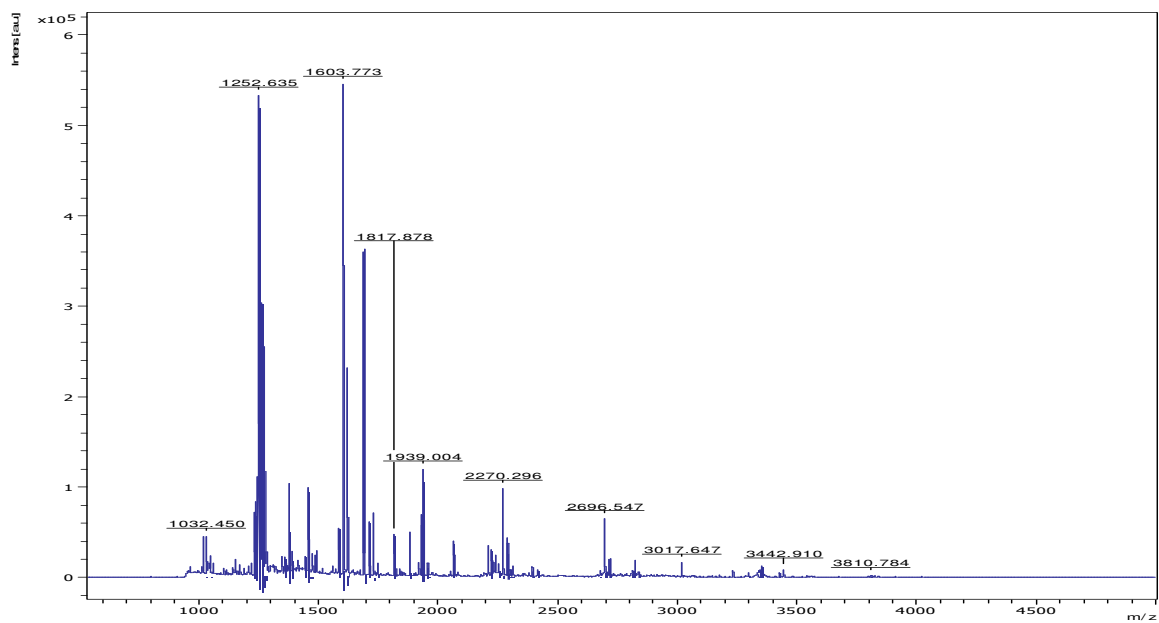


Figure 26. MALDI-TOF-MS spectrum of Hev b3 (L) within rubber particle (RP2) obtained by eluting from the gel pieces and prepared with CHCA

Table 9. Tryptic peptides assigned to beta-1, 3–glucanase (Hev b3, L) originating from RP2 band after sequence coverage of the identified peptides

Amino acid Residues ¹	Molecular mass ¹	# ²	Sequence ¹
1 - 1	1378.5384	1	-.MAEEVEEERLK.Y Oxidation (M)
18 – 35	1939.0036	0	R.AAGVYAVDSFSTLYLYAK.D
36 – 53	1881.0490	0	K.DISGPLKPGVDTIENVVK.T
54 – 68	1691.9815	0	K.TVVTPVYYIPLEAVK.F
69 – 90	2314.2630	1	K.FVDKTVDVSVTSLDGVVPPVIK.Q
73 – 105	3426.8182	1	K.TVDVSVTSLDGVVPPVIKQVSAQTYSVAQDAPR.I
106 – 124	1934.0426	0	R.IVLDVASSVFNTGVQEGAK.A
125 – 133	1018.5608	0	K.ALYANLEPK.A
134 – 143	1236.6067	0	K.AEQYAVITWR.A
144 – 168	2696.5469	1	R.ALNKLPLVPQVANVVVPTAVYFSEK.Y
148 – 168	2270.2960	0	K.LPLVPQVANVVVPTAVYFSEK.Y
175 – 194	2239.1660	1	K.LPLVPQVANVVVPTAVYFSEK.Y
183 – 194	1346.7524	0	R.VSSYLPLLPTTEK.I

¹according to the NCBI NR database

²number of missed cleavages

1	10	20	30	40	50
MAEEVEEEERLKYLDFVRAAGVYAVDSFSTLYLYAKDISGPLKPGVDTIENVVK					
60	70	80	90	100	
TVVTPVYYIPLAVKFDKTVDVSVTSLDGVVPPVIK QVSAQTYSVAQDAPRI					
110	120	130	140	150	
VLDV ASSVENTGVQ EGAKALYANL EPKAEQYAVI TWRALNKLPL VPQVAN					
160	170	180	190	200	
VVVPTAVYFSEKYNDVVRGTTTEQGYRVSSYLPLL PTEKITKVFGEAS					

The mass spectra data showed that beta-1, 3-glucanase (Hev b2, L) had 33.5 Da and *pI* value of 9.4, rubber elongation factor of 14.7 Da and *pI* value 5.0 and M.W. of small rubber particle 22.3 Da and *pI* = 4.8, respectively. Mascot search algorithm with a probability-based MOWSE scoring algorithm was used for identifying peptide mass fingerprint by which length of peptide, mass accuracy and fragment ion series were used to calculate probability-based ions score for each peptide. Probability is calculated based on the match between observed experimental data and the database sequence as a random event. The significance of this match is calculated based on the size of the sequence database. Figure 27 shows the example of procedure for Mascot searching database protein which there are ten steps to obtain the finally identification protein.

The screenshot shows the Mascot MS/MS Ions Search interface with the following fields and callouts:

- 1:** Select the database that you want to search the dataset against. (Database dropdown)
- 2:** Select enzyme used for digestion. (Enzyme dropdown)
- 3:** Select fixed and variable modifications according to the experimental set up. (Fixed and Variable modifications dropdowns)
- 4:** Select peptide charge. (Peptide charge dropdown)
- 5:** Select peptide tolerance and MS/MS tolerance at appropriate values. (Peptide tol. and MS/MS tol. dropdowns)
- 6:** Browse and select peak list for search. (Data file field)
- 7:** Select data format, and instrument used for acquiring spectra. (Data format and Instrument dropdowns)
- 8:** Select number of allowed missed cleavages for search. (Allow up to dropdown)
- 9:** (Callout for the 'Allow up to' dropdown)
- 10:** Click on "Start search". (Start Search button)

The interface includes the following text and fields:

{MATRIX} {SCIENCE}

Mascot > MS/MS Ions Search

MASCOT MS/MS Ions Search

Your name: Yo Email: yo@unimelb.edu

Search title: The most important search

Database: [dropdown]

Textonomy: All entries

Enzyme: Trypsin

Allow up to: 2 missed cleavages

Fixed modifications: ITRAQ (K), ITRAQ (N-term), ITRAQ (N), ITRAQ (K), ITRAQ (R), ITRAQ (Q), ITRAQ (Y), ITRAQ (Z), ITRAQ (G), ITRAQ (H), ITRAQ (I), ITRAQ (L), ITRAQ (M), ITRAQ (N), ITRAQ (O), ITRAQ (P), ITRAQ (R), ITRAQ (S), ITRAQ (T), ITRAQ (V), ITRAQ (W), ITRAQ (X), ITRAQ (Y), ITRAQ (Z)

Variable modifications: Silac (R)-heavy, IMMS (C), Oxidation (M), Deamidation (NQ), Pyro-glu (N-term Q)

Protein mass: [input] kDa ICAT:

Peptide tol. ±: 0.7 Da MS/MS tol. ±: 0.3 Da

Peptide charge: 1+ Monoisotopic: Average:

Data file: [input] Browse...

Data format: Mascot generic Precursor: [input] m/z

Instrument: MALDI-TOF-TOF

Overview: Report top: AUTO hits

Start Search ... Reset Form

Click on "Start search".

Figure 27. Illustration of operating procedure in Mascot search algorithm with a probability-based molecular weight searching scoring algorithm for peptide mass fingerprint (Perkins, 1999)

2.6 Conclusion

Allergen proteins have been successfully isolated and purified from fresh natural rubber latex and latex glove by using mechanical lysis with buffer solution containing detergent (0.2% Triton X-100 or 0.5% SDS) at pH 7.4 as the first step to release target protein from the cell. To enable the high purified protein allergens gel-filtration chromatography was used to separate the mixture protein according to size distribution of SephacrylTMS-100 (High Resolution), extra cross-linking of the dextran with acrylamide, which is suitable for separation of target protein due to its large working range of 1,000 Da to 100,000 Da. Purification protein of each step for purification of protein method could be evaluated by observation the percentage yield of purified protein using BCA assay or SDS-PAGE. Finally, purified allergen protein were characterized and identified by mass spectra to confirm the structure of peptide using MALDI-TOF-mass spectrometer. All the extracted and purified latex allergen protein obtained were used for further investigation of biosensor and application in following chapter.

CHAPTER 3

STUDIES FOR PROTEIN IMPRINTING SURFACE ONTO A SUBSTRATE USING A POLYMERIZABLE MONOMER

3.1 Introduction

Conventional bulk molecular imprinting is generally perceived as being inappropriate for large molecular such as proteins. During imprinting they may become permanently entrapped on damaged and during rebinding mass transfer is poor. To avoid these issues it was proposed to complex Hev b1 molecule in aqueous solution with bifunctional molecule species and subsequent attach them to functionalized cellulose surfaces before incorporation within a thin polymer film to create protein specific sites. The design and fabrication of protein imprinting surfaces, which exhibit improved binding kinetic and high mass transfer characteristics were carried out in this study. Imprinting protein template are low dynamic diffusion in polymer matrix and much function on their surface area could be generated non-specific binding sites. Moreover, they have a flexible structure and conformation could be easily affected from temperature or environmental changes (Nicholls and Rosengren 2002 and Turner et al., 2006). Two major strategies for creating polymeric receptors targeting proteins were proposed in this

study. First, functional groups forming strong template interactions with the target molecules are commonly used such as electrostatic and metal-chelating groups. Second, shape interactions between the template molecule and the synthetic receptor can be exploited including weak interaction (hydrophobic and hydrogen bonding) have also been employed. Moreover, surface imprinting of protein is alternative strategies to generate artificial recognition site through non-covalent interaction (ionic interaction, H-bond, and hydrophobic interaction). There are several advantages such as high accessibility and high selectivity when compared with bulk molecular imprinting (Bossi *et al.*, 2007 and Hansen, 2007).

The generating of artificial receptor for latex allergen protein recognition onto an immobilized membrane was investigated to gain a better understanding in the molecular feature, physical and chemical stability of template protein. For this aim, bacterial cellulose (BC) membrane and glass filter membrane were selected as a substrate for studying protein surface-imprinting, since they have high porosity, and good water absorption with a high mechanical stability (Hu *et al.*, 2009; Guo, 2003). Copolymer made either methacrylic acid (MAA) acrylamide (ACM), styrene (SY) or itaconic acid (ITA) as a functional monomer and ethylene glycol dimethacrylate (EGDMA) or *N,N'* methalenebis acylamide (BAAm) as a crosslinker in the presence of Hev b1 (G) in pH 7.4 buffer as porogen solvent. The parameters affected to imprinting factor during polymerization process were determined and such prepolymer mixture would further be employed in investigation of sensor application.

3.2 Objective

To investigate the polymerization composition of MIP for imprinting latex protein Hev b1 on the polymer and evaluation of immobilized membrane after templating polymerization.

3.3. Experimental

3.3.1 Chemicals and instruments

All solvents were of analytical grade and were dried with a molecular sieve prior to use. Methacrylic acid (MAA), styrene (SY), acrylamide (ACM), itaconic acid (ITA), ethylene glycol dimethacrylate (EDMA), *N-N'*-(1,2-dihydroxyethylene)bisacrylamide (DHE-BAAm) were obtained from Aldrich Chemical Company (Milwaukee, WI, USA). 2,2'-Azobisisobutyronitrile (AIBN) was purchased from Janssen Chimica (Geel, Belgium). MAA and EDMA were purified by distillation under reduced pressure. A bacterial cellulose membrane was locally obtained in Songkla and glass fiber filter membrane, pore size: 0.2 μm and diameter of 46 mm was obtained from Whatman Ltd. (Kent, England).

3.3.2 Preparation of Hev b1 imprinted polymer thin-film

The preparation of isopropenylate derivatives of cellulose and glass fiber filter membrane was carried out in this study using two step grafting procedure to yield a MIP by in situ copolymerization. The bacterial cellulose and glass fiber filter membranes were cut into a small circle (0.5 cm x 2 mm) and reacted with 3-trimethoxysilyl methacrylate (3-MPS) in toluene solution at 80 °C for 5 hr. After the completed reaction, the resulting membrane was then thoroughly washed with methanol and dried in vacuum overnight. A series of molecularly imprinted polymers (MIP1, MIP2, MIP3, MIP4 and MIP5) and corresponding non-imprinted polymers (NIP1, NIP2, NIP3, NIP4 and NIP5) were prepared using thermal polymerization involving free-radical mechanism of initiator. For the typical preparation procedure of grafted MIP layer, the polymerizing compositions as listed in Table 10 were dissolved in 500 μL of phosphate buffer (pH 7.4) containing 0.2% SDS and 0.15 mg of AIBN was added. The mixtures were sonicated and purged with nitrogen for 5 min. The mixtures were pre-polymerized at 70 °C for 15 min until reaching gel point and 50 μL of protein template (concentration of 1.0 mg L^{-1}) was added in the mixture. A 50 μL of pre-polymerization of protein imprinting was coated on both the functionalized bacterial cellulose membrane and glass fiber filter membrane. The coated membranes were then purged with nitrogen for 5 min and polymerized by heating in a hot-air oven at 60 °C for 24 hr. The non-imprinted control polymers were prepared as the same method above without protein template. The template removal of each grafted-MIP membrane was performed by rinsing with 0.1% SDS in water and followed with

0.1% SDS in 10% acetic acid solution. Complete extraction of the template protein in a rinse solution of immobilized membrane was measured by BCA and SDS PAGE. Finally, the resultant membrane was dried under vacuum and stored at ambient temperature prior to use.

Table 10. Polymer compositions of Hev b1-molecular imprinted polymer

MIP/NIP	Monomer (mmole)				Cross-linker (mmole)	
	MAA	ACM	ITA	SY	BAAm	EDMA
MIP1	0.4	0.4			0.2	
MIP2	0.4	0.4				0.2
MIP3		0.4	0.4		0.2	
MIP4	0.4		0.4		0.2	
MIP5			0.4	0.4	0.2	

3.3.3 Characterizations of MIP and NIP membranes

A silanized coupler as an additional anchor for the MIP was confirmed by FT-IR spectroscopy, but the result turned out as no peak of vinyl group occurred in the IR spectrum (data not shown). The morphology of membranes before and after

immobilization with MIP formulation was examined by scanning electron microscope and confocal laser scanning microscopy (CLSM).

3.3.4 Binding experiment

The ability of the MIPs prepared to selective recognizing the template molecule in comparison to the corresponding NIP control polymer was evaluated in phosphate buffer, pH 7.4 after equilibration of the polymers with a protein solution. In a typical binding assay, each membrane was added to 200 μ l of phosphate buffer containing 50 μ g of the protein solution and incubated at 25 °c for 24 h. The free Hev b1 molecule in the solution was analysed by adding BCA and absorbance of an aliquous as measured at 562 nm. The quantity of Hev b1 protein was determined by reference to a calibration curve. The amount of bound protein was obtained by subtracting the amount of free protein from the total amount of the protein added. The imprinting factor (α), which represented the effect of the imprinting process, was the ratio of the amount of substract bound by the MIP to that bound by the corresponding NIP.

3.4 Results and Discussion

3.4.1 Preparation of Hev b1-MIP in cellulose and glass membrane

The cellulose membrane and glass membrane surfaces were incorporated with MIP into polymer matrix at free hydroxyl group, subsequently this was then charged with 3-MPS to yield a repeating vinyl anchor group for MIP formulation (see Figure 28). The physical properties of membrane before and after immobilization were investigated. Micro-porous and roughness of the membrane during reaction with 3-MPS can be observed by SEM (Figure 29). The modified vinyl groups of surface membrane were generated via silane coupling procedure. Hydrolysable group of methoxy in $(\text{CH}_3\text{O})_3\text{SiCH}_2\text{CH}_2\text{CH}_2\text{CH}=\text{CH}_2$ was hydrolyzed and then silane coupling reacted hydroxyl group (OH) of a thin-layer membrane yielding of a generation of methacryloxy group and extension of cross-linked polymerization in the presence of protein template.

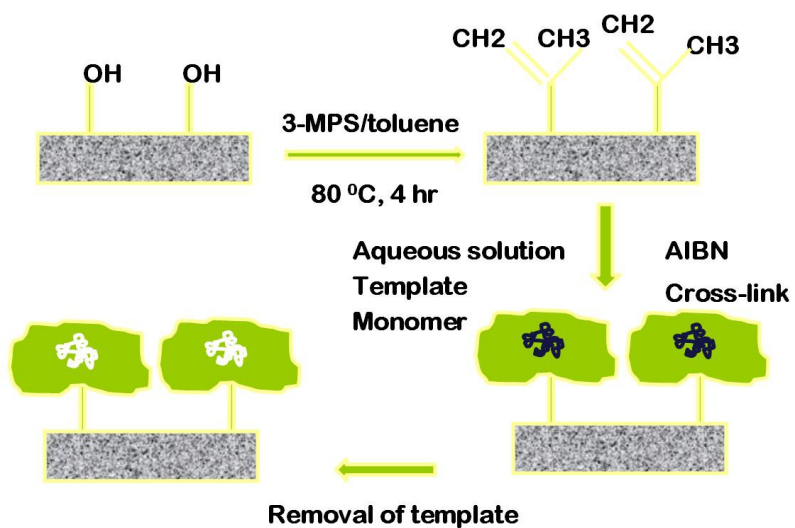


Figure 28. The incorporation of surface-molecular imprinted polymer into the polymer matrix onto the substrate

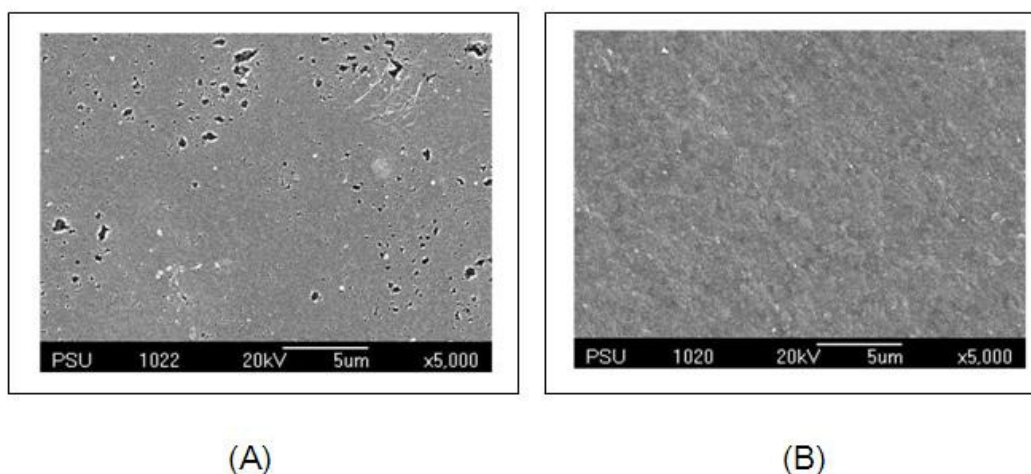


Figure 29. Scanning electron microscopy images of bacterial cellulose membrane (A) before and (B) after grafting with a MIP layer

In order to generate protein imprinting with high selective and good recognition for sensitive layer, the effect of physical parameters on protein imprinting of membrane surface was studied with regard to selectivity, robustness and adhesion of MIP layer on a substrate. First of all, in order to generate protein imprinting with high selectivity, the mixture of protein imprinting system containing protein template was prepared in aqueous solution (20 mM of phosphate buffer at pH 7.4) to maintain protein stability and their conformation which is necessary to imprinting effect during polymerization process.

The monomers were selected regarding self-assembly interaction of ionic interaction, H-bonding, hydrophobic interaction. As a result, the most common functional

monomer methacrylate acid (MAA) was used due to their acidic proton can be changed to be basic groups on the Hev b1 molecule. Moreover, acrylamide (ACM) was taken as a functional monomer because the amide group of ACM has advantageous of hydrogen bonding with the pH amine groups of protein molecule. In addition to bifunctional monomer species such as styrene was also employed in polymerization procedure because it can bind protein template via hydrophobic interaction in aqueous medium. In spite of monomer used as as component for protein imprinting, cross-linkers is important for imprinting protein molecule because the cross-linking monomer stabilized the prepolymer complex and maintain the binding site with the rigidity. A cross-linker, EGDMA gives high compactness inert and a high physical property with respect to rigidity of polymer structure was investigated and BAAM generates an imprinted polymer that is soft polymer which may reduce mass transfer of protein in polymer matrix was also investigated.

Imprinted polymer MIP1 from copolymerization between the functional monomer methacrylic acid and acrylamide and cross-linking agent, bis-methylenebiscrylamide was produced. However, MIP 2, 3, 4 and 5 consist of itaconic acid or ethylene glycoldimethacrylate as the cross-linking monomer the polymer can not be produced in aqueous solution and precipitated in solution. Therefore, MIP 1 is suitable for preparation of a grafting MIP layer on a thin-film. The result obtained described that the solubilizing of monomeric mixture is necessarily desirable since the polymer-complexes formed between the functional monomer and the templates may precipitate from solution during bulk polymerization.

The physical property and morphology templated polymer of cellulose and glass fiber membrane were investigated by CLSM. FITC was used to form a complex to protein template. The CLSM measurement of the MIP membrane was performed at maximum excitation and emission wavelength 360 and 471 nm, respectively. Figure 30 (A, C) depicts the morphology of both membranes obtained from CLSM. There were allergen proteins bound polymer matrix probably in MIP binding site of imprinted cavity in either immobilized cellulose and glass fiber membrane. In contrast to non-imprinted control polymer, no template protein bound can be seen. Taking advantage of the use of fluorophore in a dye that reacts with the protein will give fluorescence intensity, which renders its possibility to detect the protein molecule in the polymer mixture. Figure 31 shows maximum excitation and emission of FITC at 360 and 417 nm, respectively, and that maximum excitation and emission of FITC and protein complex appeared at 481 and 524 nm, respectively.

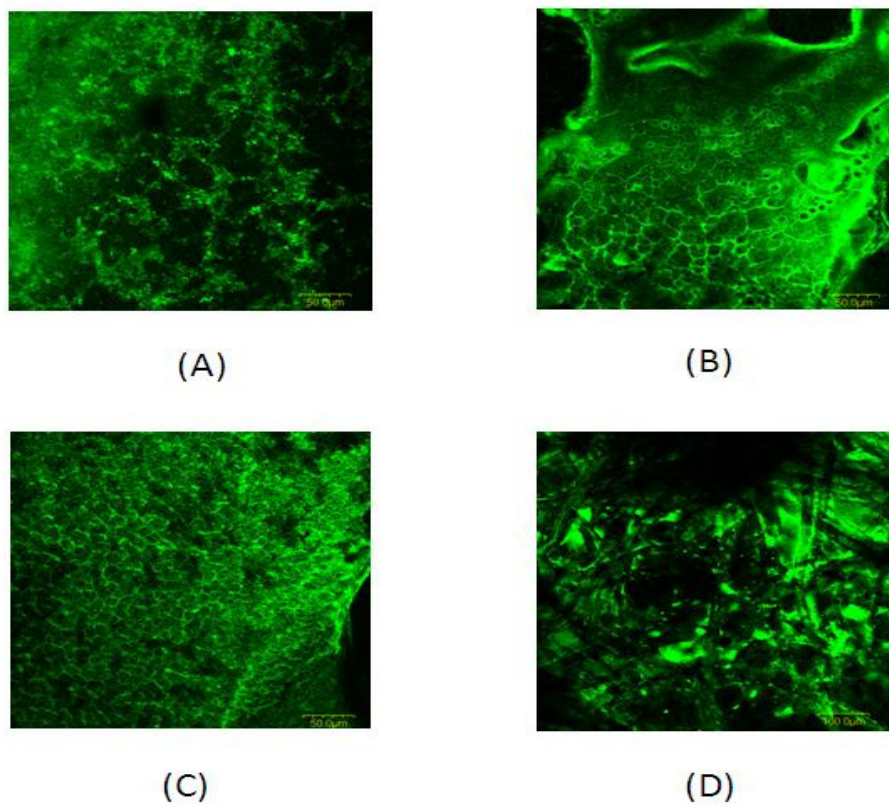
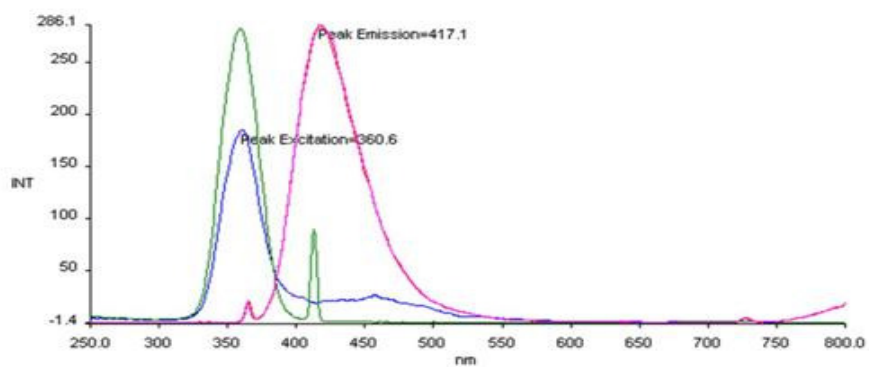
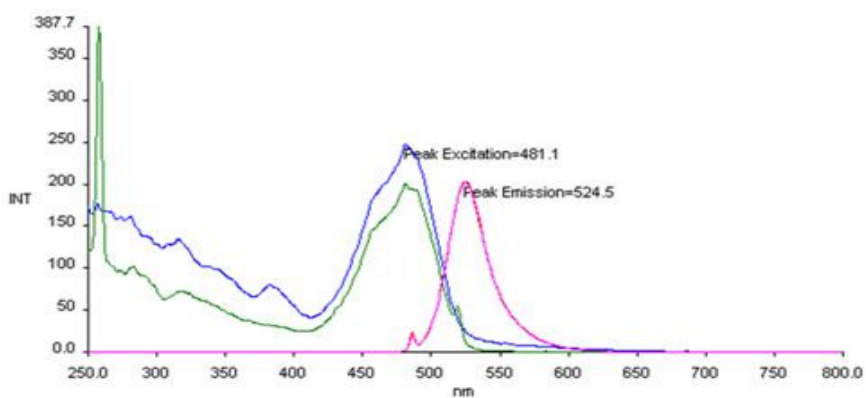


Figure 30. CLSM images of the Hev b1-FITC staining on: (A) a grafted MIP and (B) NIP layer on cellulose membrane, (C) MIP and (D) NIP on glass fiber membrane



(A)



(B)

Figure 31 Fluorescent spectrum showing the differences in emission and excitation between FITC (A) and FITC after addition of protein (B)

3.4.2 Investigation in protocol for protein template removal

A series of template removal protocols were evaluated by the use of distilled and SDS and water mixture. The template protein in a rinse solution of immobilized membrane was examined by using a SDS-PAGE method. When distilled water was used as a solvent for removing of protein template, there was no protein template detected by BCA method. This result can be interpreted as that water can not remove the protein molecule out from recognition site inside polymer matrices of either two membrane substrates because of two reason; first the interaction of Hev b1 molecule bound to the functional monomer inside polymer matrix is formed through H-bonding and ionic interactions whereas distilled water only generated strong H-bond to destroy the H-bond of protein template to functional monomer, whereas ionic interaction existing in the environment of recognition site of protein imprinting. Second, low mass transport of protein template in a polar environment occurred in this MIP system into polymer matrix with using 0.1% SDS in distilled water as solvent the protein template was found in a rinse and verified by a UV spectroscopy method. Figure 32 shows the UV absorbance at 562 nm of protein template in a rinse of 0.1% SDS from cellulose membrane in the presence of added BCA solution. The results indicated the influence of SDS which may reduce any strong interaction including hydrogen bonding and hydrophobic formation, between Hev b1 molecule and the functionality of binding site in the imprint cavity.

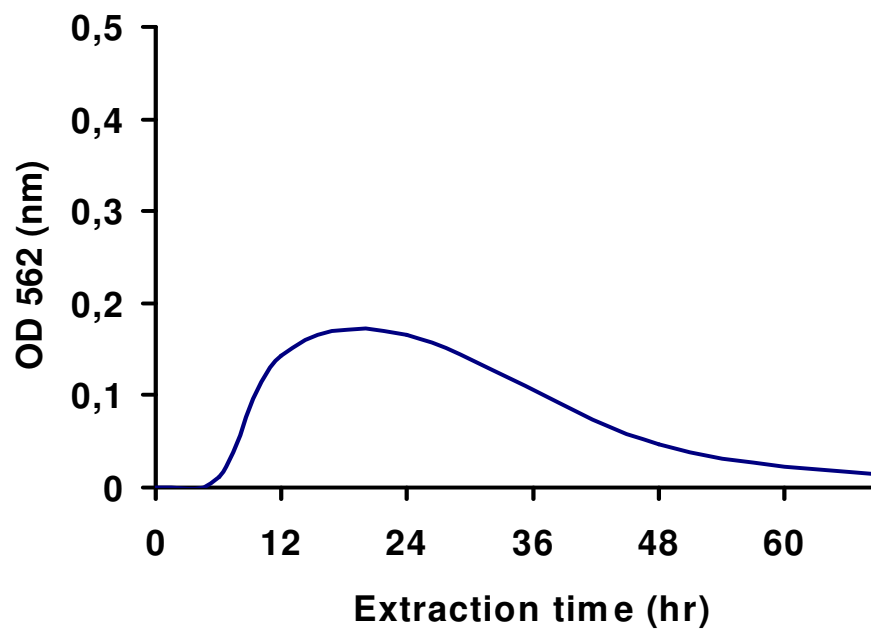


Figure 32. Absorbance spectrum of Hev b1 within a grated MIP layer of cellulose membrane after washing with 0.1% SDS in distilled water after the addition of BCA solution

3.5. Conclusions

The incorporation of Hev b1-MIP onto the surface of cellulose membrane has been done successfully by copolymerization reaction from the mixed functional monomer MAA and ACM and BAAM as the crosslinking agent. The characterization and physical properties of the MIPs onto the membrane were investigated by CLSM. The template removal was performed with different solvents and completed extraction of protein template was shown after washing the MIP membrane with SDS solution whilst the protein template is not easy to remove from the polymer matrix by distilled water.

CHAPTER 4

THE FABRICATION OF LATEX PROTEIN ALLERGEN SENSOR USING HEV B1 MOLECULARLY IMPRINTED POLYMER AS A SENSOR COATING ON QUARTZ CRYSTAL MICROBALANCE

4.1 Introduction

Quartz crystal microbalance (QCM) is an ultra-sensitive weighing device that utilizes the mechanical resonance of piezoelectric signal-crystalline quartz. QCM consists of a thin quartz disk with painting electrodes. As QCM is piezoelectric, an oscillating electric field applied across the device induces an acoustic wave that propagates through the crystal and meets minimum impedance when the thickness of the device is a multiple of a half-wavelength of the acoustic wave. The crystal orientation, thickness of the piezoelectric material, and geometry of the metal transducer determine the type of acoustic wave generated and the resonance frequency. A change in weight on the crystal can be determined by measuring the shift in resonating frequency, wave velocity, or amplitude according to the Sauerbrey equation (3) (Steinem *et al.*,2007).

$$\Delta f = \frac{f_0^2 \Delta m}{N \rho_q A} \quad (3)$$

where Δf is frequency change (Hz), f_0 is the fundamental frequency of the crystal, N the modulus of quartz (167 kHz cm), ρ_q the quartz density (2.648 g cm⁻³), and A is the piezoelectrically active.

The influence parameters in QCM sensor measurement such as electronic damping and liquid viscosity, temperature and viscoelastic film in aqueous solution should be controlled to reduce the significant dissipation of acoustic energy due to liquid contact, which translates to energy lost from the electrical circuit (Steinem *et al.*, 2007). The advantages of QCM sensor are a simple, cost effective, high-resolution mass sensing technique, which has been favorably adopted for analytical chemistry, and electrochemistry application due to its sensitive solution-surface interface measurement capability. Moreover, QCM has also been broadly applied in biology, environmental assay, analytical chemistry, pharmaceutical science (Liu *et al.*, 2006).

Dickert and coworkers have been successfully developed bioimprint polymer coated on quartz crystal microbalance sensor to detect cells (Dickert *et al.*, 2001), viruses (Dickert *et al.*, 2004), enzymes (Hayden *et al.*, 2003) and proteins (Hayden *et al.*, 2006). The soft-lithography of bioimprinted polymer is based on stamp or solution based imprinted polymer technique that directly coated on transducer. The imprinted polymer was obtained after removal the template with hot water for cell and 0.2% solution of sodium dodecyl sulfate for protein. The selective chemical recognition of the

bioanalyte by re-incorporation is achieved by a geometrical fit in combination with a pronounced adhesion to the cavities based on noncovalent phenomena as electrostatics, hydrogen bonding, vander Waals and hydrophobic forces. The geometrical dimensions range from diameters of molecules to micrometers characterizing cells. For example, bioimprinted QCM sensors have been used to detect tobacco mosaic viruses (TMV) in aqueous media. The analytical performance of this sensors showed linear range of 100 ng mL^{-1} to 1 mg mL^{-1} within minutes. Furthermore, direct measurements without time-consuming sample preparation are possible in complex matrices such as tobacco plant sap. In spite of viruses detection, this QCM sensor when combined with trypsin-imprinted polymer allowed to selectively bind lysozyme and pepsin which the mechanism of recognition for this MIP system involved electrostatic interaction and could be distinguish denatured trypsin from the native form. Therefore, for quantification of allergen protein in the biocomplex matrix of NRL or NRL glove sample, QCM sensor combined with protein-imprinted polymer may be promising alternative which can give the high sensitive, selective and reversible sensor signals when protein re-inclusion to imprint cavities.

4.1.1 Quartz crystal microbalance transducer

Piezoelectric effect can be reversed in the form of converse piezoelectric effect i.e. the production of stress and/or strain when an electric field is applied. Therefore, the creation of an electrical field in the direction of the polar axis of the crystal

leads to a mechanical deformation and by creating alternating fields across the crystal, a mechanical swing can be stimulated whose frequency can be measured using appropriate devices as illustrated in Figure 33. Among the piezoelectric substrate materials that can be used for acoustic wave sensors, the most common are quartz (SiO_2), lithium tantalate (LiTaO_3), and, to a lesser degree, lithium niobate (LiNbO_3). Each has specific advantages and disadvantages, which include cost, temperature dependence, attenuation, and propagation velocity. An interesting property of quartz and some other materials is its ability to provide temperature dependence selectivity by using optimal cut angle and wave propagation direction. With proper selection, the first order temperature effect can be minimized.

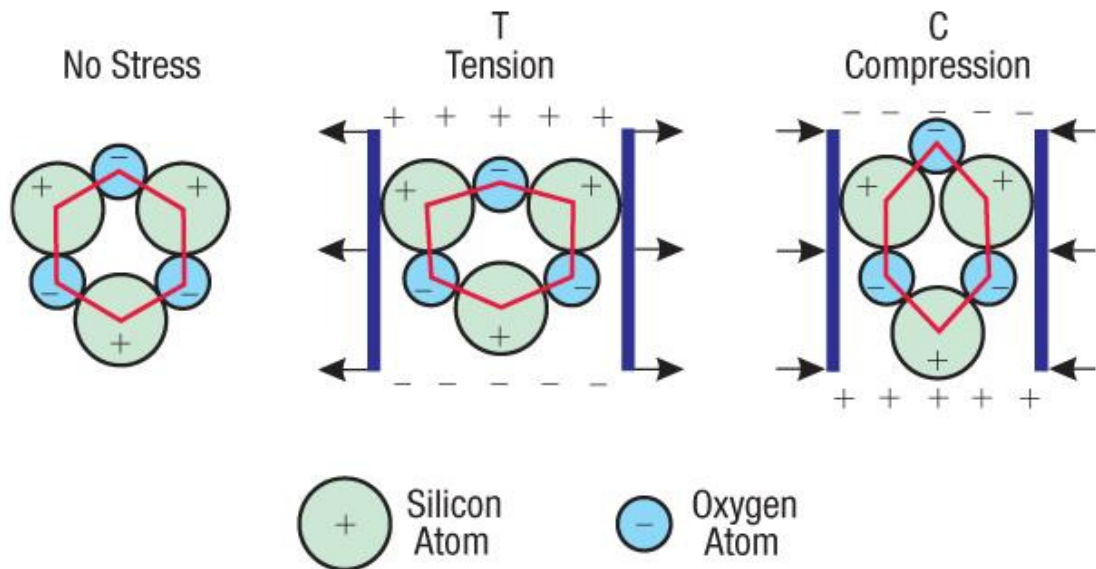


Figure 33. Illustration showing the piezoelectric effect generated of dipoles by deforming force (Bishop *et al.*, 1981)

An acoustic wave temperature sensor may also be designed by maximizing this effect. Crystalline quartz is a piezoelectric material which has low damping, extremely high mechanical stability and low temperature dependence.

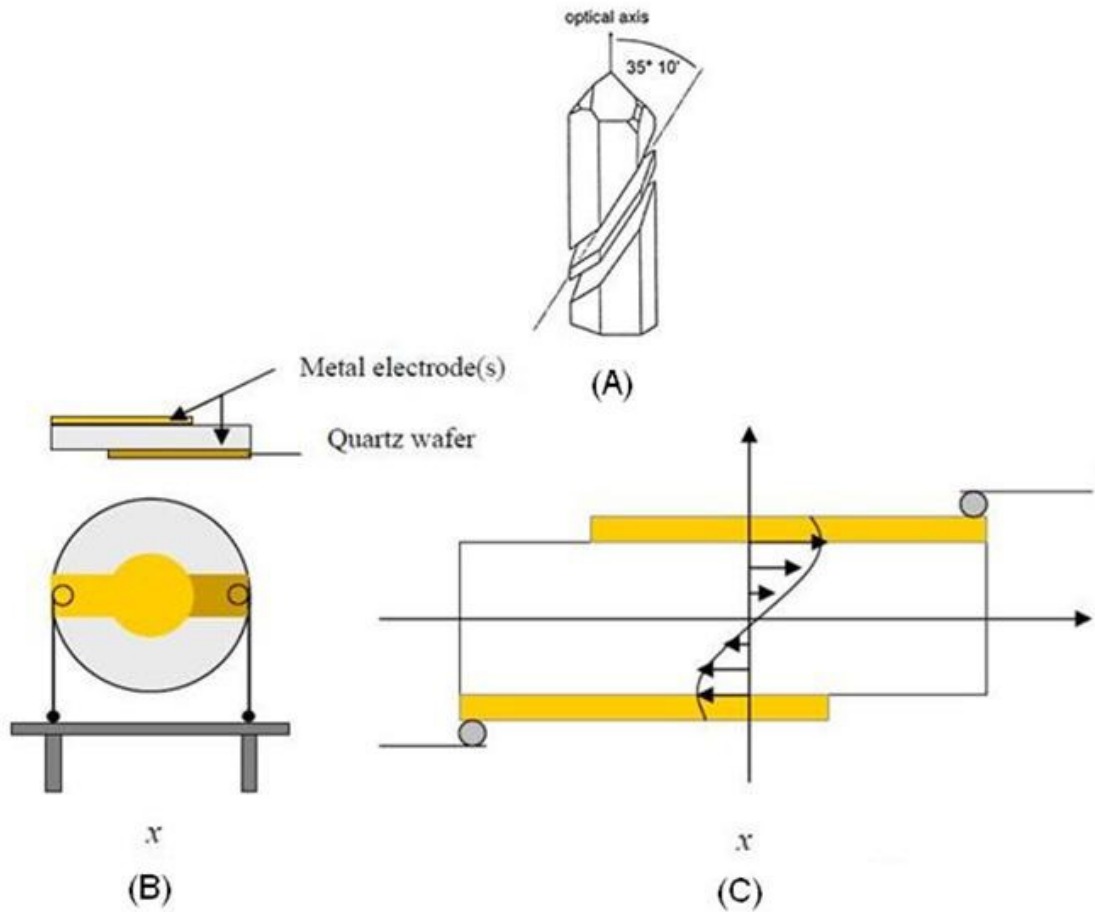


Figure 34. (A) AT-cut of a quartz crystal, (B) Piezoelectric crystal construction and (C). crystal vibrating in thickness shear mode (Suri, 2006; Marx, 2003)

Typically, for QCM applications, quartz crystals of a few tenths of a mm in thickness are cut in the AT form, at a $35^{\circ} 10'$ angle from the Z-axis as shown in Figure 34. This geometry provides a stable oscillation with almost no temperature fluctuation in f at room temperature. The QCM technique relies upon circular quartz crystals operating in the thickness shear mode (TSM) of oscillation, where motion lateral to the surface as

shown in Figure 34 C. Under these conditions, the lateral amplitude of a vibrating crystal is 1-2 nm. Any mass bound to the surface tend to oscillate with the same lateral displacement and frequency as the underlying crystal. If it did so elastically, then there was no energy loss for this process. If energy loss accompanies this mass oscillation, then the process became inelastic.

In practice, QCM sensor consists of a thin disk, sliced from a single crystal of an alpha-quartz. The crystal is sandwiched between two metal electrodes which are vapor deposited on either side of the crystal Figure 37.

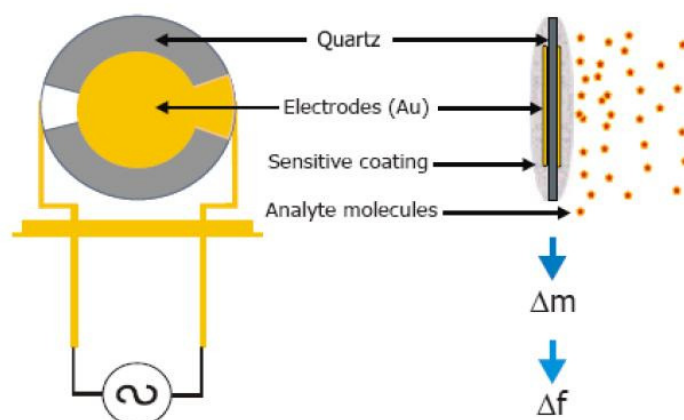


Figure 35 The QCM sensor: Quartz crystal is sandwiched between two metal electrodes that are vapor deposited on either side of the crystal. When the AC voltage is applied, quartz crystal will oscillate. Analyte molecules will be attached on the coated surface of QCM and the mass of the crystal increases, and therefore the resonance frequency of the quartz crystal changes.

The coated QCM crystal is then placed into an oscillation circuit where it resonates close to its fundamental resonance frequency. A typical equivalence circuit for a QCM is shown in Figure 36.

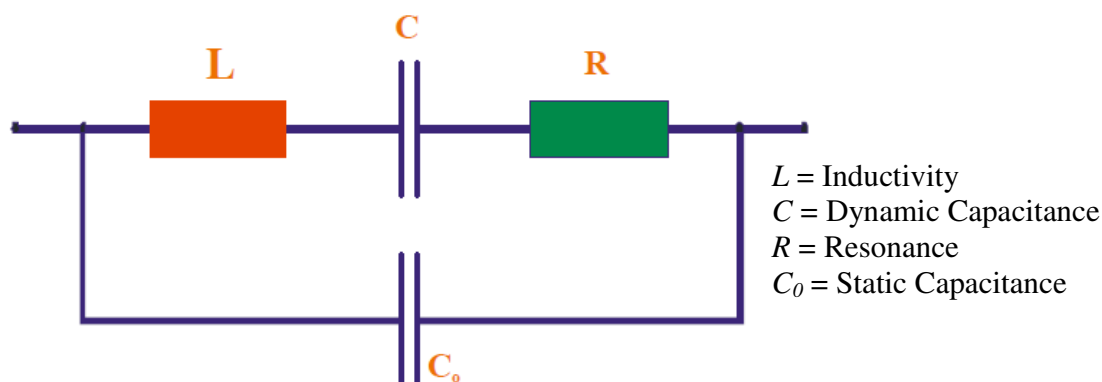


Figure 36. Schematic illustration equivalence circuit for a QCM

The inductance L in the equivalence circuit can be compared with the mechanically vibrating mass, the dynamic capacitance C complies with the elastic behavior of the resonator, the resonance resistance R represents the dynamic vibration losses, and the static capacitance C_0 is for the capacity between the two electrodes. The analyte adsorbs onto the metallic surface or absorbs into the chemical film and causes the resonance frequency of the oscillator to change. This change in frequency can then be related to the change in mass described by Sauerbrey equation. The QCM is a mass sensing device with the ability to measure very small mass changes on a quartz crystal resonator in real-

time. The sensitivity of the QCM is approximately 100 times higher than an electronic fine balance with a sensitivity of 0.1 μg . This means that QCMs are capable of measuring mass changes as small as a fraction of a monolayer or single layer of atoms. This high sensitivity and the real-time monitoring of mass changes on the sensor crystal make it a very attractive technique for a large range of applications. Especially, the development of QCM systems for use in fluids or with visco-elastic deposits has dramatically increased the interest towards this technique.

AT quartz crystal microbalance (QCM) sensors represent an alternative analytical method which they have been extensively used as QCM sensors in gaseous media (Czanderna, 1984). Konash (1980) demonstrated that the QCM could be used for liquid-phase (Kanazawa, 1985). There have been reports about the use of the quartz sensor under liquid conditions (Kurosawa *et al.*, 1990; Schumacher, 1990; Davis, *et al.*, 1989; Shana, 1990). The complete physical description of a viscoelastic load in contact with the quartz crystal resonator (QCR) has allowed the study of mechanical properties of different materials coated on the surface of the sensor, like viscoelastic properties of polymers (Behling *et al.*, 1997; Behling, *et al.*, 1998). In these cases concepts like “acoustically thin” or “acoustically thick” coating are of fundamental importance (Lucklum *et al.*, 1999). In case of a thick viscoelastic film in contact with a liquid, a complete characterization of the sensor, together with alternative techniques, is necessary for a comprehensive explanation of certain phenomena involved during the experiments (Jiménez *et al.*, 2008). On the contrary, for acoustically thin films, great simplifications can be done in the physical model and the extraction of the physical properties of interest

is simple by appropriate characterization of the sensor (Jiménez, *et al.*, 2008; Martin *et al.*, 1991), by the use of, for example, fluid physical characterization for both Newtonian and/or viscoelastic fluids (Jiménez *et al.*, 2008; Lee *et al.*, 2002; Arnau *et al.*, 2000), charge transfer analysis of conductive polymers in electrochemical processes (Gabrielli, 2007), detection of immunoreactions in biosensors (Camesano *et al.*, 2007; Lazcka, *et al.*, 2007; Hug, *et al.*, 2003; Dickert, *et al.*, 2003). However, even in the simplest cases, sensor characterization should be performed through suitable electronic interfaces that must be able to accurately measure and to monitor, even continuously, appropriate sensor parameters associated with the physical properties to be evaluated. Application of QCM sensors under in-liquid phase conditions is very much challenging. The limitations of different electronic interfaces in relation to the application will be introduced. The application will be evaluated as a function of a change in the measuring parameters. Thus, it is necessary to verify the parameters of the QCM system to be measured.

4.2 Objective

The aim of this chapter was to seek to develop Hev b1 sensor based on molecular imprinted polymer onto quartz crystal microbalance transducer system for application to screen detecting rubber latex allergen in natural rubber latex and latex gloves.

4.3. Experimental

4.3.1 Chemicals and biologicals

Acrylamide (ACM), 1-vinyl-2-pyrrolidone (NVP), methacrylic acid (MAA), *N,N'*-methylene bisacrylamide (MBA), *N,N'*-(1,2-dihydroxyethylene) bisacrylamide (DHEBA), sodium dodecyl sulfate (SDS), Triton X-100 and Tris-HCl were obtained from Aldrich Chemical Company (Milwaukee, WI, USA). 2,2'-Azobisisobutyronitrile (AIBN) was obtained from Janssen Chimica (Geel, Belgium). Lysozyme, ovalbumin and bovine serum albumin (BSA) were purchased from Sigma-Aldrich (St. Louis, MO, USA).

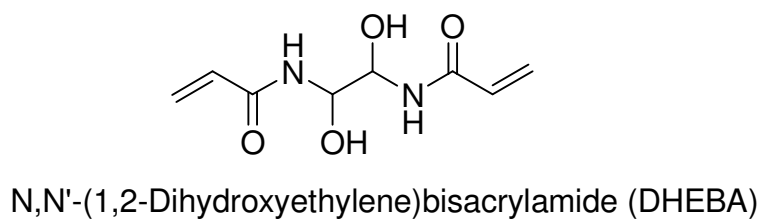
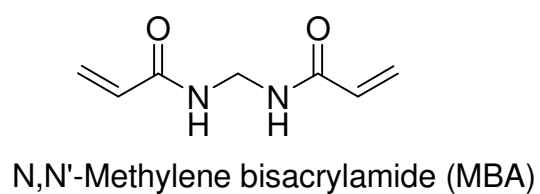
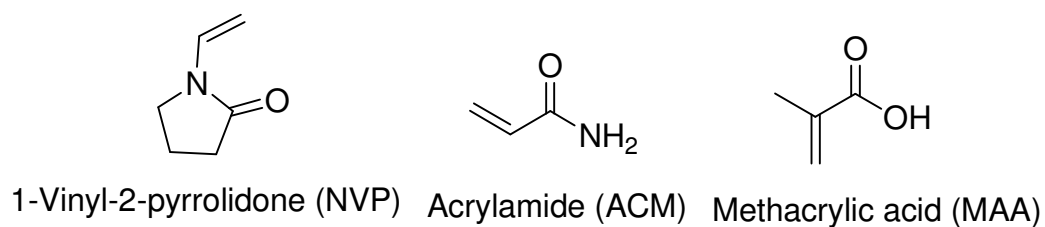


Figure 37. Chemical structures of functional monomers and cross-linking monomers used in this study

Table 11. Polymer compositions for preparing of Hev b1 rubber allergens surface-imprinted polymer.

Polymer	Functional monomer (mmol)			Cross-linker (mmol)		Porogen (ml)
	MAA	NVP	ACM	DHEBA	MBA	Water
MIP1	0.7	0	0	0.15	0	0.8
MIP2	0	0.7	0	0.15	0	0.8
MIP3	0	0	0.7	0.15	0	0.8
MIP4	0.6	0	0.2	0.15	0	0.8
MIP5	0	0.2	0.6	0.15	0	0.8
MIP6	0.6	0.2	0	0.15	0	0.8
MIP7	0.6	0.2	0	0	0.15	0.8

4.3.2 Equipment

An Ismatec peristaltic pump (MCP-Process Series, Ismatec SA, Wertheim- Mondfeld, Germany) was used to drive the sample solution into the flow cell Figure 38. An RF network analyser (8712ET 300 KHz-1300 MHz, Agilent Technologies,

Palo Alto, CA) (Figure 39) was utilized to monitor output signals which read the resistance signals from the sensor array with subsequent display on the Laptop screen.

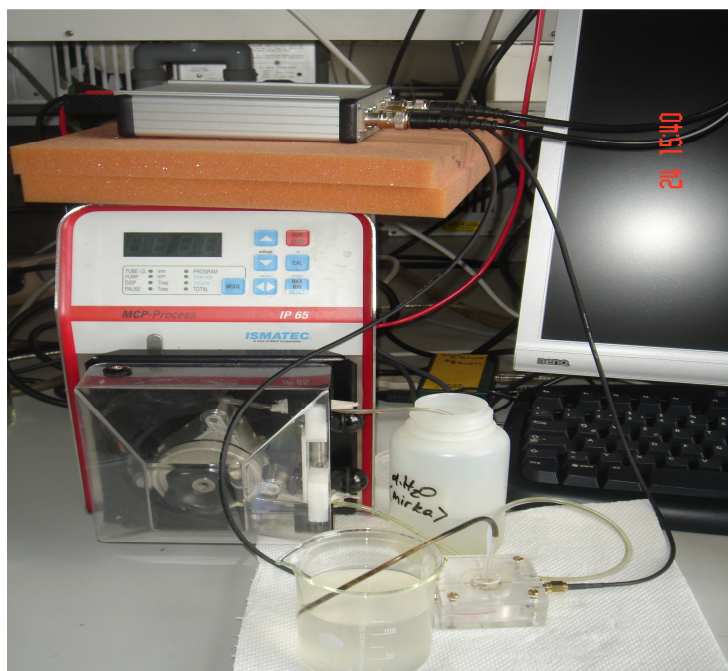


Figure 38. MCP-Process Series Ismatec peristaltic pump

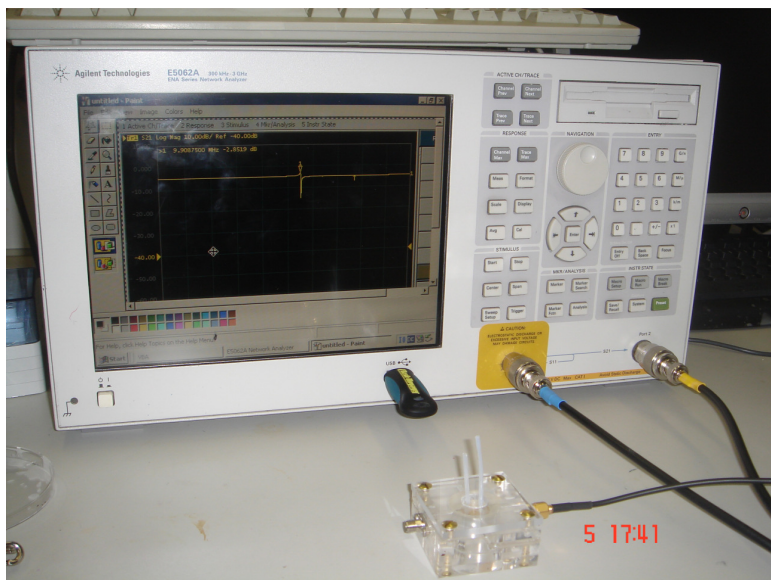


Figure 39. Illustration of an 8712ET RF network analyzer

The morphology of the polymer and protein template for imprinting as well as the thickness of thin film prepared was determined by an atomic force microscope (AFM) (Digital Instruments Inc., Santa Barbara, CA) (Figure 40) using a Nanoscope III Scanning tunnel microscope.



Figure 40. Atomic force microscope apparatus

4.3.3 QCM sensor

A quartz crystal microbalance system sensor was consisted of quartz crystal, oscillator, frequency counter and a computer. These items will be connected into a working circle as shown in Figure 41.

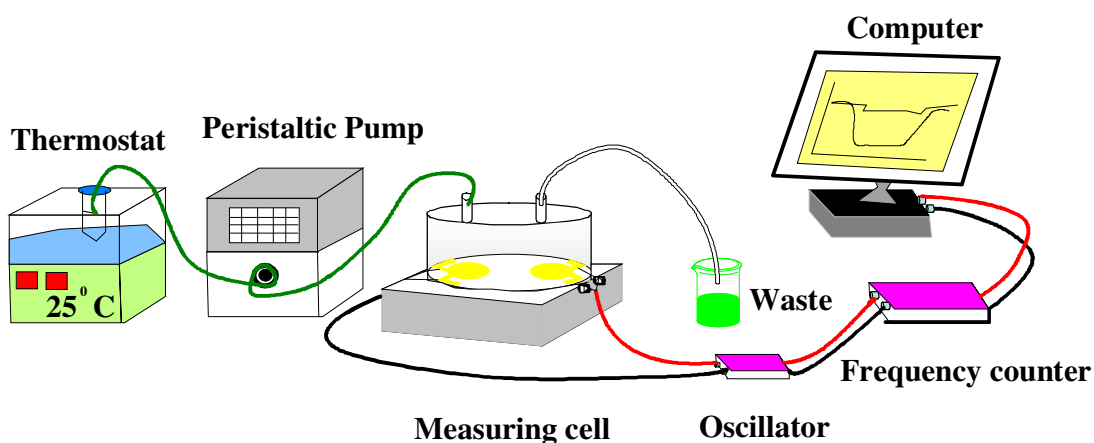


Figure 41. Schematic representation of the mass measurement circuit

4.4 Method

4.4.1 Preparation of Hev b1(G)-surface imprinted polymer

The imprinting was performed on quartz crystal microbalances with two-electrode geometry. One electrode was incorporated with the imprinted polymer layer and the other one was a reference electrode coated with the non-imprinted polymer (NIP) control polymer, prepared in the same way but with the template molecule omitted. The former is used as a working electrode and the latter is a reference for eliminating unspecific effects such as temperature changes or changes in viscosity. Dual electrode geometries were screen-printed (brilliant gold paste, GGP 2093 – 12%, from Heraeus,

Germany) onto quartz discs (10 MHz, AT-cut, 15.5 mm diameter) and burned-in at 420 °C overnight. Electrodes oriented toward the aqueous phase were grounded and 5 mm in diameter, whereas electrodes oriented to the gas phase were 4 mm in diameter, as previously reported (Dickert, 2004).

4.4.2 Protein stamp preparation

The protein stamps used in this study were prepared by incubation of the Hev b1 allergen proteins solubilized in a buffer solution on microscope glass slides (rms surface roughness of 14–16 nm, VWR International, USA) followed by allowing the film to dry, and the obtained surface inspected by the atomic force microscopy (AFM) method. The protein (0.1 mg mL^{-1}) was dissolved in 0.1 mM phosphate buffer and centrifuged at 4,000 rpm for 1 h at ambient temperature. The glass substrate surface was cleaned with detergent then with distilled water three times, followed by drying in the oven at 120°C for 2 h before it was coated. A 5 μL sample of Hev b1 (G) was deposited on the glass substrate and incubated in an incubator for 2 h at 25 °C.

4.4.3 Sensor layers

Molecularly imprinted and corresponding non-imprinted polymer film layers coated on the QCM electrodes were created according to a previously described procedure (Hayden, 2006). The chemical structures of functional monomers and cross-

linkers used in this study are presented in Figure 37. The compositions of this preparation of surface imprinted films are shown in Table 11. The polymerizing mixture was dissolved in distilled water followed by adding AIBN (1% w/w) and purged with N₂ (for 30 s) and pre-polymerizing until reaching the gel point. The viscous pre-polymer was then spin-coated onto a QCM electrode at 3,000 rpm to yield layer heights in the range of 80 to 400 nm. The final stamp was pressed into the pre-polymerized coating localized on the electrodes of a QCM. The pre-polymer mixtures were then exposed at 25°C to a UV-source to initiate photochemical polymerization. The template removal was carried out by incubation the resulting coated electrodes with distilled water at 40 °C for 30 min and followed by thoroughly rinsing with water in the measuring cell at pump velocity of 2 ml min⁻¹ until return of signals to baseline. Figure 42 shows the fabrication and polymer after procedures of Hevb1-MIP. The non-imprinted polymer (NIP) based electrodes were also fabricated with a pre-polymerized mixture including Hev b1 (L) of the rubber latex as the template during the polymerization process.

4.4.4 AFM measurements

Atomic force microscopy (AFM) measurements were performed by the use of Veeco SNL-10 silicone tips with a spring constant of 40 N/m. The topography and phase images of the protein stamps and polymer film layers on the QCM surface were obtained by contact mode AFM at a scan rate of 1 Hz under ambient laboratory

conditions. The thickness of the films was determined by scratching with a needle and measuring the depth of the scratches using an AFM.

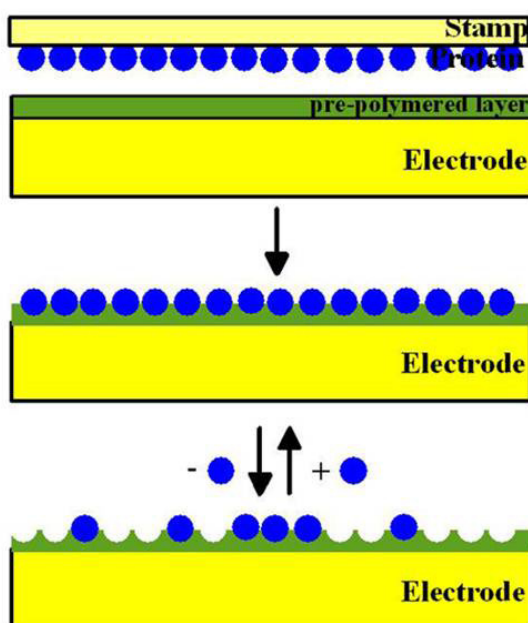


Figure 42. Schematic for the preparation of the protein surface-imprinted polymer coating on a QCM electrode. A stamp with densely packed rubber proteins is pressed into the pre-polymerized coating, templates are removed after polymerization

4.4.5 Flow cell design

Basically the quartz crystal is designed to contact with liquid at one side only (“one-side cell”). This is to eliminate the influences of conductivity, dielectric constant and liquid damping to allow the crystal reach a stable oscillation condition.

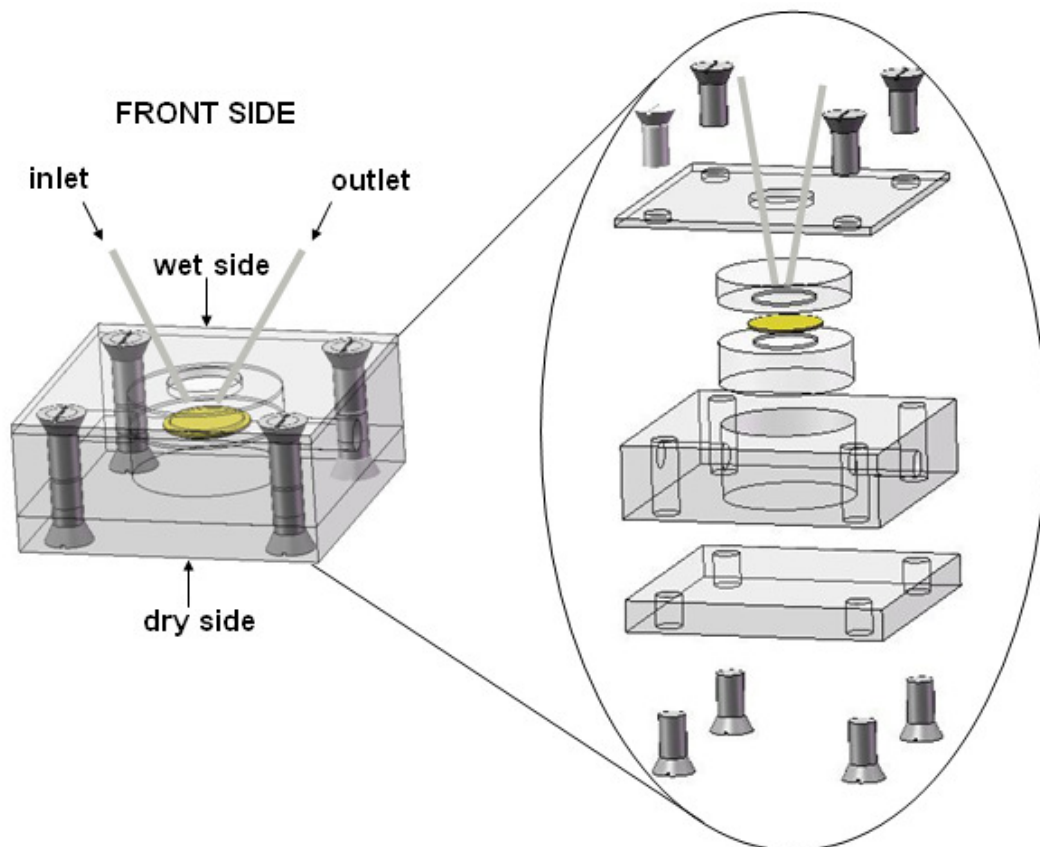


Figure 43. Flow Cell Design

In order to achieve this one-side operating condition, a cell must be designed to make sure one side of the crystal be dry and exposed to the air (see Figure 43). This cell can either be static or flow cell. For a static cell, one face of the crystal is exposed to a chamber that can hold up to 1 mL of liquid while the other face is dry and exposed to the air. For a flow cell, so one face of the crystal is exposed to a 70 μL chamber. This chamber is connected to an external peristaltic or syring pumping system. A QCM crystal was placed between two O-ring for sealing. One side of the crystal that was fabricated into flow-cell exposed to air while the other exposed to a liquid chamber.

4.4.6 QCM measurements

The coated quartz electrode was mounted in a self-made measuring cell of 250 μl volume and thermostatted at 25 $^{\circ}\text{C}$. Home-built oscillator circuits and a self-programmed frequency readout and processing software were used. The oscillator frequency was measured by means of an HP 53131A frequency counter, and the responses of the oscillator circuit were checked by means of a network analyzer (HP 8572C) to record damping and phase spectra. Sensor experiments were performed in a stopped-flow system and a 2 mL min^{-1} flow rate for solution delivery. The coated QCM devices were first stabilized in 0.1 mM phosphate buffer solution (pH 7.4), and a steady resonant frequency was obtained at room temperature (25 ± 1 $^{\circ}\text{C}$). The sensors were rinsed with distilled water to remove bound proteins and allergens followed by a background solution at the end of analysis. The frequency shift responses of QCM with

the prepared MIP and NIP control polymers were measured when exposed to Hev b1 (G) solution at its initial concentration. The sensitivity of the Hev b1 (G)-MIP-based sensor was measured as a function of the changes in frequency shift of the polymer upon exposure to Hev b1 (G) with concentrations ranging from 1-2000 $\mu\text{g L}^{-1}$.

In order to define the optimum sensor technological parameters of the prepared sensor the frequency of the sensor (Hev b1 (G)-MIP film) was measured and presented in this work. For the sample measurement using the sensor, the signal response towards the analyte sensor was reported as a frequency shift response ($-\Delta F$). Moreover, the selectivity of the MIP sensor was affirmed by comparing the signal responses of the MIP sensor and reference sensor having a NIP control polymer, as a different pair mode. The selectivity of the sensor was examined by comparing the frequency shift response of the protein analogues to the frequency shift response of the template. The protein template was considered to give 100% selectivity and all other proteins were related to this value. Every experiment was carried out in triplicate on any particular day of experimentation.

4.4.7 Binding isotherm

The kinetic adsorption of protein can be explained by different models, including the Langmuir, Freundlich, or Brunauer–Emmett–Teller (BET) isotherms. According to physical adsorption phenomena the BET model is preferably suitable for gases at porous materials. BET analysis is highly favorable, because of the physical

interpretation, according to multisite adsorption (Dickert *et al.*, 1996). A monolayer must be considered, yielding a high interaction energy, followed by less favorable adsorbates. The BET equation can be derived by considering factor ($\exp[-\Delta E/(RT)]$), the interaction energy (ΔE), the thermal energy (RT), and the exchange rates between different sites. As in the case of adsorption of inert gases, van der Waals interactions and other noncovalent phenomena are also valid for proteins. One must only consider that the pressure of the pure gas (P_0) must be substituted by the most densely packed protein concentration (C_0), and the partial pressure P must be substituted by the protein concentration C in aqueous solution according to equation (4) (Jenik *et al.*, 2009).

$$\frac{C}{n(C_0 - C)} = \frac{1}{n_m b} + \frac{b-1}{n_m b} \left(\frac{C}{C_0} \right) \quad (4)$$

The number of adsorbed proteins in the sensitive layer (n) can be derived from the frequency shift of the sensor. The QCM sensitivity can be calculated from the Sauerbrey equation. The parameter n_m describes the number of favorable sites in the layer. The parameter b is given as ($\exp[-\Delta E/(RT)]$), where ΔE is the difference between interaction energies of favorable and less-favorable binding sites.

4.4.8 Method validation

Method validation is performed to ensure that the analytical methodology is accurate and precise in the range that an analyte will be analyzed, to provide reliability during normal use, and may be submitted for both internal and official regulatory

approval. The guidances and criterion were taken from according to Taverniers *et al.*, (2004).

4.4.8.1 Recovery

The efficiency of recovery was performed by the addition of known amount of standards Hev b1 (G) into the crude proteins from rubber latex and glove extracts which were analyzed by the proposed Hev b1 (G)-MIP sensor. For this purpose, 1 g of the solid powder (or 4 g of the glove extracts) spiked with Hev b1 (G) standards was extracted according to the procedure previously described for Hevb1 (G). Spiked samples of allergen protein (250, 500, and 1000 $\mu\text{g L}^{-1}$), used in recovery studies, were prepared by adding the appropriate volume of a Hev b1 (G) standard solution to a extract of amatrix sample from a latex glove, resulting in a final volume of 15 mL. A calibration curve was prepared by dissolving Hev b1 (G) in 0.1mM phosphate buffer, pH 7.4, to obtain solutions having Hev b1 (G) of between 10 and 1000 $\mu\text{g L}^{-1}$, and then comparing them to that measured for Hev b1 (G) in the spiked samples. After several washing steps, QCM measurement was carried out which is protocol in protocol in Section 2.7. Every experiment was repeated three times at room temperature (25 ± 1 °C).

4.4.8.2 Linearity

Linearity of the proposed method was prepared by dissolving Hev b1 (G) in 0.1 mM phosphate buffer, pH 7.4, to obtain solutions having Hev b1 (G) of

between 10, 50, 100, 250, 500 and 1000 $\mu\text{g L}^{-1}$. The responses of Hev b1 (G), frequency shift were plotted *vs* the concentrations. Linearity was obtained by considering the correlation coefficient. Every experiment was repeated three times at room temperature (25 ± 1 °C).

4.4.8.3 The limit of detection (LOD)

In this work, 1000 $\mu\text{g L}^{-1}$ of Hev b1 (G) were diluted with 0.1 mM phosphate buffer solution at pH 7.4 to concentrations in the range of 1-10 $\mu\text{g L}^{-1}$. Each solution was measured by the MIP-QCM sensor system at optimum condition. After several washing steps, QCM measurement was carried out by following the protocol as in QCM analysis section. Every experiment was repeated three times at room temperature (25 ± 1 °C). Five replicates of each concentration were tested. A signal to noise ratio (S/N) of more than 3 was calculated which this was considered acceptable for estimating the detection limit of the method by ICH-Q2B guidance “Validation of Analytical Procedures” (1996).

4.4.8.4 Limit of quantitation (LOQ)

The limit of quantitative (LOQ) which is the smallest concentration of analyte gives a response that can be accurately quantified. The LOQ of the assay with MIP-QCM sensor was determined in thesis work, which requires a certain

precision at the lowest level of determination with a S/N ratio of 10. In this work, 1000 $\mu\text{g L}^{-1}$ standard stock solution were diluted with 0.1 mM phosphate buffer solution at pH 7.4 to concentrations in the range of 1-100 $\mu\text{g L}^{-1}$. Each solution was measured by the MIP-QCM sensor system using the optimum condition. Every experiment was repeated three times at room temperature (25 ± 1 °C). Five replicates of each concentration were tested.

4.4.8.5 Precision

Precision is “the degree of agreement among individual test result when the procedure is applied repeatedly to multiple samplings of a homogeneous sample” (CDER, 1994). To assess the precision of the method for the determination of Hev b1 (G) by MIP based QCM electrode, 1 g of the solid powder (or 4 g of the glove extracts) spiked with Hev b1 (G) standards was extracted according to the procedure previously described for Hevb1 (G). Spiked samples of allergen protein (250, 500, and 1000 $\mu\text{g L}^{-1}$) followed several washing steps. A sample blank was also analyzed in parallel. Five replicate analyses were performed at each concentration. The relative standard deviation (RSD) values were then calculated using the following equations (5 and 6) (Miller, 2000).

$$\%RSD = \frac{s}{x} \times 100 \quad (5)$$

$$s = \sqrt{\frac{\sum (x_i - \bar{x})^2}{n - 1}} \quad (6)$$

Where s is the standard deviation

n is the total number of measurements

\bar{x} is the mean of n measurements

4.4.9 Quantitative analysis

Quantitative analyzes of Hev b1 (L) and Hev b1 (G) of crude proteins from rubber latex and glove extracts were based on the response of the frequency shift that was proportional to the amount of analyte when the MIP-QCM sensor was used at the optimized and controlled condition. The frequency shift of Hev b1 (G) in glove extracts was first compared with the matrix match calibration curve. Hev b1 (G) responses was compared with the matrix match calibration curve. After this step if the analyte was not detectable (ND) or lower than the LOQ standard addition method was then applied.

4.4.9.1 Calibration curves

The determination of recovery for analysis with the sensor was carried out by spiking all analyzed compounds into 1 g of the solid powder (or 4 g of the

glove extracts) spiked with Hev b1 (G) standards at final concentrations of 10, 100 , 250 and 1000 $\mu\text{g L}^{-1}$. These were added directly to the samples before the sample preparation step. Spiked and unspiked samples were then measure by using Hev b1 (G) QCM-sensor under the optimum conditions and repeated three times. Calibration curves were obtained by plotting the peak area after subtracting the concentration of the analytes in the unspiked sample versus the concentration of Hev b1 (G). The response from the frequency shift per unit of concentration of Hev b1 (G) in the unknown samples is then calculated mathematically from the calibration curve.

4.4.9.2 Standard addition method

Standard addition was performed in the sample that showed non detectable response (ND) or lower than the LOQ of Hev b1 (G). The extracted sample solution was divided into 5 equal portions, Hev b1 (G) was added to all portions by increasing levels of standard concentration from 0, 100, 250, 500 and 1000 ng mL^{-1} . The samples were analyzed and peak area response versus the final concentration is plotted. The original concentration is then determined by extrapolation to the x-axis (Harris, 1995).

4.4.10 Real-life analysis to rubber allergen proteins

Quantitative analysis of the target analyte in the extracts of the latex articles and glove samples was achieved by a Hev b1 (G) sensor using optimized

sensor conditions. A latex extract was obtained from commercial rubber latex in Songkla, Thailand, from which protein was extracted according to the procedures described in section 2.2. The crude proteins from rubber latex and glove extracts were analyzed by the proposed Hev b1 (G)-MIP sensor. For this purpose, 1 g of the solid powder (or 4 g of the glove extracts) spiked with Hev b1 (G) standards was extracted according to the procedure previously described for Hev b1 (G). Spiked samples of allergen protein (250, 500, and 1000 $\mu\text{g L}^{-1}$), used in recovery studies, were prepared by adding the appropriate volume of a Hev b1 (G) standard solution to an extract of a matrix sample from a latex glove, resulting in a final volume of 15 ml. A calibration curve was prepared by dissolving Hev b1 (G) in 0.1 mM phosphate buffer, pH 7.4, to obtain solutions having Hev b1 (G) of between 10-1000 $\mu\text{g L}^{-1}$, and then comparing them to that measured for Hev b1 (G) in the spiked samples using the QCM electrodes. Every experiment was repeated three times at room temperature (25 ± 1 °C).

4.5 Results and discussion

4.5.1 Protein stamp and imprints

An MIP layer for use as a sensor system for detecting Hev b1 (G) in NRL glove samples was imprinted onto the gold surface of QCM electrodes by the use of a suitable procedure of microfabrication and protein imprinting to construct the on-chip MIP biosensors. Stabilizing the many individual weak interactions between the template

and the functional monomers is important for obtaining a large number of high-affinity binding sites in the resulting polymer. The initial evaluation was examined with a selective layer fabricated by the prepolymerization of MAA-NVP-DHEBA. Polymers based on the MAA-NVP-DHEBA copolymer can be prepared in aqueous solution and initiated by radicals, and can be devoid of denatured protein. A protein stamp technique was used for incorporating a surface-imprinted thin layer on a transducer of a QCM sensor and then the template proteins were removed from the templated (MAA-NVP-DHEBA cross-linked) polymer structures, while hopefully retaining a copy of the geometrical features of the latex allergen (Figure 44). In the preliminary study, the layer coating and stamping procedures were examined to ensure formation of cavities within the polymer matrix. A simple spin-coating procedure for surface nano-imprint lithography was found to provide easy access to nanoscale patterns of a host of active materials on the polymer surface on the gold coated transducer. Partial curing of a MAA/NVP/DHEBA based UV cross-linkable resin by spin-coating at 3,000 rpm (for 10 s) prior to imprinting resulted in a sufficient buildup of the resin molecular weight to prevent its absorption into the stamp protein yet maintaining a low enough viscosity to allow for rapid molding of nanoscale features of the rubber allergen during the subsequent imprinting process. The AFM images as depicted in Figure 45 (a-b) show a morphology and topographic of the stamps after the protein allergen was applied as described in the “Experimental” section. AFM topographies of the stamp surfaces show ridges and roughness of adsorbed rubber protein allergen in the dry state. Imprinted features were readily patterned in the underlying substrate by the stamp imprinting

procedure. The main challenge in Hevein latex allergen imprinting is adsorption and reversible binding of the protein on the polymer surface; the large interaction area between each individual latex allergen and the forming polymer does of course increase binding strength. Film thickness had to be optimized; if it was too high Hevein proteins would not penetrate as effectively into the tighter meshed polymer chains, while a very thin film would not lead to good reproduction of the specific template species patterns in the polymer due to the small interaction area. Atomic force microscopy was used to establish the optimum imprinting of the surface initiated polymerization. The AFM tests results revealed that optimal imprinting for an MAA/NVP/DHEBA MIP is when the layers have a thickness of 200 nm. An AFM of the imprinted surface, as depicted in Figure 42c, confirms a pattern height of less than 50 nm. Whereas with the 70 nm-pit in Figure 42d, the polymer layer imprinted with the Hev b1 (G) mold, shows better contrast and sharp edges. Our results indicate that the proposed stamp imprinting process is a feasible method for replicating the pattern of the allergenic proteins in a (MAA-*co*-NVP-*co*-DHEBA) cross-linked polymer structure.

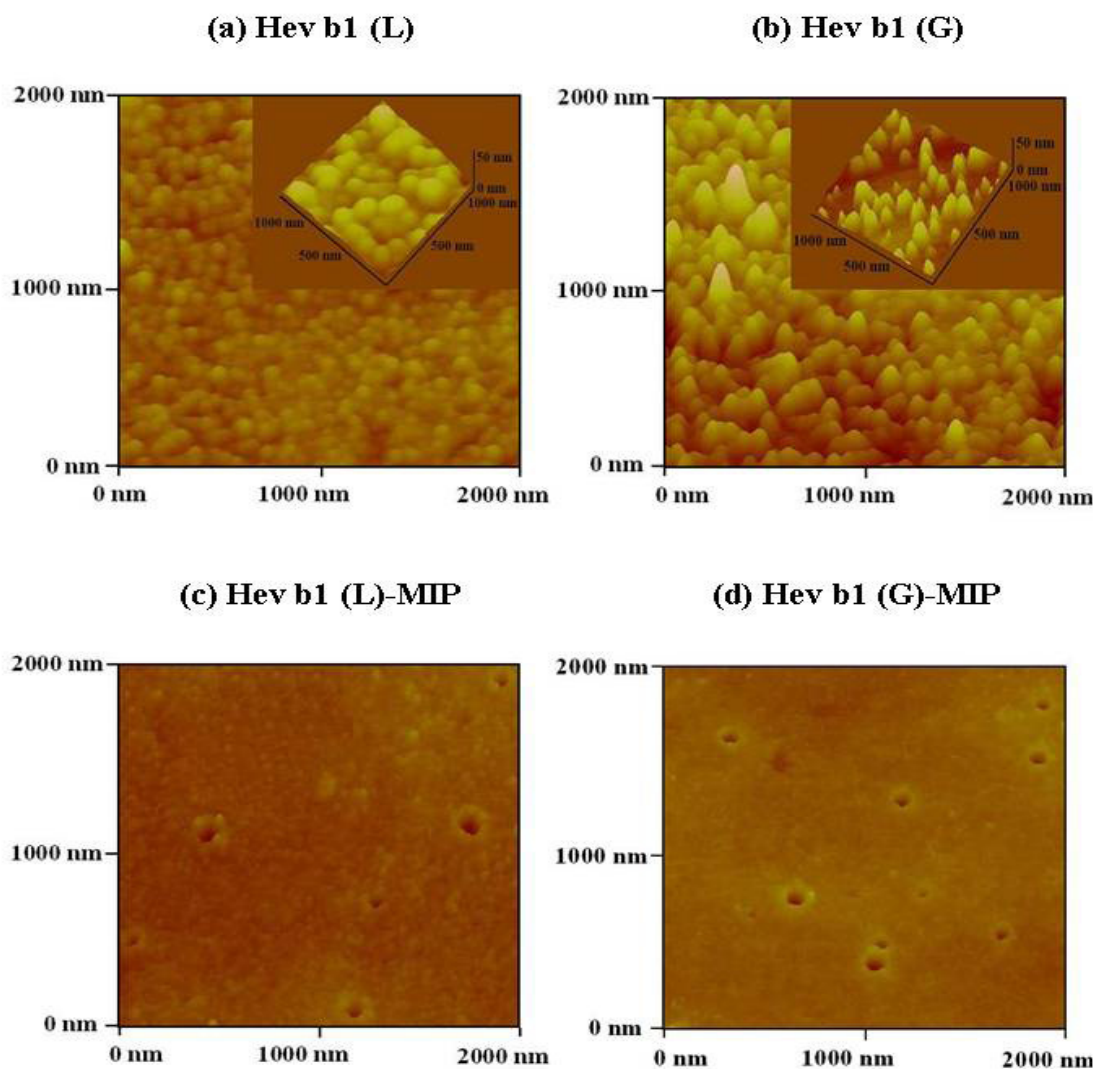


Figure 44. Topographic AFM images of poly (MAA-NVP-DHEBA-polymer) layer: (a) Hev b1 (L) and (b) Hev b1 (G) self-assembled on a surface, (c) Hev b1 (L)-MIP, and (d) Hev b1 (G)-MIP coated on a QCM electrode showing regular patterns of latex allergen imprints. Layer heights are 200 nm (spin coated, layer height tested with AFM).

Various layers of thickness of a Hev b1 (G) imprinted polymer coated on the transducer surface in a range of 80-240 nm were examined for their frequency shift responses of the sensor exposed to 2 mg L⁻¹ Hev b1 (G) solution. The frequency shifts increase with an increase of the polymer thickness, with the greatest shift occurring between 80-120 nm thickness, and the shift-increase being relatively stable between 160 and 240 nm (Figure 45).

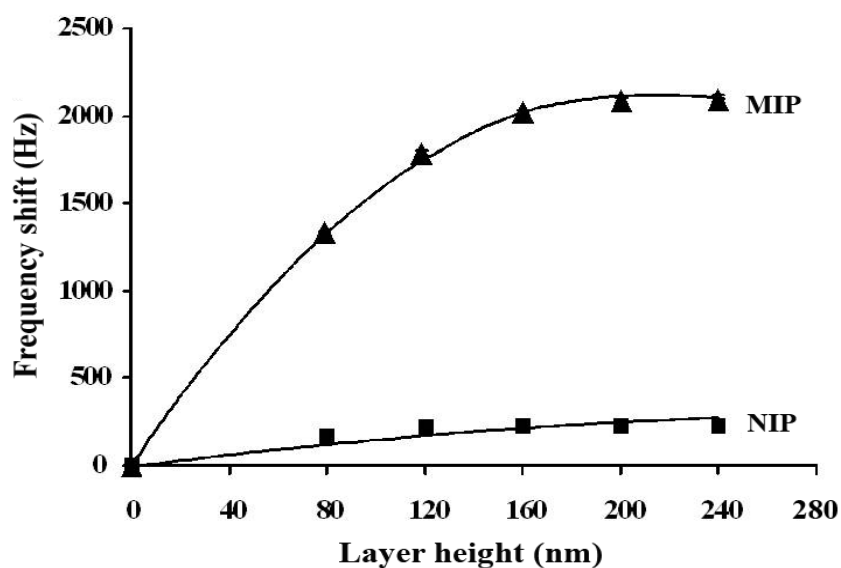


Figure 45. Effect of imprinted layer height on the frequency shift of the NIP and Hev b1 (G)-MIP (MAA-NVP-DHEBA-polymer) coated QCM exposed to Hev b1 (G) at a concentration level of 2 mg L⁻¹. Measurements were carried out in 0.1 mM phosphate buffer solution (pH 7.4) at room temperature, using an electrode polymerized at 25 °C.

For the corresponding NIP layer, the frequency shift appearance was only slight and associated with binding of proteins to non-specific binding sites. The phenomenon of this saturation condition with respect to the layer thickness has been associated in the MIP with a minor role played by nonspecific binding. This phenomenon may be attributed to the effects of a gradient in water evaporation being established in the monomeric mixture near the surface of the film layer during the imprinting process. Such a gradient would be expected to lead to an alteration in the density of the synthesized polymer network and be dependent upon the depth of the MIP layer.

4.5.2 Optimization of polymer compositions

To achieve a highly selective recognition of the target analyte, the influence of polymer components on the frequency shift response of Hev b1 (G)-MIP-based QCM was studied, using corresponding non-imprinted polymer film layers as a reference channel. Hev b1 (G)-imprinted sensor thin-films on QCM were prepared by using a single functional monomer or combinations of two different functional monomers with a fixed cross-linking concentration. DHEBA and MBA were chosen as the cross-linking agents for surface imprinting of Hev b1 (G) via a non-covalent approach, as they could minimize the non-specific interaction forces between protein and polymer in order to achieve reasonable adhesive properties of the polymer from the solvent. As shown in Figure 46, a MAA polymer gives a frequency shift response to Hev b1 (G) higher than the NVP polymer or even higher than the ACM polymer, prepared using DHEBA as a

cross-linker. For the monofunctional polymers with a molar ratio of 7:1, an excess of the functional monomer with respect to the template yielded a higher non-specific affinity. In general, the proper molar ratios of functional monomers to template are very important to enhance the specific affinity of polymers and the numbers of MIP recognition sites. High ratios of functional monomer to template result in high non-specific affinity, while low ratios produce fewer complications due to insufficient functional groups. So, the difunctional polymers were investigated for sensor effects on QCM measurements, by combining the MAA, or ACM with another functional monomer at a molar ratio of 6:2. The QCM with MIP prepared with MAA-NVP monomers gives a high frequency response for Hev b1 (G) with a minor non-specific effect compared to other MIPs (Figure 47). The polymer functionality of the MAA-ACM copolymer can interact with protein by hydrogen bonding which leads to a high effect similar to that of an MAA polymer but with selectivity factors of less than 2 toward Hev b1 (G). When the ACM was combined with the NVP monomer, the effect of either the MIP or NIP thin-films on the QCM sensor was lower than that of a single ACM monomer. For the polymer functionalities of ACM-NVP they are neutral in an aqueous solution and provide a much lower frequency response and a very low selectivity whereas with MAA-NVP, their polymer functionalities occupy more hydrogen bonding from MAA and a good wetting or adhesive properties from the NVP. Moreover, NVP stabilizes the inclusion of protein in the MIP and also stabilizes the protein conformation after inclusion (Bühler, 2005).

When the selectivity of the Hev b1 (G)-MIP prepared with the MAA and NVP functional monomers with DHEBA and MBA as cross-linkers was determined in

QCM experiments, the DHEBA in the polymer matrix produced a high selectivity for the response to Hev b1 (G) by a factor of 12, compared with MBA in the polymer which obtained a selectivity factor value of only 3 (data not shown). The superior binding capacity and effective recognition properties achieved by the optimized imprinted polymer, in which DHEBA provides an –OH surface on the polymer, can be attributed to the greater polarity and higher wettability of poly(methacrylic acid-*co*-vinylpyrrolidone) cross-linked with DHEBA rendered protein preferentially included in MIP (Lin, 2006).

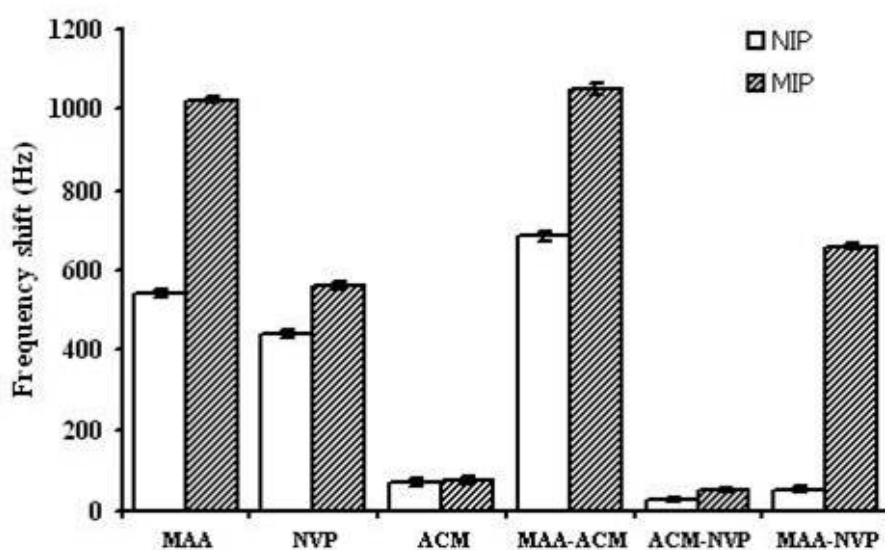


Figure 46. Effect of the polymer components for an MIP- or NIP-modified QCM sensor on the frequency shift responses to $500 \mu\text{g L}^{-1}$ Hev b1 (G) in phosphate buffer (pH 7.4) at room temperature.

The imprinted polymer from cross-linked poly(MAA-NVP-DHEBA) displays a high efficacy of recognition for the target analyte; therefore this polymer would have been used for investigations in the following experiments.

4.5.3 The investigation of the technological parameters

4.5.3.1. Influence of the background solutions on the sensor response

Figure 47 shows the effect of the solvent on the frequency shift response of Hev b1 (G) ($500 \mu\text{g L}^{-1}$) to Hev b1 (G)-MIP-modified and NIP-modified QCM electrodes when exposed in either water, pH 7.4 buffer (0.1 mM): Tris-HCl buffer (0.1 mM), or NaCl solution (0.1 mM). The frequency shift of the imprinted sensor coating from the pH 7.4 buffer was as high as 660 Hz, and was only half the value with distilled water. The frequency response of Hev b1 (G) for the imprinted polymer was low for both NaCl and the Tris-HCl buffer solutions compared to that in distilled water. With water as the solvent, it may be the fact that the protein surface is not charged properly to bind to the active sites of the cavities of the MIP, and hence produces a lower selective signal. The selective response of MIP decreased when exposed in NaCl solutions such that it is possible that the electrolytes cause a salting out of the proteins, thus altering the protein structure so that it can no longer be recognized by the imprint. While in the Tris-HCl buffer, the binding interaction of MIP and protein might be inhibited by conjugation of amine-based cross-linkers (Ahmed, 2005). The phosphate buffer, which was used in

the preparation phase of the imprinted layer, was found to be a better solvent for selective rebinding of Hev b1 (G) to MIP, as the optimized sensor signal was achieved in this solvent with a very low non-selective signal.

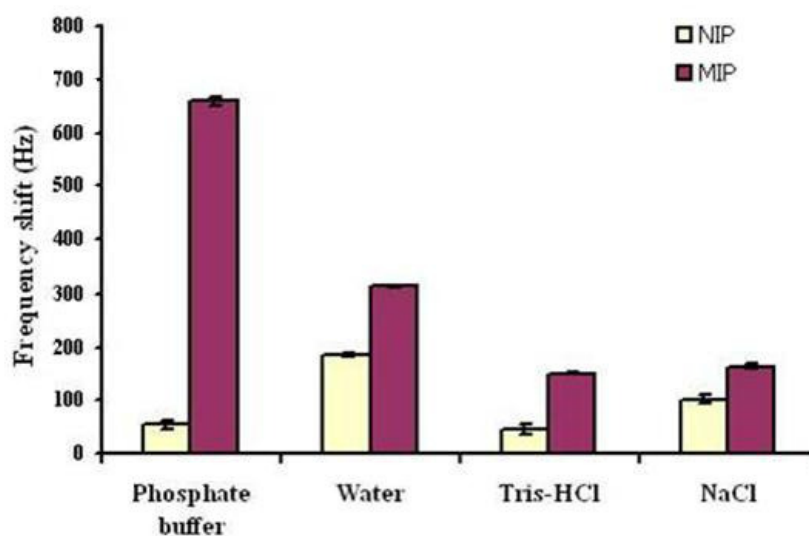


Figure 47. Effect of the background solution on the frequency responses of the NIP and Hev b1 (G)-MIP (MAA-NVP-DHEBA-polymer) layer coated 10 MHz-QCM using an electrode polymerized at 25 °C. Measurements were carried out in 0.1 mM phosphate buffer solution pH 7.4 and at room temperature. Responses were initiated by the addition of 500 $\mu\text{g L}^{-1}$ Hev b1 (G). Each value represents the average of three independent measurements.

4.5.3.2. Influence of the medium pH on the sensor response

The pH of the background solution had a large effect on the frequency response of Hev b1 (G) on Hev b1 (G)-imprinted and non-imprinted sensors (see Figure 48), with a low pH (pH 5) leading to a much lower frequency response of Hev b1 (G) (*pI* value = 5.0) on the sensors than when the sensors were exposed to protein at a higher pH (pH 6-8). At acidic pH, renaturation was achieved and this affects the binding motifs on the latex proteins (Wagner, 2009). This effect causes a decrease of adsorption interactions between protein and polymer, and results in a loss of the frequency signal at a low pH value (pH 5). The binding property of Hev b1 (G) to the MIP artificial receptor was optimized at pH 7.4. This can be attributed to the structural rearrangement of the MAA-NVP-DHEBA-polymer in the pH 7.4 buffer, which was used in the preparation phase for the sensor layer to provide a successful rearranging of the functional groups of the template and monomers in the imprint cavity with a defined surface structure optimized for recognition of the template. Furthermore, the Hev b1 (G) allergen proteins retained their native structure on adsorption to the MIP layer.

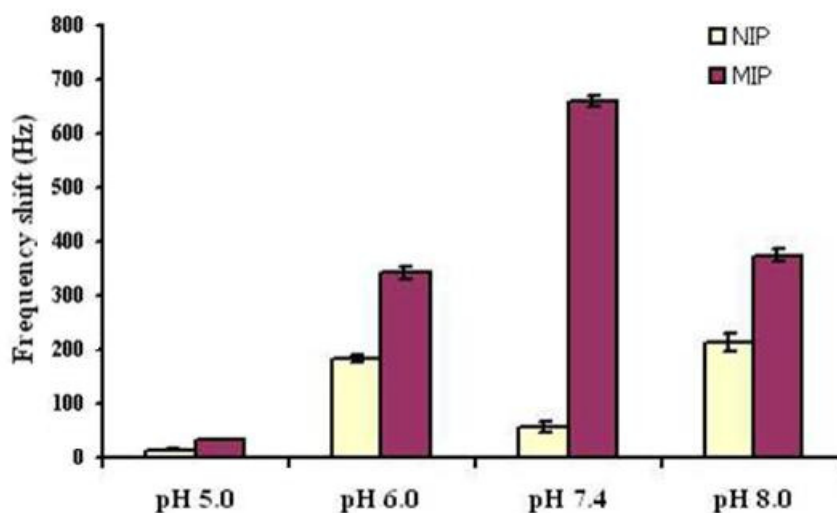


Figure 48. Effect of medium pH on the sensor response using $500 \mu\text{g L}^{-1}$ of Hev b1 (G) for NIP sensor and MIP sensor, using an electrode polymerized at $25 \text{ }^\circ\text{C}$. Responses were initiated by the addition of $500 \mu\text{g L}^{-1}$ Hev b1 (G)

Consequently, while strong polymer surface-protein interactions are desirable for surface coverage and charge compensation, this depends not only upon the binding affinity of MIP, but also on the relative stability of the structure under the exposed conditions. This effect causes a decrease of adsorption interactions between protein and polymer, and results in a loss of the frequency signal at a low pH value (pH 5). The binding property of Hev b1 (G) to the MIP artificial receptor was optimized at pH 7.4. This could be due to the structural rearrangement of the MAA-NVP-DHEBA-polymer in the pH 7.4 buffer, which was used in the preparation phase for the sensor layer to provide a successful rearranging of the functional groups of the template and

monomers in the imprint cavity with a defined surface structure optimized for recognition of the template. Furthermore, the Hev b1 (G) allergen proteins retained their native structure on adsorption to the MIP layer. Consequently, while strong polymer surface-protein interactions are desirable for surface coverage and charge compensation, this depends not only upon the binding affinity of MIP, but also on the relative stability of the structure under the controlled relevant.

4.5.3.3. Influence of the polymerization temperature on the sensor response

The effect of the polymerization temperature on the frequency shift response of the sensor exposed to Hev b1 (G) ($500 \mu\text{g L}^{-1}$) at $25 \text{ }^\circ\text{C}$ was examined over a temperature range of $25\text{-}75 \text{ }^\circ\text{C}$ during the polymerization process. The frequency response of the imprinted sensor was reduced at a polymerizing temperature above $25 \text{ }^\circ\text{C}$ because of the template/polymer exothermic interaction (Figure 49). During the polymerization of the layers, NIP interaction sites are minimized at high temperatures. The interactions of the protein and solvent molecules inside and outside the backbone of the polypeptides are greater for NIP, and are thus endothermic. Temperature has a complex effect on monomer-template and polymer-template interactions. In the previous study, a complex behavior of the imprinting effect with the change of polymerization temperature was observed. This enabled a good selectivity for the template being present in the binding groups of the resulting materials (Dickert *et al.*, 2001). The selective

sensor response of the optimized imprinted polymer for the present study was, after polymerization, the highest at room temperature (25 °C). The incorporation at the optimum condition of the QCM sensor in exposure to the protein template solution may occur by hydrogen bonding between a proton donor and acceptor, typically involving oxygens and nitrogens of protein and MIP. Moreover, a geometrical fit can occur by a part incorporation of the protein template to MIP.

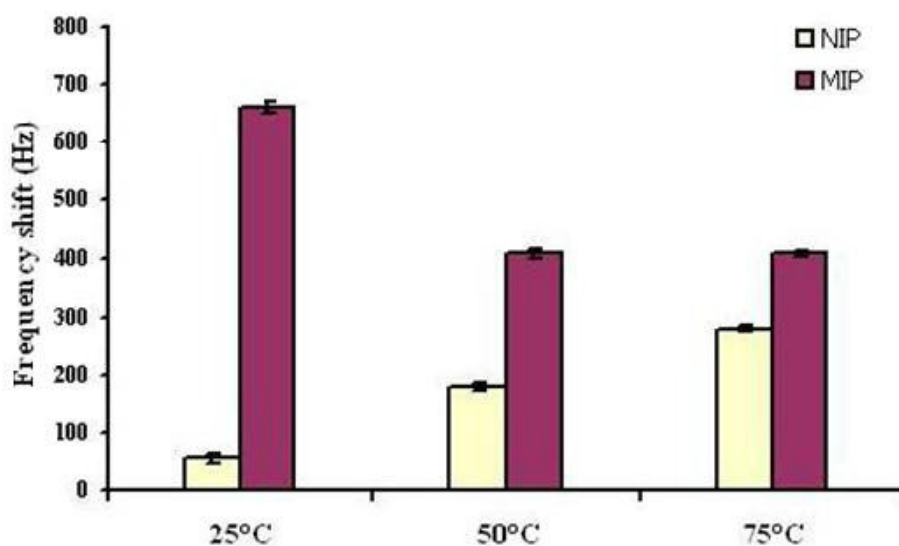


Figure 49. Effect of polymerization temperature on the frequency shift response of the NIP sensor and MIP sensor. Responses were initiated by the addition of $500 \mu\text{g l}^{-1}$ Hev b1 (G)

4.5.4 Binding of template to Hev b1 (G) MIP

Figure 50 shows the response of the Hev b1 (G) MIP layer and the adsorption by the NIP control electrodes. It appears that the normal baseline of an MIP-based sensor changes to 110 Hz upon the addition of $10 \mu\text{g L}^{-1}$ Hev b1 (G) in phosphate buffer, pH 7.4. The present study demonstrates that the Hev b1 (G)-MIP sensor has a high sensitivity. This can be explained by the protein readily interacting with the high-affinity binding sites in the cavities of MIP that have a low surface free energy and the binding energy stabilizes the template protein as in the behavior of a monolayer thin polymer film. Adsorption leads to a stable plateau value being attained within 10 min, which this may be interpreted as the re-orientation of Hev b1 (G) in the conformational spaces of cavities on the molecularly imprinted polymer material surfaces. On the other hand, the frequency shift due to Hev b1 (G) for the non-printed sensor turns out to be as low as 8 Hz; this is because there is no specific site on the polymer surface that can geometrically include the protein. This indicates that there is very low unspecific adsorption of the Hev b1 (G) proteins on the polymeric material. These results demonstrate the binding ability of Hev b1 (G) via non-covalent interaction with the imprinted polymer, and the regulation of protein orientation by the active binding site in the imprints.

The concentration dependence of these relatively small effects achieved on the reference electrodes can be used for verification during cross-selectivity

measurements, for which it is needed to choose the appropriate concentration of analyte. The sensitivity of the QCM was 1.04 Hz/ng. At the highest concentration measured, the overall mass effect is 2.1 KHz, that corresponds to 2.52×10^{17} Hev b1 (G) proteins bound to the sensitive layer. We have found that allergen concentration versus frequency change is linear over $10 \mu\text{g l}^{-1}$ to $1500 \mu\text{g l}^{-1}$. Above this range, the dynamic behavior shows a leveling off and thus the onset of a plateau. One explanation could be that above this concentration of Hev b1 (G) all to the sensitive layer.

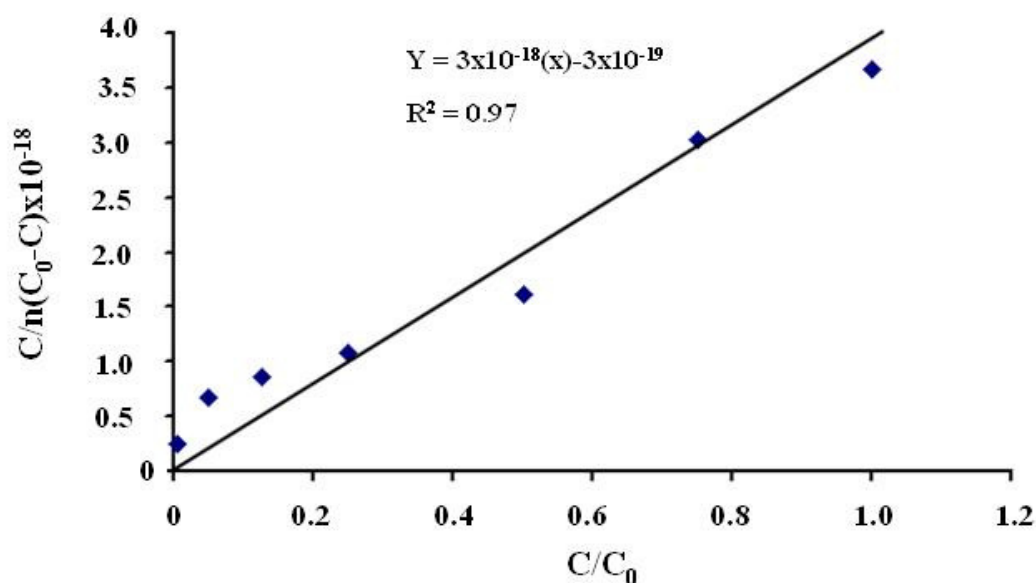


Figure 50. Linearized BET adsorption isotherm of Hev b1(G) on MIP at 25°C, according to equation 6 (correlation coefficient of linear regression, $R^2 = 0.97$)

The mass response generated by the selective layers is correlated to the allergen concentration in the buffer, as shown in Figure 51. Figure 52 shows QCM sensor

response for the MIP and corresponding NIP thin-layer coated onto QCM electrode when expose to the concentration of template as low as $10 \mu\text{g L}^{-1}$ in pH 7.4 phosphate buffer solution. Allergen concentration versus frequency change is linear over $10 \mu\text{g L}^{-1}$ to $1500 \mu\text{g L}^{-1}$. Above this range, the dynamic behavior shows a leveling off and thus the onset of a plateau. One explanation could be that above this concentration of Hev b1 (G) all available selective cavities are occupied and hence increasing the amount of proteins in the sample, will not further increase the sensor response. This also confirms that any possible non-specific adsorption of a double layer of proteins did not form on the sensor surfaces leading to an additional Sauerbrey effect.

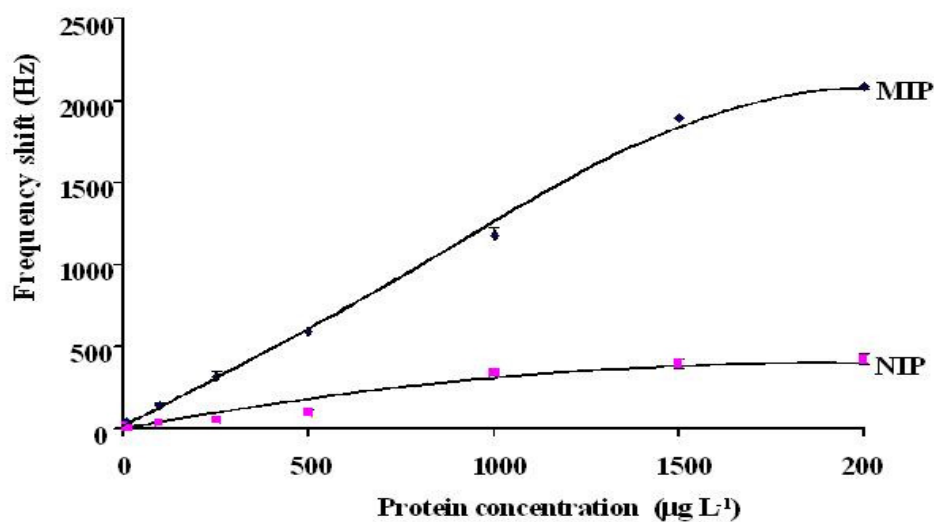


Figure 51. QCM sensor show the characteristics of NIP, and Hev b1 (G)-MIP coated 10 MHz QCM. Measurements were carried out in 0.1 mM phosphate buffer solution (pH 7.4) at room temperature.

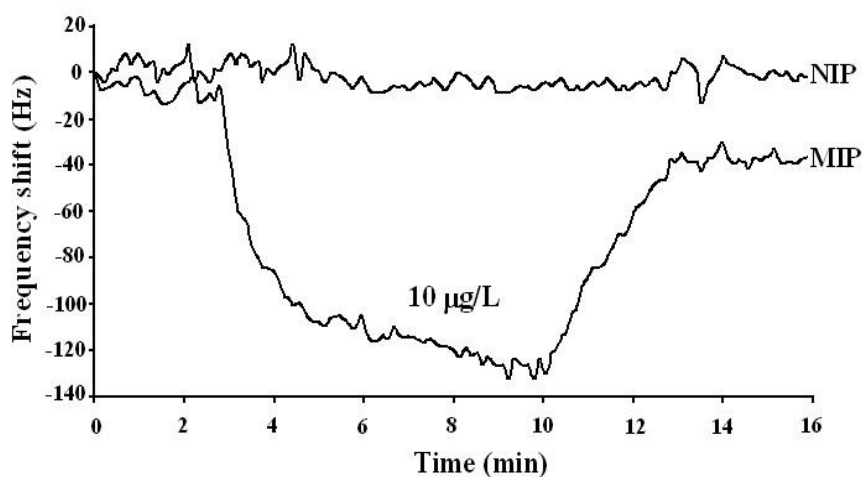


Figure 52. QCM sensor responses for non-imprinted reference and a Hev b1 (G)-MIP coated electrodes exposed to $10 \mu\text{g L}^{-1}$ Hev b1 (G) solution. Measurements were carried out in 0.1 mM phosphate buffer solution (pH 7.4) at room temperature.

4.5.5 The effect of matrix on the Hev b1 analyses

In the current study, the investigation whether the matrix from glove samples would affect the difference of quantitation analysis of Hev b1. For this, calibration curve produced between Hev b1 in a solution and the presence of matrix from glove sample were compared. The slopes of standard curve and matrix match calibration curve were tested using two-way ANOVA (analysis of variance).

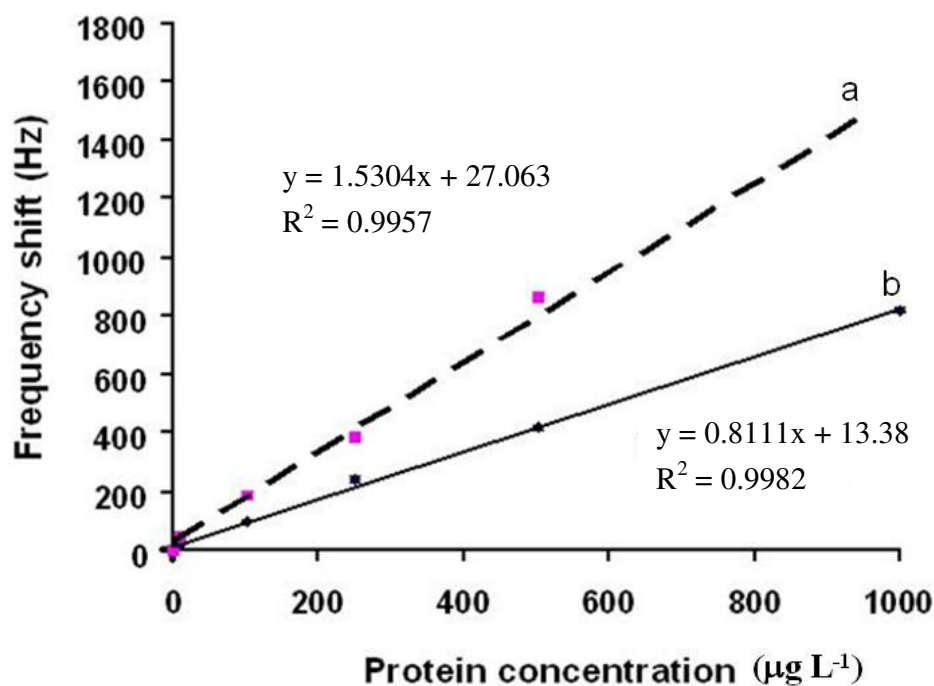


Figure 53. Calibration curve of Hev b1 either in the absence and presence of the matrix from latex glove sample measurement were performed with with poly-DHEBA-MAA-NVP, (2:6:2, w/w/w) coated on QCM sensor exposed with Hev b1 (G) between 10 to 1000 $\mu\text{g L}^{-1}$ in 0.1 mM phosphate buffer pH 7.4, a: a Hev b1 solution; b: Hev b1 solution with added matriculate liquid of latex glove.

The standard and matrix matched calibration curves of Hev b1 are shown in Figure 53. The result showed that the slope of regression line of standard curve and matrix match calibration curve were significantly different ($P < 0.0001$) for MIP as showed in Table

12. Therefore, quantitative analysis of these compounds should be analysed from matrix calibration curve.

Table 12 Statistical values for the comparison between the slope for Hev b1 (G) standard curve and matrix match calibration curve of glove extract using two-way ANOVA of R software (R development Core Team, 2006).

Matrix	D_f	Sum S_q	Sum S_q	F	P
Glove extract	3	218.0	72.7	31.436	$8.908 \times 10^{-5***}$

Significant codes: '*' ($\alpha = 0.01$), '**' ($\alpha = 0.05$), '***' ($\alpha = 0.001$)

Where D_f : Degree of freedom

Sum Sq: Sum square

Mean Sq: Mean square

F: ratio of two variances

P: Probability

4.5.6 Specific binding of Hev b1 protein surface-imprinted polymers

In the present study, the evaluation of the synthesized MIP system as selective recognition elements has been further explored through sensitive QCM measurements using non-imprinted polymers as a reference channel. The cross-selectivity of Hev b1 (G)-MIP and Hev b1 (L)-MIP with templates Hev b1 (G), Hev b1 (L) and their analogues was studied, with measurements performed under controlled conditions. The

value of the cross-reactivity, obtained from the signal responses of the particular MIP on the sensor for the analogue relative to that for the respective template, is shown in Figure 54. Clearly, in both cases the imprinted sensors results in a substantial frequency shift response when exposed to the respective template. The non-selective adsorption of all proteins binding to a non-imprinted polymer is much lower than that on an imprinted polymer due to the lack of selective recognition on the non-imprinted references.

The imprinted polymers exhibit greater cross-reactivity for proteins related to Hev b1 than for non-Hev b proteins; while Hev b1 (L)-MIP has a higher cross-reactivity toward Hev b (L) proteins, to a much greater degree than an analogous MIP obtained by Hev b1 (G) as the templating protein. Although Hev b1 (G), Hev b1 (L) and lysozyme have the same geometrical dimension (14 kDa), at the same concentration level

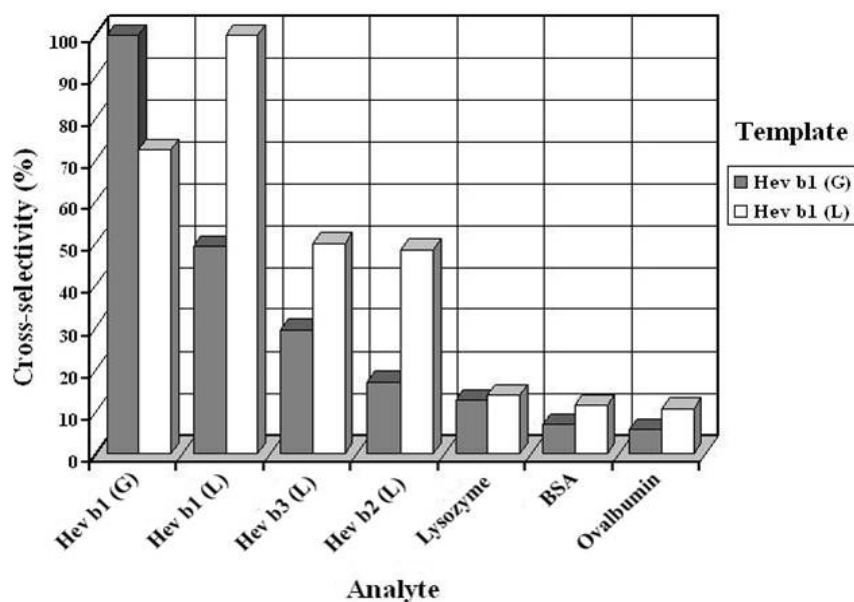


Figure 54. Selectivity profiles of the surface-imprinted polymers for Hev b1 (G), and Hev b1 (L) templates from stopped flow QCM experiments at an analyte concentration level of $500 \mu\text{g L}^{-1}$ in phosphate buffer (pH 7.4).

they lead to distinct sensor responses of the Hev b1 (G)-MIP-modified-QCM. The closely related structural protein Hev b1 (L) generates a signal approximately 44% of that obtained when exposed to the template. With the non-related protein lysozyme, the cross-reactivity value governing selective recognition, is much lower (about 12%), and thus is about four times larger than the non-selective responses on the non-imprinted sensor materials, since it is a hydrophilic protein and its conformation is more globular. This result confirms the difference in conformation between Hev b1 (G), Hev b1 (L), and

lysozyme. Thus, it was proven that the shape selectivity of proteins by the MIP is important in the selection of proteins.

Both the Hev b1 (G)-MIP and Hev b1 (L)-MIP based receptors provide a high selective recognition for Hev b2 (L) and the closely related protein Hev b3 (L), while non-related proteins such as ovalbumin and BSA, which are different in size and shape, have a less selective recognition interaction. The cross-reactivity shown for Hev b3 (L) may arise from the fact that the Hev b3 protein-associated latex allergen shares a 47% sequence identity with Hev b1 at the amino acid level, and the two molecules have been shown to share IgE epitopes (Banerjee, 2000). However, there appears to be cross-selectivity between Hev b1 (G) and Hev b1 (L) because of their similar functional groups and dimension of protein. Hence, it can be concluded that the Hev b1 (G) surface-imprinted polymer has a selective recognition to a template with a geometrical fit and functional group interaction that depends on the conformation of the protein. It is noted that Hev b1 naturally interacts with the specific binding sites created for the non-native protein recognition, showing a 50% reduction in cross-reactivity to the template protein. This indicates that the substrate protein, bound to the “active site” in a non-native conformation to the imprint, has been made use of in the MIP-QCM sensor method. Interestingly, the recognition site generated by Hev b1 (L) leads to the greatest selectivity for Hev b1 (L) (the template) as well as Hev b1 (G). The difference of signal response for Hev b1 (G) on the imprint of Hev b1 (G) and Hev b1 (L) is ~13% to the case of Hev b1 (L) on the Hev b1 (L) imprint. This indicates that it is possible that non-native Hev b1 undergoes re-orientation onto the surface near or adjacent to the active site of MIP, and is

specifically able to bind species of naturally derived Hev b1. This may be because the non-native Hev b1 protein refolds to a stable state in the Hev b1 (L)-imprinted cavity to its native conformation. Although the sensor readily detected proteins from other partially purified sources because they had the same epitopes, this sensor would be advantageous to detect the proteins extracted from NRL products other than gloves or were similar epitopes on the proteins recognized on crude latex samples.

4.5.7 Method validation

Method validation is performed to ensure that an analytical methodology when employing the MIP-based QCM sensor for Hev b1 analyses and further intended application is accurate, specific, reproducible and rugged over the specified range that an analyte will be analyzed. Method validation provides an assurance of reliability during normal use (Swartz, 1997).

4.5.7.1 Determination of percentage recovery of Hev b1 (G)

Recovery of Hev b1 (G) in glove extract was investigated by spiking known amount of Hev b1 (G) standard solution into glove extract at concentration level of 250, 500 and 1000 $\mu\text{g L}^{-1}$ as described the experimental section. The responses obtained from a spiked glove extract and from Hev b1 (G) standard

solution were compared. The results are in the range of 95-105% (Table 13) and these levels are within the range, *i.e.* 70-120% (EPA, 1996).

Table 13 Percentage recovery of Hev b1 (G) in glvoe sample at various spiked concentration

Spiked concentration ($\mu\text{g kg}^{-1}$)	% Recovery* \pm SD	% RSD
1000	102 \pm 7	6.5
500	105 \pm 4	3.8
250	97 \pm 5	4.6

* 5 replications, RSD < 5 %

4.5.7.2 Determination of MDL and LOQ

Glvoe extract was spiked with Hev b1 (G) standard solution to make final concentrations in the range of 1 to 10 $\mu\text{g L}^{-1}$ and analyzed together with nonspiked (blank) samples. The analyte peak areas were corrected for any interference found in blank samples by subtraction the peak area of the interference in blanks from the analyte peak areas in spiked samples. The method detection limit (MDL) of this MIP-QCM sensor method which was obtained by a signal to noise ratio (S/N) ≥ 3 was 1.0 $\mu\text{g L}^{-1}$ for Hev b1 (G) in glove sample. The LOQ was calculated as the analyte concentration

giving a signal to noise ratio of a factor of 10. The LOQ of Hev b1 (G) in glove sample is $10 \mu\text{g L}^{-1}$.

4.5.7.3 Determination of precision for Hev b1 assay in MIP sensor

In this study, glove sample were evaluated at three spiking level of 250, 500 and 1000 $\mu\text{g kg}^{-1}$ in sample followed by sample preparation procedure before measure by propose Hev b1 (G) QCM sensor at optimum conditions as described in Experimental section. Five replicates were performed at each concentration. The results are shown in Table 13. It shows good precision, their relative standard deviation (RSD) were lower than 7% at all spike concentrations. This value was better than the recommendation by Taverniers and coworker (2004) that accepted RSD less than or equal to 15%.

4.5.8 QCM assays using Hev b1 (G) surface-imprinted polymer

Using the Hev b1 (G) surface-imprinted polymer as a selective layer in QCM is important for determination of the analyte in the extracts of NRL articles and finished products of gloves. MIP-QCM sensor-based assay was performed for measuring the analyte, and studied its analytical performance. As a label-free detection method, QCM allows for a rapid and simple continuous Hev b1 assessment. The assay covered a linear range of 10 to 1000 $\mu\text{g L}^{-1}$ ($R^2 > 0.996$). The analytical detection limit, calculated

using a signal-to-noise ratio of 3, was $1.0 \mu\text{g L}^{-1}$. The more sensitive Hev b1 (G) surface-imprinted polymer was applied to glove extracts. The principal intention of the MIP-QCM sensor is to minimize the matrix effects of real samples, owing to the selectivity of the Hev b1 (G) imprinted polymer. Initially, evaluation of the matrix effect on QCM measurement was carried out; and secondly, a study was performed on the extraction efficiency of Hev b1 (G) from spiked glove samples to verify the accuracy of the QCM-based assay of Hev b1 (G). For this purpose we used an extract of the matrix sample from a latex glove spiked with a standard solution of Hev b1 (G) at concentration levels of 250, 500 and $1000 \mu\text{g L}^{-1}$. The method showed high selectivity and good precision and compatibility with the biological complex matrix. Recoveries were in the range of 97 to 105%, with RSD values between 3 and 6.5. The measurement of latex allergens in real samples was performed by the developed MIP-QCM assay method. The amount of latex allergens in natural rubber latex mattresses and latex gloves were found to be 1822 ± 41 and $22 \pm 4 \mu\text{g/g}$ of rubber material, respectively, which correspond well to the previous report by other authors using different methods (Yagami, 2009; Deborah, 1995; Raulf-Heimsoth, 2000).

4.6 Conclusions

This chapter presents the development and optimization of a surface imprinted polymer for detection of the latex allergen proteins in natural rubber latex products. Surface imprinting allows for the selective recognition of proteins based on

shape selection and the positioning of functional groups that can memorize Hev b1 protein in a molecular recognition process. Polymers as sensor coatings enable for a variety of modifications of composition and functionality, ensuring optimum modification of the sensitive surface to the analyte. The results of the present study proved that surface imprinting of thin films does produce molecularly imprinted synthetic receptors that allow accessibility for target analytes and can be a fast and cost-effective method for detection and determination of Hev b1 rubber latex allergens. The fast frequency shifts, as well as the fully reversible responses, also indicates the presence of non-covalent interactions to the bioanalyte in the cavity of the MIP. Hev b1 (G) imprinted methacrylic acid/vinylpyrrolidone/dihydroxyethylene bisacrylamide copolymer as the recognition system on a transducer of QCM sensor showed a high sensitivity and selectivity for the response toward Hev b1 (G). It can readily distinguish between the template and others (i.e. lysozyme, ovalbumin, and bovine serum albumin), and demonstrates the geometrical and functional selective fitting of the imprinted cavities of the resulting polymers. The MIP material has conformational memory. The surprising distinct orientation of the non-native protein Hev b1 arises from interaction of the binding group ordering with a preferred conformation due to a gain in entropy on the molecularly imprinted polymer material surfaces produced with native Hev b1 as a templating protein. The results of the present study may provide a better insight into the structure and conformation arrangements in the supramolecular structure and physicochemical properties of the latex allergen Hev b1, that has been implicated in life-threatening immunological reactions. Additionally, the results demonstrate that QCM sensor

measurements using MIP as a recognition material can be used to screen and detect Hev b1 in such complex matrices as manufactured rubber latex gloves.

CHAPTER 5

HEV B1 SURFACE-MOLECULARLY IMPRINTED POLYMER AS A SENSITIVE LAYER ON INTERDIGITATED CAPACITIVE ELECTRODE FOR DETECTION OF RUBBER LATEX ALLERGENS

5.1 Introduction

Inter-digital capacitance (IDC) transducer is an electronic transducer system, becomes important transducer in medical, biological and environmental diagnostics. This transducer consists of a planar glass support with interdigitated gold electrode pairs on one surface in a planar configuration. The principle of the capacitor detection is based on the changes of the dielectric value or insulation properties between two parallel electrodes by many biochemical reactions in solution. One major attractive feature of the IDC detection mode has an advantage that a large number of reactions involve either consumption or production of charged species and therefore, lead to a change in ionic composition of the reacting solution. Therefore, such thin film capacitor electrodes were used to realize sensors sensitive to various target analytes in respect of

organic and inorganic substances. From a technological point of view, thin-film metal electrodes are suitable for miniaturization, multisensory network design and production on a large scale using the low cost thin-film technology. The advantage of IDC sensor proposes good linearity and gave high specific sensitivity to the target analyte, stable, portable and reasonable signal response in a solution containing inorganic anions. The capacitor consists of two metal plates separated by an insulating material called dielectric according to this equation (7) (Gebbert *et al.*, 1992):

$$C = \frac{\epsilon_0 \epsilon_r A}{d} \quad (7)$$

where A = plate area [m^2] = cross section of electric field, d = distance between plates [m], ϵ_0 = permittivity of free space = 8.854×10^{-12} F/m and ϵ_r = relative permittivity of the dielectric between the plates (dimensionless). This calculated value is based on the assumption that the charge density on the plates is uniformly distributed.

Cheng *et al.*, (2001) developed MIP-glucose sensor based on capacitive detection. The sensitive layer was prepared by electropolymerization of *o*-phenylenediamine on a gold electrode in the presence of glucose. The template molecules were removed from the modified electrode surface by washing with distilled water. The imprinted polymeric layer had a high selectivity for glucose when the electrode surface has a good insulating property. The capacitance decreased with increasing glucose concentration. No cross-reactivity was observed on the capacitive sensor when the ascorbic acid or fructose was injected into the system sensor (Cheng *et al.*, 2001). The improvement of the insulating properties of a capacitive chemical sensor for fenvalerate

is reported Gong and coworker (2004). The sensor layer was prepared by a deposition of a self-assembled monolayer of 2-mercaptobenzimidazole (2-MBI) before electropolymerization of 2-MBI and subsequent treatment with *n*-dodecanethiol to eliminate pinholes and defects in the polymerized 2-MBI film. From the calibration curve concentrations of fenvalerate up to $9 \mu\text{g mL}^{-1}$ could be detected with a linear determination range up to $5 \mu\text{g mL}^{-1}$ and a detection limit of $0.36 \mu\text{g mL}^{-1}$. No significant interference was observed from common pyrethroid insecticides (Gong *et al.*, 2004). A novel capacitive sensor for pazufloxacin mesilate (pazufloxacin) determination was developed by electropolymerizing *p*-aminobenzene sulfonic (*p*-ABSA) and molecularly imprinted polymers (MIPs), which was synthesized through thermal radical copolymerization of methacrylic acid (MAA) and ethylene glycol dimethacrylate (EGDMA) in the presence of pazufloxacin template molecules, on the gold electrode surface. Furthermore, 1-dodecanethiol was used to insulate the modified electrode. Under the optimum conditions, the sensor showed linear capacitance response to pazufloxacin in the range of 5 ng mL^{-1} to $5 \mu\text{g mL}^{-1}$ with a relative standard deviation (RSD) 5.3% ($n=7$) and a detection limit of 1.8 ng mL^{-1} . The recoveries for different concentration levels of pazufloxacin samples varied from 94% to 102%. Electrochemical experiments indicated the capacitive sensor exhibited good sensitivity and selectivity and showed excellent parameters of regeneration and stability (Lu *et al.*, 2007).

5.1.1 Interdigital capacitors transducer

Capacitive sensors directly sense electrode motion, conductive or dielectric object motion, or the dielectric properties of a local material. Signal conditioning circuits convert capacitance variations into a voltage, frequency, or pulse width modulation. Very simple circuits can be used, but simple circuits may be affected by leakage or stray capacitance, and may not be suitable for applications with very small capacitance sense electrodes. The excitation frequency should be reasonably high so that electrode impedance is as low as possible. Typical electrode impedance is 1-100 Mohms. Excitation wave shape is usually square or trapezoidal, but a triangle waveform can be used to allow a simpler amplifier with resistive feedback and a sine wave offers better accuracy at high frequency. This electrode configuration is referred to as two interdigitated electrodes, and is illustrated in the top-view drawing in Figure 55.

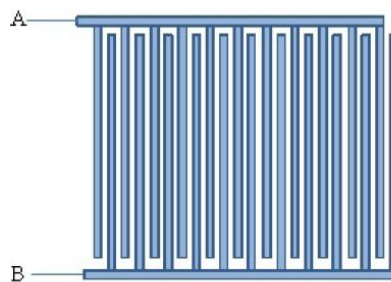


Figure 55. Illustration of interdigitated electrodes

In the measurement, the electrode overlapping area or the relative permittivity of the dielectric between the electrodes can be sensed with a capacitor structure. Fringing field

capacitive detection has the advantage of allowing the electrodes to be physically isolated from the sensing environment, as the fringing electric field is projected into the object or material being detected without altering the electrode configuration. Interdigitated electrode structures are particularly suitable for this sensing technique, as they can be designed to maximize the capacitance due to fringing. There have been reports in the use of measuring soil moisture content (Majid, 2009), grain moisture content (McIntosh, 2008) or rain detection (Bord, 2006) as proximity sensors (Chen, 1998), as capacitive touch switches (Sample *et al.*, 2009) and also application in biomedical sensors (Dewarrat *et al.*, 2008). Many of these sensors operate by measuring the change in capacitance due to the fringing fields in air ($\epsilon_r = 1.0006$) and in water ($\epsilon_r = 80$) (Hayt, 1981). Since the ratio of relative permittivities of water and air is approximately 80:1, there is typically a very large change in capacitance due to the presence of water or an object containing water. The electrodes can be coated with solder mask to isolate them from the sensing environment, typically water based, to prevent electrical shorting. Additionally, the Cu thickness can be tailored to the solder mask thickness in order to minimize measurand induced non-fringing capacitive effects directly between the electrodes. A cross-sectional illustration of this concept is presented in Figure 56, where interdigitated electrodes, "A" and "B", are only realized on one side of the PCB. The electric field, including fringing, is illustrated in Figure 57. It is observed that the fringing field extends out beyond the solder mask layer where it can interact with objects or fluid in close proximity to the PCB. The other side of the PCB can also be used for additional interdigitated electrodes, a Cu ground plane or for attached sensor interface electronics.

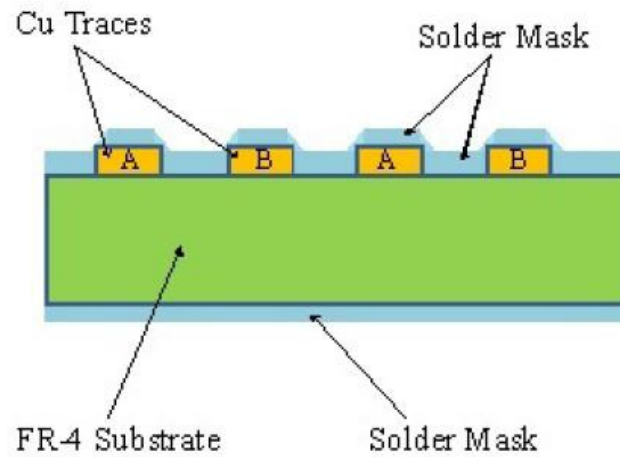


Figure 56. A cross-sectional drawing of interdigitated electrodes realized in the Cu foil on one side of a PCB

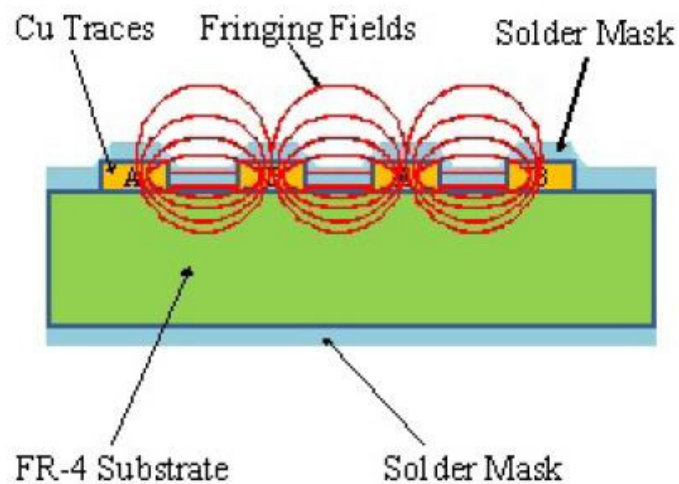


Figure 57. A cross-sectional drawing of interdigitated electrodes realized in the Cu foil on one side of a PCB where the red lines represent the electric field lines between the electrodes

The development of the affinity based interaction sensor using imprinted polymer has been investigated in this thesis work for application to the detection of Hev b1 allergen in rubber glove samples. A surface imprinting approach that enhances recognition by the imprinted polymer surfaces is used, to ensure generation of sufficient receptor binding sites from the bound protein templates during the polymerization process. The adsorptive cross-link is made of a copolymer between methacrylic acid and vinylpyrrolidone with *N,N'*-dihydroxyethylene-bisacrylamide as the crosslinker allows for some control of the binding characteristics of the resultant polymeric recognition material. As a result of surface-diffusion from the imprinted layer, the specific spatial requirements for achieving significant levels of binding capacity and affinity of the corresponding polymer, compared to those obtained with a conventional polymer surface reference material are obtained. This is followed by a substantial increase of the dielectric constant and to corresponding changes of the surface of the capacitance components on the IDC transducer system when analyte binds.

In this research an interdigitated capacitive microelectrode (for detection) with molecularly imprinted polymerization (for specific capture) were integrated to form chemical probes that resulted in changes to the electrical capacitance due to modification of the dielectric constant of the polymer after binding of the rubber protein molecules. The MIP-based capture system was prepared by a solution-based imprinting polymerization with Hev b1 proteins extracted from rubber gloves as the template (see Figure 58). The technique was based on a simple casting of the template-containing

polymer solutions on the cross-linking prepolymer layer coating on the surface of an IDC electrode attached to the glass chip. This avoided the unfavorable action of photochemical stress on the templates and pre-polymerization complexes. The presence of Hev b1-MIP-IDC biosensors fabricated as a lab-on-chip device is directly incorporated into a miniaturized sampling system, that allows for an online measurement of the allergen proteins. So with this approach the rubber allergens can be detected without labeling (label-free) them and provides an inexpensive production process and a low consumption of sample. The new flow-through conductometric sensor was applied to the measurement of the Hev b1 rubber allergen in simple extracts from the complex matrices of manufactured rubber latex gloves. Substantial differences occurred in the capacitance signals of the Hev b1 imprinted electrode and non-imprinted reference electrode after exposure of the protein analyte to an IDC in an aqueous solvent using the IDC-based assay protocol. Parameters that influence the protein-specific selectivity of the imprinted polymer on the IDC sensor had been discussed.

5.2 Objective

The aim of this chapter was to study the possibility of fabricating Hev b1 sensor for Hev b1 assessment in natural rubber latex and latex glove by the use of copolymer of methacrylic acid-vinylpyrrolidone-dihydroxyethylene-bisacrylamide cross-linked polymers as sensitive material in interdigitated capacitive sensor.

5.3 Materials and methods

5.3.1 Chemicals and biologicals

Methacrylic acid (MAA), 1-vinyl-2-pyrrolidone (NVP), *N,N'*-dihydroxyethylene-bisacrylamide (DHEBA), sodium dodecyl sulfate (SDS), Triton X-100 and Tris-HCl were obtained from Aldrich Chemical (Milwaukee, WI). 2,2'-Azobisisobutyronitrile (AIBN) was purchased from Janssen Chimica (Geel, Belgium). Ammonium persulfate was obtained from Amresco (Solon, OH). Lysozyme, ovalbumin, and bovine serum albumin (BSA) were from Sigma-Aldrich (St. Louis, MO).

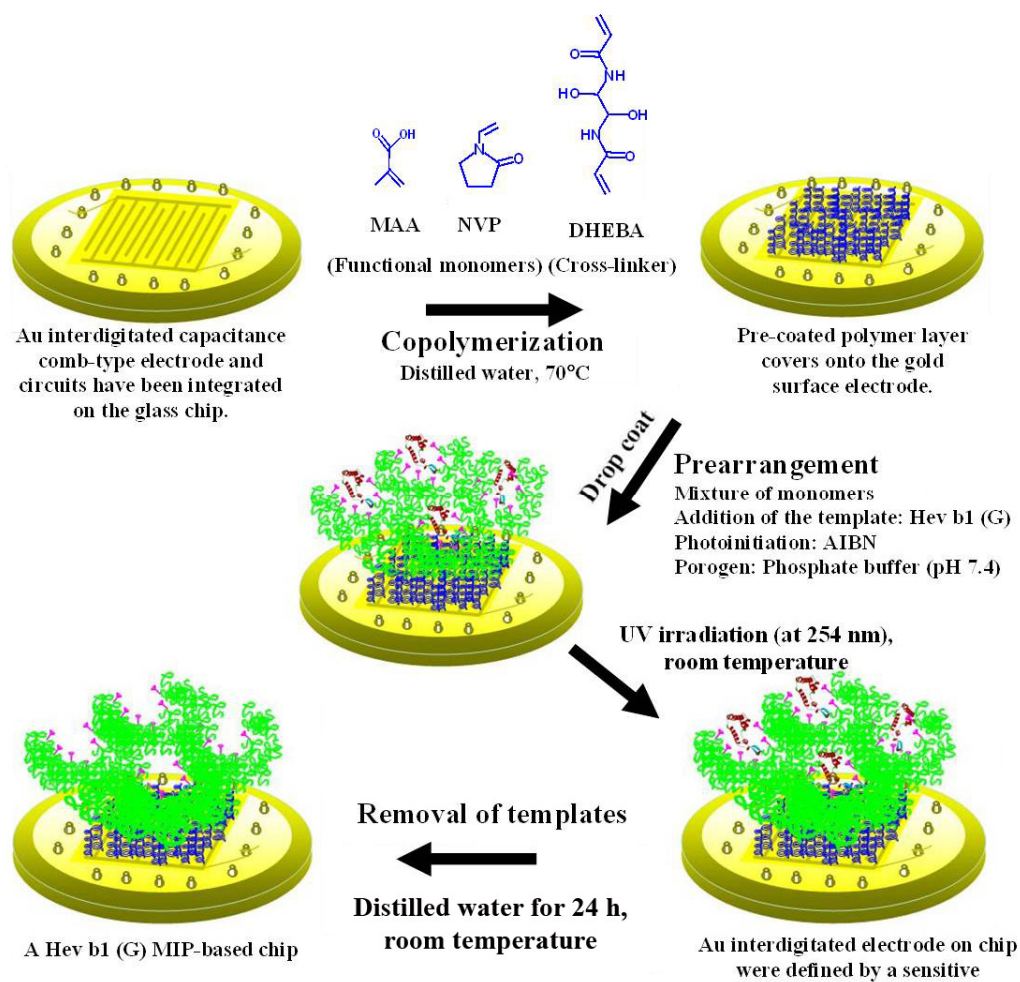


Figure 58. Schematic illustration of the surface imprinting process of a pre-coated IDC microelectrode on the chip; The monomeric solutions of the MAA and NVP functional monomers and DHEBA as a crosslinker and the Hev b1 (G) template in phosphate buffer (pH 7.4) is dripped onto the coated transducer surface to produce self-organizing receptor sites on the thin-film surface

5.3.2 Fabrication of MIP biosensors

A gold (Au) interdigitated electrode with dimensions of 4 mm × 4 mm × 1 μm and with a 10 μm gap between the digits was used, in which a planar inductor interdigital capacitor pair is photolithographically. The capacity of the IDC in the air was approximately between 5 to 10 pF. The IDC microelectrodes had a conductivity of $62.3 \pm 2.1 \text{ } \Omega/\text{cm}$ in the 0.01 mM NaCl solution and increased to $108.5 \pm 4.0 \text{ } \Omega/\text{cm}$ in 0.2 mM NaCl solution. The sensor coating layers were prepared from an aqueous solution with distilled water as porogen solvent with functionality ratios of methacrylic acid and vinylpyrrolidone of 6:2 and a 17 mol% content of DHEBA as cross-linking agent. After adding the radical polymerization initiator (AIBN) polymerization was continued under stirring conditions at 70 °C until the gel point was reached. The polymerizing solutions were diluted with distilled water and used for the coating process and patterning for rubber protein allergen. To prepare the template layers, the polymer coating was as already described, except that the pH had been adjusted to 7.4 with 100 mM KOH (in order to prevent denaturation of the protein template) and ammonium persulfate as catalyst, was mixed with Hev b1 (G) in 0.1 mM phosphate buffer ($0.2 \text{ } \mu\text{l}$, 12.5 mg ml^{-1}). The freshly prepared template-containing polymer solution was coated onto the surface of the pre-polymer coated electrode. The curing process of methacrylic acid-vinylpyrrolidone-DHEBA-polymer layer was overnight UV exposure at 254 nm under ambient conditions. After the immobilization step, the chip was immersed in 5 x 100 ml

of distilled water for 24 h at room temperature. This removed the templates, leaving the nanometer pits of the imprinted process on the IDC microelectrodes. The coated layers were responsible for transferring the capacitive signal of the analytes when they were rebound in the MIP cavities. The reference electrode with a non-imprinted polymer (NIP) was used to evaluate the efficiency of the MIP electrode, which was fabricated in the absence of the template during the polymerization process.

5.3.3 Interdigitated capacitance electrode and measurements

In this work, the construction of IDC microelectrodes both with the imprinted and non-imprinted reference polymer was done. Allergen detection was performed using a 4284A LCR precision bridge (Agilent Technologies, Santa Clara, CA) with the PC software developed in-house. The sampling and capacitive analytical system consists of: a liquid port for delivery of the sample from a sample reservoir; a peristaltic pump; and the flow-through microcell/integrated MIP sensor with a sample volume of 100 μl were connected to the test and counter electrodes on the network analyzer. The tested frequency range was from 0.1 kHz to 1 MHz with an alternating potential voltage of 100 mV. After washing the electrode several times with a background solution, the difference in capacitance before and after the protein binding was taken as the signal produced by reaction between the MIP biosensors and proteins. Finally, capacitance values (C) were extracted from the measurements at certain frequency (f). The signal response toward the protein of the sensor was reported as ΔC (fF; femtofarad), where ΔC

is the capacitance shift in response to the addition of known amounts of the protein of interest. After several times washing with distilled water, sensors were stored at room temperature until use.

5.3.4 Method validation

5.3.4.1 Recovery

The efficiency of recovery was performed by the addition of known amount of standards Hev b1 (G) into the crude proteins from rubber latex and glove extracts which were analyzed by the proposed Hev b1 (G)-MIP sensor. For this purpose, 1 g of the solid powder (or 4 g of the glove extracts) spiked with Hev b1 (G) standards was extracted according to the procedure previously described for Hevb1 (G). Spiked samples of allergen protein (50, 100, and 200 $\mu\text{g L}^{-1}$), used in recovery studies, were prepared by adding the appropriate volume of a Hevb1 (G) standard solution to an extract of a matrix sample from a latex glove, resulting in a final volume of 15 mL. A calibration curve was prepared by dissolving Hev b1 (G) in 0.1mM phosphate buffer, pH 7.4, to obtain solutions having Hev b1 (G) of between 10 and 1000 $\mu\text{g L}^{-1}$, and then comparing them to that measured for Hev b1 (G) in the spiked samples. After several washing steps, IDC measurement was carried out by following the protocol in Section 2.7. Every experiment was repeated three times at room temperature (25 ± 1 °C).

5.3.4.2 Linearity and method detection limit (MDL) of the IDC sensor was studied same as that in QCM experiment in section 4.4.8.2 to 4.4.8.5.

5.3.5 Sample and assays

In order to validate the biosensor performances, one disposable powder glove and one powder-free glove from a glove manufacturer in Songkla, Thailand were sampling for analysis protocol using the MIP-based IDC assay. Rubber-based gloves were cut into small pieces and extracted in 0.2 M phosphate buffer, pH 7.4, containing 0.5% SDS. After that, the mixtures were centrifuged at 10,000 g for 15 min at 4 °C. The liquid was dialyzed against distilled water for 48 h at room temperature. A typical protein sample has a conductivity ranged from 150-153 Ω /cm. The crude protein extract from the rubber gloves was analysed using the developed MIP-IDC biosensor at the optimized sensor conditions. After several washing steps, a further IDC measurement was carried out by following the protocol described in section 5.3.3. Every experiment was carried out in triplicate on any particular day of experimentation.

5.4 Results and discussion

5.4.1 MIP immobilization

Atomic force microscopy (AFM) was used to confirm the immobilization of the chemical detectors (artificial antibodies) onto the coated biosensor surface. The MIPs, were made by photochemical polymerization of the monomeric mixtures after being doped with a free radical initiator in distilled water as a porogen solvent. An Hev b1 (G)-imprinted poly(MAA-NVP-DHEBA) was fabricated on the glass chip by following the method mentioned in the experimental section and as presented in Scheme 1. A section analysis with an AFM image showed the depth of the imprinted sites was ~70 nm. Due to the surface imprinting process using a solution-based polymerization with templates we were able to generate imprinted surfaces at several nanometer thicknesses of film by changes to the dilution of the pre-polymer. The Hev b1 (G) imprinted surface had nanosized pits on the gold IDC microelectrode. An MIP layer, 200 nm-thick, was measured by the AFM spectroscopy method after the film was scratched with a needle see Figures 59 (A & B). At 200 nm thick the layer was also suitable for imprinting the polymer and provided the optimum imprinting effect to achieve the optimum capacitance signal (when the measured capacitance was carried out in the open air after the electrode was soaked with sample at ambient temperature). The size distribution of the rubber allergen imprints is reflected through the surface imprinting process and when the templates are removed by solvent the hardened material is left with polymeric-coated

cavities that have a memory for the contours and charge distributions of the chemical groups in the original biological molecule. Figure 60A illustrates the regular pattern of the imprinted sites and some remaining rubber allergens included in the imprinted pits on the surface of the polymer layer coated onto a IDC transducer. The surface imprinting procedures allow generation of micropatterns of the rubber allergen protein on the polymer surface that results in a randomly distributed nano-pitch pits on the coated surfaces (Figure 60B).

5.4.2 Sensor coating layer

The effect of the washing procedure on the efficiency of extracting the template was studied by using the resulting MIP coating layer on the IDC surface and IDC measurement. Allergenic rubber proteins are well known for their ability to adhere to the inner and outer surfaces of manufactured rubber gloves. To ensure that remaining allergens in the used electrodes can be effectively removed. Therefore, always first performed the removal experiment of remaining templates from the films by soaking the coated electrodes with distilled water at room temperature ($25 \pm 1^\circ\text{C}$). It can be seen that the resistance of the surface, when measured in the air, gradually decreased the more times the imprinted electrodes were washed in distilled water up to 24 h. A 24% increase in the capacitance response in the air occurred for the MIP film after consecutive immersions of the MIP-coated electrodes in distilled water.

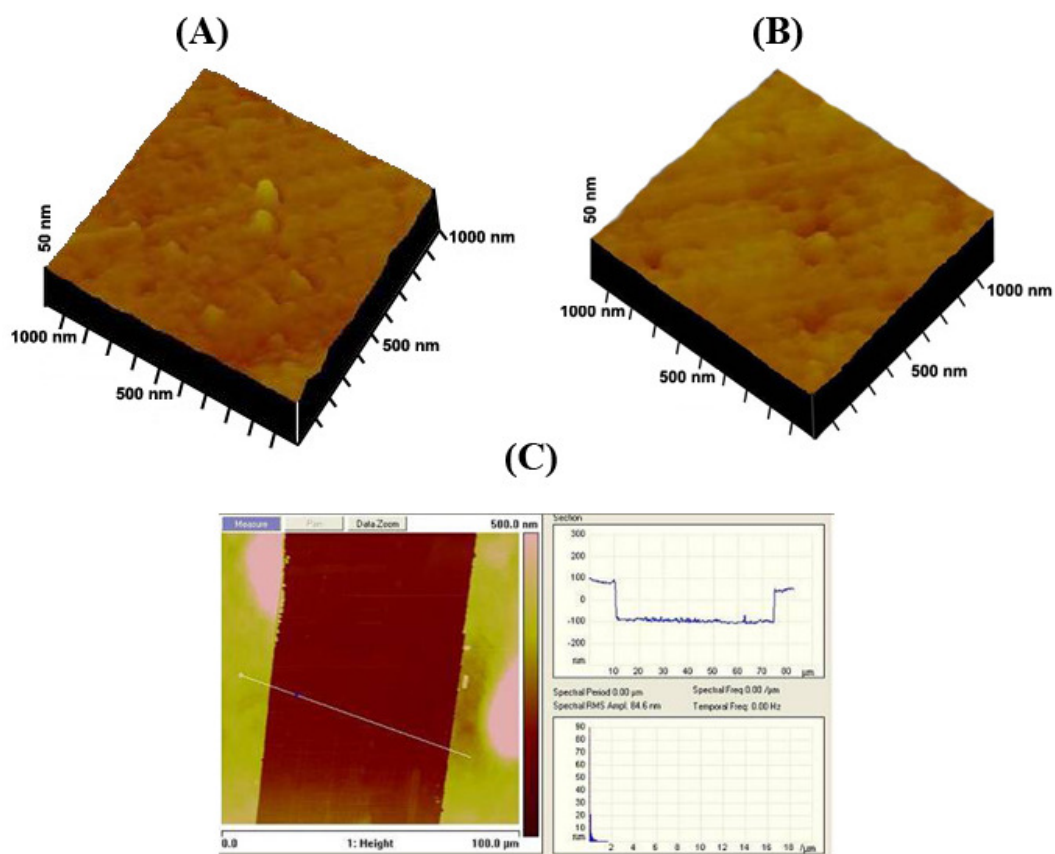


Figure 59. Contact mode AFM images of: (A) MIP with partially removed template showing the rubber allergens retained in the polymerized material. (B) imprinted layer showing Hev b1 (G) pits on a MAA-NVP-DHEBA polymer after hardening of the layer and washing with distilled water for 24 h. (C) cross-section analyses of the scratch on the imprinted layer and the measured 200 nm layer

This indicates that the templates diffuse through the imprinted cavities within the MIP matrix. In contrast there was only a 7.1% increase in capacitance for the reference polymer coated surface. This capacitance behavior indicates that water penetrates into the bulk of the polymer layer in this type of polymer material. The washing of the MIP electrode with water reduces the contribution of any non-specific binding, and also effectively extracts the specifically bound template Hev b1 (G). Under the washing protocol used, the existence of Hev b1 (G) imprints on the surface of polymer films was shown to be ~90%, as determined from the amount of template that was removed from the sensor coating layers.

5.4.3 Capacitance characteristics of the immobilization process

Figure 60(a) illustrates the scanning electron microscope (SEM) image obtained with the micro-interdigitated capacitor, showing the inter-digitated comb capacitor structure on top of a glass chip, and equivalent circuit model of the biosensor is depicted in Figure 60(b). Equivalent circuit consists of ohmic resistance of the electrolyte (R_s) between two electrodes and double layer capacitance (C_{dl}), electron transfer resistance (R_{ct}) and the Warberg impedance (Z_o) around each electrode was proposed for interpretation of the capacitance components of the gold planar microelectrode arrays. The total current through the electrode area is the sum of Faradaic current and double layer current in the branch circuit and the impedance and the electron transfer resistance both of them connected in parallel with double layer capacitance. If there is a change in

the dielectric constant, then a counter change occurs in the capacitance value between the two sets of array electrode. Unlike other detection mechanism used to quantify protein concentration, capacitance method does not need labeling of protein sample. The protein bound to the surface of the immobilized capture molecularly imprinted polymers yields dielectric properties between the IDC electrodes changes and measurement can be taken immediately after the protein binding (Figure 60c). Taking into account that the capacitance of a planar capacitor is determined by its geometry (area and thickness) and dielectric constant, any modification of its capacitance with no change of geometry indicates a definite modification of the dielectric constant (Patolsky *et al.*, 1999).

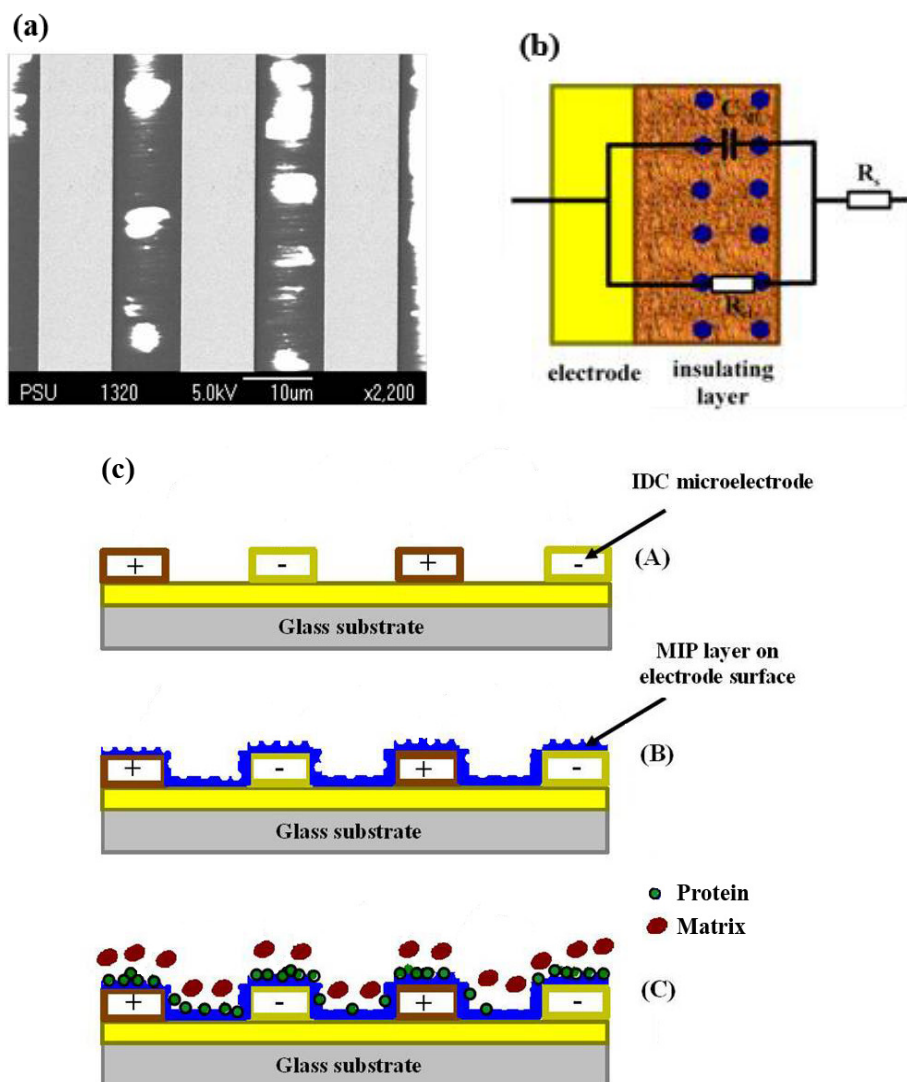


Figure 60. (a) SEM image of inter-digital capacitor and (b) equivalent circuits used to describe impedance spectra of coated electrodes: R_s electrolyte resistance; R_{ct} charge transfer resistance and C_{dl} is double layer capacitance. (c) Hev b1 (G)-MIP capacitive biosensor fabrication and process. (A) bare electrode; (B) with MIP layer; (C) with Hev b1 (G) binding. Circle = Hev b1 (G); Oval = matrix

Figure 61 shows the Bode plots and phase degree of bare electrodes and electrodes coated by Hev b1 (G) MIP thin-film. As expected, the impedance spectra of the bare microelectrodes can be described by the interfacial interactions, the Randles equivalent circuit with an essential contribution of Warburg's impedance. Modification of the molecularly imprinted polymer of the IDC electrode led to major alterations to the impedance spectra. At a frequency of more than 100 Hz, the coated electrodes have mainly capacitive properties (the phase angle becomes close to 90°). The $\log |Z|$ vs $\log f$ function is a straight line with a slope of -1 and remains nearly unchanged at low frequencies (where the resistive components dominate) and is decreased at high frequencies. The strong capacitance properties of the MIP-coated electrode at 1 kHz allow us to relate the changes in the capacitive current at this frequency to changes in the electrode capacitance, hence this frequency is used for further experiments. An inductive behavior after 10 MHz, therefore capacitance values for frequencies higher than 10 MHz were not considered. According to the equivalent circuit model obtained by impedance measurement, we can calculate the value for the double layer capacitance and reaction resistance on the interfacial electrode of IDC biosensor, was calculated which was $1560 \mu\text{F}/\text{cm}^2$ and $3975 \text{ M}\Omega/\text{cm}^2$, respectively.

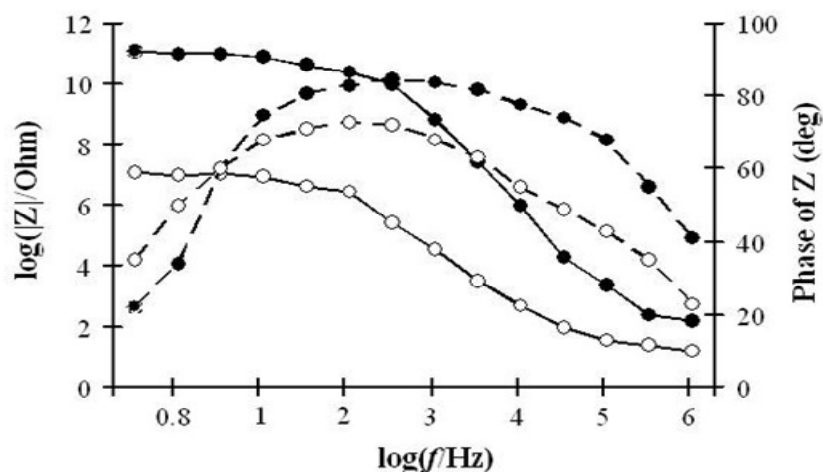


Figure 61. Bode plots refer to representation of the impedance magnitude (or the real or imaginary components of the impedance) and phase angle as a function of frequency for IDC electrode (open symbols) and IDC electrodes coated with an Hev b1 (G)-MIP (filled symbols), exposed to 0.1 mM phosphate buffer solution (pH 7.4) containing Hev b1 (G) at a concentration of $250 \mu\text{g L}^{-1}$ at room temperature. Impedance = black line; phase degree = dotted line

5.4.4 Optimum content of cross-linker

The presence of imprint structures in the polymerized MIP coating obtained by the solution-based imprinting polymerization was demonstrated by atomic force microscopy. Regular patterns of bioimprinting sites in a thin-film of sensor coating are preferred rather than a high number of densely imprinted sites. This can allow for

pronounced re-visits of protein templates onto the surface of the polymer layer. Prepolymer formulations generally contain the functional monomer and protein template at high concentration levels, such as comonomers, cross-linking agents and porogenic solvents. Under polymerization conditions, functional monomers supposedly change to form stable dimers or oligomers. Sometimes, disposition of pendent groups of a functional monomer can be hidden within polymer domains so limit some conformational changes and impair the pendent's ability to establish the subtle network of noncovalent contacts essential for efficient and selective protein binding.

In this work we have determined the optimal amount of DHEBA for cross-linking the MAA-NVP-DHEBA-polymer layer to allow for the formation of a complementary shape with a high affinity for the template in the imprint. This also produced the most effective sensor response from the Hev b1 (G) MIP when immobilized onto the IDC electrode. As can be seen in Figure 62, this degree of cross-linking, 10 mol%, produced a lower imprinting effect than at the other cross-linker contents which indicates a low stability of the binding sites on the MIP thin-layer. In contrast, a high cross-linked density of the polymer beyond 15% causes a reduced diffusion of the protein template onto the binding sites of the MIP resulting in just surface imprinting on the polymer, and tends to interact more by binding non-specifically bound protein to the residues of the functional groups of the cross-linker. The sensitive and highly selective MIP have been successfully generated for recognizing Hev b1 (G) by using mixtures of MAA and NVP as the functional monomers (6:2, mole ratio) with 15 mol% of DHEBA and a solubilized Hev b1 (G) as template. The fact that the affinity and selectivity for the

Hev b1 (G) is superior to those of other components (an imprinting factor of 4), indicates that there should be a significant population of template selection sites on this polymer.

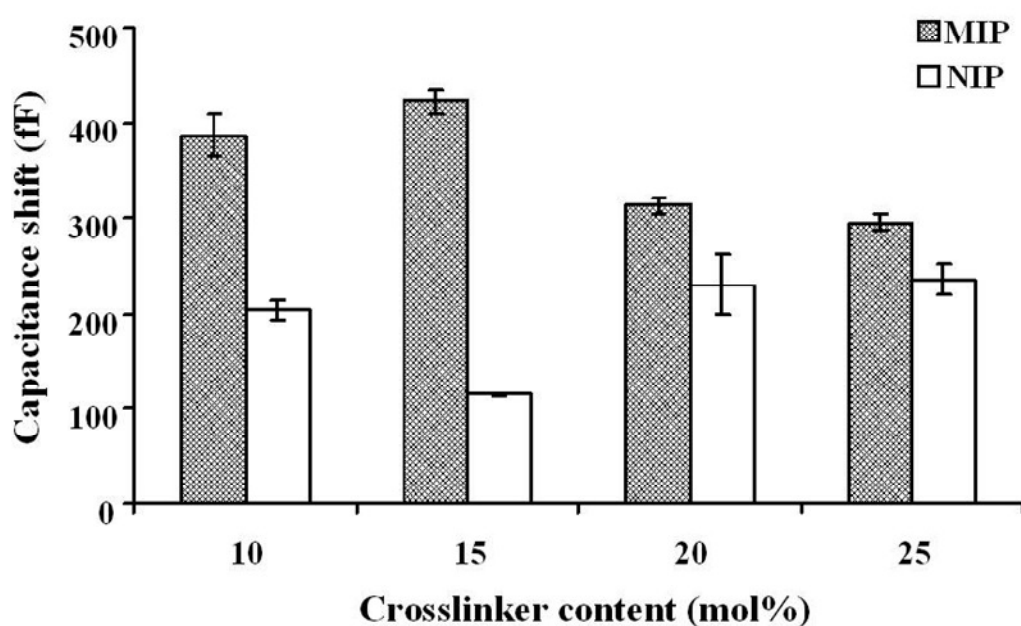


Figure 62. Effect of the amount of cross-linking monomer (DHEBA) on the capacitive responses of the MIP and NIP layer on the IDC microelectrode biosensor exposed to Hev b1 (G) in phosphate buffer solution (pH 7.4) at a concentration of $400 \mu\text{g L}^{-1}$. The methacrylic acid and vinylpyrrolidone acted as functional monomers at a mole ratio of 6:2 were used

At this degree of cross-linking the fraction of the monomer being nonfunctional due to steric restriction was low. The high binding affinity and the excellent molecular level complementary of this template-monomer combination was anticipated to give rise to a

high concentration of monomer-template complexes in the polymerization mixture. The decreased capacitance upon the binding events of the protein analyte on the electrode surface can be accounted for the template interact with the binding sites within the imprints, which associate to the change in the dielectric property of the selective imprint material due to the orientation polarization changes upon binding.

Hence, the imprinting approach has proven to be successful in reproducing the structural features of the latex allergy protein within the imprinted matrix, allowing for the artificial recognition surfaces to interact with the accessible surface residues of Hev b1 (G) in solution. In order to exploit the new, selective Hev b1 (G)-imprinted MAA-NVP-DHEBA-polymer by measuring the change to its capacitive property after binding of the specific molecule (targets) into the imprint cavity, and to investigate any analytical applications for detecting rubber allergen proteins, in products such as rubber gloves.

5.4.5 Chemical parameters

The effect of the medium pH of the reaction conditions was studied by using phosphate buffer solutions in IDC measurement under controlled condition. The highest sensor effect to Hev b1 (G) was around pH 7.4 (Figure 64). At a pH of 5.0, both the MIP and NIP thin films gave the lowest capacitance shift response for Hev b1 (G) (Figure 63). The allergen undergoes a renaturation process in acidic conditions, therefore all measurements at pH 5 were performed with freshly prepared samples (van der Merwe,

2000). The results can be explained if the Hev b1 (G) ($pI = 5$) does not bind to the binding sites on the polymer film surface at a pH of 5. As the amount of Hev b (G) increases in the MIP layer due to the increase in pH and the MIP polymer material returns to its original size when at pH 7.4, which mimics the conditions under which the polymer were created, produced a similar response to the original interaction. Therefore pH 7.4 was chosen for sensor measurement and applications to gain the highest allergen sensitivities in detecting Hev b1 (G) from manufactured rubber gloves.

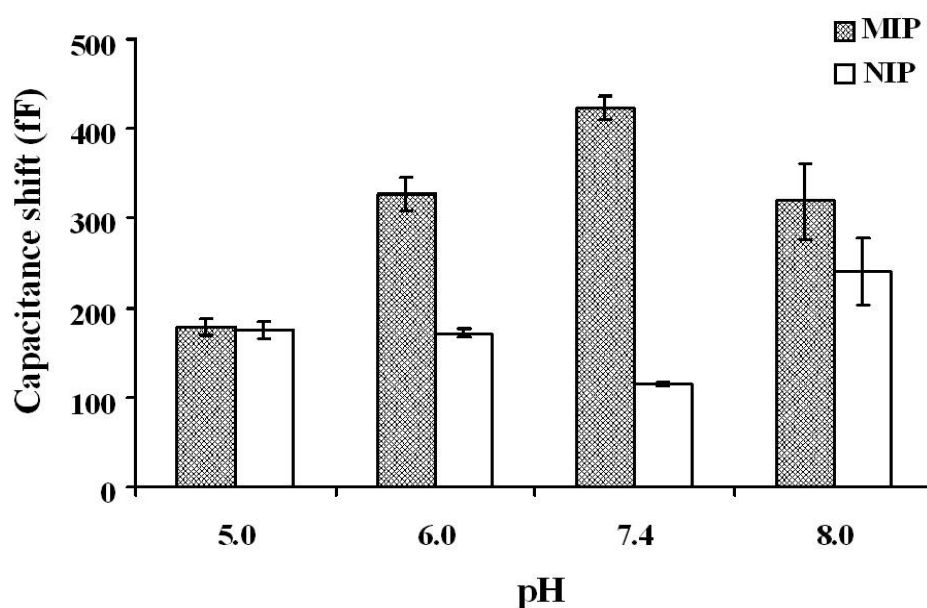


Figure 63. Effect of pH of the medium on the capacitance response upon 400 ng ml^{-1} of Hev b1 (G) MIP sensor and reference sensor at 1 kHz and at room temperature. (b) Effect of NaCl on the capacitive shift response of the MIP and NIP copolymer of MAA and NVP at 6:2 mole ratio and 15 mol% DHEBA (pH 7.4). Responses were initiated by the addition of $250 \mu\text{g mL}^{-1}$ Hev b1 (G)

Using the same layer compositions the further investigation was carried out in testing the effectiveness of our sensor coating immersed into a phosphate buffer solution containing Hev b1 (G) ($250 \mu\text{g L}^{-1}$) and an NaCl concentration of between 0.01 to 0.2 mM and a small-amplitude ac potential (100 mV). Increasing concentrations of NaCl up to 0.2 mM resulted in a decrease in the selective sensor responses to Hev b1 (G) (see Figure 64). Chloride ions will displace water molecules from the inner coordination polymer layer. A 70% increase of the magnitude of capacitance was observed for the MIP-based electrode, while there was a 180% increase of the magnitude of capacitance for the NIP-based electrode. The reduction of the selective signal of the biosensor, as the amount of Na^+ increases, is due to the polymer crosslink binding to the salt instead of the protein template causing the network to lose this proportion of its cross-linking thus allowing the protein to be released from the MIP. Therefore, the concentrations of salts have to be kept below 0.01 mM for effective molecular recognition and selectivity by the selective MIP layer.

5.4.6 Capacitance measurements and optimization of the capacitive biosensor

The detecting a single rubber protein allergen-MIP interaction has been carried out successfully using this IDC microelectrode transducer system. It can be applied for rapid and selective detection and provides an increased active area for interdigitated electrode arrays that can be used in order to increase the sensitivity to

binding events. The adhesion of the protein allergen to the IDC surface was measured by an IDC-based assay protocol and the effect in Figure 65 could be interpreted as the adhesion of the rubber protein into the selective

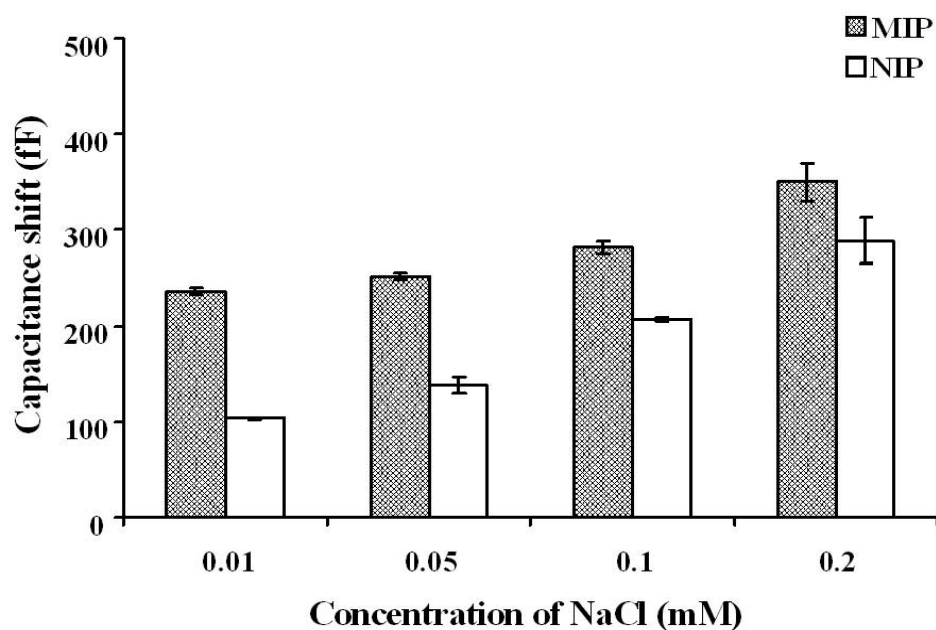


Figure 64 Effect of NaCl on the capacitive shift response of the MIP and NIP copolymer of MAA and NVP at 6:2 mole ratio and 15 mol% DHEBA (pH 7.4). Responses were initiated by the addition of $250 \mu\text{g L}^{-1}$ Hev b1 (G).

layer. A capacitance decrease of ~63% on the MIP-modified electrode, and a decrease of 3.7% for the NIP-modified electrode after binding of a Hev b1 (G) ($250 \mu\text{g L}^{-1}$) allergen was observed. The efficiency of the imprinting process is greatly enhanced and re-dissolution of the template can occur without the process being modified, and achieved a

rapid signal response within 5 minutes, which enables multiple measurements without time-consuming surface regeneration. This complete availability of the surface imprinting protocol is a reflection of the thin film of the cross-linking polymer, that allows for fast and efficient mass transport.

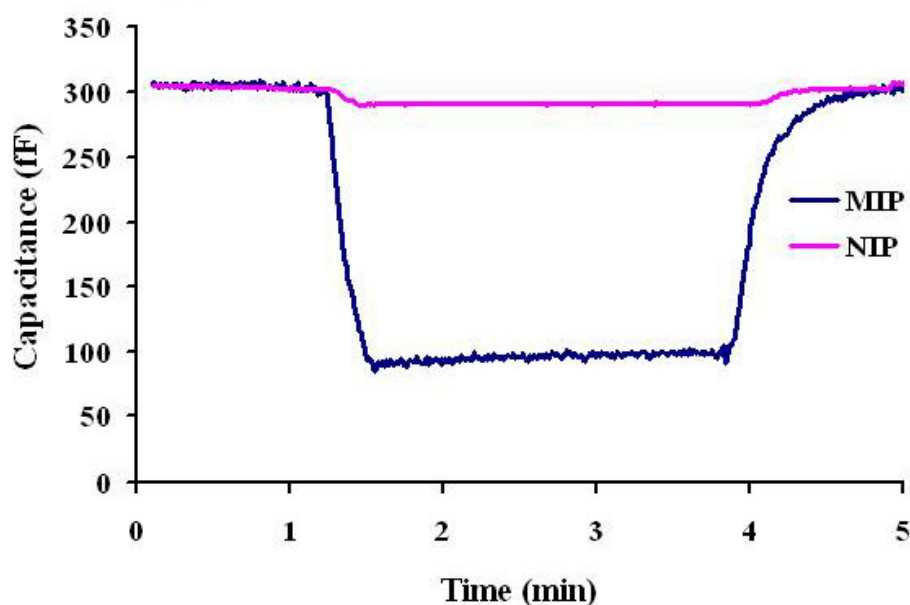


Figure 65. A typical sensor response of both a non-imprinted control polymer and Hev b1 (G)-MIP illustrates the effectiveness of rubber allergen adhesion via surface imprinting using solution-based polymerization with Hev b1 (G) proteins (pH 7.4, room temperature and flow rate of 1 mL min⁻¹)

In the current investigation of this thesis, the optimization of capacitance for the Hev b1 (G)-MIP-IDC biosensor was carried out to assess whether regeneration of the

selective electrode remove any non-covalently bound Hev b1 (G) analyte without disrupting the activity of the biomimetic recognition materials on to the electrode. The residual activity of the imprinted electrode was obtained from the capacitance change as a result of the binding between Hev b1 (G) (i.e. $250 \mu\text{g L}^{-1}$ of Hev b1 (G) standard) and the Hev b1 (G)-imprinted layer on the IDC transducer system before and after regeneration. Successful regeneration allows the surface to be reused of capacitive biosensor for many times. The criteria for successful regeneration of the electrode surface is if post regeneration binding still retains above 90% binding efficiency compared to that before regeneration (van der Merwe, 2000). It was shown that residual binding values above 95% after up to 50 cycles of regeneration steps (Figure 66).

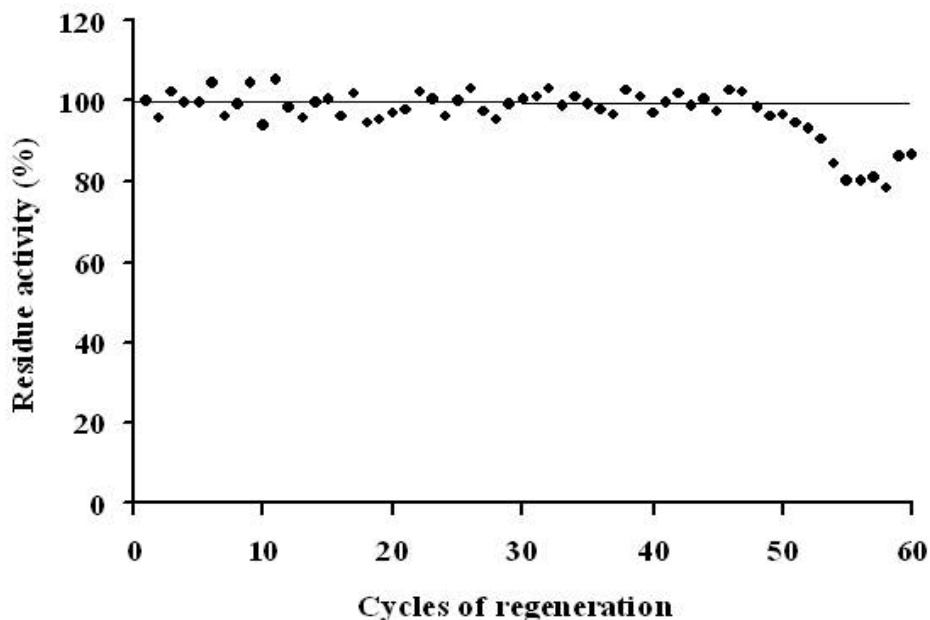


Figure 66. Reproducibility of the response from the Hev b1 (G)-MIP modified electrode to injections of fixed volume of a standard solution of Hev b1 (G) ($250 \mu\text{g L}^{-1}$) with regeneration and reconditioning steps between each individual assay

5.4.7 Concentration dependence of the biosensors

As can be seen from Figure 67, the MIP sensor gives a signal response that depends on the concentration of Hev b1 (G), in the range of $10\text{-}1000 \text{ ng ml}^{-1}$. In contrast the reference sensor shows only a slight capacitance response towards added Hev b1 (G) in phosphate buffer solutions (pH 7.4). The sensitivity of these sensor layers is therefore in the ng ml^{-1} range of template concentrations. The sensor response was selective with a selectivity factor of about 6 at low rubber protein concentrations ($10\text{-}400$

$\mu\text{g L}^{-1}$) but highly selective when challenged with protein concentrations of between 400-900 $\mu\text{g L}^{-1}$ with a factor of 10 for Hev b1 (G). The template polymerization procedures used produced a pronounced titration point at around 400 $\mu\text{g L}^{-1}$ Hev b1 (G) with a capacitance change of about 450 fF that corresponds to the formation of a Hev b1 (G) imprint cavity. This observation indicates that for the IDC sensor there may be an optimum thickness for the MIP layer for achieving a favorable compromise between the response characteristics, sensitivities and selectivity. This observed concentration dependence could depend on the surface diffusion, as such that at very low concentrations the template will rapidly bind to the highly specific affinity sites. Because of the multiple-point interactions experienced in this environment, template dissociation from these sites, and thus surface diffusion should be slow. In the presence of higher template concentrations, however, the sparsely populated high-affinity sites are rapidly saturated; further template binding will then occur at randomly distributed nonselective sites, the dissociation kinetics of which are presumed to be much faster, because of the lack of specific interactions. Further increases in the quantity of allergen on the non-

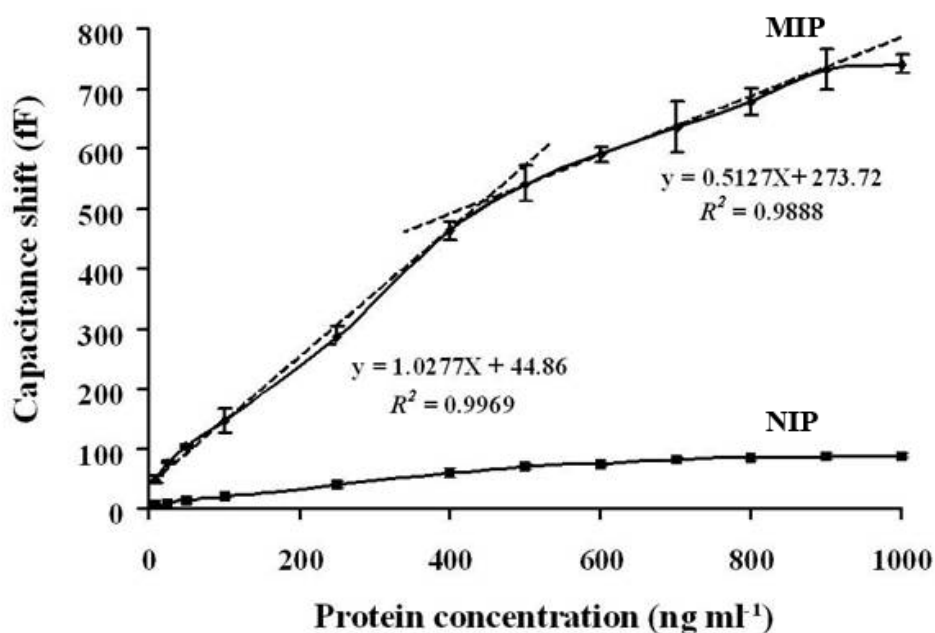


Figure 67. Concentration dependence of the capacitance response to Hev b1 (G) for the imprinted poly(MAA-NVP-DHEBA)-coated IDC and the control. Each point represents the average of three independent measurements. A separate regression line has been fitted for the data in each stratum. Those regression lines are the dashed lines in the plot.

imprinted electrode produced a very slight increase in the capacitance responses due to the electrostatic repulsions of the charges on the additional proteins that results in hydrophobic protein-protein aggregations on the electrode surface. Therefore, the increase in capacitance sensitivity i.e. ~1000 times is related to the specific protein-MIP interactions and the dynamic structural changes that occur upon binding. Incorporation of this protein-monomer complex onto the surface imprinting procedures may successfully

compete with their structurally identical, conformationally unrestricted, and readily accessible surface cavities. In addition to these, the corresponding control materials also generated signals in the absence of Hev b1 (G) in a phosphate buffer.

Fitting the isotherm data to the Langmuir adsorption models enabled quantification of the association energies and densities of the individual binding sites of the MIP and NIP onto the capacitance electrode, the values of the amounts bound were plotted against the concentrations of Hev b1 (G) as shown in Figure 68 and Figure 69, respectively. The binding constants were determined from the following equation (8):

$$\frac{B}{[Hev\ b1]} = \frac{(B_{max} - B)}{K_d} \quad (8)$$

where K_d is the equilibrium dissociation constant, B is the amount of Hev b1 bound to the polymer, B_{max} is the apparent maximum number of binding sites, and $[Hev\ b1]$ represents the equilibrium concentration of Hev b1. The binding profile of our thin-films indicated simple two-phase binding interactions. This finding demonstrates that the polymerizable component provides the significant imprinted sites with heterogeneous binding characteristics. Thus, the Hev b1 (G) MIP had pronounced affinity ($K_a = 1.25\ \mu\text{M}$) which is approximately 62.5 times compared to that of the corresponding NIP ($K_a = 0.02\ \mu\text{M}$). The capacity (B_{max}) was $0.021\ \mu\text{mol}/\text{mm}^2$ for Hev b1 (G), which is more than ten times higher than the polymer layer's capacity.

The K_D and Q_{max} of the higher and lower affinity binding sites of both MIP and NIP can be calculated and shown in Table 14. Most MIPs prepared with non-covalent imprinting approach, correspondingly Hev b1 (G) formed a heterogeneous distribution of binding sites (Takeuchi, 2000 and Matsui, 2000). This phenomenon was probably associated with imprinting process which can produce binding sites through the polymer matrix after removal of the template. Therefore, the possibility of imprinting sites located at the surface position is accordingly less than those located inside polymer matrix. The imprinting sites situated at the surface can be considered as high affinity to the template, so easy diffusion into by template molecule. The lower affinity binding sites were assumably believed that located deeply inside the polymer particle (Zhi Zhu *et al.*, 2002). It was mostly due to the more difficult diffusion process of the template to these binding sites. The binding events of the inside imprinting hole can occur after the saturation of the imprinted sites from the template binding at the surface attained. This explanation can be clearly revealed from two slopes in Schatchard analysis which the higher affinity binding sites represented the higher slope at lower template concentration and correspondingly, lower slope of a straight line at high template concentration showed the lower affinity imprinted sites. Comparing between MIP and NIP, the high affinity region of MIP has higher negative slope than NIP. It revealed the sensitivity of binding site in the MIP to the template. Q_{max} of both MIP and NIP were produced from the high affinity and low affinity binding site. The amount of high affinity of MIP has less than the amount of low affinity because the imprinting site located at surface area of imprinting polymer has less

than the inside imprinting hole similar to NIP. Comparing between MIP and NIP, Q_{\max} shown that the binding site of MIP is higher than NIP because the imprinting sites consist of specific binding and non-specific binding whereas NIP was obtained from non-specific only.

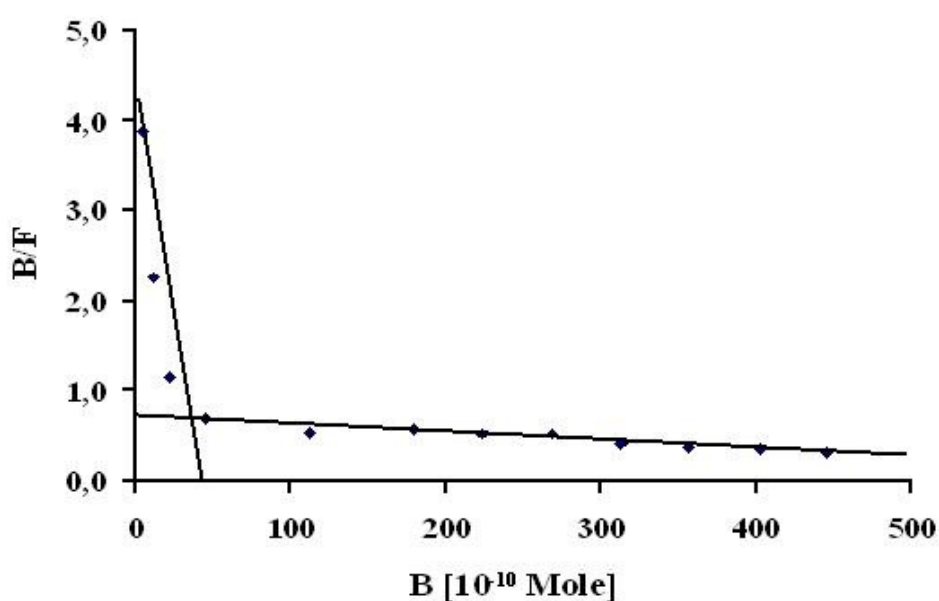


Figure 68. Scatchard plot of the binding of Hev b1 (G) to MIP. Q: bound Hev b1 (G) [Hev b1 (G)]:concentration of free Hev b1 (G)

Table 14 displays the equilibrium dissociation constant and maximum number of binding site of two classes of binding sites in both imprinting polymer. The K_d was obtained from the reciprocal of slope of two straight lines which consist of high affinity and low affinity from Scatchard plot of MIP and NIP. The K_d indicates the ability of the dissociation of complex form which obtained imprinting site bind to template. Therefore high K_d , the

complex form can be easily dissociated or unstable while low K_D produced complex has more stable and difficult to dissociation.

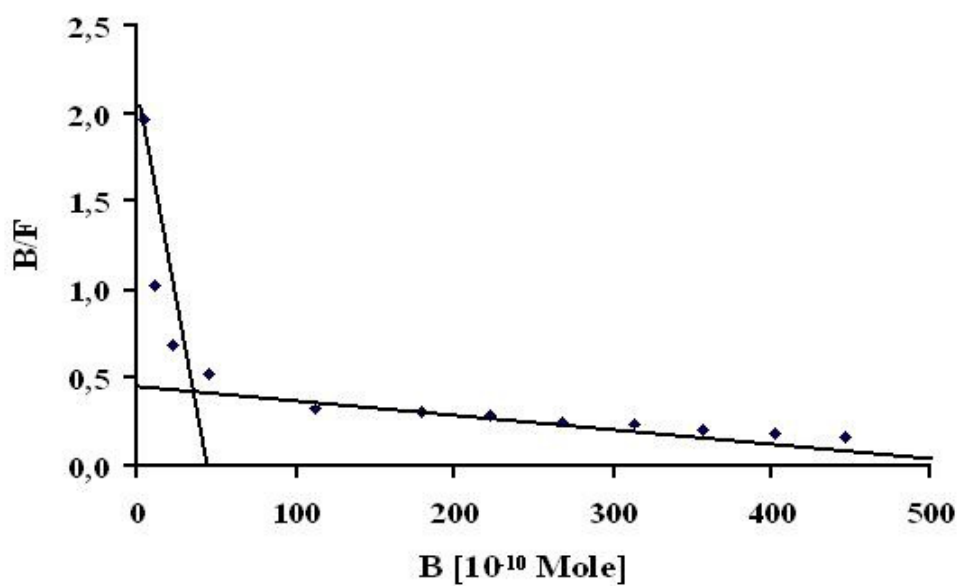


Figure 69. Scatchard plot of the binding of Hev b1 (G) to NIP. Q: bound Hev b1 (G) [Hev b1 (G)]:concentration of free Hev b1 (G)

Table 14. Equilibrium dissociation constant (K_d) and maximum number (Q_{max}) of binding sites value of two classes of binding sites in both imprinting polymer

Constant	MIP		NIP	
	High affinity	Low affinity	High affinity	Low affinity
K_d (M)	1.6×10^{-6}	4.0×10^{-5}	2.0×10^{-6}	2.0×10^{-5}
Q_{max} (mole/cm ²)	3.04×10^{-9}	2.07×10^{-8}	2.06×10^{-9}	8.77×10^{-9}

5.4.8 The selectivity and sensitivity of the Hev 1 (G) MIP layer on the IDC

Incorporation of protein-monomer complexes into the cavity formed by the Hev b1 (G) MIP may shape binding sites around complexes with the potential to enhance selectivity and substrate specificity. It is justified to expect that the surface imprinting procedures used may also form pits imprinted with the ability to memorize specific structural features, in particular the size and shape of the template. Thus the Hev b1 (G) surface imprinted polymer should show an enhanced level of substrate specificity, that will preferentially recognize the original template by providing a geometrical fit and a conformation memory for the rubber protein allergen. The results indicate that the NRL latex proteins are capable of inducing changes in the capacitance of MIP due to being located in the Hev b1 (G)-imprinted cavity, but at different degrees of fitting for each rubber allergenic protein (see Figure 70). The cross-reactivity results are illustrated in

Figure 71. The experiment was carried out with a NIP-based sensor to confirm that the test proteins did not bind specifically to the sensor with a similarly embedded Hev b1 (G) MIP. High sensitivities are only obtained when the analyte is identical to the template. As shown in Figure 71, solutions of Hev b1 (G) of $250 \mu\text{g L}^{-1}$ in buffer are readily detectable, whereas the Hev b1 isolated from rubber-tree-derived latex produced a 1.8 times lower sensitivity. Although they have exactly the same size, they differ slightly in their exact conformation around the receptor site. Compared to Hev b1 (G), the different allergenic proteins Hev b2 and Hev b3 isolated from natural latex proteins produced a smaller capacitance signal response on a Hev b1 (G) MIP-based electrode by a sensitivity factor of 2.25. The Hev b1 (G) MIP has a cross-reactivity to Hev b2 (L) (47%) and Hev b3 (L) (43%). These two latex allergens are different in size: the molecular weight of Hev b2 is 35 kDa and that of Hev b3 is 23 kDa, so they do not fit comfortably into the smaller Hev b1 (G) imprinting.

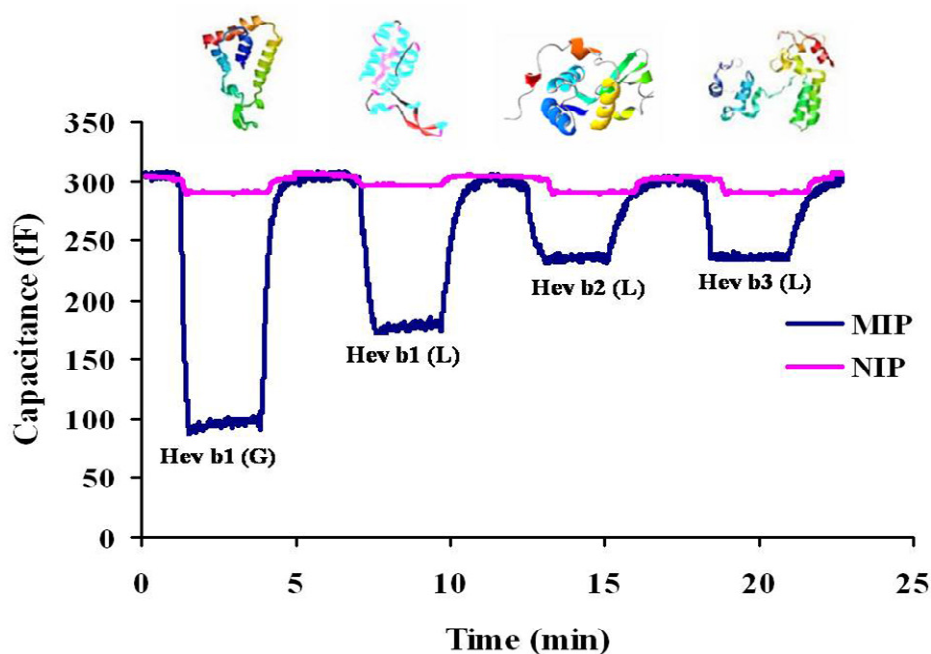


Figure 70. The Hev b1 (G) imprinted MAA-NVP-DHEBA copolymer on the IDC transducer. The sensor response shows different degrees of enrichment for Hevein latex allergenic proteins tested at an analyte concentration level of $250 \mu\text{g L}^{-1}$, room temperature and pH 7.4.

While Hev b3 has structurally similar epitopes to the template, and Hev b3 is related to Hev b1 by a sequence identity of 47% (Banerjee *et al.*, 2000); but the Hev b1 (G) MIP yielded similar bindings to Hev b2 ($pI = 9.3$) and Hev b3 ($pI = 4.8$) (Posch *et al.*, 1997). Hev b2 of the allergenic NRL proteins may have a part of its structure similar to part of the structure of Hev b3. However this interaction area between this part of the larger latex allergens and individual cavities of the MIP will be restricted to the upper

edge of the recognition site, and this will not be sufficient for a strong, non-covalent binding to the imprinted layer. When comparing Hev b1 (G) and the structurally related protein Hev b1 (L) with a non-Hev b protein (lysozyme) that has similar dimensions (14 kDa), there was a clear difference observed in the binding and hence demonstrates the sensor effects of the imprinted layer for these proteins. The much lower cross-reactivity value of the lysozyme protein (cross-reactivity value = 25%) can be due to its having a more globular structure, and also indicates the difference in surface functionality and protein configuration between the template and lysozyme that renders lysozyme unable to fit well into the cavities. The selectivity value of the distinct larger non-related proteins (ovalbumin and BSA) is as low as ~20%. The specificity shown with the MIP sensor could be explained on the basis of electrostatic interactions combining to size and shape memories on the template. The Hev b1 (G) imprinted polymer can distinguish between Hev b-related proteins and non-Hev b proteins such as lysozyme, ovalbumin and BSA; the Hev b1 (G) MIP favors binding to Hev b. The imprinted polymer has the defined oriented protein assembly found on the surfaces of the latex allergens. Hev b1 (G)-selective polymers can also distinguish between extractable Hev b1 allergens from latex mattresses made from rubber tree latex and rubber latex gloves.

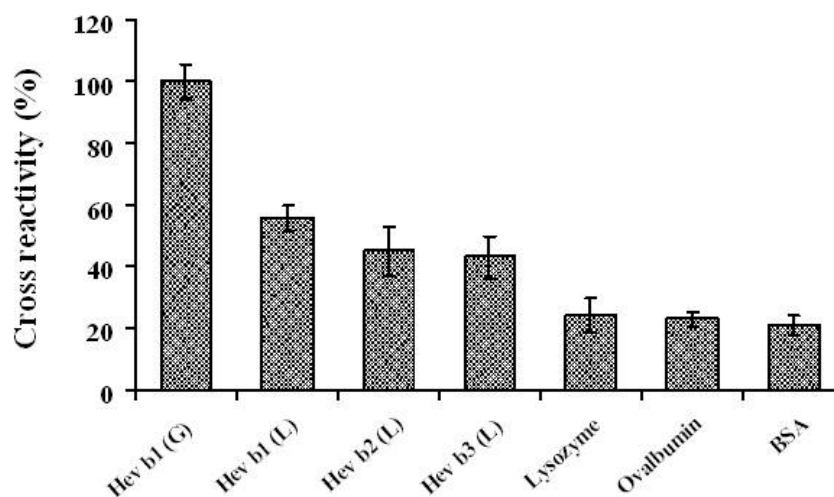


Figure 71. The selectivity pattern of Hev b1 (G)-imprinted polymer as obtained by IDC measurements. The proteins Hev b and non-Hev b are detected at a concentration of $250 \mu\text{g L}^{-1}$ in phosphate buffer (pH 7.4) at room temperature. Each value represents the average of three independent measurements.

5.4.9 Analytical characteristics

The calibration curves constructed from the capacitance shift parameter dependency provided reasonable results. The capacitance shifts of Hev b1 (G) measured on the MIP sensor has good linear relations with its concentration in the two ranges of $10\text{-}400 \text{ ng ml}^{-1}$ with a correlation coefficient (R^2) of 0.9969, and for $400\text{-}900 \mu\text{g L}^{-1}$ with a correlation coefficient (R^2) of 0.9888. When the capacitance shift response of the Hev b1 (G) microelectrode was taken as the threshold of the signal, the detection limit of this biosensor was 10 ng ml^{-1} and corresponded to a 3:1 signal to noise ratio, which is

comparable with the sandwich ELISA for assessment of latex allergen proteins that had a detection range of 125-4000 $\mu\text{g L}^{-1}$ with a detection limit of 1.25 μg of Hev b1/g of rubber (Yagami, 2009 and Raulf-Heimsoth, 2000). The MIP can undergo at least 50 generation steps without losing its recognition ability, which is limited to only 4-6 cycles for the natural compounds. A recovery study was carried out by spiking Hev b1 (G) at 50, 100 and 200 ng ml^{-1} with extracts prepared from latex gloves. A calibration curve was prepared by dissolving Hev b1 (G) in 0.1 mM phosphate buffer, pH 7.4, to attain solutions having Hev b1 (G) between 10-1000 $\mu\text{g L}^{-1}$, and then comparing them to that measured for Hev b1 (G) in spiked samples. The recovery data were in the range of 95–100%, with a relative standard deviation (RSD) of 4%.

5.4.10 Analysis of rubber latex gloves

To examine the selectivity and sensitivity of the Hev b1 (G) imprinted polymer in the presence of a complex matrix, rubber gloves supplied by a local manufacturer were chosen to test the MIP-based capture system. Figure 72 shows the sensor response of Hev b1 (G) imprinted to powder-free gloves and powdered latex surgical glove samples. A control experiment was also performed with non imprinted electrodes (Figure 73). The effects on the sensor of a spiked sample with standard Hev b1 (G) solutions of 50, 100 and 200 $\mu\text{g L}^{-1}$ are also compared. As shown in Figure 10b the sensor effect was not influenced by the complex matrix in the manufactured rubber latex gloves and finished products of natural rubber latex. A non-specific effect was obtained

for the imprinted polymer and non-imprinted polymer reference sensor – a capacitive sensor response which is very slight and did not change with increasing Hev b1 (G) in the samples. Moreover, the sum of the absolute capacitance changes of the imprinted and non-imprinted electrode are similar for every sample tested, which indicates that small compounds are present in the powder-free examination gloves and powdered latex gloves after extraction and dialysis and can compete for adhesion to the interaction sites on the polymer surface.

When one powdered latex glove was treated with SDS and centrifuged, the capacitive effects were only observed for the contents of the pellet from three different batches in which the average of three independent measurements was shown. The amount of Hev b1 (G) in a specimen of the rubber latex gloves was found to be 25 ± 6 $\mu\text{g/g}$ of rubber material. The IDC measurement for non-powder manufactured gloves was examined and from which the protein level is shown to be very low at 3.1 ± 0.5 $\mu\text{g/g}$. The values of protein content obtained from the MIP-IDC biosensor-based assay correspond well to the previous report by other authors (Yagami, 2009 and Raulf-Heimsoth, 2000; Yunginger, 1994).

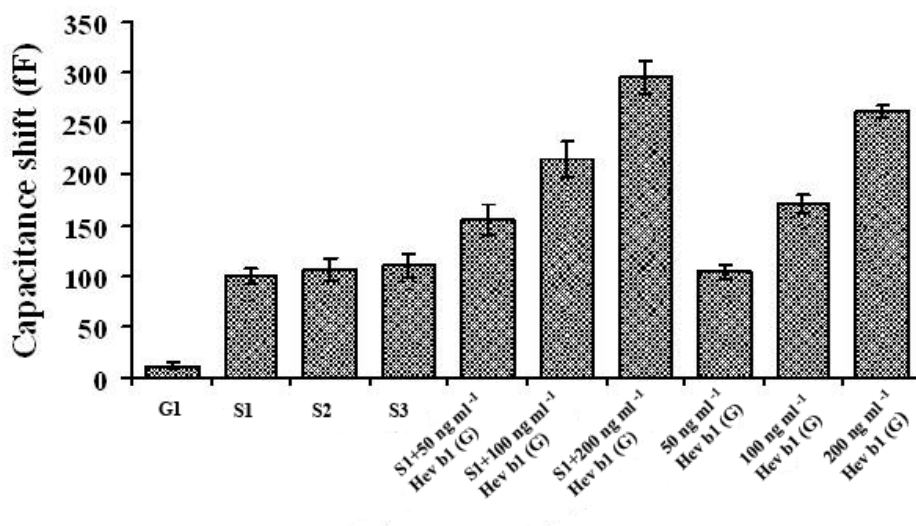


Figure 72. Response of Hev b1 (G)-imprinted polymer layer coated IDC sensors for the rubber latex allergen proteins to Hev b1 (G) from powder-free (G1) and powdered rubber latex gloves (S1, S2, S3) and powdered gloves (S1) spiked with Hev b1 (G) standards, and pure Hev b1 (G) standards. Measurements were carried out in 0.1 mM phosphate buffer solution (pH 7.4) at room temperature and flow rate of 1 mL min⁻¹. Each value represents the average of three independent measurements.

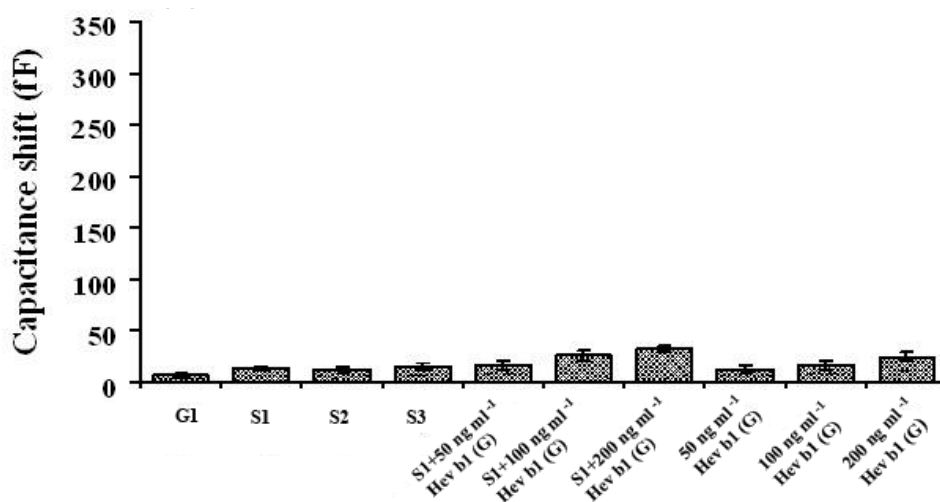


Figure 73. Response of non-imprinted reference polymer layer coated IDC sensors for the rubber latex allergen proteins to Hev b1 (G) from powder-free (G1) and powdered rubber latex gloves (S1, S2, S3) and powdered gloves (S1) spiked with Hev b1 (G) standards, and pure Hev b1 (G) standards. Measurements were carried out in 0.1 mM phosphate buffer solution (pH 7.4) at room temperature and flow rate of 1 mL min⁻¹. Each value represents the average of three independent measurements.

5.5 Conclusions

In this study, the development of a biosensor for the detection of Hev b1 rubber tree latex allergens has been investigated using an efficient surface imprinting process with the rubber allergenic proteins combined with an advanced microelectrode technology. This biosensor, based on MIP-protein interactions, can be used for

quantification of hevea latex allergens present as contaminants in rubber latex gloves. The MIP-IDC sensor showed a rapid shift in capacitance and a reasonable capacitive response that was clearly dependent on the concentration of the Hev b1 allergen proteins. The ability of the artificial recognition material to recognize the presence of defined organized structures on the protein surface allows for interaction and binding that can be recognized by the sensor system. The MIP chemical probes on the IDC sensor could distinguish Hev b1 from analogues such as lysozyme, ovalbumin and bovine serum albumin. This is extremely beneficial for the application of this analytical system to quantify hevein latex allergens in real-life samples. Moreover, the IDC microelectrode is one effective approach to miniaturize MIP biosensors that will allow for the detection of specific allergens in small sample volumes without reducing sensitivity and selectivity. The IDC microelectrode-based on-chip MIP biosensors when integrated with microfluid systems for sample delivery can further improve the overall stability and reproducibility of the interdigitated electrodes based biosensor. Interdigitated electrodes can be further designed in different array formats and integrated into microdetection device/systems for biomedical and biotechnological applications. Using an array of capacitors may allow us to quantify more than one marker at the same time and enhance the diagnostic power of the biosensor.

CHAPTER 6

MOLECULARLY IMPRINTED A SURFACE POLYMER AS A SENSOR LAYER COATED ONTO SURFACE PLASMON RESONANCE ELECTRODES

6.1 Introduction

Surface plasmon resonance (SPR) is a real-time, label-free, optical detection method for studying the interaction of soluble analyte with immobilized ligand (Green *et al.*, 2000). In principle, the SPR measures the mass concentration change caused by binding of an antigen (or antibody) to corresponding antibody (or antigen) immobilized of the sensor surface. The SPR phenomenon occurs when plane polarized light is reflected from a gold film deposited on a glass support. Photons react with the free electron cloud in the metal film at a specific angle, the SPR-angle, and cause a drop in the reflected light. Refractive index changes near the surface give rise to a shift of the resonance angle. The shift is directly proportional to the mass increase and mass concentration can thus be measured. An important side effect of total internal reflection is the propagation of an evanescent wave across the boundary surface (Luppa *et al.*, 2001).

Figure 74 shows the configuration of the SPR, a monochromatic p -polarized light source is used and the interface between the two optically dense media is coated with a thin metal film, commonly is gold, (of thickness less than one wavelength of light).

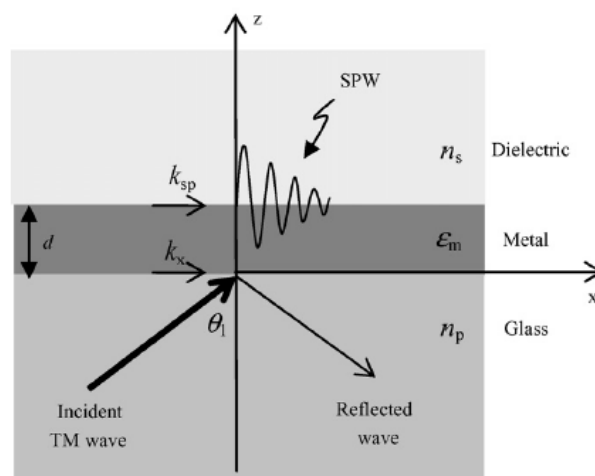


Figure 74. Three-layer Kretschmann configuration of SPR

The wave vector of the evanescent field (k_{ev}) is given by equation (9)

$$k_{ev} = \frac{\omega_0 n_g \sin \theta_1}{c} \quad (9)$$

where ω_0 is the frequency of incident light, n_g the refractive index of the dense medium (glass), θ_1 is the angle of incidence of the light and c the speed of the light in a vacuum.

The wave vector of a surface plasmon (k_{sp}) can be approximated to equation (4)

$$k_{sp} = \frac{W_0}{C} \sqrt{\frac{\epsilon_m n_s^2}{\epsilon_m + n_s^2}} \quad (9)$$

where ϵ_m is the dielectric constant of the metal film and n_s is the refractive index of the dielectric medium (Gebbert *et al.*, 1992).

Matsunaga *et al.*, (2007) reported lysozyme imprinted polymer coated on SPR sensor chips with acrylic acid and *N, N'*-methylenebisacrylamide. The high selectivity recognition of MIP to lysozyme and analog was obtained in the presence of NaCl. Electrostatic interactions would mainly contribute to the formation of lysozyme-acrylic acid complexes in the prepolymerization mixture and the resulting polymer thin films. A combination of SPR sensing technology with protein-imprinted thin films is a promising tool for the construction of selective protein sensors.

The electrochemical transducer provides the high sensitive and selective to detect target analyte when incorporated with a MIP system. However, the MIP-modified electrode procedure is the lack of stability of the non-crosslinked film which it is possible destruction of protein recognition site. Therefore, in this thesis work, three different transducer devices (capacitive, quartz crystal microbalance and surface plasmon resonance transducer) as a transduction system in biosensor when combined to a crosslinked polymeric networks having recognition sites, have been studied.

6.1.1 Surface plasmon resonance (SPR)

Optical sensors are based on various phenomena connected with the interaction of light and matter. One of such phenomena is surface plasmon resonance (SPR) (Liedberg, 1983), where resonance of an electromagnetic wave propagating along the metal–dielectric boundary are fulfilled. The main parameter influencing the conditions of resonance to SPR measurement is the refractive index of the examined substance. In order to measure a different parameter, such as concentration or biospecific interactions, the sensor will be designed in a way which combines the change of the parameter with the change of the refraction index. So far, the refraction index (RI) has been established by means of measuring the intensity of the electromagnetic wave near the resonance (Nylander *et al.*, 1982), measuring its intensity depending on the angle of the incident light (Matsubara *et al.*, 1988), or its intensity depending on the wavelength (Zhan *et al.*, 1988). There are also setups where the phase change (Shen *et al.*, 1998) and the polarization of light are examined (Kruchinin *et al.*, 1996). Theoretically, the highest precision of measurement is achieved for angular interrogation-based sensors (Homola, 1999). This precision will be defined as the derivative of the monitored SPR parameter (angle or wavelength) with respect to the parameter to be determined (refraction index). In order to increase the measurement precision and partly eliminate the factors distorting the measurement, such as temperature, one can either simultaneously measure the change of the angle and

the wavelength (Karlsen, 1995) or use multi-channel setups (Berger, 1998). The typical resolution of the SPR sensors is 10^{-6} RIU (refraction index unit) (Homola, 1999).

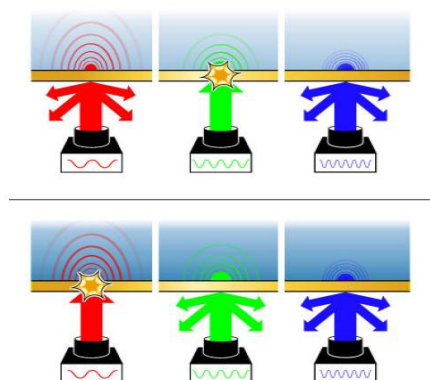


Figure 75. Change in permittivity shifts SPR excitation: this phenomenon is analogous to resonant frequency in a mechanical system in that there must be a precise match between the light's frequency and momentum and the characteristics of the gold. Any mismatch between the wavelength of the light: either too short (a.k.a. "blue-shifted") or too long (a.k.a. "red-shifted"), and the gold will fail to exhibit the plasmon oscillation. The matching wavelength is also dependant on the permittivity of the material on the opposite side of the gold film.

Permittivity is a measure of a material's capability to store energy in an electric field and is defined in terms of the material's dielectric constant (see Figure 75). In a thin film, the light actually induces an interrogation field on the opposite side of the gold. This field interrogates the relative permittivity for a distance on the order of 1 wavelength of the light striking the surface. A biological system is not likely to be disturbed by an electromagnetic field of low optical intensity. A biological system can,

however, invoke a change in permittivity. This change of permittivity within the interrogation field of the SPR system can cause a measurable shift in the wavelength required to excite the plasma state, as illustration in Figure 76.

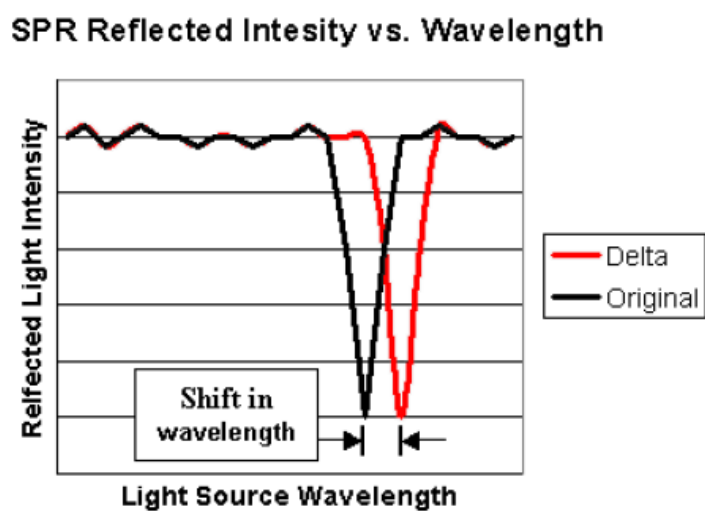


Figure 76. Depiction of measurable shift in SPR curve

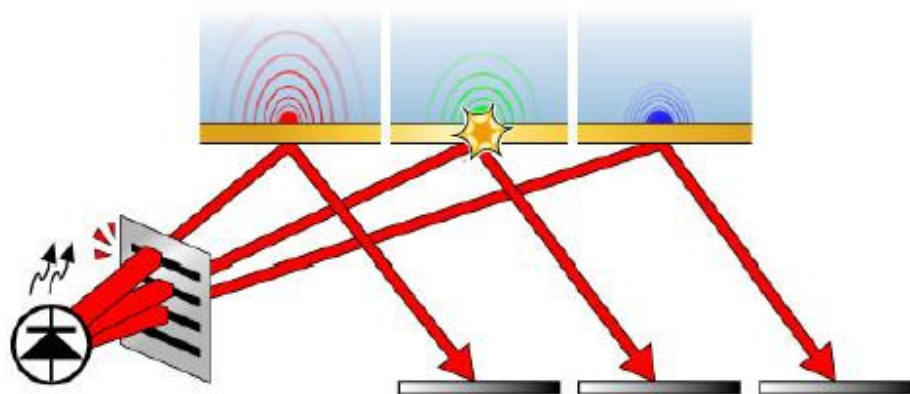


Figure 77. Spreeta's multiple SPR interrogation design

As shown in Figure 77, the Spreeta device has a rather ingenious design based on a single light source shining on the entire gold surface and reflecting onto an array of 128 light sensors. Thus a single Infrared ($\lambda = 840\text{nm}$) LED is the source for the Spreeta's entire range of SPR interrogation wavelengths. The gold film is tilted relative to the light source; this tilting results in a continuous change in the angle of incidence along the face of the film. When transverse magnetic (TM) polarized light strikes the film at an angle, the component of the wavelength that is parallel to the film is projected onto the film's surface. An interrogation field induced by angled incidence is identical to that induced by perpendicular incidence at the projected (shorter) wavelength. Thus with a simple application of trigonometry it is easy to visualize that the steepest angle of incidence generated at the point on the film closest to the light source projects the longest

interrogation wavelength (analogous to the “red-shift”), and the shallowest angle of incidence generated at the point on the film farthest away from the source projects the shortest interrogation wavelength (analogous to the “blue-shift”). A SPR component with sensor surface, biological to electrical transducer and analog electrical interface all contained in a surprisingly small package (~1 in. x 1 in. x ½ in.) offer low cost and readily available. Based on this sensor component, portable self-contained biosensor system was implemented with a MIP sensor layer for detecting of the protein analyte sample.

In this study, the Spreeta sensor consists of a plastic prism molded to a microelectronic circuit contained on a printed circuit board (PCB) (see Figure 78). The circuit contains an infrared LED (830 nm peak wavelength), a 128-pixel linear diode array detector, and a non-volatile memory chip for recording identification and calibration information. The LED emits a diverging beam that passes through a polarizer and strikes an elliptical region of the sensor surface at a range of angles above the critical angle. The angle at which light is incident upon this surface will vary with the location on the surface: smaller incident angles strike closer to the base of the sensor. The sensor surface is formed by a glass chip coated with a 50 nm layer of gold and epoxied to the plastic prism.

The thin layer of gold produces the SPR effect: for certain angles of incidence, part of the energy of the transverse-magnetic (TM) polarized incident light will couple into a surface plasma wave traveling along the interface between the gold layer and the analyte. The loss of this energy is observed as a sharp attenuation of

reflectivity. The angles at which this occurs vary with the surface RI of the analyte; therefore one can measure the surface RI by measuring the reflectivity across a range of angles and analyzing the resulting reflection spectrum. In the Spreeta (see this illustration of this equipment in Figure 78) the light reflected from the sensor surface then reflects from the sensor's top mirror and back down onto the PCB. A portion of this light strikes the diode array detector. Because each detector pixel will collect light which struck the sensor surface at a different angle, a reflectivity versus angle spectrum may be obtained by reading the detector array. The active area on the sensor surface (i.e. the area on which the RI is sensed) is defined by the portion of the light cone which projects onto the detector, and is a strip 0.2 wide by 3 mm long.

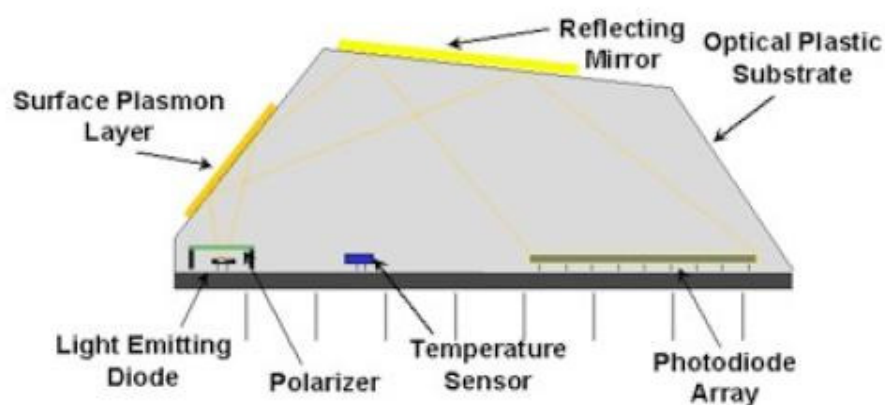


Figure 78. Internal design of spreeta sensor

Next, the development and characterization of successful Hev b1 imprints in nanometer scale with molded polymers and template containing an aqueous solution

have been made and this yielded randomly receptor site on the polymer coated onto surface plasmon transducer surface. The sensitive layer coating together with a surface imprinting onto gold metal film SPR sensor chip in flow cell (see Figure 79) enable binding sites of MIP are more accessible, fast binding kinetic simple and quick detection procedure.

6.2 Objective

The aim of this chapter was to study the feasibility of developing Hev b1 sensors for screening detection of the target protein in natural rubber latex and latex glove by the use of copolymer of methacrylic acid-vinylpyrrolidone-dihydroxyethylene-bisacrylamide cross-linked polymers coated onto the surface plasmon resonance electrode.

6.3 Experimental

6.3.1 Chemicals and materials

1-Vinyl-2-pyrrolidone (NVP), methacrylic acid (MAA), and *N,N'*-(1,2-dihydroxyethylene) bisacrylamide (DHEBA) were obtained from Aldrich Chemical Company (Milwaukee, WI, USA). 2,2'-Azobisisobutyronitrile (AIBN) was purchased from Janssen Chimica (Geel, Belgium). Lysozyme, ovalbumin and bovine serum

albumin were purchased from Sigma-Aldrich (St. Louis, MO, USA). All solvents were analytical grade and purified prior to use.

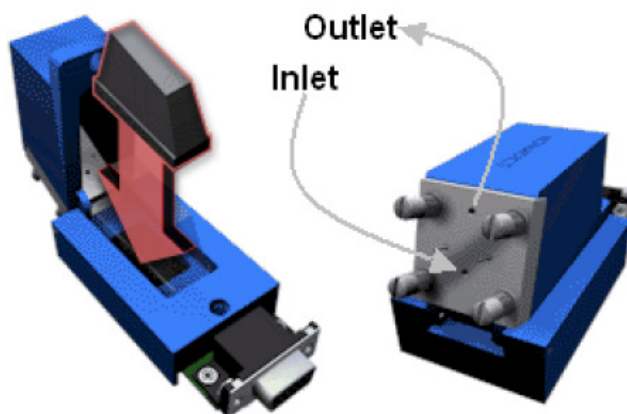


Figure 79. Spreeta flow cell

6.3.2 Preparation of SPR sensor chip

Solution-based protein surface imprinting created on gold metal film of SPR sensor chip (Figure 80) that involves non-covalent type imprinting and self-assembly around protein template and subsequently washing out of template, resulting the recognition cavities on mass-producible polymer surface. The SPR transducer system was prepared by soft lithography using gold pastes after that was immobilized on transducer surface by the pre-polymerizing phase consisting of the copolymer of (0.6 mmol) MAA, (0.2 mmol) NVP and (0.15 mmol) DHEBA in distilled water prior to imprinting process. The immobilization of sensitive layer was carried out with Hev b1

(G) solubilized in copolymer mixture which adjusted to pH 7.4 by 100 mM KOH in order to prevent protein template to be denaturated. The 2 μ L of pre-polymerizing mixture was coated on gold surface SPR chip electrode as a very thin layer to increase binding of the film to the transducer and then, sensitive layer was drop coated and spreaded with 2 μ L polymer mixture onto the gold surface of SPR chip. The curing process of the polymer layer was performed under UV light and the protein template was removed by distilled water. A non-imprinted polymer (NIP) was also prepared following exactly the same procedure as the MIP, but excluding the template Hev b1 (G) from the formulation protein template.

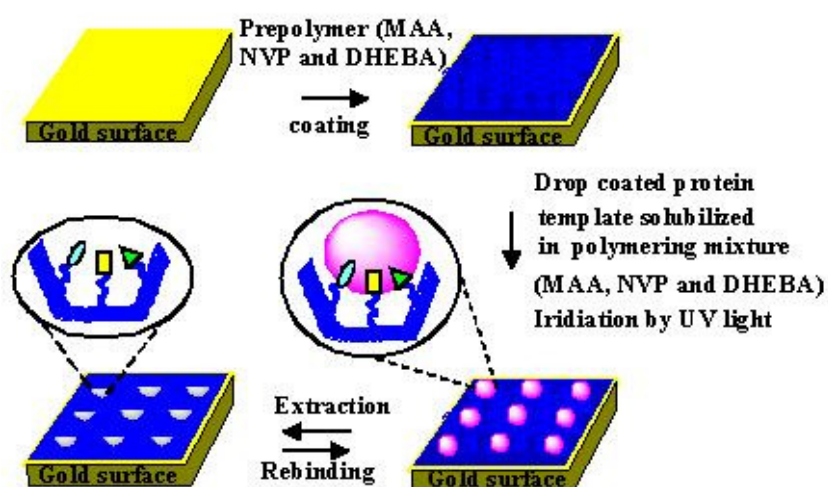


Figure 80. Illustration of the preparation of Hev-b1-surface imprinted layer by a solution based imprinting coated onto gold surface as a sensitive recognition layer of SPR sensor chip

6.3.3 Scatchard analysis

The binding isotherm of Hev b1 (G)-MIP coated SPR sensor exposed with Hev b1 (G) was investigated at 10, 50, 100, 150, 200, 250, 300, 400 and 500 mg L⁻¹. The angle shift was plotted with the concentration level of Hev b1 (G). The amount of substrates bound to the polymer (Q) was calculated from the concentration difference between the concentration of the substrate in the filtrate and the initial substrate concentration. Scatchard analysis was also used for binding affinity evaluation. The apparent maximum number of binding sites (Q_{\max}) and the equilibrium dissociation constant (K_d) were determined from the Scatchard equation shown in Equation 9.

6.4 Results and discussion

6.4.1. Morphology of protein imprinting

The morphology of nanopatterned recognition layers obtained during imprinting process through solution-based Hev b1 (G)-imprinted polymer was examined by AFM. The molecularly imprinted films examined prior to washing showed the presence of Hev b1 allergen proteins to be approximately 80–90 nm in diameter (Fig. 81A) and after template removal, the film surface shows the cavities that the depth of the imprinted sites was approximately 70 nm.

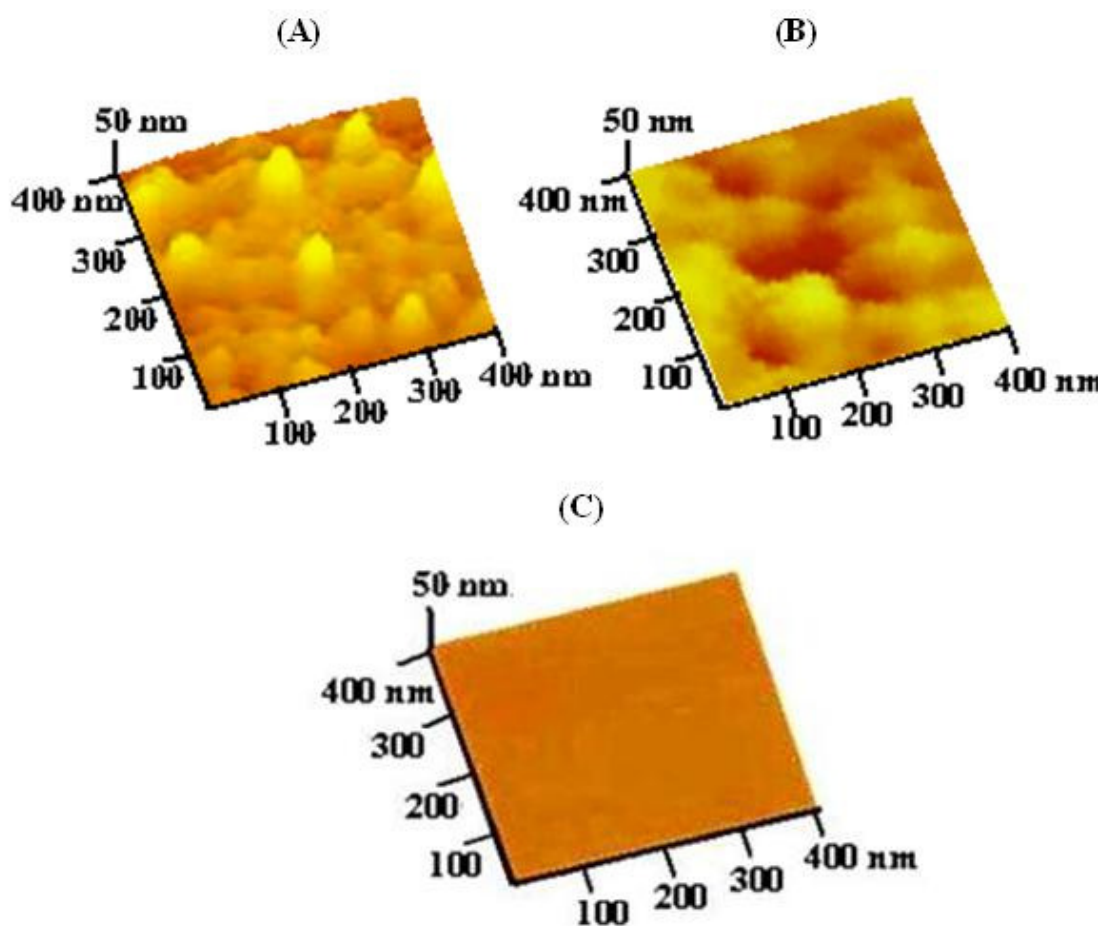


Figure 81. Contact mode AFM images: (A) MIP with partially removed template showing the rubber allergens retained in the polymerized material; (B) imprinted layer showing Hev b1 (G) pits on a MAA–NVP–DHEBA polymer after hardening of the layer and washing with distilled water for 24 h

(Figure 81B) and some residual surface protein still attached possibly entrapped by irreversibly binding to the surface and greatly improve the binding capacity and also site

accessibility of imprinted materials, comparing to non-imprinted layer of copolymer MAA/NVP/DHEBA having of smooth surface and a low roughness (Figure 81C).

6.4.2 Binding of Hev b1 (G) on surface Plasmon resonance

SPR measurement was used to quantify interaction between the MIP and NIP layer and Hev b1 (G) template. Figure 82 shows representative time course of the SPR angle change of a SPR surface immobilized MIP layer upon injection of the Hev b1 (G) solution contain the interaction molecule the sensor surface. As the Hev b1 (G) binds to the specific site of imprinted polymer at the gold surface causes the angle of incidence of light changes and have an increase in resonance units. As the binding of Hev b1 (G) to imprint site of the specific layer reaches steady state, the SPR angle will create to change and upon removal of protein from the flowing buffer and under the appropriate elution conditions, the SPR angle will change as the protein dissociates from the surface and return to its value prior to exposure of the surface to analyte. Surface imprinting is also successfully applicable to form fingerprints from nanometer sized templates. The imprinted exhibited the highly effective and selective to the template protein which can be effectively enriched on imprinted layers, whereas the non-imprinted layers show minor effects. The template-monomer interaction was designed in aqueous solution to avoid protein template denature and provided high selective and sensitive sensor layer for SPR sensor. Therefore, water-soluble polymer of MAA-NVP-DHEBA were utilized for biomacromolecule imprinting at a molar ratio of template and monomer of 1:8.

combining of the acrylate and pyrrolidone functional monomer into MIP, the carboxylic groups MAA are capable of interaction to the amine and hydroxyl of the template molecule via electrostatic hydrogen bond interaction.

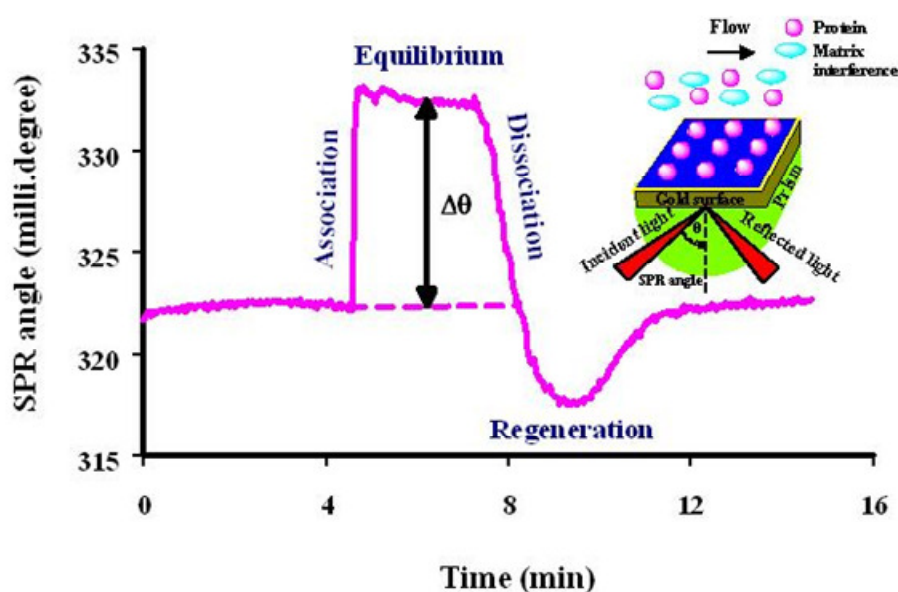


Figure 82. Schematic diagram depicting a typical surface plasmon resonance (SPR) experiment which the MIP layer is immobilized on the gold surface of SPR biosensor chip and the protein passes through a micro-fluidic flow cell which SPR sensor chip is used to monitor the change in SPR angle shift ($\Delta\theta$) caused as protein adsorption on the biosensor surface and reversible binding of the protein template.

Moreover, NVP with a good wetting and adhesive properties gives binding interaction between protein and functional group of polymer and also stabilize the protein conformation after protein inclusion (Chen *et al.*, 1997). In addition, the dihydroxy group of DHEBA as a cross-linker is able to minimize the non-specific

binding of protein template and enhance the rigidity of binding site into imprint cavities. Moreover, the long chain cross-linker is important for imprinting process allowing the polymeric matrix to conform to the protein molecule and stabilize the imprinted cavities. The inclusion of protein interaction into the binding site of imprint cavities was found to be the greatest selective recognition to Hev b1 in the microenvironment surrounding that created imprint site. Moreover, a number of factors, including solution temperature, pH, and ionic strength have to monitor avoiding the conformational change of target protein upon polymerization process and during analysis with biosensor. Molecularly imprinted polymers synthesized for the selective recognition of Hev b1 in aqueous solutions most certainly exploit template-receptor complexation through non-covalent interaction. The results have shown that specific binding of Hev b1 to the imprinted polymer was based on a hydrogen bonding that is the hydroxyl group of amino acid residues (asparagine, serine or glutamic acid) onto surface of Hev b1 molecule interact with the carboxylic group of MAA rather than the secondary amine group of NVP.

6.4.3 Scatchard analysis

The SPR sensor chip for Hev b1-MIP-MAA-NVP-DHEBA yielded response SPR angle shift to exposed Hev b1 at different concentration. The linear regression equation for standard Hev b1 solution in the range 10 and 200 mg L⁻¹ was $y = 0.0188x + 0.182$ ($R^2 = 0.995$, $n=3$) with a detection limit of 10 mg L⁻¹. As shown in Figure 81, the binding kinetics of the surface imprint films emerge as a profile of the saturation

curve which compose of high binding affinity from protein-MIP interaction and low affinity region which was the higher concentration of analyte of interest to protein interactions may be as dominant as a multilayer and leading to the loss of linearity in the low affinity region.

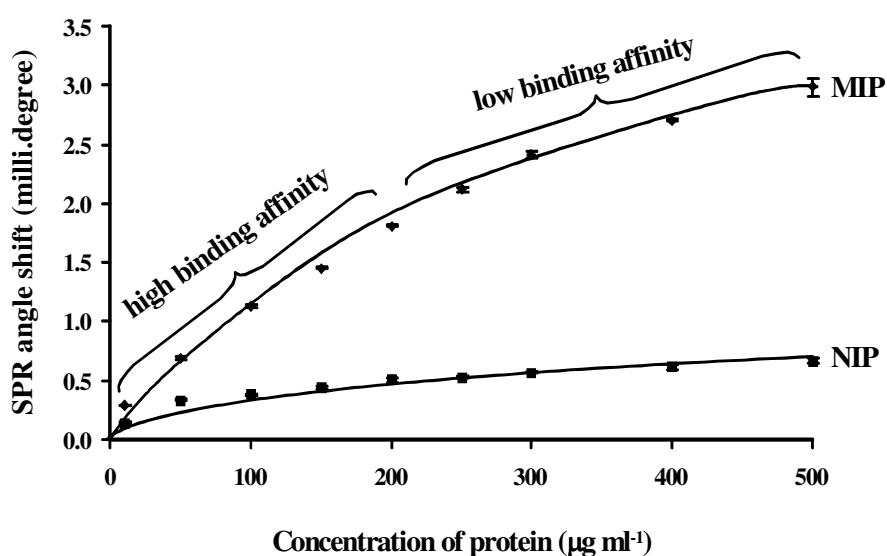


Figure 83 Concentration dependence of the SPR angle shift to Hev b1 (G) for the specific Hev b1-imprinted polymer coated gold surface SPR chip in 0.1mM phosphate buffer (pH 7.4) at 25°C with a flow rate 0.25 mL min⁻¹.

Figures 84 and 85 show the Scatchard plot of MIP and NIP which shows two straight lines with different slope. These suggested that the binding sites in the MIP and NIP were heterogeneous in respect to the affinity for Hev b1 (G), and indicates that the binding sites in the imprinted polymer could be classified into two distinct groups

with specific binding properties (Zhi Zhu *et al.*, 2002). The K_d and Q_{max} of the higher and lower affinity binding sites of both MIP and NIP can be calculated and shown in Table 15. Most MIPs prepared with non-covalent imprinting approach, correspondingly Hev b1 (G) formed a heterogeneous distribution of binding sites (Shea *et al.*, 1993; Matsui *et al.*, 1995). This phenomenon was probably associated with imprinting process which can produce binding sites through the polymer matrix after removal of the template. Therefore, the possibility of imprinting sites located at the surface position is accordingly less than those located inside polymer matrix. The imprinting sites situated at the surface can be considered as high affinity to the template, so easy diffusion into by template molecule. The lower affinity binding sites were assumably believed that located deeply inside the polymer particle (Zhi Zhu *et al.*, 2002). It was mostly due to the more difficult diffusion process of the template to these binding sites. The binding events of the inside imprinting hole can occur after the saturation of the imprinted sites from the template binding at the surface attained. This explanation can be clearly revealed from two slopes in Schatchard analysis which the higher affinity binding sites represented the higher slope at lower template concentration and correspondingly, lower slope of a straight line at high template concentration showed the lower affinity imprinted sites. Comparing between MIP and NIP, the high affinity region of MIP has higher negative slope than NIP. It revealed the sensitivity of binding site in the MIP to the template. Q_{max} of both MIP and NIP were produced from the high affinity and low affinity binding site. The amount of high affinity of MIP has less than the amount of low affinity because the imprinting site located at surface area of imprinting polymer has less than the inside imprinting hole

similar to NIP. Comparing between MIP and NIP, Q_{\max} shown that the binding site of MIP is higher than NIP because the imprinting sites consist of specific binding and non-specific binding whereas NIP was obtained from non-specific only.

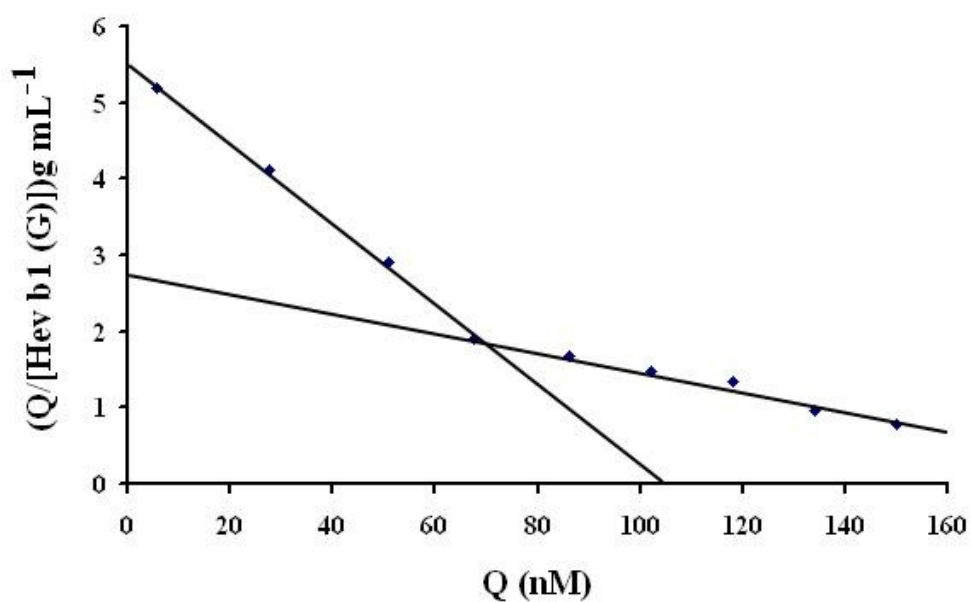


Figure 84. Scatchard plot of the binding of Hev b1 (G) to MIP. Q: bound Hev b1 (G) [Hev b1 (G)]:concentration of free Hev b1 (G)

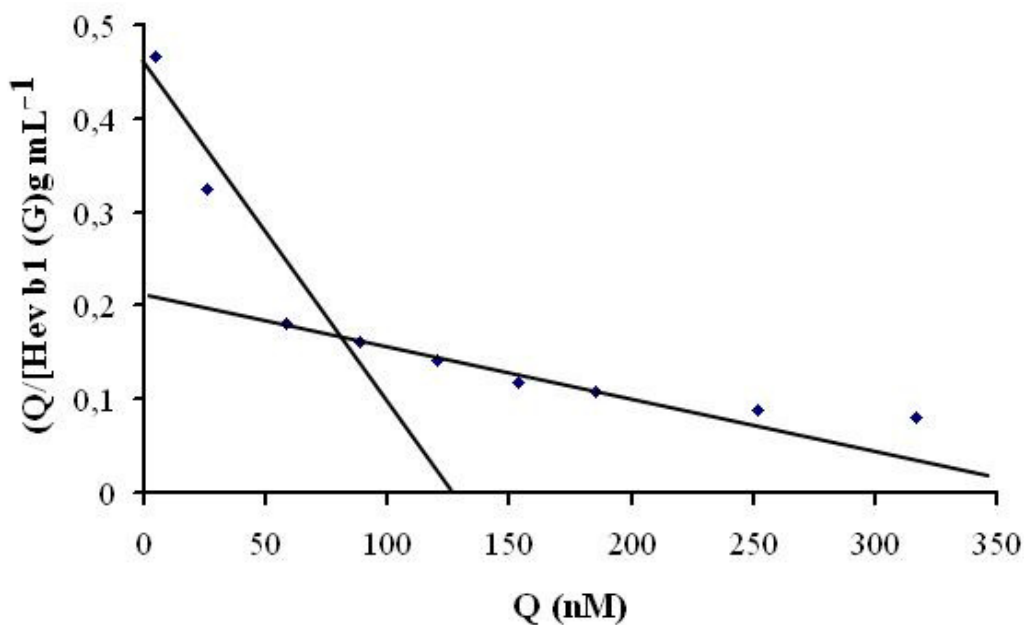


Figure 85. Scatchard plot of the binding of Hev b1 (G) to NIP. Q: bound Hev b1 (G)
[Hev b1 (G)]:concentration of free Hev b1 (G)

Table 15 shows the equilibrium dissociation constant and maximum number of binding site of two classes of binding sites in both imprinting polymer. The K_d was obtained from the reciprocal of slope of two straight lines which consist of high affinity and low affinity from Scatchard plot of MIP and NIP. The K_d indicates the ability of the dissociation of complex form which obtained imprinting site bind to template. Therefore high K_d , the complex form can be easy dissociated or unstable while low K_d , produced complex has more stable and difficult to dissociation.

Table 15 Equilibrium dissociation constant (K_d) and maximum number of binding sites (Q_{max}) value of two classes of binding sites in both imprinting polymer

Constant	MIP		NIP	
	High affinity	Low affinity	High affinity	Low affinity
K_d (mol/L)	12±1	152±5	263±7	3333±2
Q_{max} (µg/g)	119±2	300±4	119±2	573±23

6.4.4 The selectivity and sensitivity of the Hev 1 (G) MIP layer on the IDC

The geometrical fit and a functional memory of Hev b1 (G) imprinting layer is a key successful for selective recognition of the original protein template or related proteins. Figure 86 depicts SPR angle shift of Hev b1 (G)-MIP-SPR sensor in an aqueous system. It was shown that Hev b1 (G) greatly selective binding to MIP layer coating with a factor of 7.3 compared to the NIP-control polymer. This could be explained that the inclusion of Hev b1 (G) into active site of the layer are preferable specific binding site than non-specific area. Moreover, this SPR angle shift has higher sensitive to Hev b1 (G), extract from rubber glove, when compared to Hev b1 (L), Hev b2 (L) and Hev b3 (L), extract from natural rubber latex, and lysozyme, ovalbumin and BSA, respectively. Although, Hev b1 (G), Hev b1 (L) and lysozyme have the same size. The SPR angle shift data showed the cross-reactivity to Hev b1 (L) of 75% and lysozyme

of 4%, respectively. Because, the allergen proteins are different in multitude of size and shape which may induce the steric hindrance during incorporation of protein–monomer complexes into the cavity formed and also may be occupied low binding energy which cause distances proximity are not match to the specific binding site of imprint cavities. Moreover, all of the other proteins are different in size (Hev b2: 35 kDa, Hev b3: 23 kDa, ovalbumin: 45 kDa and BSA: 65 kDa) that can be distinguished by the sensor layer provided a slightly SPR angle shift according to the geometrical and functionality fitting to the imprinted cavities of the protein template molecule.

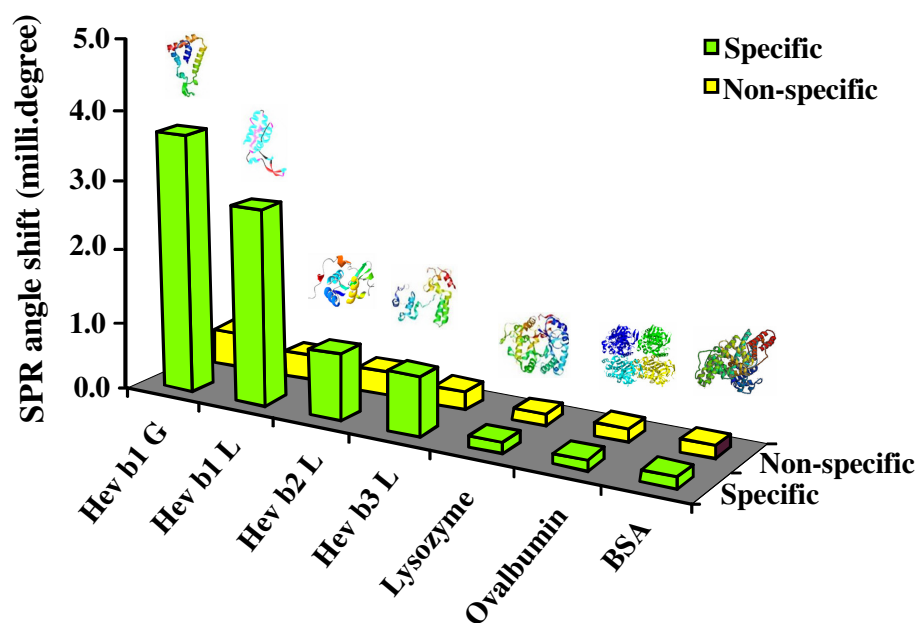


Figure 86 Selectivity test of Hev b1, related Hev b1 and non-related Hev b1 on the Hev b1 (G)-imprinted polymer coated gold surface SPR chip in 0.1mM phosphate buffer (pH 7.4) at 25°C with a flow rate 0.5 ml min⁻¹.

6.5 Conclusions

In summary, high affinity and selective polymer for the latex allergen Hev b1 were synthesised by a surface imprinting polymerization through solution polymerization process. Protein surface imprint fabricated onto gold metal surface SPR sensor chip as a sensitive layer displayed a high selective and sensitive to allergen protein detection. The nano-imprinted cavities are expected to greatly improve the binding capacity and also site accessibility of imprinted materials. A miniaturized surface plasmon resonance (SPR) sensor chip on-line monitoring is a feasible as a screening tool for detection of allergen proteins remain in rubber latex glove and natural rubber latex.

CHAPTER 7

GENERAL DISCUSSION AND FUTURE WORK

7.1 Extraction and purification of rubber latex allergen

Both natural rubber latex and latex glove as a source to produce protein latex allergy were isolated for Hev b proteins to use as the template and the proteins of this study. For this, Hev b1 (L), Hev b2 (L), Hev b3 (L) and Hev b1 (G) were found to be the subject of protein in samples. Rubber particle of natural rubber latex comprise of protiolipid protein that islated from the rubber particle by extracting with 1% SDS and 0.05 Triton X-100 in Tris-HCl, pH 7.4 at 4°C. All of the latex allergen proteins were purified by gel filtration chromatography and visualized by SDS PAGE method. The allergen proteins of 13.9 and 23.0 kDa which were identified to be Hev b1 and Hev b3, respectively. Using Western blot assay found that Hev b1 and Hev b3 had IgE reactivity to serum of one patient from Songkhlanakarind hospital. Moreover, the purified allergen protein was verified by the use of trypsin digention and MALDI-TOF-MS mass spectrometry and MASCOT searching program that was accepted according to probability value greater than 95.0% as specified by the Peptide Prophet algorithm (Craig, 2004) as compared with the mass spectrum of standard protein from data blank.

The successful extraction and purification process of natural rubber allergen protein from natural latex and latex glove have been achieved with the extraction protocol as described here and the percentage yield of about 71-75%. Moreover, natural rubber proteins were extracted from the bottom membrane fraction of rubber particle which was isolated by 0.2% Triton X-100 in 50 mM Tris-HCl, pH 7.4 with yield of purified protein more than 40%. After purification employing gel filtration chromatography, the allergen proteins of 38.2 kDa Hev b2 could be observed in a acrylamide gel on SDS-PAGE and purified and characterized by using same protocols as those for Hev b1 and Hev b3. This extracted Hev b2 was not shown to have IgE reactivity. Furthermore, allergen protein from latex glove samples obtained from a local supplier was isolated by 0.1% SDS in 0.2 M phosphate buffer. The purification and characterization of the extrated protein was performed same as that achieved from the natural rubber latex proteins. The percent yield of Hev b1 extracted from rubber glove was 75%. All of the extractable protein were lyophilized for use as purified Hev b1 (G) for imprinting process and for analysis protein of the sensor.

7.2 Hev b1-molecularly imprinted polymer coated quartz crystal microbalance sensor

Sensor for allergen protein form natural rubber latex has been successfully developed by surface imprinting technique combined with mass-sensitive and interdigitated capacitance transduction system. Copolymers made from methacrylic acid-

vinyl pyrrolidone-dihydroxy ethylene bisacrylamide are soluble in aqueous solution and allowed to avoid the denaturing protein. The polymerization was performed at ambient temperature and radical UV light. The recognition property and sensing performance of the Hev b1 (G)-imprinted polymers integrated in all these transducer systems have been assessed for the application of these sensors in detection.

A typical QCM measurement device was first prepared using a stamp imprinting procedure after mixing optimum amounts of methacrylic acid-vinylpyrrolidone-dihydroxyethylene bisacrylamide and the Hev b1 latex allergen proteins. QCM measurements showed that the resulting polymer layers after removal of the allergen templates used in their preparation could reincorporate that allergen into the imprinted polymer far more effectively than a non-specific control polymer also produced under controlled sensor conditions and an optimized polymerization process. The sensor layers selectively adsorbed Hev b1 within minutes in amounts that ranged from 10 to 1000 $\mu\text{g L}^{-1}$. The imprinted polymer layer exhibited specificity, in that it distinguished between the latex allergen Hev b1 and proteins such as lysozyme, ovalbumin and bovine serum albumin, with a selectivity factor of from 2 to 4, and the response of the template by an astonishing factor of 12. QCM sensor measurements using MIP as the recognition material was applied to detect and measure Hev b1 in such complex matrices as manufactured rubber latex gloves. Good recoveries of 97-105% from spiked allergens were achieved with RSD values between 3 and 6.5.

In order to improve the speed of analysis of the Hev b1-MIP based on the QCM sensor an alternative development method of using an inter-digitated capacitance

(IDC) an transducer was developed. This combined with the surface imprinted layer allowed for label-free measurements. The immobilized imprinted polymers are the probed that bind the rubber allergen proteins. Copolymers made from methacrylic acid-vinylpyrrolidone-dihydroxyethylene bisacrylamide are soluble in aqueous solution and this eliminates any denaturation of protein. The surface imprinting process using Hev b1 (G)-MIP based IDC allows for the generation of micropatterns of the rubber allergen protein on the polymer surface and produce a series of a randomly distributed nano-path pits on the coated surface with the depth of the imprinted site being around 70 nm. When deposited as a coating onto a IDC microelectrode transduction system, such materials lead to sensors that produced capacitance responses that were clearly dependent on the concentration of the latex protein (10 to 900 $\mu\text{g L}^{-1}$) and showed a rapid shift within 5 minute in a pH 7.4 buffer. The selective layer recognized Hevea latex proteins better than non-Hev b proteins such as lysozyme, ovalbumin and bovine serum albumin by a factor of 2. IDC sensor measurements using MIP as a recognition material was applied to analyze Hev b1 in such complex matrices as manufactured rubber latex gloves and good recovery of 95-100% was achieved with RSD values of less than 4.

Finally, to compare the label-free and the fast analysis of Hev b1-MIP based on either QCM and IDC an optical detection method was developed for the allergen protein using a surface plasmon resonance (SPR) transducer combined to a surface imprinted layer. The surface molecularly imprinted layer containing poly(methacrylic acid-vinylpyrrolidone-dihydroxyethylene-bis-acrylamide) was prepared onto a miniaturized surface plasmon resonance (SPR) device by a solution based

imprinting procedure. Protein surface imprint fabricated onto gold metal surface SPR sensor chip as a sensitive layer displayed a high fabricated onto gold metal surface SPR sensor chip as a sensitive layer displayed a high selective and sensitive to allergen protein detection. The nano-imprinted cavities are expected to greatly improve the binding capacity and also site accessibility of imprinted materials. Finally, miniaturized surface plasmon resonance (SPR) sensor chip on-line monitoring in a feasible as a screening tool for detection of allergen proteins remain in rubber latex glove and natural rubber latex, even though the sensitivity and selectivity of the proposed imprint layer on this transducer are desirable to be improved the work on this line will be a future work on molecular imprinting technology.

The proposed sensor method allows the sensor signal more selectively, specifically and effectively precision, especially Hev b1 QCM and IDC sensors when are used for selective detection allergen protein in rubber latex glove. In comparison to the results of this work to ELISA and Lowry assay in detecting allergen protein and total soluble protein, found in detection limit of the proposed method was same as the ELISA (see Figure 16) but that the present method with Hev b1-QCM and IDC sensor present rapidly detection and ease of operation and handling process.

Table 16. Comparison of the analytical features for the analysis of Hev b1 from latex glove using development allergen sensor and conventional method

Sensor Characteristics	QCM	IDC	SPR	ELISA ASTM D6499-03	Lowry ASTM D5712-05
LOD ($\mu\text{g L}^{-1}$)	1	10	1000	0.1	10
R²	0.996	0.997	0.995	-	-
Recovery (%)	97-105	95-100	-	-	-
Specific	Hev b1	Hev b1	Hev b1	Non-specific	Non-specific
Preparation complexity	√	√	√	√	√
Durability	√	√	√	-	-

Future work

An artificial antibodies towards allergen protein based molecularly imprinted polymers is a strategy to mass production. Therefore, an artificial master stamp which it realized by introducing a copy of the geometry and the chemical properties of the protein surface that may be straightforward improved the sensitive layer manufacturing process. It would be certainly be attempting to apply the mass sensor and IDC sensor to the

detection of rubber allergen protein in a very complex matrix as a biological sample for clinical analysis and Hev b1 assessment in the manufactured gloves during manufactory process. The development of the sensitive layer and transduction to lab-on-a-chip is beneficial for use of the device in quality control of the products latex.

REFERENCES

- Ahram, M., Best, C.J., Flaig, M.J., Gillespie, J.W., Leiva, I.M., Chuaqui, R.F., Zhou, G., Shu, H. 2002. Proteomic analysis of human prostate cancer. *Molecular Carcinogenesis*, **33**: 9-15.
- Akasawa, A., Hsieh, L.S. and Lin, Y. 1995. Serum reactivities to latex proteins (*Hevea brasiliensis*). *Journal of Allergy and Clinical Immunology*, **95**: 1196-1205.
- Akasawa, A., Hsieh, L.S. and Tanaka, K. 1996. Identification and characterization of avocado chitinase with cross-reactivity to a latex protein. *Journal of Allergy Clinical Immunology*, **97**: 321.
- Alenius, H., Kalkkinen, N., Yip, E., Hasmin, H., Turjanmaa, K. and Maëkinen-Kijunen, S. 1996. Significance of rubber elongation factor as a latex allergen. *International Archives of Allergy and Immunology*, **109**: 362-368.
- Alenius, H.N.K. and Lukka, M. 1995. Prohevein from the rubber tree (*Hevea brasiliensis*) is a major latex allergen. *Clinical & Experiment Allergy*, **25**: 659-665.

Alenius, H., Palosuo, T., Helly, K., Kurup, V., Reunala, T., Makinen-Kiljunen, S., Turjanmaa, K. and Fink, J. 1993. IgE reactivity to 14-kD and 27 –kD natural rubber proteins in latex-allergic children with spina bifida and other congenital anomalies. *International Archives of Allergy and Immunology*, **102**: 61-66.

Alenius, H., Turjanmaa, K. and Palosuo, T. 2002. Natural rubber latex allergy *Occupational Environment Medicine*, **59**: 419-424.

Alexander, C., Andersson, H.S. Andersson, L, Ansell, R., Kirsch, N. and Nicholls, L., O'Mahony, J. and Whitcombe, M.J. 2006. Molecular imprinting science and technology: a survey of the literature for the years up to and including 2003. *Journal of molecular recognition*, **19**:106-180.

Andersson, L.I., Müller, R., Vlatakis, G. and Mosbach, K. 1995. Mimics of the binding sites of opioid receptors obtained by molecular imprinting of enkephalin and morphine. *Proceeding of the Natinal Academy of Sciences of the United States of America*, **92**: 4788-4792.

Archer, B.L., Audley, B.G., Cockbain, E.G. and McSeeney, **G.P.** 1963. The biosynthesis of rubber: incorporation of mevalonate and isopentenyl pyrophosphate into rubber by *Hevea brariliensis* latex fractions. *Biochemical Journal*, **89**: 565-574.

- Archer, B.L. and Audley, B.G. 1973. Rubber, gutta perch and chicle. In: *Phytochemistry*, New York: Van Nostrand-Reinhold., pp. 10-343.
- Archer, B.L. and Cockbain, E. G. 1955. The proteins of *Hevea brasiliensis* latex isolation of the α -globulin of fresh latex serum. *Biochemical Journal*, **61**: 508-514.
- Archer, B.L., Audley, B. G., McSweeney, G. P. and Tan, C. H. 1969. Studies on composition of latex serum and bottom fraction particles. *Journal of the rubber Research Institute of Malaysia*, **21**: 560–569.
- Archer, B.L. and Cockbain, E. G. 1960. The proteins of *Hevea brasiliensis* 4. Isolation and characterization of crystalline hevein. *Biochemistry Journal*, **75**: 236-242.
- Arnau, A. Jiménez, Y. and Sogorb, T. 2000. Thickness shear mode quartz crystal resonators in viscoelastic fluid media. *Journal of Applied Physics*, **88**: 4498-4506.
- Arif, S.A.M., Hamilton, R. G. and Yusof, F. 2002. Multiple 43 kDa allergenic proteins in natural rubber latex [Abstract]. *Journal of Allergy Immunology*, **109**: S332–S333.
- Backhaus, R. A. 1998. Natural Rubber from Plants. In: *Biopolymers From Renewable Resources*, Berlin: Springer-Verlag., pp 323-354.

- Backhaus, R.A., Cornish, K., Chen, S.F., Huang, D.S and Bess, V.H. 1991. Purification and characterisation of an abundant rubber particle protein from Guayule. *Phytochemistry*, **30**: 2493-2497.
- Backhaus, R.A. 1985. Rubber formation in plants -a mini review. *Israel Journal of Botany*, **34**: 283-293.
- Backhaus, R.A. 1998. Natural Rubber from Plants. In: *Biopolymers from Renewable Resources*, Berlin: Springer-Verlag, pp 323-354.
- Backhaus, R.A., Cornish, K., Chen, S.F., Huang, D.S and Bess, V.H. 1991. Purification and characterisation of an abundant rubber particle protein from Guayule. *Phytochemistry*, **30**: 2493-2497.
- Beezhold, D.H. Hickey, V.L. and Kostyal, D.A.2003.Lipid transfer protein from *Hevea brasiliensis* (Hev b 12), a cross-reactive latex protein. *Annals of Allergy, Asthma and Immunology*, **90**: 439–445.
- Bernstein, D.I., Biagini, R. E. and Karnani, R. 2003. In vivo sensitization to purifiedbv*Hevea brasiliensis* proteins in health care workers sensitized to natural rubber latex. *Journal of Allergy Clinical Immunology*, **111**: 610–616.

- Bernardini, R., Novembre, E., Ingargiola, A., Veltroni, M., Mugnaini, L. and Azzari, C. 1998. Prevalence and risk factors of latex sensitization in an unselected pediatric population. *Journal of Allergy Clinical Immunology*, **101**: 621-625.
- Beezhold, D.H., Sussman, G. L., Kostyal, D. A. and Chang, N. S. 1994. Identification of a 46-kD latex protein allergen in health care workers. *Clinical Experiment Immunology*, **98(3)**: 408– 413.
- Benedict, C.R., Madhavan, S., Greenblatt, G.A., Venkatachalam, K.V. and Foster, M.A. 1989. The enzymatic synthesis of rubber polymer in *Parthenium argentarum* Gray. *Plant Physiology*, **92**: 816-821.
- Bealing, F.J. 1969. Carbohydrate metabolism in Hevea latex - availability and utilization of substrates. *Journal of the Rubber Research Institute of Malaysia*, **21**: 445-455.
- Behling, C. Lucklum, R. and Hauptmann, P. 1997. Possibilities and limitations in quantitative determination of polymer shear parameters by TSM resonators. *Sensors and Actuators A*, **61**: 260-266.
- Behling, C. Lucklum, R. and Hauptmann, P. 1998. The non-gravimetric quartz crystal resonator response and its application for polymer shear moduli determination. *Measurement Science and Technology*, **9**: 1886- 1893.

- Berger, C.E., Baumer, T.A., Kooyman, R.P. and Greve, J. 1998. Surface plasmon resonance multisensing. *Analytical Chemistry*, **70(4)**: 703-706.
- Boatman, S.G. 1966. Preliminary physiological studies on the promotion of latex flow by plant growth regulators. *Rubber Research Institute of Malaysia*, **19**: 243–258.
- Bowler, W.W. 1953. Electrophoretic mobility of fresh Hevea latex. *Industrial & Engineering Chemistry*, **45**: 1790-1795.
- Bossi, A., Piletsky, S.A., Piletska, E.V., Righetti, P.G. and Turner, A.P.F. 2001. Surface-grafted molecularly imprinted polymers for protein recognition. *Analytical Chemistry*, **73**: 5281-5286.
- Bonner, P.L.R. 2007. Protein Purification. New York: Taylor & Francis Group.
- Bossi, A., Bonini, F., Turner, A.P.F., Piletsky, S.A. 2007. Molecularly imprinted polymers for the recognition of proteins: The state of the art. *Biosensors and Bioelectronics*, **22**: 1131-1137.
- Bord, I., Tardy, P. and Menil, F. 2006. Influence of the electrodes configuration on a differential capacitive rain sensor performances, *Sensors and Actuators B*, **114**: 640-645.

- Bradford, M.M. 1976. A rapid and sensitive method for the quantitation of microgram quantities of protein utilizing the principle of protein-dye binding. *Analytical Biochemistry*, **72**: 248-254.
- Burow, M. and Minoura, N. 1996. Molecular imprinting: Synthesis of polymer particles with antibody-like binding characteristics for glucose oxidase. *Biochemical and Biophysical Research Communications*, **227**:419-422.
- Camesano, T.A., Liu, Y.T., Datta, M. 2007. Measuring bacterial adhesion at environmental interfaces with single-cell and single-molecule techniques. *Advances in Water Resources*, **30**:1470- 1491.
- Chen, Z., Cremer, R., Posch, A., Raulf-Heimsoth, M., Rihs, H.P. and Baur, X. 1997. On the allergenicity of Hev b1 among health care workers and patients with spina bifida allergic to natural rubber latex. *Journal Allergy Clinical Immunology*, **100**: 684-693.
- Chen, Z., Van Kampen, V. and Raulf-Heimsoth, M. 1996. Allergenic and antigenic determinants of latex allergen Hev b 1: peptide mapping of epitopes recognized by human, murine and rabbit antibodies. *Clinical & Experimental Allergy*, **26**: 406-415.

- Cheng, Z., Wang, E. and Yang, X. 2001. Capacitive detection of glucose using molecularly imprinted polymers. *Biosensors & Bioelectronics*, **16**: 179-185.
- Chen, Z. and Luo, R.C. 1998. Design and implementation of capacitive proximity sensor using microelectromechanical systems technology, *IEEE*, **45**: 886-894.
- Cook, A.S. and Sekhar, B. C. 1953. Fractions from *Hevea brasiliensis* latex centrifugation at 59,000 g. *Journal of Rubber Research Institute of Malaya*, **14**: 163-168.
- Cornish, K. and Siler, D.J. 1996. Characterization of *cis*-prenyl transferase activity localized in a buoyant fraction of rubber particles from *Ficus elastica* latex. *Plant Physiology and Biochemistry*, **34**: 377-384.
- Cornish, K. 1993. The separate roles of plant *cis* and *trans* prenyl transferases in *cis*-1,4-polyisoprene biosynthesis. *European Journal of Biochemistry*, **218**: 267-271.
- Cornish, K. and Backhaus, R.A. 1990. Rubber transfrase activity in rubber particles of guayule. *Phytochemistry*, **29**: 3809-3813.
- Cornish, K., Castillon, J. and Chapman, M.H. 1998. Membrane bound *cis*-prenyl transferase: Regulation and substrate specificity. *Teldran* (USDA).

- Craig, R. and Beavis, R.C. 2004. TANDEM: matching proteins with tandem mass spectra. *Bioinformatics*, **20**: 1466–1467.
- Creighton, T.E. 1993. *Proteins: Structures and Molecular Properties*, 2nd, San Francisco: W.H. Freeman.
- Czuppon, A.B., Chen, Z. and Rennert, S. 1993. The rubber elongation factor of rubber trees (*Hevea brasiliensis*), is the major allergen in latex. *Journal of Allergy and Clinical Immunology*, **92**: 690-697.
- Czuppon A.B., Chen, Z., Rennert, S., Engelke, T., Meyer, H.E., Heber, M. Baur, X. 1993. The rubber elongation factor of rubber trees (*Hevea brasiliensis*) is the major latex allergen. *Journal of Allergy and Clinical Immunology*, **92**:690-697.
- Czanderna, A.W., Lu, C. 1984. *Applications of Piezoelectric Quartz Crystal Microbalances*. Amsterdam: Elsevier., pp. 1-393.
- D’auzac, J., Jacob, J.L. and Prevot, J.C. 1997. The regulation of *cis*polyisoprene production (natural rubber) from *Hevea brasiliensis*. *Plant Physiology*, **1**: 273-32.

- D' Amato, A., Bachi, A, Fasoli, E., Boschetti, E., Peltre, G., Sénéchal, H., Sutra, J.P. Citterio, A. and Righetti, P.G. 2010. Righetti, In-depth exploration of *Hevea brasiliensis* latex proteome and “hidden allergens” via combinatorial peptide ligand libraries. *Journal of Proteomics*, **73**: 1368–1380.
- Davis, K.A., Leary, T.R. 1989. Continuous liquid-phase piezoelectric biosensor for kinetic immunoassays. *Analytical Chemistry*, **61**:1227-1230.
- De Fay, E. and Jacob, J.L. 1989. The anatomical organization of the laticiferous system in the bark. In: Physiology of rubber tree latex: the laticiferous cell and latex-a model of cytoplasm, Boca Raton: CRC Press., pp. 51-55.
- De Beer, C., Cilliers, J., Truter, E.J. and Potter, P.C. 1999. Latex Gloves: More harm than good. *Medical Technology SA*, **13 (1)**: 282-288.
- Dewarrat, F., Falco, A., Cadu, M.S., Talary, Y. Feldman and Puzenko, A. Measurement and simulation of conductive dielectric two-layer materials with a multiple electrodes sensor. *IEEE*, **15**:1406-1414.
- Dickenson, P.B. 1969. Electron microscopical studies of latex vessel system of *Hevea brasiliensis*. *Rubber Research Institute of Malaysia*, **21**: 543-559.

- Dickenson, P.B. 1963. *The Chemistry and Physics of Rubber-like Substances*, London: Maclaren and Sons Ltd., pp. 43-45.
- Dickert, F.L. and Hayden, O. 2002. Bioimprinting of polymers and sol-gel phases. Selective detection of yeasts with imprinted polymers. *Analytical Chemistry*, **74**: 1302-1306.
- Dickert, F.L., Hayden, O., Bindeus, R., Mann, K.J., Blaas, D. and Waigmann, W. 2004. Bioimprinted QCM sensors for virus detection – screening of plant sap. *Analytical Bioanalytical Chemistry*, **378**: 1929–1934.
- Dickert, F.L., Hayden, O. and Halikias, K.P. 2001. Synthetic receptors as sensor coatings for molecules and living cells. *Analyst*, **126**: 766-771.
- Dickert, F.L., Lieberzeit, P. and Hayden, O. 2003. Sensor strategies for micro-organism detection – from physical principles to imprinting procedures. *Analytical and Bioanalytical Chemistry*, **377(3)**: 540-549.
- Dennis M.S. and Light D.R. 1989. Rubber elongation factor from *Hevea brasiliensis*: identification, characterization and role in rubber biosynthesis reactions. *Journal of Biological Chemistry*, **264**: 18608-18617.

- Dennis, M.S., Henzel, W.J., Bell, J., Kohr, W. and Light, D.R. 1989. Amino acid sequence of rubber elongation factor protein associated with rubber particles in Hevea latex. *Journal of Biological Chemistry*, **264** (31): 18618-18626.
- Ekberg, B. and Mosbach, K. 1989 Molecular imprinting: A technique for producing specific separation materials. *Trends in Biotechnology*, **7**: 92-96.
- Fuchs, T., Spitzauer, S. and Vente, C. 1997. Natural latex, grass pollen, and weed pollen share IgE epitopes. *Journal of Allergy and Clinical Immunology*, **100**: 356-364.
- Gabrielli, C., Perrot, H., Rose, D., Rubin, A., Pham, M.C. and Piro, B. 2007. New frequency/voltage converters for ac-electrogravimetric measurements based on fast quartz crystal microbalance. *Review Scientific Instruments*, **78**(7):74-103.
- Ganglberger, E., Radauer, C., Wagner, S., O'Riordain, G., Beezhold, D.H., Brehler, R., Niggemann, B., Scheiner, O., Jensen-Jarolim, E. and Breiteneder, H. 2001. Hev b8, the Hevea brasiliensis latex profilin, is a cross-reactive allergen of latex, plant foods and pollen. *International Archeiv of Allergy Immonology*, **125**: 216-227.
- Gebbert, A., Alvarez-Icaza, M., Stocklein, W. and Schmid, R.D. 1992. Real-time monitoring of immunochemical inteactions with a tantalum capacitance flow-through cell. *Analytical Chemistry*, **64**: 997-1003.

- Gomez, J.B. and Samsidar, H. 1989. Frey-Wyssling complex in Hevea latex-Uniqueness of the organelle. *Journal of Natural Rubber Research*, **4**: 75-85.
- Gomez, J.B., and Moir, G.F.J. 1979. The ultracytology of latex vessels in Hevea Brasiliensis. Malaysian Rubber Research and Development Board, Kuala Lumpur., pp. 39- 40.
- Guo, T.Y., Xia, Y.Q., Hao, G.J., Song, M.D. and Zhang, B.H. 2004. Adsorptive separation of hemoglobin by molecularly imprinted chitosan beads. *Biomaterials*, **25**: 5905-5912.
- Guo, W. and Ruckenstein, E. 2003. Crosslinked glass fiber affinity membrane chromatography and its application to fibronectin separation. *Journal of Chromatography B*, **795**, 61-72.
- Gygi, S.P. and Aebersold, R. 2000. Mass spectrometry and proteomics. *Current Opinion in Chemical Biology*, **4**: 489-94.
- Hasma H. 1992. Proteins of natural rubber latex concentrate. *Journal of Natural Rubber Research*, **7**:102-12.

- Hasma, H. 1987. Proteolipids of natural rubber particles. *Journal of Natural Rubber Research*, **2**: 161-133.
- Harris, E.L.V. and S. Angal. 1990. Protein purification applications: a practical approach. New York: Oxford.
- Hayden, O., Haderspock, C., Krassnig, S., Chen, X. and Dickert, F.L. 2006. Surface imprinting strategies for the detection of trypsin. *Analyst*, **131**: 1044-1050.
- Hansen, D.E. 2007. Recent developments in the molecular imprinting of proteins. *Biomaterials*, **28**: 4178-4191.
- Hasma, H. 1987. Proteolipids of natural rubber particles. *Journal of Natural Rubber Research*, **2**: 129-133.
- Hayden, O., Bindeus, R., Haderspock, C., Mann, K.J., Wirl, B. and Dickert, F.L. 2003. Mass-sensitive detection of cells, viruses and enzymes with artificial receptors. *Sensors and Actuators B*, **91**:316-319.
- Haupt, K. and Mosbach, K. 2000. Molecularly Imprinted Polymers and Their Use in Biomimetic Sensors. *Chemical Reviews*, **100**: 2495-2504.

- Homola, J., Yee, S.S. and Gauglitz, G. 1999. Surface plasmon resonance sensor: Review. *Sensors and Actuators B*, **54**: 3-15.
- Hillberg, A.L. and Tabrizian, M. 2008. Biomolecule imprinting: Developments in mimicking dynamic natural recognition systems. *ITBM-RBM*, **29**: 89-104.
- Ho, C.C., Subramaniam, A. and Yong, W.M. 1975. Lipids associated with the particles in Hevea latex. *Proceeding of the International Rubber Conference*, **2**: 441-456.
- Hsia, R.C.H. 1958. Oxygen Absorption by Hevea brasiliensis Latex. *Trans. Inst. Rubb. Ind*, **34**: 267-290.
- Huang, J.T., Zhang, J., Zhang, J.O. and Zheng, S.H. 2005. Template imprinting amphoteric polymer for the recognition of proteins. *Journal of Applied Polymer Science*, **95**:358-361.
- Hu, W., Chen, S., Li, X., Shi, S., Shen, W., Zhang, X. and Wang, H. 2009. In situ synthesis of silver chloride nanoparticles into bacterial cellulose membrane. *Materials Science and Engineering C*, **29**: 1216-1219.
- Hug, T.S. 2003. Biophysical methods fro monitoring cell-substrate interactions in drug discovery. *Assay and Drug Development Technologies*, **1(3)**: 479-488.

- Itzhaki, R.F. and Gill, D.M. 1964. A micro-biuret method for estimating proteins. *Analytical Biochemistry*, **9**: 401–410.
- Jaeger, D., Kleinhans, D., Czuppon, A.B. and Baur, X. 1992. Latex-specific proteins causing immediate-type cutaneous, nasal bronchial and systemic reactions. *Journal of Allergy and Clinical Immunology*, **89**: 759-768.
- Janeway, J.C., Travers, P., Walort, M. and Shlomchik, M. 2005. Allergy and hypersensitivity. In: Immunobiology the immune system in health and disease. 6th edition, New York: Garland Science Publishing., pp. 517-555.
- Jenik, M., Schirhagl, R., Schirk, C., Hayden, O., Lieberzeit, P., Blaas, D., Paul, G. and Dickert, F.L. 2009. Sensing picornaviruses using molecular imprinting techniques on a quartz crystal microbalance. *Analytical Chemistry*, **81**: 5320-5326.
- Jewtragoon, P. 2004. Bottom fraction membrane: Involvements in natural rubber latex allergy. *Doctor of Philosophy Thesis in Biochemistry*. pp. 65-173.
- Jiménez, Y., Otero, M. and Arnau, A. 2008. *Piezoelectric Transducer and Applications*, (2nd) Heidelberg: Springer-VerlagBerlin.

- Kanazawa, K.K.; Gordon II, J.G. 1985. The oscillation frequency of a quartz resonator in contact with a liquid. *Analytica Chimica Acta*, **175**: 99-105.
- Kempe, M. and Mosbach, K. 1995. Separation of amino acids, peptides and proteins on molecularly imprinted stationary phases. *Journal of Chromatography A*, **691**: 317-323.
- Kaur-Atwal, G., Weston, D.J., Green, P.S., Crosland, S. Bonner, P.L. and Creaser, C.S. 2007. Analysis of tryptic peptides using desorption electrospray ionization combined with ion mobility spectrometry/mass spectrometry. *Rapid Communications in Mass Spectrometry*, **21(7)**: 1131-1138.
- Kay, A.B. 2001. Allergy and allergic diseases. First of two parts. *The New England Journal of Medicine*, **344**: 30-37.
- Katz, A. and Davis, M.E. 2000. Molecular imprinting of bulk, microporous silica. *Nature*, **403**: 286-289.
- Karlsen, S.R., Johnston, K.S., Jorgenson, R.C. and Yee, S.S. 1995. Simultaneous determination of refractive index and absorbance spectra of chemical samples using surface plasmon resonance. *Sensors and Actuators B*, **25**: 747-749.

- Kim, H. and Guiochon, G. 2005. Comparison of the Thermodynamic Properties of Particulate and Monolithic Columns of Molecularly Imprinted Copolymers. *Analytical Chemistry*, **77**: 93-102.
- Kjeldahl, J.Z. 1883. A new method for the determination of nitrogen in organic bodies. *Analytical Chemistry*, **22**:366.
- Kleno, T.G., Andreasen, C.M., Kjeldal, H.O., Leonardsen, L.R., Krogh, T.N., Neilsen, P.F., Sorensen, M.V. and Jensen, O.N. 2004. MALDI MS peptide mapping performance by in-gel digestion on a probe with prestructured sample supports. *Analytical Chemistry*, **76**: 3576-3583.
- Konash, P.L. and Bastiaans, G.J. 1980. Piezoelectric crystals as detectors for liquid chromatography. *Analytical Chemistry*, **52**: 1929-1931.
- Ko, J.H. and Chow, K.S. 2003. Transcriptome analysis reveals features of the molecular events occurring in the laticifers of *Hevea brasiliensis* (para rubber tree). *Plant Molecular Biology*, **53**: 479-492.

- Kleno, T.G., Andreasen, C.M., Kjeldal, H.O., Leonardsen, L.R., Krogh, T.N., Neilsen, P.F., Sorensen, M.V. and Jensen, O.N. 2004. MALDI-MS peptide mapping performance by in-gel digestion on a probe with prestructured sample supports. *Analytical Chemistry*, **76**: 3576-3583.
- Kruchinin, A.A. and Vlasov, Y.G. 1996. Surface plasmon resonance monitoring by means of polarization state measurement in reflected light as the basis of a DNA-probe biosensor. *Sensors and Actuators B*, **30**: 77-80.
- Kurosawa, S., Tawara, E. 1990. Oscillating frequency of piezoelectric quartz crystal in solutions. *Analytica Chimica Acta*, **230(1)**: 41-49.
- Kurup, V.P., Yeang, H.Y., Sussman, G.L., Bansal, N.K., Beezhold, D.H., Kelly, K.J., Hoffman, D.R., Williams, B. and Fink, J.N. 2000. Detection of immunoglobulin antibodies in the sera of patients using purified latex allergens. *Clinical and Experimental Allergy*, **30**: 359-369.
- Laemmli, U.K., 1970. Cleavage of structural proteins during the assembly of the head of bacteriophage T4. *Nature*, **227**: 680-685.
- Larche, M., Akdis, C.A. and Valenta, R. 2006. Immunological mechanisms of allergen-specific immunotherapy. *Nature Reviews Immunology*, **6**: 761-771.

- Lazcka, O., Del Campo, F.J. and Muñoz, F.X. 2007. Pathogen detection: A perspective of traditional methods and biosensors. *Biosensors & Bioelectronics*, **22(7)**:1205-1217.
- Levy, D., Allouache, S., Chabane, M., Leynadier, F. and Burney, P. 1999. Powder-free protein-poor natural rubber latex gloves and latex sensitization. *Journal of the American Medical Association*, **281**: 988-994.
- Lewis, J.K., Wei, J. and Siuzdak, G. 2000. Matrix-assisted laser desorption/ionization mass spectrometry in peptide and protein analysis. *Encyclopedia of Analytical Chemistry*, R.A. Meyers (Ed.) □ Chichester: John Wiley & Sons Ltd., pp. 5880-5894.
- Liedberg, B., Nylander, C. and Lundstrom, I. 1983. Surface plasmon resonance for gas detection and biosensing, *Sensors and Actuators*, **4**: 299–304.
- Light, D.R. and Dennis, M.S. 1989. Purification of prenyltransferase that elongates as polyisoprene rubber from the latex of *Hevea brasiliensis*. *The Journal of Biological Chemistry*, **264**: 18589-18597.

- Liu, F., Liu, X., Siu-Choon, N., and Chan, H.S. 2006. Enantioselective molecular imprinting polymer coated QCM for the recognition of L-tryptophan. *Sensors and Actuators B*, **113**: 234-240.
- Little, D.P., Speir, J.P., Senko, M.W., O'Connor, P.B. and McLafferty, F.W. 1994. Infrared multiphoton dissociation of large multiply charged ions for biomolecule sequencing. *Analytical Chemistry*, **66**: 2809-2815.
- Lee, S.W. Hinsberg, W.D. and Kanazawa, K.K. 2002. Determination of the viscoelastic properties of polymer films using a compensated phase-locked oscillator circuit. *Analytical Chemistry*, **74(1)**:125-131.
- Loo, J.A., Edmonds, C.G. and Smith, R.D. 1990. Primary sequence information from intact proteins by electrospray ionization tandem mass spectrometry. *Science*, **248**: 201-204.
- Lowry, O.H., Rosebrough, N.J., Farr, A.L., and Randall, R.J. 1951. Protein measurement with the Folin phenol reagent. *Journal of Biological Chemistry*, **193**: 265-275.

- Lucklum, R., Behling, C. and Hauptmann, P. 1999. Role of mass accumulation and viscoelastic film properties for the response of acoustic-wave-based chemical sensors. *Analytical Chemistry*, **71**: 2488-2496.
- Luppa, P.B., Sokoll, L.J., and Chan, D.W. 2001. Immunosensor-principles and applications to clinical chemistry. *Clinica Chimica Acta*, **314**: 1-26.
- Lynen, F. 1969. Biochemical properties of rubber synthesis. *Journal of the Rubber Research Institute of Malaysia*, **21**: 389-406.
- Madhavan, S., Greenblatt, G.A., Foster, M.A. and Benedict, C.R. 1989. Stimulation of isopentenyl pyrophosphate incorporation into polyisoprene in extracts from guayule plants (*Parthenium argentatum* Gray) by low temperature and 2-(3, 4-dichlorophenoxy) triethylamine. *Plant Physiology*, **89**: 506-511.
- Martin, M.N. 1991. The latex of *Hevea brasiliensis* contains high levels of both chitinases and chitinases/lysozymes. *Plant Physiology*, **95**: 469-476.
- Manchester, K.L., 1996. Use of UV methods for measurement of protein and nucleic acid concentrations. *Biotechniques*, **20**: 968-970.

- Marx, K.A. 2003. Quartz crystal microbalance: A useful tool for studying thin polymer films and complex biomolecular systems at the solution-surface interface. *Biomacromolecules*, **4**: 1099-1120.
- Mc Fadden, E.R. 2002. Natural rubber latex sensitivity seminar conference Summary: *Journal of Allergy and Clinical Immunology*, S137-140.
- Majid, H.A., Razali, N., Sulaiman, M.S. and A'ain A.K. 2009. A capacitive sensor interface circuit based on phase differential method. *Engineering and Technology*, **55**: 636-639.
- Makinen-Kiljunen, S., Turjanmaa, K., Palosuo, T and Renula, T. 1992. Characterization of latex antigens and allergens in surgical gloves and natural rubber by immunoelectrophoretic methods. *Journal of Allergy and Clinical Immunology*, **90**: 230-5.
- Marchetti-Deschmann, M. and Allmaier, G. 2009. Allergenic compounds on the inner and outer surfaces of natural latex gloves: MALDI mass spectrometry and imaging of proteinous allergens. *Journal of mass spectrometry*, **44**:61-70.

- Martin, S.J., Granstaff, V.E. and Frye, G.C. 1991. Characterization of a quartz crystal microbalance with simultaneous mass and liquid loading. *Analytical Chemistry*, **63**: 2272-2281.
- Matsunaga, T., Hishiya, T. and Takeuchi, T. 2007. Surface Plasmon resonance sensor for lysozyme based on molecularly imprinted thin films. *Analytical Chimica Acta*, **591**: 63-67.
- Matsubara, K., Kawata, S. and Minami, S. 1988. Optical chemical sensor based on surface plasmon measurement. *Applied Optics*, **27(6)**: 1160–1163.
- McIntosh, R.B. and Casada, M.E. capacitance sensor for measuring the moisture content of agricultural commodities. *IEEE*, **8**: 240-247.
- Michael, J., Whitecome, M., Rodrigue, E. and Villar, P. 1995. A new method for the introduction of recognition site functionality into polymers prepared by molecular imprinting: synthesis and characterization of polymeric receptors for cholesterol. *Journal of the American Chemical Society*, **117**: 7105-7111.
- Molinelli, A., 2004. Molecularly imprinted polymer : towards a rational understanding of biomimetic materials, Doctoral thesis, Georgia Institute of Technology, U.S.A.

Moir, G.F.J. 1959. Ultracentrifugation and staining of Hevea latex. *Nature*, **184**: 1626-1628.

Moir, G.F.J. and Tata, S.J. 1960. The proteins of Hevea brasiliensis. The soluble proteins of bottom fraction. *Journal of the Rubber Research Institute of Malaysia*, **16**: 155-165.

Moir, G.F.J. 1959. Ultracentrifugation and staining of *Hevea* latex. *Nature*, **184**:1626-28.

Morrissey, B. and Downard, K.M. 2006. A proteomics approach to survey the antigenicity of the influenza virus by mass spectrometry. *Proteomics*, **6**: 2034-41.

Nicholls, I. and Rosengren, J.P. 2002. Molecular imprinting of surfaces. *Bioseparation*, **10**: 301-305.

Nieto, A., Mazon, A. and Estornell, F. 1998. Profilin, a relevant allergen in latex Allergy. *Journal of Allergy and Clinical Immunology*, **101**: S207-S215.

Nylander, C., Liedber, G.B. and Lind, T. 1982. Gas detection by means of surface plasmon resonance. *Sensors and Actuators*, **3**: 79-88.

- Ou, S.H., Wu, M.C., Chou, T.C. and Liu, C.C. 2004. Polyacrylamide gels with electrostatic functional groups for the molecular imprinting of lysozyme. *Analytica Chimica Acta*, **504**: 163-166.
- Pampi, P. and Kofinas, P. 2004. Biomimetic glucose recognition using molecularly imprinted polymer hydrogels. *Biomaterials*, **25**: 1969-1973.
- Pan, S., Gu, S., Bradbury, E.M. and Chen, X. 2003. Single peptide-based protein identification in human proteome through MALDI-TOF MS coupled with amino acids coded mass tagging. *Analytical Chemistry*, **75**: 1316-1324.
- Patterson, S.D. and Aebersold, R. 1995. Mass spectrometric approaches for the identification of gel-separated proteins. *Electrophoresis*, **16**: 1791-814.
- Perkins, D.N., Pappin, D.J.C., Creasy, D.M. and Cottrell, J.S. 1999. Probability-based protein identification by searching sequence databases using mass spectrometry data. *Electrophoresis*, **20**: 3551-3567.
- Pendle, T.D. and Swinyard, P.E. 1991. The Particle Size of Natural Rubber Latex Concentrates by Photon Correlation Spectroscopy. *Journal of Natural Rubber Research*, **6(1)**: 1-11.

- Pingoud, A., Urbanke, C., Hoggett, J. and Jeltsch, A. 2002. *Biochemical Methods*. Weinheim: Wiley-VCH Verlag GmbH., 76-82.
- Rashidi, H.H. and Buehler, L.K. 2000. *Bioinformatics basics: Application in biological science and medicine*, Boca Raton: CRC Press., pp. 133-4.
- Reid, G.E. and McLuckey, S.A. 2002. Top down protein characterization via tandem mass spectrometry. *Journal of Mass Spectrometry*, **37**: 663-675.
- Rihs, H.P., Chen, Z., Schumacher, S., Rozynek, P., Cremer, R., Lunderg, M., Raulf-Heimsoth, M., Petersen, A. and Baur, X. 2000. Recombinant Hev b 1: large-scale production and immunological characterization. *Clinical and Experimental Allergy*, **30(9)**: 1285-1292.
- Roby, J.F., White, B.J. 1978. *Biochemical Techniques: Theory and Practice*. California Wadsworth, Inc., pp.116-118.
- Sample, A.P., Yeager, A.J. and Smith, J.R. 2009. A capacitive touch interface for passive RFID tags. *Proceeding of the IEEE International Conference*, pp., 103-109.

- Schumacher, R.1990. The quartz microbalance: a novel approach to the in-situ investigation of interfacial phenomena at the solid/liquid junction. *Angewandte Chemie International Edition in English*, **29(4)**: 329-343.
- Senko, M.W., Speir, J.P. and McLafferty, F.W. 1994. Collisional activation of large multiply charged ions using fourier transform mass spectrometry. *Analytical Chemistry*, **66**: 2801-2808.
- Shana, Z.A. Radtke, D.E. 1990. Theory and applications of quartz resonator as a sensor for viscou liquids. *Analytica Chimica Acta*, **231(2)**: 317-320.
- Shen, S., Liu, T. and Guo, J. 1998. Optical phase-shift detection of surface plasmon resonance. *Applied Optics*, **37**: 1747–1751.
- Schoon, T.G.F. and Van, G.J.. 1995. Particle-size distribution in brominated Hevea lattices. *Journal of Polymer Science*, **15**: 63-88.
- Southorn, W.A. 1969. Physiology of Hevea latex flow. *Rubber Research Institute of Malaysia*, **21**: 494–512.
- Smith, P.K. 1985. Measurement of protein using bicinchonic acid. *Journal Analytical Biochemistry*, **76**:150-158.

- Sobott, F. and Robinson, C.V. 2002. Protein complexes gain momentum. *Current Opinion in Structural Biology*, **12**:729–734.
- Subramaniam, A. 1972. Gel permeation chromatography of natural rubber. *Rubber Chemistry & Technology*, **45**: 346-358.
- Sellergren, B., Kenneth, J.S. 1993. Influence of polymer morphology on the ability of imprinted network polymers to resolve enantiomers. *Journal of Chromatography*, **635**: 31-49.
- Scopes, R.K. 1994. Separation by Precipitation. In: Protein Purification, New York: Springer., pp. 71-101.
- Senko, M.W., Speir, J.P. and McLafferty, F.W. 1994. Collisional activation of large multiply charged ions using fourier transform mass spectrometry. *Analytical Chemistry*, **66**: 2801-2808.
- Slater, J.E. and Chhabra, S.K. 1992. Latex antigens. *Journal of Allergy and Clinical Immunology*, **89**:673-8.
- Steinem, C. and Janshoff, A. 2007. Chemical Sensors and Biosensor. 5th ed. New York: Springer Berlin Heidelberg., pp. 7-22.

- Sunderasan, E.H., Samsidar, H., Sharifah, H., Ward, M.A., Yeang, H.Y. and Cardosa, M. J. 1995. Latex B serum β -1, 3-glucanase (Hev b II) and a component of the microhelix (Hev b IV) are major latex allergens. *Journal of Natural Rubber Research*, **10**: 82–99.
- Sunderasan, E., Bahari, A., Arif, S.A.M., Zainalw, Z., Hamilton, R.G. and Yeang, H. Y. 2005. Molecular cloning and immunoglobulin E reactivity of a natural rubber latex lecithinase homologue, the major allergenic component of Hev b 4. *Clinical Experiment Allergy*, **35**: 1490–1495.
- Suedee, R., Intakong, W. and Dickert, F.L. 2006. The use of trichloroacetic acid imprinted polymer coated quartz crystal microbalance as a screening method for determination of haloacetic acids in drinking water. *Talanta*, **70**: 194-201.
- Suedee, R., Seechamnaturakit, V., Canyuk, B., Ovatlarnporn, C., Martin, G.P. 2006. Temperature sensitive dopamine-imprinted (N, N-methylene-bis-acrylamide cross-linked) polymer and its potential application to the selective extraction of adrenergic drugs from urine. *Journal of Chromatography A*, **1114**: 239-249.

- Sunderasan, E., Hamzah, S., Hamid, S., Ward, M.A., Yeang, H.Y. and Cardosa, M.J. 1996. Latex B-serum β -1 3-glucanase (Hev b 2) and a component of the microhelix (Hev b 4) are major latex allergens. *Journal of Natural Rubber Research*, **10**:82-99.
- Suri, C.R. 2006. Quartz crystal based microgravimetric immunobiosensors. *Sensors & Transducers Magazine*, **66(4)**:543-552.
- Svenson, J., Karlsson, J.G. and Nicholls, I.A. 2004. ¹H nuclear magnetic resonance study of the molecular imprinting of (-)-nicotine: template self-association, a molecular basis for cooperative ligand binding. *Journal of Chromatography A*, **1024**: 39–44.
- Takeuchi, T. and Haginaka, J. 1999. Separation and sensing based on molecular recognition using molecularly imprinted polymers. *Journal of Chromatography B*, **728**: 1-20.
- Towbin, H., Staehelin, T. and Gordon, J. 1979. Electrophoretic transfer of proteins from polyacrylamide gels to nitrocellulose sheets: Procedure and some applications. *Proceedings of the National Academy of Sciences*, **76**: 4350-4354.

- Takeda, K. and Kobayashi, T. 2005. A. imprinted polymer adsorbents with selective recognition and binding characteristics. *Science and Technology of Advanced Materials*, **6**: 165-171.
- Tao, Z., Tehan, E.C., Bukowski, R.M., Tang, Y., Shughart, E.L., Holthoff, W.G., Cartwright, A.N., Titus, A.H. and Bright, F.V. 2006. Templated xerogels as platforms for biomoleculeless biomolecule sensors. *Analytica Chimica Acta*, **564**: 59–65.
- Tomazic-Jezic, V.J. and Lucas, A.D. 2002. Protein and allergen assays for natural rubber latex products. *Journal Allergy Clinical Immunology*, **110**: S40-46.
- Tata, S.J. 1975. Hevein, its isolation, purification and some structural aspects. *Proceedings International Rubber Conference*, Rubber Research Institute of Malaysia, Kula Lumpur, **2**: 441-447.
- Tata, S.J. and Moir, G.F.J. 1964. The proteins of *Hevea brasiliensis* latex: Starch gel electrophoresis of C-serum proteins. *Journal of Rubber Research Institute of Malaya*, **18**: 97-108.

- Tata, S.J., 1975. A study of the proteins in the heavy fraction of *Hevea brasiliensis* latex and their possible role in the destabilisation of rubber particles. University Malaya, Kuala Lumpur.
- Tata, S.J. 1976. Hevein: Its isolation, purification and some structural aspects. *Proceeding International Rubber Conference*. Kuala Lumpur., pp. 499-517.
- Tata, S.J. and Edwin, E.E. 1970. Hevea latex enzymes detected by zymogram technique after starch gel electrophoresis. *Journal of Rubber Research Institute of Malaya*, **23**: 1-12.
- Tata, S.J., Beintema, J.J. and Balabaskaran, S. 1983. The lysozyme of *Hevea brasiliensis* latex. Isolation, enzyme kinetics and a partial amino acid sequence. *Journal of Rubber Research Institute of Malaya*, **18**: 97-108.
- Tata, S.J. 1980. Distribution of proteins between the fractions of *Hevea* latex separated by ultracentrifugation. *Journal of the Rubber Research Institute of Malaysia*, **28**: 77-85.
- Tata, S.J. 1980. Studies on the lysozyme and components of microhelices of *Hevea brasiliensis* latex. Thesis for a degree of Doctor of Philosophy. University Malaya, Kuala Lumpur.

- Turner, N.W., Jeans, C.W., Brain, K.R., Allender, C.J., Hlady, V. and Britt, D.W. 2006. From 3D to 2D: A Review of the Molecular Imprinting of Proteins. *Biotechnology Progress*, **22**: 1474-1489.
- Venton, D.L. and Gudipati, E., 1995. Entrapment of enzymes using organo-functionalized polysiloxane copolymers. *Biochimica et Biophysica Acta*, **1250**: 117-125.
- Wagner, B., Krebitz, M., Buck, D., Niggemann, B., Yeang, H.Y., Han, K.H., Scheiner, O. and Breiteneder, H. 1999. Cloning, expression and characterization of recombinant Hev b 3, a *Hevea brasiliensis* protein associated with Latex allergy in Spina bifida patients. *Journal of Allergy and Clinical Immunology*. **104**: 1084-1092.
- Wagner, S., Breiteneder, H., Simon-Nobbe, B., Susani, M., Krebitz, M., Niggemann, B., Brehler, R., Scheiner, O. and Hoffmann-Sommergruber, K. 2000. Hev b 9, an enolase and a new cross-reactive allergen from hevea latex and molds. Purification, characterization, cloning and expression. *Journal of Biochemistry*, **267**: 7006-7014.

- Wagner, S., Sowka, S. and Mayer, C. 2001. Identification of a *Hevea brasiliensis* latex manganese superoxide dismutase (Hev b 10) as a cross-reactive allergen. *International Archives of Allergy Immunology*, **125**: 120–127.
- Wititsuwannakul, R., Rukseree, K. and Kanokwiroon, K. 2008. A rubber particle protein specific for *Hevea* latex lectin binding involved in latex coagulation. *Phytochemistry*, **69**: 111-1118.
- Wan, J., Wang, J. and Cheng, H. 2001. Proteomic analysis of apoptosis initiation induced by all-trans retinoic acid in human acute promyelocytic leukemia cells. *Electrophoresis*, **22**: 3026-37.
- Ward, W.W. and Swiatek, G. 2009. Protein Purification. *Current Analytical Chemistry*, **5(2)**: 1-21.
- Weber, K. Osborn, M. 1969. Reliability of molecular weight determinations by dodecyl sulphate-polyacrylamide gel electrophoresis. *Journal of Biological Chemistry*, **244**: 4406-4412.
- Wititsuwannakul, D., Rattanapittayaporn, A., Koyama, T. and Wititsuwannakul, R. 2004. Involvement of *Hevea* latex organelle membrane proteins in rubber biosynthesis activity and regulatory function. *Macromolecular Bioscience*, **4**: 314-323.

- Wood, D.F. and Cornish, K. 2000. Microstructure of purified rubber particle. *International Journal of Plant Sciences*, **161**: 435-445
- Wysocki, V.H., Resing, K.A., Zhang, Q. and Cheng, G. 2005. Mass spectrometry of peptides and proteins. *Methods*, **35**:211-222.
- Yagami, T., Sato, M., Nakamura, A. and Shono, M. 1995. One of the rubber latex allergens in a lysozyme. *Journal Allergy Clinical Immunology*, **96**: 677-686.
- Yates, J.R. 1998. Database searching using mass spectrometry data. *Electrophoresis*, **19**: 893-900.
- Yates, J.R. 2000. Mass spectrometry: from genomics to proteomics. *Trends in Genetics*, **16**: 5-8.
- Yeang, H.Y., Ghandimathi, H. and Paranjothy, H. 1977. Protein and enzyme variation in some Hevea cultivars. *Journal of Rubber Research Institute of Malaya*, **25**: 9-18.

- Yeang, H.Y., Cheong, K.F., Sunderasan, E., Hamzah, S., Chew, N.P., Hamid, S., Hamilton, R.G. and Cardoso, M.J. 1996. The 14.6 kd rubber elongation factor (Hev b1) and 24 kd (Hev b3) rubber particle proteins are recognized by IgE from patients with spina bifida and latex allergy. *Journal of Allergy and Clinical Immunology*, **98**: 628-639.
- Yeang, H.Y., Siti, A. M., Arif, F.Y. and Sunderasan, E. 2002. Allergenic proteins of natural rubber latex. *Methods*, **27**: 32-45.
- Yeang, H.Y., Ghandimathi, H. and Paranjothy, H. 1977. Protein and enzyme variation in some Hevea cultivars. *Journal of Rubber Research Institute of Malaya*, **25**: 9-18.
- Yeang, H.Y., Ward, M.A., Dennis, M.S. and Light, D.R. 1998. Amino acid sequence similarity of Hev b 3 to two previously reported 27- and 23-kDa latex proteins allergenic to spina bifida patients. *Allergy*, **53**: 513– 519.
- Yeang, H.Y., Chow, K.S. and Yusof, F. 2000. Appraisal of latex glove proteins in the induction of sensitivity to multiple latex allergens. *Journal of Investicational Allergology and Clinical Immunology*, **10**: 215–222.
- Yilmaz, E., Haupt, K. and Mosbach, K. 2000. The use of immobilized templates-A new approach in molecular imprinting. *Angewandte Chemie*, **39**: 2115-2118.

Yip, L., Hickey, V., Wagner, B., Liss, G., Slater, J. and Breiteneder, H. 2000. Skin prick test reactivity to recombinant latex allergens. *International Archives of Allergy and Immunology*, **121**: 292-299.

Ylitalo, L., Alenius, H., Turjanmaa, K., Palosuo, T. and Reunala, T. 1998. IgE antibodies to prohevein, hevein, and rubber elongation factor in children with latex allergy. *Journal of Allergy and Clinical Immunology*. **102(4)**: 659-664.

VITAE

Name Mr. Chonlatid Sontimuang

Student ID 5010730001

Educational Attainment

Degree	Name of Institution	Year of Graduation
M.Sc. (Analytical Chemistry)	Prince of Songkla University	2549
B.Sc. (Chemistry)	Prince of Songkla University	2541

Scholarship Awards during Enrolment

The scholarship support from the National research council of Thailand and NANOTEC Center of Excellence, Prince of Songkla University, 2 months scholarship from Institute of Analytical Chemistry, Faculty of Chemistry, University of Vienna, Vienna, Austria.

List of Publication and Proceeding

Sontimuang, C., Suedee, R., Canyuk, B., Phadoongsombut, N. and Dickert, F.L. 2011.

Development of a rubber elongation factor, surface-imprinted polymer-quartz crystal microbalance sensor, for quantitative determination of Hev b1 rubber latex allergens present in natural rubber latex products. *Analytica Chimica Acta*. **687**:184-192.